Volume of Inter- and Intra-hemispheric Connections and the Efficiency of Higher Cognitive Processing

by

Jacek Jonca-Jasinski, M.A.

A Dissertation

In

EXPERIMENTAL PSYCHOLOGY

Submitted to the Graduate Faculty
of Texas Tech University in
Partial Fulfillment of
the Requirements for
the Degree of

DOCTOR OF PHILOSOPHY

Alice Young
Chair of Committee

Roman Taraban

Steven Sawyer

Gregory Schrimsher

Marek Kubicki

Peggy Gordon Miller
Dean of the Graduate School

August, 2011

ACKNOWLEDGEMENTS

Author would like to thank Marian and Ranjit Bessy, Alma and Tom Taubensee, Deborah Harding, Donna Rogers, Shannon Samson, and the staff of the Office of Graduate Admissions and the Graduate School for their continuous support. Author would like to acknowledge kind mentorship and feedback of Richard P. McGlynn during early stages of this project and inspirations for this research provided by Michael O'Boyle. This project would not be possible without training provided by the Multimodal Neuroimaging Training Program (MNTP) at the University of Pittsburgh, in collaboration with Carnegie Mellon University, and with funding from the National Institutes of Health (NIH)(grants R90DA023420 and T90DA022761) as well as training provided by the APA Advanced Training Institute in Magnetic Resonance Imaging. Special acknowledgments are due for Julie Price, James Becker, Howard Aizenstein, Megan Nable, Seong-Gi Kim, and Bill Eddy. Data used in the preparation of this article were obtained from the NIH Pediatric MRI Data Repository created by the NIH MRI Study of Normal Brain Development. Finally, author would like to acknowledge the High Performance Computing Center (HPCC) at Texas Tech University whose computing resources were a significant contribution to this dissertation. Special acknowledgements are due for Srirangam V. Addepalli, David Chaffin, Philip W. Smith, and James Abbott.

Table of Contents

List of Figures

List of Tables

ABSTRACT

The brain is one of the most complex biological systems known to man. While neuroscientists understand many of the basic aspects of brain operation, how these basic aspects merge together to give rise to more complex phenomena such as consciousness or higher cognitive function remains a mystery. This study explores the idea that higher cognitive function arises from the integration of processing resources distributed across hemispheres and across brain areas. This integration owes much to white matter tracts creating information highways between hemispheres. In this study a well-defined set of cognitive processes engaged by a specific subset of measures of processing speed, spatial working memory, visuo-spatial abilities, and non-verbal reasoning is related to a network of areas previously demonstrated to be involved in higher cognitive functioning. Of special interest is the corpus callosum, the largest white matter structure in the brain and the highest order integrator of the processing resources from brain hemispheres. In a series of hypotheses the relation between sections of the corpus callosum and a group of cognitive tasks was examined. Selected cognitive measures included CANTAB Spatial Working Memory (SWM), WASI Block Design, WASI Matrix Reasoning, and WISC-III Coding CANTAB SWM, B subtests.

Author predicted that (1) Volume and of the anterior fifth of the corpus callosum carrying connections between frontal areas will be positively related to scores on CANTAB Spatial Working Memory, WASI Block Design, WASI Matrix Reasoning, and WISC-III Coding B subtest and that (2) volume of the posterior two-fifths of the corpus callosum carrying connections between parieto-occipital areas will be positively related to scores on WASI Block Design, WASI Matrix Reasoning, WISC-III Coding B.

Hierarchical regression analyses conducted on a representative sample of the U.S. population for ages 4 years 10 months through 18 years 5 months for CANTAB SWM, 4 years 10 months through 18 years 5 months for WASI Block Design, WASI Matrix Reasoning, and 8 years 1 month through 16 years 11 months for WISC-III Coding B provided no support for proposed hypotheses.

From all predictors entered into hierarchical regression analyses age emerged as a sole consistent and highly significant predictor of dependent measures of cognitive ability. Age universally accounted for a large and significant amount of variance in each dependent measure. Ex-

planations for lack of predictive power of the volumes of the corpus callosum are presented and significant effects of nuisance variables are discussed.

THESIS

Individual differences in the volume of the white matter relate to levels of cognitive functioning by affecting bandwidth of inter-hemispheric (e.g. corpus callosum) and intra-hemispheric connections (e.g. frontal and parietal medial white matter) involved in pooling and coordination of neural resources distributed across the brain regions and brain hemispheres.

GOALS AND MOTIVATION

Rationale

Information in the nervous system is transferred through axons. On the macroscopic level collections of axons appear is the tissue as the white matter. Volume of white matter is related to number and size of axons it contains. Both number of axons and axonal size are positively related to the amount of information that can be transferred per unit of time because: (a) larger axons have faster conduction velocity, and (b) more axons can transfer more information. Since (1) volume of white matter is positively related to the number and sizes of axons it contains, and (2) since number and sizes of axons are positively related to bandwidth, on the basis of the De Morgan's laws it can be concluded that white matter volume is also positively related to amount of information that can be transferred per unit of time. Amount of information transferred per unit of time, in turn, optimizes cognition by: (1) facilitating recruitment of additional processing resources, and by (2) inhibiting interference between activated areas when localized processing is more efficient than a distributed process. Inhibition of activations may be particularly important when task is simple and delay associated with information transfer outweighs gains stemming from distributed processing.

Purpose

The primary purpose of this study is to test whether volume of the sections of the corpus callosum corresponds to cognitive performance on cognitive test that are likely to invoke inter-hemispheric transfer through those callosal subsections. Secondary purpose of this study is to evaluate feasibility of a mathematical formalism intended to estimate relative contributions of anterior and posterior portions of the corpus callosum (inter-hemispheric integration), frontal and parietal white matter volumes (intra-hemispheric integration), as well as frontal and parietal gray matter volumes (rudimentary processing) to performance on cognitive tests.

Research questions

Guiding research questions include: (1) Is volume of the anterior corpus callosum related to performance on CANTAB SWM, WASI Block Design, WASI Matrix Reasoning, and WISC-III Coding B? (2) Is volume of the posterior corpus callosum related to performance on WASI Block Design, WASI Matrix Reasoning, and WISC-III Coding B?

Predictions

Author predicts that:

1. Volume and of the anterior fifth of the corpus callosum carrying connections between frontal areas will be positively related to performance on CANTAB Spatial Working Memory, WASI Block Design, WASI Matrix Reasoning, and WISC-III Coding B subtest. Those tasks have been shown to invoke inter-hemispheric transfer between frontal brain areas.

2. Volume and of the posterior two-fifths of the corpus callosum carrying connections between parieto-occipital areas will be positively related to performance on WASI Block Design, WASI Matrix Reasoning, and WISC-III Coding B. Those tasks have been shown to invoke inter-hemispheric transfer between posterior brain areas.

Methodology

Predictions presented above are tested using data provided by the NIH MRI Study of Normal Brain Development, a national study of a well constructed and well screened sample of normally developing children and adolescents. In the present study, data is representative of the U.S. population in the age ranges corresponding to the selected cognitive measures including: CANTAB SWM (ages 4 years 10 months through 18 years 5 months), WASI Block Design, WASI Matrix Reasoning (ages 4 years 10 months through 18 years 5 months), and WISC-III Coding B (ages 8 years 1 month through 16 years 11 months). This dataset was selected in order to address selection bias and sample size issues present in some of the previous studies of relations between callosal morphology and cognitive performance. In contrast to many previous studies conducted on convenience samples of normal or clinical populations this study is based on (1) a well screened sample of normally developing participants, (2) a well constructed sample intended for drawing inferences to the general U.S. population limited to normally developing children in

age groups defined by cognitive tests used in this study. This study aims at demonstrating that while processing resources distributed among frontal and parietal areas are important, of importance are also the connections formed among those areas allowing integration of distributed processing resources.

INTRODUCTION

The human brain has a hierarchical-modular organization, allowing progressively more complex integration of inputs and information processing from lower organizational levels. On the highest levels, there are fiber tracts connecting higher-order (e.g. multi-modal) association areas that, by themselves, represent already complex integration of information from both unimodal association areas and the primary cortices.

Relation between structure of axons, their function, bandwidth, and cognitive functioning

Size, density, and myelination of fibers together determine the bandwidth of connections. Thickness and degree of myelination of an axon affects the speed of transmission of information, (Gutierrez, Boison, Heinemann, & Stoffel, 1995; Tolhurst & P. R. Lewis, 1992; Waxman, 1980), while the density of the fiber tracts in the bundle, and the size of a bundle itself may relate to the amount of information that can be simultaneously transferred. Both density and integrity of axons in the bundle influence bandwidth by affecting the amount of information that can be transferred per unit of time. Bandwidth, in turn, is important for the integration, synchronization, and recruitment of the distributed information processing resources. Speed and efficiency with which information is integrated affects ability to recruit additional processing resources in service of a goal-oriented action (Turken et al., 2008). Speed and efficiency of information coordination and synchronization depends on temporal precision (Engel, Fries, & Singer, 2001) and temporal precision depends on the structural properties of axons that carry neural signals. Temporal precision affects temporal synchrony, which in turn has been proposed as one of the mechanism of binding (C. M. Gray, 1999, Singer, 1999, Singer & C. M. Gray, 1995; for critique see Shadlen & Movshon, 1999) which in turn is necessary for normal higher cognition. For example, in multiple sclerosis, a diminished conduction velocity in demyelinated axons affects temporal precision, temporal synchrony, and it has been linked to cognitive deficits (Kesselring, 1997; Rao, 1996).

In addition to temporal aspects of neural transmission, structure of axons and myelin sheath affects the distance neural signal can travel. Long distance transmission in the brain is contingent on the ability to reduce signal degradation (Turken et al., 2008) that is partially assured by the myelin sheath. Consequently, structure of axons and myelin sheath is particularly important for long association and commissural fibers that project over longer distances interconnecting

brain lobes and hemispheres respectively.

In sum, macro- and micro-structure of fiber bundles affects speed, efficacy, as well as temporal precision and temporal synchrony of neural transfer. Efficiency of neural transfer affects efficiency of cognitive processes through recruitment of additional processing resources during challenging tasks or/and through inhibition of competing brain regions and consequently decreasing interference or time penalty associated with long distance transfer. Schematic representation of relation between axon properties, white matter properties, bandwidth, and cognitive efficiency is summarized in figure 1 on page 19.

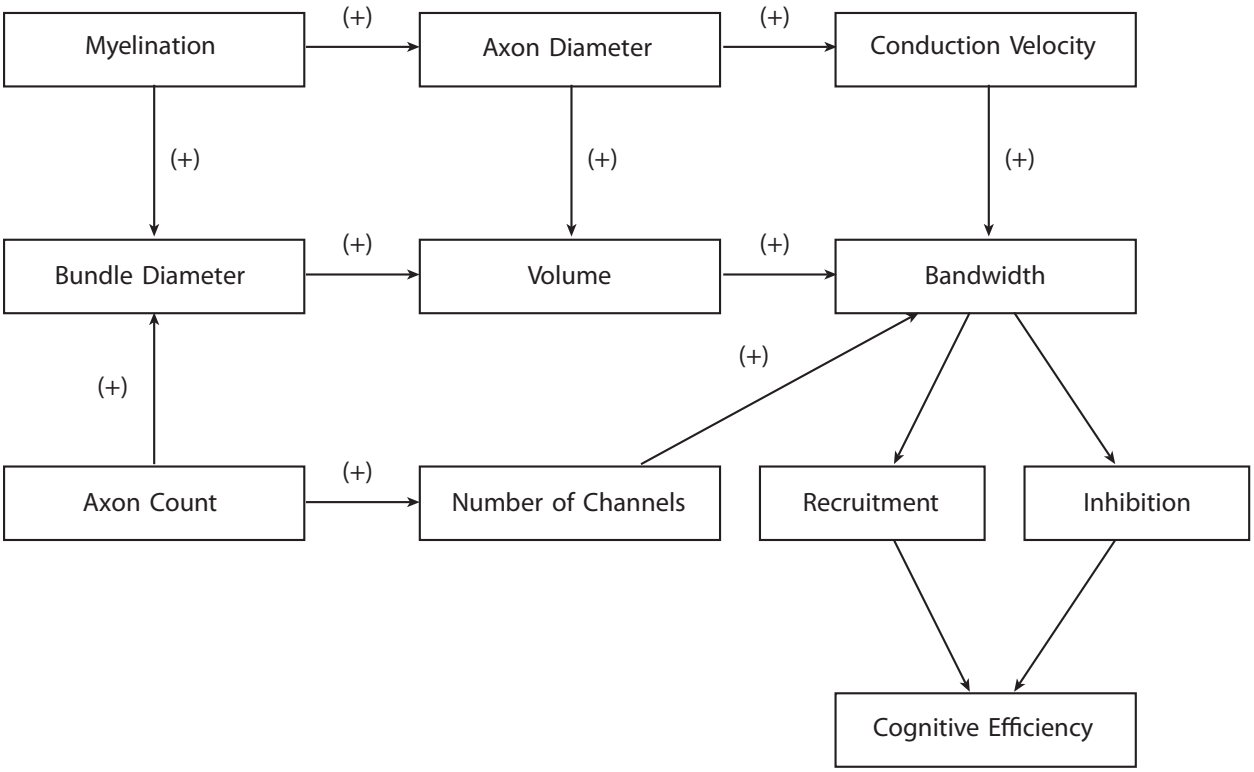

Figure 1: Schematic representation of relations between axon properties, white matter properties, bandwidth, and cognitive efficiency.

Development of white matter

Development of the white matter is only partially complete at birth and at the age of two estimated 90% of the myelination is complete (Byrd, Darling, & Wilczynski, 1993). The remainder of myelination progresses through the lifespan as late as through the sixth decade of life

(Benes, Turtle, Khan, & Farol, 1994; Filley, 2001). The ontogenetic sequence of white matter maturation mirrors phylogenetic sequence of brain development. Brain areas acquired last in the course of phylogenesis also mature last in the course of ontogenesis. In general, myelination progresses in the posterior to anterior order with occipital and parietal lobes maturing before the frontal and temporal lobes (Byrd et al., 1993; Klingberg, Vaidya, Gabrieli, Moseley, & Hedehus, 1999).

The development of white matter as indicated by the fractional anisotropy reaches asymptote in the second to third decade of life (Ben Bashat et al., 2005; T.-Q. Li & M. D. Noseworthy, 2002; McLaughlin et al., 2007) and pattern of white matter development over time is largely linear (Toga, Thompson, & E. R. Sowell, 2006). First longitudinal study to compare growth curves for brain lobes reported linear increase in white matter up until the age of 20 accompanied by non-linear increase in the gray matter (J. Giedd, J. Blumenthal, Jeffries, Castellanos et al., 1999).

Among fiber tracts, great commissures and association fibers tend to mature last (Filley, 2001; Yakovlev & Lecours, 1967). Previous studies have shown that both the fractional anisotropy in the corpus callosum, and the volume of corpus callosum increases linearly through childhood and adolescence until young adulthood reaching plateau in the second decade of life (McLaughlin et al., 2007). Others reported that great cerebral commissures finish development much earlier, between 7th and 10th year of life (Yakovlev & Lecours, 1967). However, development of the corpus callosum is not uniform across all its parts. Thompson, Giedd et al. (2000) reported that between the ages 3 and 6 there is a robust maturation of anterior parts of the corpus callosum while between the ages of 11 and 15 fastest maturation takes place in the area or isthmus / posterior body.

White matter development in specific cortical areas parallels cognitive development of variety of specific cognitive functions (Mabbott, M. Noseworthy, Bouffet, Laughlin, & Rockel, 2006; Nagy, Westerberg, & Klingberg, 2004; Fields, 2008) including cognitive control, inhibition, and executive decisions (Liston et al., 2006) as well as language related cognitive functions including reading (Kraft, O. Mitchell, Languis, & Wheatley, 1980), and acquisition of vocabulary (Pujol et al., 2006). Furthermore, there is preliminary evidence that acquisition of skill correlates with localized changes in white matter structure in the areas involved in those tasks. For example, in Bengtsson et al. (2005) learning to play piano correlated in white matter changes

in fiber tracts that varied by age. In children, extensive changes took place in the cortico-spinal tract and increased complexity of white matter correlated with the number of practice hours. Converging evidence for experience related changes in the corpus callosum emerges from animal studies. In rats enriched environment was associated with increased number of myelinated axons traveling in the corpus callosum (Juraska & Kopcik, 1988; Markham & Greenough, 2004; Fields, 2008). This finding suggests that normal development of white matter goes beyond genetically pre-determined program and at least during critical development periods can be significantly modified by experience (Fields, 2008). In addition to traditionally recognized mechanisms of cellular learning such as the long term potentiation, white matter plasticity may represent an additional long-term learning mechanism that so far has not received sufficient attention (Fields, 2008).

White matter and cognitive functioning

Networks of white matter fiber tracts facilitate integration and synchronization of information processing taking place across the brain (Mesulam, 1998, 2000; Turken et al., 2008). The importance of the white matter fiber tracts in cortical function is emphasized by theoretical models of brain connectivity (Kotter & Sommer, 2000) and clustering analyses (Hilgetag, Burns, O'Neill, Scannell, & Young, 2000) both indicating that patterns of brain wiring can largely account for patterns of cortical activity (Turken et al., 2008). As early as 1924, it has been suggested that there is a close correlation between myelination of the fiber tracts and acquisition of function (Tilney & Casamajor, 1924; Davison & Dobbing, 1966; van der Knaap et al., 1991; Yakovlev & Lecours, 1967).

Global changes in white matter have been documented in children with congenital hydrocephalus where cognitive impairment correlated with delayed myelination (van der Knaap et al., 1991) and in patients diagnosed with multiple sclerosis (MS). Patients diagnosed with MS show 7 to 10 points gap between Wechsler's measures of Verbal IQ (higher) and Performance IQ (Rao, 1996). Rao (1996) further pointed out that MS patients show diminished performance on variety of neuropsychological and cognitive measures of conceptual and abstract reasoning including the Category Test (Heaton, L. M. Nelson, D. S. Thompson, Burks, & Franklin, 1985; Peyser, Edwards, Poser, & Filskov, 1980; Reitan, Reed, & Dyken, 1971), Wisconsin Card Sorting Test (Heaton et al., 1985; Rao, Hammeke, & Speech, 1987; Rao, Leo, Bernardin, & Unverzagt,

1991), Grassi Block Substitution Test (Parsons, K. D. Stewart, & Arenberg, 1957), Levine Concept Formation task (Rao & Hammeke, 1984), and Weigl Sorting Test (Jambor, 1969). MS patients have difficulty sequencing pictures (Beatty & Monson, 1994) and planning in the Tower of Hanoi task (Arnett et al., 1997). Pattern of symptoms discussed above is consistent with deficits associated predominantly with frontal and parietal functions. In cognitively normal samples individual differences in IQ (Schmithorst, Wilke, Dardzinski, & Holland, 2005), reading skills (Gold, Powell, Xuan, Jiang, & Hardy, 2007; Klingberg, Hedehus et al., 2000; S. N. Niogi & McCandliss, 2006), working memory (Gold et al., 2007; Nestor et al., 2007), and musical abilities (Bengtsson et al., 2005; Hyde, Zatorre, Griffiths, Lerch, & Peretz, 2006) all correlate with white matter in brain regions differentially involved in those abilities (see also Fields, 2008). Some support for the role of white matter in general, and corpus callosum in particular, in cognitive performance comes from studies of mathematically gifted individuals. In one study O'Boyle, Cunnington et al. (2005) reported that during mental rotation task mathematically gifted male adolescents activated more extensive brain network than controls. Mathematically gifted individuals showed activations in more distributed network of bilateral homologous brain regions consisting of the frontal and parietal regions as well as the anterior cingulate. Authors suggested that this pattern of activation reflects enhanced inter-hemispheric communication that may involve the corpus callosum (cf. O'Boyle, 2008).

White matter development, cognitive development, and age

Human development reflects a complex and dynamic interplay of parallel developmental processes occurring according to genetically programmed sequence of stages that correspond to approximate periods of chronological age and are affected by environmental influences. Development of white matter is no exception following a sequence of developmental processes ranging from synaptogenesis to myelination (Yakovlev & Lecours, 1967). White matter development is closely paralleled by changes in function, for example gradual acquisition of the motor skill in newborns follows a head to toe pattern, reflecting gradual myelination of the cortico-spinal tracts (Coffey & Brumback, 2006), and falls into an approximately defined period of chronological age. Similar parallels exist with regard to cognitive development and emergence of cognitive abilities. For example, it was suggested that progression through Piagetian stages of cognitive development reflects cortical myelination in general, and inter-hemispheric connectivity in particular (Kraft

et al., 1980). In the animal studies, rhesus monkeys raised in enriched habitats showed increase in the size of the corpus callosum that was also paralleled by performance gains on the delayed non-matching to sample test (M. M. Sanchez, Hearn, Do, Rilling, & Herndon, 1998).

Cognitive maturation, maturation of white matter, and chronological age, represent to large extent different facets of the same underlying process. There are documented links between age and cognitive control, between white matter properties and cognitive control, and between white matter micro-structure and age. Liston et al. (2006) in their study employing go/no-go task reported that both diffusivity in the fronto-striatal tract and efficiency of cognitive control changed with age. Reflecting increasing complexity and integrity of myelin, the diffusivity in the white matter decreased with myelination and age while efficiency of cognitive control increased with age. Liston et al. (2006) noted that accuracy of responses on the go/no-go task changed with both age and diffusion. Accuracy of responses on this task increased with age and with decreased radial diffusivity in the fronto-striatal tract. Changes in diffusion were also associated with changes in reaction time. Decreased diffusivity mapped onto decreased reaction time. This link was independent of age and accuracy thus suggesting a relation between structure of white matter and reaction time possibly mediated by speed of transfer. Furthermore, association between diffusion in the fronto-striatal tract and response time strengthened for trials involving greater degree of cognitive control providing additional evidence for relation between white matter micro-structure in the fronto-striatal tract and executive function.

Altogether, results reported by Liston et al. (2006) (1) confirm a positive link between complexity of micro-structure including integrity of myelin sheath and age, (2) confirm a positive relation between age and cognitive control, (3) document a positive relation between complexity of micro-structure in the fronto-striatal tract and response time in tasks involving cognitive control, (4) suggest a positive relation between complexity of micro-structure and degree of cognitive control, (5) confirm a positive relation between age and accuracy of performance on the go/no-go task and (6) suggest an additional positive link between diffusivity in the fronto-striatal tract and accuracy of performance on this task. In sum, Liston et al. (2006) not only demonstrates importance of accounting for age in research designs, but also demonstrates complexity of interrelations between age, cognitive control, and white matter structure. Shared source and interrelatedness of those factors pose a significant challenge in attempts to separate their contributions in

statistical models (Mabbott et al., 2006).

Section that follows will provide brief introduction to the nodes of brain network responsible for higher cognitive function and relate those nodes to specific white matter tracts responsible for integration of processing resources subserved by those nodes.

Higher-order cognitive abilities, higher-order association areas, highest-order integrator tracts

Higher-order cognitive abilities rely on higher-order association areas and connections they form. Higher-order association areas located in the prefrontal, posterior parietal, and temporal cortex have been implicated in a variety of highest-level cognitive processes including working memory, attention, and response selection (for review see Goldman-Rakic, 1988). Prefrontal (J. Duncan, Emslie, P. Williams, Johnson, & Freer, 1996; J. Duncan, R. J. Seitz et al., 2000; J. Duncan & A. M. Owen, 2000) posterior parietal (Andersen, L. H. Snyder, Bradley, & Xing, 1997; Shulman et al., 1997), and temporal (Shulman et al., 1997) cortical areas are frequently recruited in variety of cognitive tasks (Turken et al., 2008) and together with fiber tracts connecting them are part of the network that is believed to be responsible for emergence of higher cognitive function (Colom, Haier et al., 2009). From among fiber tracts in human brain, of particular interest are fibers at the top of the resource-integration hierarchy. Those fibers include some of the commissural fibers interconnecting cortical areas in the hemispheres, and the long association fibers interconnecting brain lobes. This study focuses on commissural fibers interconnecting higher-order association areas that in turn are frequently recruited in a variety of cognitive tasks (Jung & Haier, 2007). Anterior and posterior portions of the corpus callosum carry fibers interconnecting homologous higher-order association areas in the frontal and parietal lobes. Frontal and parietal medial white matter carries fibers interconnecting anterior and posterior brain areas and includes fiber tracts such as the superior longitudinal fasciculi interconnecting the multimodal association areas in the parietal lobe with the frontal association cortex.[1] Fronto-parietal

[1]The Superior Longitudinal Fasciculi cannot be partitioned from the medial white matter using traditional MRI scanning sequences. An additional study will be performed when DTI portion of the NIH Pediatric database becomes available. While present study examines relation between macro-structure of the corpus callosum (inter-hemispheric transfer), medial white matter of the frontal and parietal lobes (intra-hemispheric transfer), and cognitive performance, future study will specifically focus on both micro- and macro-structure of the corpus callosum and the

integration has been suggested to be an important factor in higher cognitive functioning (Fuster, 2004; Goldman-Rakic, 1988; Jung & Haier, 2007).

In sum, higher cognitive function emerges from integration of processing resources distributed across brain areas. At the highest level of the resource integration hierarchy are the association areas interconnected by highest level integration tracts including commissural and association fibers. Association areas in the frontal and parietal areas are of special importance for higher cognitive function. Those areas are connected across hemispheres by the corpus callosum, and within hemispheres by the association fibers including but not limited to the superior longitudinal fasciculus. A simplified diagram of this network is summarized in figure 2 on page 26. The section that follows will extend introduction of the corpus callosum presented on page 24 and discuss both basics on callosal anatomy, evidence of its involvement in inter-hemispheric transfer, and relate corpus callosum to cognition.

Corpus Callosum

The corpus callosum is the largest white matter structure and the largest of the commissures in the human brain. It consists of more than 200 million axon fibers (Aboitiz, Scheibel, Fisher, & Zaidel, 1992; Innocenti, 1986; Tomasch, 1954) interconnecting largely homologous areas in the cerebral hemispheres. In order to demonstrate relative size of the corpus callosum to brain as a whole figure 3 on page 27 depicts sagittal cut through a brain specimen with corpus callosum appearing in the middle.

The corpus callosum is the information superhighway and one of the highest-level integrators of the processing resources in the neocortex. It is the most important venue of cortical inter-hemispheric transfer (Sperry, Gazzaniga, & Bogen, 1969; Zaidel & Iacoboni, 2003) and belongs to a network of brain areas and tracts that show genetically determined associations with intelligence (VIQ/PIQ; Hulshoff Pol et al., 2006). In addition to binding representations of outside world between left and right hemispheres, the corpus callosum has been also implicated in attention control (Banich, Hugdahl, & R. J. Davidson, 2003; Dimond, 1976).

Anatomy of callosal connections. The topographic organization of the corpus callosum mapped in primate studies (Pandya & Seltzer, 1986) grossly corresponds to the topographic distribution of the regions of overlying cortex. Medial and ventral prefrontal fibers cross the midline

Superior Longitudinal Fasciculi in relation to cognitive performance.

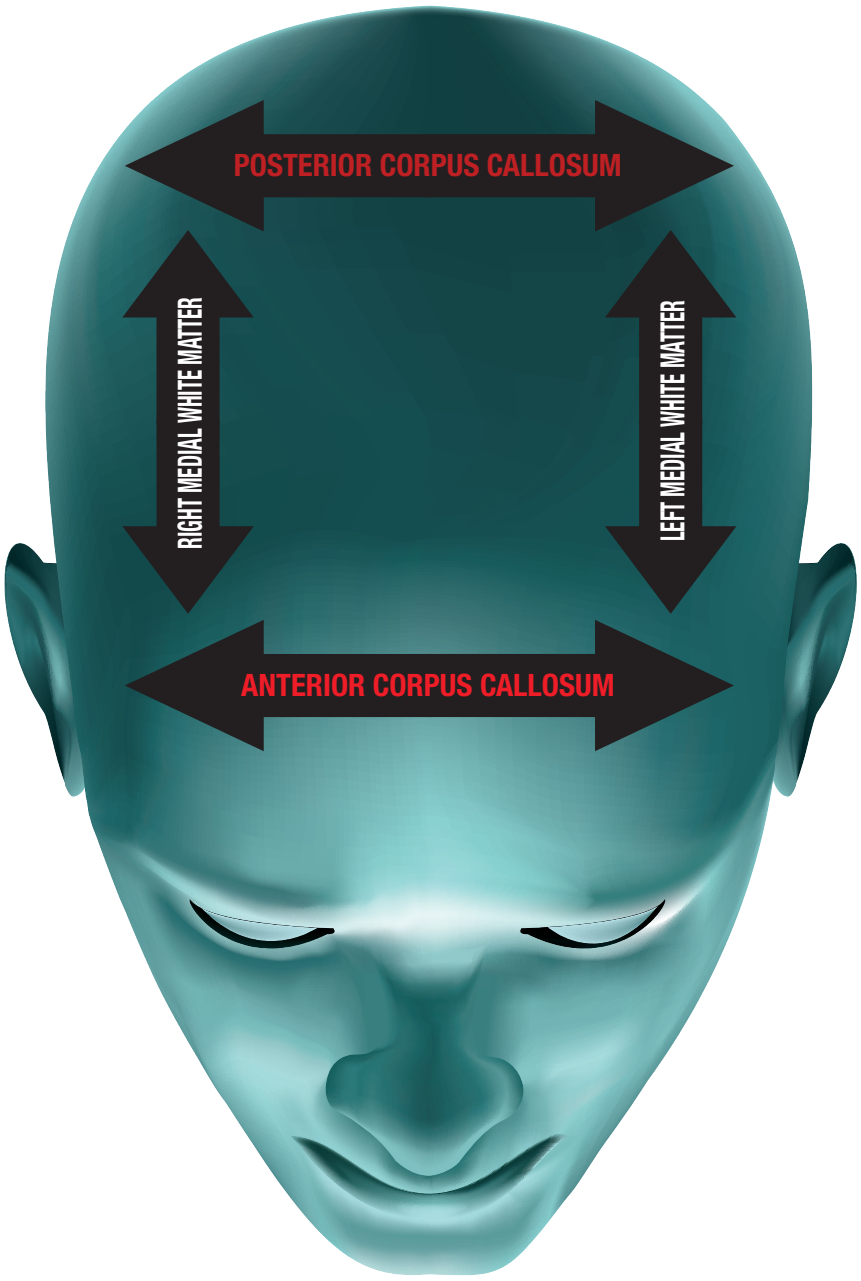

Figure 2: Inter- and Intra-Hemispheric Connectivity. Modified from Vector Open Stock.

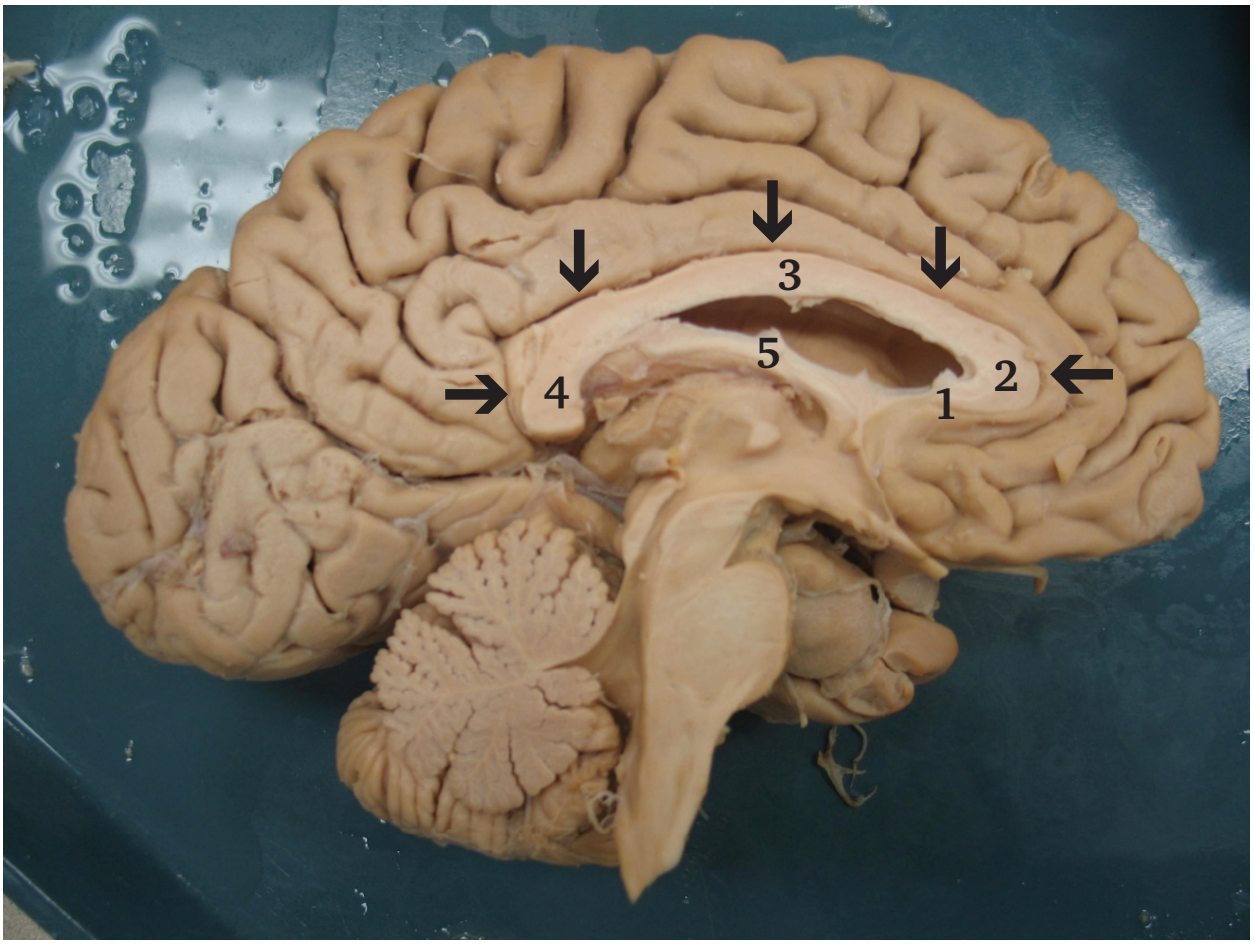

Figure 3: Midsagittal cut through the brain with septum pellucidum removed for clarity. Arrows point to the corpus callosum. 1 – rostrum, 2 – genu, 3 – trunk, 4 – splenium. Brain specimen courtesy of Prof. Steven Sawyer, Department of Rehabilitation Sciences, Texas Tech Health Sciences Center.

in the rostrum and ventral genu of the corpus callosum. Lateral prefrontal fibers cross the midline in the dorsal genu. Premotor fibers cross the midline in the rostral portion of the trunk of the corpus callosum. Sensori-motor fibers cross the midline in the mid-trunk of the corpus callosum. Fibers from the posterior parietal cortex and the middle and caudal superior temporal region cross the midline in the posterior trunk of the corpus callosum (Pandya & Seltzer, 1986). Fibers originating in the superior parietal lobules, the temporo-parieto-occipital region including the planum temporale, and the occipital lobes cross the midline in the splenium (de Lacoste, Kirkpatrick, & E. D. Ross, 1985; Pandya & Seltzer, 1986). Fibers originating from the caudal infero-temporal cortex and caudal parahippocampal gyrus cross the midline at the intersection of the callosal trunk and splenium. Fibers originating from the cingulate gyrus cross the midline in the dorsal portion of the trunk of the corpus callosum. Fibers originating from the insula cross the midline in the ventral portion of the trunk of the corpus callosum (Pandya & Seltzer, 1986).

Gender and the morphology of the corpus callosum. Studies of the gender differences in callosal morphology often show inconsistent pattern of results. While both S. Clarke, Kraftsik, Van der Loos, and Innocenti (1989) and Witelson (1989) found that the corpus callosum on midsagittal slices was larger in males than in females, nine other studies conducted by different research teams did not replicate similar difference (Byne, Bleier, & Houston, 1988, de Lacoste-Utamsing & Holloway, 1982, Demeter, Ringo, & Doty, 1988, Harris, Sundsten, & Fischer-Wright, 1987, Holloway & de Lacoste, 1986, Kertesz, Polk, Howell, & S. E. Black, 1987, O'Kusky et al., 1988, Poltana, Poulpanich, Withyachumnarnkul, Suriyaprapadilok, & Inthisean, 2001, Weber & Weis, 1986; cf. J. Clarke, 1990). In another study de Lacoste-Utamsing and Holloway (1982) reported that due to larger maximal splenial width the posterior fifth of the corpus callosum was more bulbous in females than in males. In their relatively weak sample of 12 subjects the maximal splenial width was bimodally distributed across sexes. Holloway and de Lacoste (1986) subsequently replicated the sex difference in callosal size on a larger sample ($n = 16$) and found that despite the significant difference in maximal splenial width, the difference in splenial area ($p = 0.08$; de Lacoste-Utamsing & Holloway, 1982) did not reach the traditional level of significance. Authors suggested possible presence of sex differences in the splenial shape rather than splenial size. Interestingly, no other research team was able to replicate sex differences in the maximum splenial width (S. Clarke et al., 1989, Demeter et al., 1988, Harris et al., 1987, We-

ber & Weis, 1986, Witelson, 1989; cf. J. Clarke, 1990). Similarly, some research teams reported a larger ratio of splenial area to the total area of the corpus callosum in females (S. Clarke et al., 1989; Reinarz, Coffman, Smoker, & Godersky, 1988) while others did not find this difference (Byne et al., 1988; Oppenheim, B. C. Lee, Nass, & Gazzaniga, 1987; Witelson, 1989). Bishop and Wahlsten (1997) reported that their meta-analysis of 49 studies published between 1980 and 1997 revealed no significant difference in the size or shape of the splenium of the corpus callosum between males and females. Bishop and Wahlsten (1997) concluded that the belief that women have larger splenium of the corpus callosum than men is a myth.

Results of studies discussed above suggest that sex differences in callosal size may exist but either their detection may be contingent on methods employed, or they are pronounced only in a subset of the population. In light of the often inconclusive evidence of gender differences in morphology of the corpus callosum, choosing gender as a covariate may shield results of studies from being attributed to possible gender differences rather than to the impact of independent variables.

Section that follows will connect previous sections discussion anatomy of the corpus callosum with callosal function by presenting results of the neuropsychological studies documenting callosal involvement in inter-hemispheric transfer. Impact of callosal structure on inter-hemispheric transfer and in turn on cognition will be discussed based on an example of individuals with the agenesis of the corpus callosum.

Inter-hemispheric Transfer. Some of the evidence for the role of the corpus callosum in the inter-hemispheric transfer comes from the response time studies performed in the Poffenberger paradigm (Poffenberger, 1913; Zaidel & Iacoboni, 2003). In this paradigm, participants respond to light flashes presented in the left or right visual hemi-field by pressing a key with the right or left hand. When the participant is responding to the light flash in the right visual hemi-field by pressing a key with the right hand, or by responding to the light in the left visual hemi-field by pressing a key with the left hand, no callosal relay is invoked, because both visual input and motor response are localized in the same hemisphere. This type of trial is referred to as uncrossed.

However, if the light flash is presented in the right visual hemi-field and the response is given by the left hand, or the reverse, the light flash is in the left visual hemi-field and the key

press is made by the right hand, visual inputs are received by the hemisphere contralateral to the one that needs to execute a motor response. Therefore, a callosal replay is necessary in order to integrate visual inputs and motor responses. This type of trial is referred to as crossed.

In essence, Poffenberger proposed that by subtracting the reaction time on the uncrossed trials from the reaction time on the crossed trails and dividing it by two, we can get the crossed-uncrossed difference and compute the inter-hemispheric transfer time (for a complete description of this paradigm see (Zaidel & Iacoboni, 2003). In individuals with an intact corpus callosum, the crossed-uncrossed difference is about three to four milliseconds, indicating relay time between the two hemispheres. By contrast, patients with callosal agenesis show a crossed-uncrossed difference of 15 ms, three to five times longer than controls. Split-brain patients who have undergone complete commissurotomy show crossed-uncrossed differences of 30 to 60 milliseconds, two to four times longer than individuals with callosal agenesis, and ten to twenty times longer than controls (J. M. Clarke & Zaidel, 1989; Iacoboni & Zaidel, 1995, 2003; Marzi, Bisiacchi, & Nicoletti, 1991).

Agenesis of the Corpus Callosum.

Agenesis of the corpus callosum (AgCC) is one of the most common brain malformations occurring in approximately 1 to 4000 individuals (L. Paul et al., 2007). While it is a heterogeneous malformation coinciding with a number of developmental disorders and stemming from many etiologies, it also can occur in a near-asymptomatic fashion in individuals with normal intelligence (Brown & L. K. Paul, 2000). While it often co-occurs with colpocephaly (L. Baker & Barkovich, 1992), Probst bundles (Tovar-Moll et al., 2007) and other more subtle anatomical changes that may complicate patterns of observed signs, it gives rise to a naturally occurring split-brain syndrome that may inform our knowledge of inter-hemispheric integration (L. Paul et al., 2007). Discussion of neuropsychological findings associated with the agenesis of the corpus callosum that follows focuses on individuals with normal IQ scores.

General Intelligence. In their review of AgCC cases reported in the literature Chiarello (1980) listed 19 cases with IQ scores above 70, including 14 cases with IQ scores above 80, and 7 cases with IQ scores above 90. Sauerwein and Lassonde (1994) summarized 17 cases reported in the literature between 1980 and 1994 listing 13 cases with IQ scores above 80, and eight cases with IQ scores above 90. Two cases reported by Brown and L. K. Paul (2000) also showed nor-

mal range intelligence with IQ scores of 87 and 108. Altogether, the full-scale IQ scores for individuals with AgCC tend to fall in the lower to middle quadrants of normal spectrum (Chiarello, 1980). Because of the bias of the IQ score towards previous knowledge this finding is most likely indicative of relatively unaffected crystallized intelligence.

While individuals with AgCC may not clearly show diminished performance on measures of general intelligence, more subtle deficits become evident on tests targeting specific cognitive abilities (Sauerwein & Lassonde, 1994). Review of the literature notes common discrepancies between VIQ and PIQ (Sauerwein & Lassonde, 1994; Chiarello, 1980) but no consistent directionality of the differences is evident (L. Paul et al., 2007). However, on specific subtests a trend of differentially impaired results emerges. Brown and L. K. Paul (2000) reported that in their study none of the WISC subtests were abnormal suggested presence of a trend for lower scores on subtests involving fluid intelligence including Arithmetic, Digit Span, and Coding. This report is consistent with Sauerwein et al. that reported lowest performance on Digit Symbol and Arithmetic (cf. Brown & L. K. Paul, 2000) and with Y. Lee, Hung, T. Chang, and C. Huang (2008) that reported digit coding score as the lowest. Altogether, those reports support selection of WISC-III Coding B in this study establishing possible link between absence of the corpus callosum and performance deficits on the digit coding tasks.

Concept Formation. The Category Test (Halstead, 1947) is a category formation task where concepts are formed on a that requires ability (1) to recognize recurring similarities and differences in presented stimuli, (2) to formulate hypotheses about noted similarities and differences, (3) to test formulated hypotheses based on feedback received after each trial, and (4) to modify formulated hypotheses based on received feedback (Reitan & Wolfson, 2004). In Brown and L. K. Paul (2000) performance of acallosal participants fell into the impaired to low average range with joint probability suggesting presence of a deficit in recognition of abstract categories. The Category Test is similar to non-verbal tests such as the Matrix Reasoning and scores on the two tests show a correlation of r = -.58 (Dugbartey et al., 1999). Because abstraction is a crucial part of both tests it can be expected that performance on this test may be associated with performance on tests of non-verbal reasoning such as the WASI Matrix Reasoning, and the Raven's Coloured Progressive Matrices.

Non-Verbal Reasoning. Raven's Coloured Progressive Matrices is a measure of complex reasoning based on non-verbal visual and spatial stimuli (Raven, 1965; Raven, Court, & Raven, 1976). In Brown and L. K. Paul (2000) performance of tested AgCC individuals fell into the impaired to low average range with joint probability suggesting presence of a deficit. However, authors concluded that performance on this task was inconsistent across their two participants. WASI Matrix Reasoning is modeled after Raven's Progressive Matrices test, and although not conclusive, evidence of impaired performance on this test for the AgCC individuals supports proposed hypothesis relating corpus callosum and inter-hemispheric transfer to performance on WASI Matrix Reasoning. Presence of deficits on both The Category Test and Raven's Coloured Progressive Matrices may suggest that abstraction abilities may be impaired in acallosal individuals. This interpretation provides additional support for the important role of the corpus callosum in higher cognitive performance.

Block Design. Jeeves and Rajalakshmi (1964) reported a case of male AgCC individual and with normal intelligence measured by WISC-I (FSIQ = 75). On the block design subtest participant P.H. was slower a group of younger controls with time to completion of 45 minutes vs. 32 minutes for controls (SD = 1.5, N = 19). Y. Lee et al. (2008) reported case of an AgCC individual with Turner's Syndrome and normal intelligence measured by WISC-III (FSIQ = 83). Author indicated that in his case study Block Design was a second lowest score (score of 7) across all subscales preceded only by Digit Coding (score of 3). In contrast, Matrix Reasoning score remained unaffected with score of 12. While firm conclusions cannot be drawn based on only two cases and including Turner's Syndrome diagnosis, it is important to note that reported diminished performance on block test is consistent with proposed hypotheses linking corpus callosum and performance on block design task.

Summary. Altogether, discussed results suggest that most pronounced deficiencies in individuals with AgCC and of normal intelligence levels relate to abstract reasoning, concept formation, and problem solving. Tasks showing most pronounced impairments are predominantly assessing fluid intelligence (G_f) and novel problem solving with relatively unaffected performance on tasks predominantly associated with crystallized intelligence (G_c). Because of this pattern of G_c and G_f impairments it is likely that in case of individuals with the Agenesis of the Corpus Callosum, deficits in performance on cognitive tests is due to callosal transfer between

frontal lobes rather than parietal lobes. Frontal lobes are more closely associated with fluid intelligence than with crystallized intelligence while parietal lobes show the opposite pattern and are more closely associated with crystallized intelligence rather than with fluid intelligence.

Performance of AgCC individuals on cognitive tests is qualified by task complexity/difficulty with no apparent decrements in performance on simple or familiar task, and affected performance on more complex tasks, tasks that require integration of the outcomes of complex cognitive operations, or tasks contingent on rapid processing. This finding informs selection of cognitive tests implemented in this study. Selected cognitive test are intended to be relatively complex and involve bilateral pattern of brain activations. Those tests include CANTAB Spatial Working Memory, WASI Block Design, WASI Matrix Reasoning, and WISC-III Coding B.

Results of neuropsychological studies of individuals with Agenesis of the Corpus Callosum collectively provide support for the callosal integration and recruitment theory for complex but not for simple tasks. Efficient cognitive performance on complex or difficult tasks may be contingent on recruitment of processing resources from the contra-lateral hemisphere through commissural fibers carried by the corpus callosum. While some of the smaller diameter commissural connections, most notably the anterior commissure, may be sufficient for inter-hemispheric integration during simpler tasks, more extensive callosal connections, and greater volume of callosal connections may be necessary for efficient performance on more complex tasks. This section suggests that relatively high degree of complexity is required of a cognitive test in order to index callosal function. Section that follows builds on those findings and will discuss research relating structure of the corpus callosum to cognitive functioning in both normal and clinical populations.

Corpus callosum and higher cognitive function. Studies of the association between callosal morphology and cognitive performance often show contradicting patterns of results. Positive, negative, and zero relationships are reported between different aspects of callosal morphology and measures of cognitive performance. Some studies reported positive relation between callosal morphometry and cognitive abilities (e.g. Luders, Narr, Bilder et al., 2007), while number of other studies reported no significant correlations between corpus callosum and cognitive performance (B. Anderson, 1999; Haier, Jung, Yeo, Head, & Alkire, 2004; Haier, Jung, Yeo, Head, & Alkire, 2005; Nosarti et al., 2004; Tramo et al., 1998). In contrast, another study of Luders and

colleagues conducted on a different age group reported reversed pattern of correlations. Luders, Thompson et al. (2011) reported negative correlations between anterior callosal thickness and both VIQ and FSIQ. This report was corroborated by analogous reports of negative relation between posterior callosal area and FSIQ (e.g. Ganjavi et al., 2011) and for callosal area and VIQ or PIQ (Hutchinson, Mathias, Jacobson et al., 2009). In the paragraphs that follow I will discuss in more detail some of the relations between corpus callosum morphology and cognitive performance. Section will end with discussion of callosal changes in disease states involving altered cognition.

In one study employing mesh-based method of assessing differences in callosal shape, a significant positive correlations between callosal thickness and full-scale IQ was reported (Luders, Narr, Bilder et al., 2007). This correlation was most pronounced at the boundary of the posterior body and the isthmus and extended anteriorly throughout most of the posterior body, and posteriorly throughout anterior aspect of splenium. Significant correlations were also present in a small portion of the anterior corpus callosum at the intersection of anterior third and anterior body. Because significant correlations between callosal thickness and FSIQ were localized to the posterior region, elsewhere Luders, Narr, Thompson, and Toga (2009) conclude that interhemispheric communication via posterior parietal and occipital fibers interconnecting association areas is "fundamental in determining individual differences in intelligence" (Luders, Narr, Thompson et al., 2009, p. 161).

In contrast to findings of Luders, Narr, Bilder et al. (2007), studies that employed more traditional two-dimensional voxel-based methods reported no significant correlations between higher cognitive abilities and the corpus callosum (B. Anderson, 1999; Haier, Jung, Yeo, Head, & Alkire, 2004; Haier, Jung, Yeo, Head, & Alkire, 2005; Nosarti et al., 2004; Tramo et al., 1998) or report negative relation between callosal area and verbal or performance intelligence quotients (Hutchinson, Mathias, Jacobson et al., 2009). Negative correlations were also present in a recent study conducted on a sample children and adolescents. Ganjavi et al. (2011) reported a significant negative correlation between total CC midsagittal area and IQ ($r = –0.147$; $p = 0.040$) controlled for total brain volume and age. In their analysis of the subsegments authors found no correlation between area of segments within anterior corpus callosum and WAIS FSIQ, PIQ, and VIQ for males, females, and the full sample. However, when sample was divided into two age groups

split at 12 years, significant negative correlations between 3 segments within corpus callosum and FSIQ and PIQ emerged. This finding was further qualified by an interaction with gender with correlations significant for males under the age of 12 but not for the females. In their combined sample of males and females Ganjavi et al. (2011) reported a single segment in the mid-posterior and posterior callosal region where the correlation between the area and FSIQ approached significance ($r = –0.196$; $q = 0.06$; $p = 0.007$) at $FDR = .10$. This correlation, admittedly small at least by J. Cohen (1988) classification, was further qualified by gender becoming moderate and significant for males ($r = –0.348$; $q = 0.011$; $p = 0.001$) but not females. When considered separately for each age group, negative correlation in this posterior segment was significant for participants below the age of 12 at $FDR = .05$. Ganjavi et al. (2011) argues that the general negative correlation between the area of the midsagittal corpus callosum and FSIQ was driven by this posterior segment. Overall, results of this study suggest that the negative association between callosal thickness and FSIQ is present in pre-pubescent males and only in the posterior portion of the corpus callosum.

Another study (Luders, Thompson et al., 2011) conducted on the same dataset as Ganjavi et al. (2011) and investigating link between corpus callosum morphology and IQ reported negative correlations between callosal thickness and WASI FSIQ and VIQ that were confined to the splenium of the corpus callosum. Reported correlations were small, in the -0.01 range, but survived correction at $FDR = .0043$ for FSIQ, and $FDR = 0.0033$ for VIQ. Remainder of correlations presented in Luders, Thompson et al. (2011) did not achieve significance after correction for multiple tests.

Altogether, reported studies show inconsistent pattern of results with regard to presence of relation between corpus callosum and cognitive abilities. Magnitude of correlations presented in both Luders, Thompson et al. (2011) and Ganjavi et al. (2011) collectively suggest that variations in callosal morphology associated with cognitive performance are small and may be difficult to detect and may be qualified by age and gender. In the larger context of literature covering this subject, when correlations are detected their directions are often inconsistent even within studies conducted by the same authors and employing similar methodologies (e.g. Luders, Narr, Bilder et al., 2007; Luders, Thompson et al., 2011). Presented results suggest that correlations are of small to moderate magnitude and may diminish depending on additional factors such as age, gender,

and method employed to quantify callosal size.

Structural changes in the corpus callosum have been documented in several disorders affecting cognitive functioning, including autism (Egaas, Courchesne, & Saitoh, 1995), mild cognitive impairment (Thomann, Wustenberg, Pantel, Essig, & Schroder, 2006; P. J. Wang et al., 2006), Alzheimer's disease (Janowsky, Kaye, & Carper, 1996; Teipel et al., 2002; P. J. Wang et al., 2006; Weis, Jellinger, & Wenger, 1991), multiple sclerosis (Pelletier et al., 2001), traumatic brain injury (Mathias et al., 2004), attention deficit hyperactivity disorder (Hutchinson, Mathias, & Banich, 2008; Valera, Faraone, K. E. Murray, & Seidman, 2007), schizophrenia, and psychosis (Downhill et al., 2000; Kubicki et al., 2008; Shenton, Dickey, Frumin, & McCarley, 2001; Walterfang et al., 2008). Structure of the corpus callosum correlated with cognitive outcomes in hydrocephalus (Fletcher et al., 1992), epilepsy (Atkinson, Abou-Khalil, Charles, & Welch, 1996; Strauss, Wada, & Hunter, 1994), mental retardation (Spencer et al., 2005), sickle cell disease (Schatz & Buzan, 2006), lacunar infarcts (Yamauchi, Fukuyama, Ogawa, Ouchi, & Kimura, 1994), anterior callosal tumors (Osawa, Maeshima, Kubo, & Itakura, 2006), and pre-term birth (Allin et al., 2007; Caldu et al., 2006; Narberhaus et al., 2007; B. S. Peterson, Vohr et al., 2000). Changes in the integrity of callosal fibers as measured by the fractional anisotropy have been documented in Alzheimer's disease (Rose et al., 2000).

Inconsistent pattern of results concerning gender differences in the morphology of the corpus callosum, and the relation between callosal structure and cognitive abilities may collectively suggest that additional factors modify results of morphometric studies. Several previously discussed possibilities exist with most viable one concerning sample selection bias and differences in methodology between discussed studies. It is important to note that none of the discussed studies disproved the notion that integration of distributed processing resources is important for cognitive performance, and that corpus callosum is involved in this process. To the contrary, discussed studies show that there are differences in callosal structure that are related to cognitive performance but may not be universally present, or their detection may depend on methodological factors.

Present study proposes that structural differences in the corpus callosum reflecting additional myelination, better myelination, or larger number of commissural fibers, may translate onto a more efficient inter-hemispheric transfer of information, which in turn will facilitate in-

tegration and coordination of distributed processing resources resulting in enhanced cognitive abilities (Luders, Narr, Bilder et al., 2007; Luders, Narr, Thompson et al., 2009). Consequently, differences in both the micro-structure and the macro-structure of the corpus callosum should be related to cognitive performance. More specifically, the partitions of the corpus callosum carrying projections interconnecting the homologous frontal (region of the genu) and parietal (region of the splenium and isthmus) association areas in each hemisphere may show variation across the spectrum of cognitive measures adopted in this study (CANTAB Spatial Working Memory, WASI Block Design, WASI Matrix Reasoning, and WISC-III Coding B).

Sections that follow introduce concepts essential to this study and in preparation for presenting hypotheses. Essential concepts include intelligence, cognitive abilities, and processing speed. In order to justify selection of the regions of interest the relation between cognitive abilities and brain lobes is discussed. Finally, the hypotheses relating to the role of the corpus callosum and the comprehensive regression model are presented.

Cognitive Abilities and Intelligence

Within the field of intelligence and cognitive abilities research two approaches can be distinguished: classic unitary intelligence approach (Spearman, 1927; Wechsler, 1939) and the multiple intelligences approach (Gardner, 1999; Sternberg, 1985). Classic approach to intelligence postulates that there is a single unitary factor underlying most of cognitive abilities and that the role of intelligence testing is to assess this factor. This idea was first mastered by Spearman (1923, 1927), who discovered that second-order factor analyses performed on measures of cognitive ability yield a single factor solution: a g-factor or general intelligence. In Spearman's view, the g-factor is a general problem-solving skill at the apex of the hierarchy of cognitive abilities. G-factor underwrites all cognitive abilities and accounts for a person's performance on all cognitive tests (Newman & Just, 2005). Spearman's idea was further extended by dividing the g-factor into a fluid intelligence G_f and crystallized intelligence G_c (Cattell, 1971). G_c results from accumulation of factual knowledge over the lifespan and thus increases with time (Toga & Thompson, 2005). In contrast, G_f is the analytical intelligence, information processing speed, and working memory (Prabhakaran, Rypma, & Gabrieli, 2001) believed to be independent of education (Toga & Thompson, 2005). G_f has a significant genetic component and reflects state of underlying biological substrate. It peaks in early adulthood and shows slow decline during rest

of the lifespan. In contrast, G_c increases with accumulation of knowledge. Consequently, during most of the lifespan G_c either increases or remains stable (Dixon & Baltes, 1986; Horn & Cattell, 1967; J.-J. Wang & Kaufman, 1993). G_f correlates with frontal gray matter volumes (Thompson, Cannon et al., 2001) and with brain activation during cognitively demanding tasks (J. R. Gray, Chabris, & Braver, 2003).

More recent approaches to intelligence postulate that intelligence measured by tests assessing the g-factor, in particular G_c, are incomplete. Theories such as the Triarchic Theory of Intelligence (Sternberg, 1985) and the Theory of Multiple Intelligences (Gardner, 1999) emphasize that intelligence measurement should go beyond cognitive tasks and should assess a wider range of abilities. This dissertation instead on focusing on all encompassing concepts such as intelligence focuses on specific cognitive processes or abilities underwritten by neurological networks. In addition to specific cognitive abilities, this dissertation will also examine contributions of white matter to overall processing speed. Processing speed links behavioral measures of cognitive ability with properties of white matter and with the concept of bandwidth.

Processing Speed

Processing speed is one of the most fundamental properties that all cognitive processes rely on (Fry & Hale, 1996, 2000) and should be considered as a fundamental building block of the cognitive architecture (Kail & Salthouse, 1994) next to resources such as attention, working memory, or inhibition (Turken et al., 2008). There is a modest yet significant relation between g and information processing speed (Vernon, 1987, 1990; A. R. Jensen, 1987). Two explanations for the modest magnitude of this correlation can be presented. First, information processing variability can be partitioned into central cognitive processing measured by speed of response (decision), and peripheral non-cognitive variance measured by speed of movement. Carroll (1991) found that while response time loaded on g-factor, movement time loaded on a second-order factor orthogonal to g (cf. Kranzler, 1997). Second, correlation between processing speed and g may be moderated by task complexity. In general, correlation between cognitive test and g-factor is a monotonic function of task complexity with tasks requiring higher complexity of information processing also having higher loadings on g-factor (A. Jensen, 1992; Vernon, 1993). Since Digit Coding task is only moderately complex it also has only modest loading on g-factor (cf. Kranzler, 1997). Irrespective, processing speed has been reported to vary across mental ability on both low

(e.g. Baumeister & Kellas, 1968) and high end of the spectrum (A. R. Jensen, 1990; A. R. Jensen, S. J. Cohn, & C. M. G. Cohn, 1989; S. J. Cohn, Carlson, & A. R. Jensen, 1985; Kranzler, Whang, & A. R. Jensen, 1994). Based on hierarchical factor analysis of a large battery of psychometric tests Carroll (1991) concluded that speed and efficiency of information processing is an important aspect of g (see also Kranzler, 1997). Faster processing speed is often associated with greater working memory capacity (Fry & Hale, 1996, 2000) and in turn with enhanced fluid intelligence (Fry & Hale, 1996, 2000).

Processing speed is associated with performance on a variety of cognitive tasks (Kail & Salthouse, 1994; Kail, 2007; Salthouse, 2005), developmental changes in cognition in children (Kail, 1991, 2007) and older adults (Salthouse, 1996) and with changes in white matter associated with aging (Gunning-Dixon & Raz, 2000; Turken et al., 2008). Processing speed is also associated with cognitive performance in multiple sclerosis (Forn, Belenguer, Parcet-Ibars, & Avila, 2008; Kail, 1998; Rao, St Aubin-Faubert, & Leo, 1989) as well as pathological changes in white matter in multiple sclerosis (Sperling et al., 2001; Swirsky-Sacchetti et al., 1992), traumatic brain injury (Verger et al., 2001) and white matter volume in temporal lobe epilepsy (Dow, Seidenberg, & Hermann, 2004). Performance on test of processing speed differs by gender. Females tend to perform faster on paper-and-pencil tests of processing speed including the Digit Symbol subtest in the Wechsler tests (Camarata & Woodcock, 2006; Majeres, 2007; Sheppard & Vernon, 2008; Wechsler, 1997; Roivainen, 2011). Similarly, analysis of the standardization samples of Woodcock–Johnson III (n = 1987), Woodcock–Johnson Revised (n = 4253), and Woodcock–Johnson 77 (n = 4225) revealed consistent across lifespan and across samples advantage of the processing speed factor for females (Camarata & Woodcock, 2006; Roivainen, 2011). Based on the analysis of the WAIS and WAIS-R standardization samples (n = 1880) Feingold (1992) reported average gender difference in performance on the Digit–Symbol subtest of d = .34. Majeres (2007) explained this difference in terms of phonological coding (e.g. matching digits) speed advantage and demonstrated that gender differences diminished for tasks involving matching geometrical shapes rather than numbers (cf. Roivainen, 2011).

Correlation between processing speed and g-factor is moderated by task complexity. Increase in task complexity, or increase in information load, is accompanied by increased advantage of fast processing speed on cognitive performance. In other words, processing speed mat-

ters more on complex, difficult, or taxing working memory tasks. This finding parallels results of neuropsychological testing conducted on individuals with the agenesis of the corpus callosum (G. E. Larson & Saccuzzo, 1989; G. E. Larson, Merritt, & S. E. Williams, 1988). AgCC individuals show unaffected performance across domains on relatively simple, or familiar tasks. However, the same individuals also show performance deficits complex or novel tasks. Considered together, those findings demonstrate a link between processing speed, inter-hemispheric transfer, and task complexity. Sections that follow will discuss functions of the frontal and parietal lobes as well as link between those lobes and g-factor. This section will close with discussion of fronto-parietal integration as an essential factor in efficient cognitive performance.

G-factor and Brain Lobes

As the field of neuroscience moves beyond global correlates of intellect, the focus of research shifts from global indices such as total brain volume to increasingly specific markers. In the brain, the volume of both gray and white matters positively correlate with the g-factor (Posthuma et al., 2002), as do the estimates of the total brain volume (McDaniel, 2005; Rushton & Ankney, 2007) and the volumes of the separate brain lobes (Posthuma et al., 2002).

Frontal Lobes. The correlation between g-factor and gray matter was reported to be the strongest in the frontal lobes (Thompson, Cannon et al., 2001; see also Haier, Jung, Yeo, Head, & Alkire, 2004) and frontal gray matter accounted for a significant amount of variance in the g-factor even after controlling for the total brain volume (Thompson, Cannon et al., 2001). This finding is consistent with brain-lesion evidence pointing to the involvement of the frontal lobes, and consequently the g-factor, in abstract reasoning (J. Duncan, Emslie et al., 1996; Piercy, 1964). The importance of the frontal lobes in cognitive abilities stems from their role in integrating crucial relations (Waltz et al., 1999), as well as attention and response selection. These functions are believed to be particularly important for solving novel problems and involve predominantly G_f. Consequently, frontal lesions affect G_f (J. Duncan, Burgess, & Emslie, 1995; J. Duncan, Emslie et al., 1996), leaving $G_c$largely intact (J. R. Gray & Thompson, 2004). Frontal lesions do not affect performance on tests of intelligence that rely on previous knowledge and skill such as the Wechsler Adult Intelligence Scale (WAIS; J. R. Gray & Thompson, 2004). G_f and frontal lobe function are best assessed by nonverbal tests such as Raven's Advanced Progressive Matrices (J. Raven, J. C. Raven, & Court, 1998) or by measures of working memory and executive function.

Parietal Lobes. Parietal lobes are the hotspot of information integration from occipital, temporal, and parietal regions. Parietal lobes have been implicated in sensory integration of visual, auditory, vestibular, cutaneous, and proprioceptive information (Strub & F. W. Black, 1977), cross modal association and cross modal transfer of information, visuo-motor coordination, visuo-spatial imagery, retrieval from episodic memory, first-person perspective taking, experience of agency (Cavanna & Trimble, 2006), coding position of body-parts in a body-referenced coordinate system (Duffy & Burchfiel, 1971, Lacquaniti, Guigon, Bianchi, Ferraina, & Caminiti, 1995, Mountcastle, Lynch, Georgopoulos, Sakata, & Acuna, 1975, Sakata, Takaoka, Kawarasaki, & Shibutani, 1973; cf. Makris et al., 2005). In the dominant hemisphere parietal lobe is involved in comprehension of written language (Geschwind, 1965a, 1965b) as well as semantic representation and perception of meaning.

Function of parietal lobes is more closely related to G_c than to G_f. Brain lesions involving parietal lobes often affect classic measures of IQ involving G_c (J. R. Gray & Thompson, 2004) including the Wechsler Adult Intelligence Scale. This finding is consistent with the notion that G_c is associated with prior knowledge and with the involvement of the parietal lobes in memory. K. H. Lee et al. (2006) after comparing patterns of activation on Raven's Advanced Progressive Matrices between individuals scoring high and low on g-factor concluded that superior general intelligence is likely to emerge from fronto-parietal integration driven by strong posterior parietal activation.

Fronto-Parietal Network. Activations in the frontal and parietal regions have been reported during intelligence tests (J. R. Gray, Chabris et al., 2003), and the magnitude of those activations in both frontal and parietal lobes correlates with the g-factor (J. Duncan, R. J. Seitz et al., 2000; Prabhakaran, J. A. L. Smith, Desmond, Glover, & Gabrieli, 1997; Prabhakaran, Rypma et al., 2001). Substantial overlap in frontal and parietal activations exists during intelligence tests and working memory tasks (Cabeza & Nyberg, 2000; Ruff, Knauff, Fangmeier, & Spreer, 2003; E. E. Smith & Jonides, 1999), suggesting involvement of both frontal and parietal regions in higher cognitive faculties. Integration of function between parietal lobes involved in cross-modal integration and visuo-spatial/visuo-motor processes and the frontal lobes involved in working memory, attention, response selection, inhibition is crucial for cognitive functioning. Fronto-parietal integration has been suggested to be an important component of higher cognitive func-

tions (Fuster, 2004; Goldman-Rakic, 1988; Jung & Haier, 2007; K. H. Lee et al., 2006).

In sum, there is a body of evidence from both functional and lesion studies linking frontal and parietal lobes with higher cognitive functions. Task employed in this study such as CANTAB Spatial Working Memory (SWM), WASI Block Design, WASI Matrix Reasoning all invoke activations in those regions. CANTAB SWM, a spatial working memory task with significant executive decision component, activates bilaterally the ventro-lateral and dorso-lateral prefrontal cortical areas (A. M. Owen, Evans, & Petrides, 1996). WASI Block Design is associated bilateral frontal and parietal activations (Fangmeier, Knauff, Ruff, & Sloutsky, 2006). Parietal activations are likely to reflect the spatial reasoning process as this area is activated during reasoning but not during working memory tasks (Jung & Haier, 2007). WASI Matrix Reasoning and its analogs, non-verbal visuo-spatial and abstract reasoning tasks, are linked among other regions to the frontal and parietal regions by a large body of PET and fMRI studies summarized in Table 5 on page 61. WISC-III Coding B, a task indexing processing speed, is linked to general white matter properties. Processing speed is believed to be fundamental aspect of cognitive architecture and a significant aspect of psychometric g-factor underlying variety of cognitive processes. Altogether, there is evidence linking frontal and parietal lobes with both general intellectual functioning, and with specific cognitive tasks employed in this study and assessing specific cognitive abilities.

Next section will introduce set of hypotheses relating anterior and posterior corpus callosum to performance on cognitive tests involving frontal and/or parietal lobes. Corpus callosum is proposed to integrate cognitive processes distributed across brain hemispheres. Hypotheses regarding the role of the white matter in cognitive performance will be summarized by a regression model of resource integration including intra-hemispheric frontal-parietal integration through lobar medial white matter and inter-hemispheric connectivity through corpus callosum. This model attempt to describe unique contributions of the frontal and parietal anatomies and of white and gray matter to variance on examined cognitive tests.

Corpus Callosum Hypotheses

This study investigates two hypotheses about the role of the corpus callosum in cognitive functioning across a selected subset of cognitive tasks. First hypothesis addresses the role of the region of the genu of the corpus callosum in the performance on cognitive tasks involv-

ing inter-hemispheric transfer between the frontal lobes. Second hypothesis addresses the role of the region of the splenium and isthmus of the corpus callosum in the performance on cognitive tasks involving inter-hemispheric transfer between posterior regions including parietal lobes. Tasks invoking inter-hemispheric transfer include CANTAB Spatial Working Memory previously shown to bilaterally engage dorsal and ventral prefrontal cortices, WASI Block Design previously shown to bilaterally engage frontal, parietal, cingulate regions, and the WASI Matrix Reasoning previously shown to bilaterally engage the frontal, parietal, temporal, cingulate, occipital cortices. Neural correlates of those tasks and their likely requirement of inter-hemispheric callosal transfer is discussed in detail in section "Assessment of Cognitive Function: WASI, CANTAB, and WISC-III Coding B" on page 51. WISC-III Coding B is included as measures of global processing speed and behavioral correlates of white matter structure.

Hypothesis 1. The volume of the anterior fifth of the corpus callosum will be larger for individuals scoring higher on cognitive tasks/tests invoking inter-hemispheric transfer between frontal brain areas (CANTAB Spatial Working Memory, WASI Block Design, WASI Matrix Reasoning, and WISC-III Coding B).

Hypothesis 2. The volume of the posterior two fifths of the corpus callosum will be larger for individuals scoring higher on cognitive tasks/tests invoking inter- hemispheric transfer between posterior brain areas (WASI Block Design, WASI Matrix Reasoning, WISC-III Coding B).

Comprehensive Regression Model

This study focuses on the role of the white matter in cognitive performance while acknowledging the elementary role of gray matter in cognitive performance. White matter is the agent of conduction of information and the source of integration of computational resources distributed across brain areas and brain hemispheres. Grey matter is a sheer computational power, providing inputs, outputs, and summation of axon potentials transported within the white matter. Without cell bodies, no form of information processing in the nervous system would exist. While cell bodies are agents of elementary information processing, more complex information processing emerges from an intricate network of differentially weighted connections formed amongst them.

The proposed model is divided into three stages. The first stage aims at controlling the im-

pact of potentially confounding variables. The second stage second aims at evaluating the fundamental effects of gray matter on intellectual ability. The third stage aims at evaluating the unique effects of white matter on intellectual ability. Paragraphs that follow will begin by discussing each of the nuisance covariates chosen in this study and subsequently will discuss each of the stages of the proposed comprehensive regression model.

eTIV. In the present study estimate of brain size is covaried in order to control for a potentially confounding relation between brain size and cognitive performance. There are both theoretical and empirical reasons for correcting for brain size. The most fundamental theoretical reason stems from a moderate correlation between brain size and intelligence (Luders, Narr, Thompson et al., 2009; McDaniel, 2005; Rushton & Ankney, 2007; Toga & Thompson, 2005). People with larger crania also tend to have higher IQs. Correcting for brain size safeguards conclusions from an alternative explanation that any revealed differences between an independent variable and IQ are due to head size. For example, if a study of children of varying ages reports that children with larger corpora callosa also have higher IQ scores but also that children with larger brain sizes also have higher IQ scores the first finding is not particularly insightful in light of the second finding. In contrast, if it was discovered that there is a relation between size of the corpus callosum and intelligence that goes beyond the relation between brain size and IQ, this would certainly deserve further investigation. In that case, the conclusion would be that individuals with larger than expected corpora callosa also have larger IQ scores thus linking relative size of the corpus callosum to IQ. While correcting for eTIV is important in this study as volume of the corpus callosum and forebrain are geometrically related, correction for eTIV may not be recommended for metrics other than volume such as cortical thickness as its relation to brain size is much less pronounced. Empirical reasons for correcting for brain volume are linked to the efficiency of the design. In their study aiming at detecting optimal combination of covariates in Voxel Based Morphometry (VBM) studies G. S. Pell et al. (2008) tested inferential power of analyses of two groups, a control group, and a group with known volume loss due to pathological process. G. S. Pell et al. (2008) concluded that a combination of covariates optimal for detection of known volume difference included only eTIV for gray matter studies, and age, gender, and eTIV for white matter studies.

Linear and quadratic age. In the present study chronological age is entered as a covariate because dependent cognitive measures are in a raw form with no correction for age. Because cognitive abilities develop during childhood and adolescence this advancement needs to be accounted for in the design either in a form of age normalized scores or age as additional variable. Previously discussed study by Liston et al. (2006) provides additional support for accounting for age in studies of white matter. In their study Liston et al. reported that both micro-structure of the fronto-striatal tract, and efficiency of cognitive control changed with age. Furthermore, two recent analyses of the relationship between the corpus callosum and IQ conducted on the same sample of participants reported age as a significant factor (Ganjavi et al., 2011; Luders, Thompson et al., 2011).

Because the indices of brain maturation may not be linearly related to cognitive performance both age and its quadratic term (E. R. Sowell, B. S. Peterson et al., 2003) were initially included as covariates (Naftali Raz, personal communication, November 9, 2009) in all planned analyses. Karama et al. (Karama et al., 2009) reported that in their analyses, in addition to the linear model, also quadratic (E. R. Sowell, B. S. Peterson et al., 2003) models were tested. Quadratic model did not provide significant improvement in fit over the linear solution. White matter in general and corpus callosum in particular show linear pattern of development for the age groups targeted in this study (J. Giedd, J. Blumenthal, Jeffries, Castellanos et al., 1999; McLaughlin et al., 2007; Toga, Thompson, & E. R. Sowell, 2006). In contrast, gray matter shows non-linear pattern of development (J. Giedd, J. Blumenthal, Jeffries, Castellanos et al., 1999; Shaw, D. Greenstein et al., 2006; Shaw, Kabani et al., 2008; E. R. Sowell, B. S. Peterson et al., 2003).

Gender and handedness. Gender and handedness are associated with variability in brain organization. Sex differences in brain organization stem from sex differences in brain lateralization, and from regional sexual dimorphisms. Brain asymmetry differs between males and females with brains of the former being on average more asymmetrical than brains of the latter (B. A. Shaywitz et al., 1995; Toga & Thompson, 2003). Structural asymmetries among genders exist in the plana temporale and parietale, with greater asymmetry in males than females (Jancke, Schlaug, Y. Huang, & Steinmetz, 1994; Toga & Thompson, 2003). Planum parietale tends to be on average larger in the right hemisphere than in the left hemisphere for males and females alike. However, in right-handers, asymmetry between left and right planum parietale is larger for males,

while for left-handers this asymmetry is larger for females (Jancke, Schlaug et al., 1994).

Sexual dimorphisms are particularly well pronounced in the cerebral cortex where females have larger ratio of cortical volume to cerebrum size than males. This gender dimorphism is accentuated in frontal and medial paralimbic cortices. Males in contrast, have larger ratio of volumes to cerebrum size in fronto-medial cortices, the amygdala, and the hypothalamus (J. M. Goldstein et al., 2001). J. M. Goldstein et al. (2001) reported that greater sexual dimorphisms are present in brain areas that in animal studies were shown to have more sex steroid receptors during critical periods of brain development. Males and females also differ with regard to the rate of brain development. For example females tend to peak on morphometric measures of total brain volume, as well as on volume of gray and white matter (J. Giedd, J. Blumenthal, Jeffries, Castellanos et al., 1999; J. Giedd, J. Blumenthal, Jeffries, Rajapakse et al., 1999; Jernigan & Tallal, 1990; Jernigan, D. Trauner, Hesselink, & Tallal, 1991; Giedd, 2008; R. K. Lenroot et al., 2007; Gogtay & Thompson, 2010). Sex differences in brain anatomy between males and females are also related to intelligence. Haier, Jung, Yeo, Head, and Alkire (2005) reported that comparison of brains of IQ matched males and females revealed that female brains tend to have more white matter and fewer gray matter areas related to intelligence. While in males strongest correlations with IQ are present in both frontal and parietal lobes, in females strongest correlations are present in the fronto-polar frontal cortex and in the Broca's area. Haier, Jung, Yeo, Head, and Alkire (2005) interpreted those results as indicating that different intelligence brain networks may operate in males than in females.

In addition, although often inconsistent, there have been reports of gender differences in the morphology of the corpus callosum and gender was one of the significant factors of recent analyses of the relation between callosal mid-sagittal area and IQ (Ganjavi et al., 2011). Gender is also a factor in processing speed with consistent reports of females showing faster performance of processing speed tests across age groups and across tested samples (Camarata & Woodcock, 2006; Majeres, 2007; Sheppard & Vernon, 2008; Wechsler, 1997; Roivainen, 2011).

Differences in brain organization associated with handedness stem predominantly from differences in lateralization of function and cerebral dominance. In chimpanzees differences in patterns of gyrification between hemispheres relate to functional measures of laterality (Hopkins, Cantalupo, & Taglialatela, 2007). Virtually all right-handers are left hemisphere dominant for

language as compared to only half of the left-handers. An estimated quarter of the left-handers process language in both hemispheres.

Discussed evidence for sex differences between males and females ranges from gross brain volumes, volumes of white and gray matter, to possible differences in callosal morphology. Females outperform males on coding task selected as a measure of processing speed in this study. In addition, some of the differences in brain organization between males and females are directly related to general cognitive abilities. Collectively, those studies provide support for accounting for sex in proposed statistical models.

First stage. In the first step of the comprehensive regression model, effects of the brain size in the form of estimated Total Intracranial Volume (eTIV; Buckner et al., 2004), chronological age, quadratic term of chronological age, as well as dummy coded gender and handedness are entered as covariates[2].

Second stage. In the second stage of the comprehensive regression model, estimates of gray matter volume are entered for the frontal and parietal lobes. Inclusion of gray matter removed fundamental effect of cell bodies on information processing. Gray matter volume for frontal lobe is defined as a sum of the volumes of the following gyri: Superior Frontal, Rostral and Caudal Middle Frontal, Pars Opercularis, Pars Triangularis, and Pars Orbitalis, Lateral and Medial Orbito-frontal, Precentral, Paracentral, Frontal Pole. Gray matter volume for parietal lobe is defined as a sum of the volumes of the following gyri: Superior and Inferior Parietal, Supra-marginal, Postcentral, and Precuneus. Volumes of the left and right frontal gray matter are summed into a single index of frontal gray matter and volumes of the left and right parietal gray matter are summed into a single index of parietal gray matter.

Third stage. In the third stage of the comprehensive regression model, estimates of white matter volume are entered for the frontal lobes, parietal lobes, and the corresponding callosal partitions. White matter volume for frontal lobe is defined as a sum of the white matter volumes corresponding to the following overlying cortical gyri: Superior Frontal, Rostral and Caudal Middle Frontal, Pars Opercularis, Pars Triangularis, and Pars Orbitalis, Lateral and Medial Orbito-frontal, Precentral, Paracentral, Frontal Pole, and is analogous to operational definition of gray matter for frontal lobes. White matter volume for parietal lobe is defined as a sum of the white matter

[2]Only significant covariates are retained in final analyses

$$
\begin{aligned}
Stage\ 1: \quad Y &= \beta_{11} \times Cov_1 + \cdots + \beta_{1n} \times Cov_n \\
Stage\ 2: \quad Y &= \beta_{21} \times F_{Gv} + \beta_{22} \times P_{Gv} \\
Stage\ 3: \quad Y &= \beta_{31} \times F_{Wv} + \beta_{32} \times P_{Wv} + \beta_{33} \times F_{CCv} + \beta_{34} \times P_{CCv}
\end{aligned}
$$

Figure 4: Algebraic representation of stages of the Comprehensive Regression Model. $\beta_{s1\ldots n}$ denote beta weights for predictors *1* through *n* in stage *s*. In *Stage 1* $Cov_{1\ldots n}$ denote significant covariates *1* through *n*. In *Stages 2 and 3* capital letters denote lobes F for frontal and P for parietal and the subscript denotes target substrate and measure. In the subscript capital letters denote substrate $_W$ for white matter, $_G$ for gray matter, and $_{CC}$ for corpus callosum. Lower case $_v$ denotes measure of volume. Intercept is implicit.

volumes corresponding to the following overlying cortical gyri: Superior and Inferior Parietal, Supra-marginal, Postcentral, Precuneus, and is analogous to operational definition of gray matter for frontal lobes. Volumes of the left and right frontal white matter are summed into a single index of frontal white matter and volumes of the left and right parietal white matter are summed into a single index of parietal white matter.

By inclusion of the anterior and posterior portions of the corpus callosum this step models the inter-hemispheric integration of distributed homologous frontal and parietal resources. By inclusion of the frontal and parietal white matter volumes this step models intra-hemispheric integration of distributed frontal and parietal resources. This model is summarized in figure 4 on page 48.Pattern of beta significances predicted *a priori* is presented in table 1 on page 49. Predictions are derived from patterns of involvement of brain regions differentially engaged by each measure.

Summary of the study and discussion of new contributions. While the field of neuroscience largely moved beyond focusing on global indices of anatomy such as brain size and began to investigate more and more detailed anatomical hypotheses, the dependent measures of cognitive ability selected for brain-behavior studies often remain very general. One of the contributions and strengths of this research is use of focused cognitive measures paired with lobe-level anatomical indices. This study correlates well defined sets of cognitive tests with theory-driven anatomical hypotheses. Consequently, this project will provide new data on the relation between

Table 1

Predicted pattern of beta weights based on previous data on localization of function for selected dependent measures. Capital letters denote lobes F for frontal and P for parietal and the subscript denotes target substrate and measure. In the subscript capital letters denote substrate W for white matter, G for gray matter, and CC for corpus callosum. Lower case v denotes measure of volume. + denotes a positive beta value significant at alpha = .05, n.s. denotes a beta that did not reach traditional level of significance with alpha = .05

	CANTAB Spatial Working Memory	WASI Block Design	WASI Matrix Reasoning	WISC-III (Coding B)
FWv	+	+	+	+
FGv	+	+	+	+
PWv	*n.s.*	+	+	+
PGv	*n.s.*	+	+	+
FCCv	+	+	+	+
PCCv	*n.s.*	+	+	+

selected subtest of CANTAB and WASI and the general anatomy of the frontal and parietal lobes and the anterior and posterior corpus callosum. In this study both behavioral and anatomical measures were selected on the basis of an *a priori* theoretical model, and are informed by the evidence present in the literature.

This study also represents at least three developments over previous studies. First, this project does not focus on a single region but on a network on interconnected regions that have been previously shown to be involved in higher cognitive functioning. Second, this project focuses on both the inter-hemispheric and to a lesser degree the intra-hemispheric integration of processing resources. Third, sample employed on this project has been extensively screened for physiological, neuropsychological, and neurological pathologies and other factors that could potentially confound results. Sample of participants is representative of the population of the Unites States as of the year 2000 U.S. Census for ages 4 years 10 months through 18 years 5 months for CANTAB SWM, 4 years 10 months through 18 years 5 months for WASI Block Design, WASI Matrix Reasoning, and 8 years 1 month through 16 years 11 months for WISC-III Coding B. Because all attempts have been made to build an unbiased sample this project may help resolve some of the inconsistencies present in the literature regarding brain-cognition relation. In contrast to many early magnetic resonance studies that were conducted on small samples, this study is based on a large sample of participants. Due to increase in sample size and consequently power of inferences, this study may help resolve some of the inconsistencies present in early MR morphometry studies.

In sum, in this project a well-defined set of cognitive processes engaged by a specific subset of measures of processing speed, spatial working memory, visuo-spatial abilities, and non-verbal reasoning is related to a inter- and intra-hemispheric network of areas previously demonstrated to have an involvement in higher cognitive functioning. Consequently, this project will provide new data on the relation between selected subtests of CANTAB and WASI and the volume of the frontal and parietal lobes as well as the anterior and posterior corpus callosum.

The final regression equation summarizes hypotheses and attempts to describe the relations between volume of white and gray matters and higher cognitive functioning in terms of a formal mathematical model. Such a mathematical formalism integrates previously proposed explicitly mechanistic and reductionist hypotheses about the role of connectivity on tasks invoking

different nodes of the brain network. This framework may allow for separation of unique contributions of bulk cells bodies and axons to cognitive performance and for separation of overall frontal and parietal contributions to cognitive performance on selected tasks.

Section that follows will discuss data source selected for this study, rational for the selection of cognitive measures, and each of the selected cognitive measures. Discussion of cognitive tests will list cognitive processes involved in completing each test, and based on empirical studies will link those processes and cognitive test to brain regions differentially involved in performance on those tests.

The NIH Pediatric MRI Data Repository

Most of the studies regarding relations between brain structures and specific cognitive abilities in normal populations (B. J. Casey, Trainor et al., 1997; E. R. Sowell, Thompson, & Toga, 2004) were not conducted on racially, ethnically, and economically representative samples (Evans, 2006). Consequently, generalizibility of those reports is limited and may be a source of controversy regarding the relation between brain anatomy and intellectual performance (Finger, 1994). Due to the high cost of acquisition of the magnetic resonance imaging data, the need for sampling from geographically diverse locations, and the relatively large number of subjects required to build a representative sample, data collection at a single site is not feasible. Those difficulties are overcome by using data sharing initiatives such as the NIH Pediatric MRI Data Repository that provides data used in this study. Inferences from this data set are limited by age ranges investigated in this study and corresponding to the age ranges for particular instruments: CANTAB SWM Between Trial Return Errors (4.8 – 18.4 years), WASI Block Design Total Raw Score (6 – 18.4 years), WASI Matrix Reasoning Total Raw Score (6 – 18.4), WISC-III Coding B (8.1 – 16.9 years).

Assessment of Cognitive Function: WASI, CANTAB, and WISC-III Coding B

In addition to Magnetic Resonance Imaging (MRI) data, the NIH Pediatric MRI Data Repository provides a variety of behavioral, neuropsychological, neurological, and physiological assessments (for complete description of the NIH Pediatric MRI Data Repository procedures and methods see B. D. C. Group (2006)). Among the measures of most interest for this study are subtests of the Cambridge Neuropsychological Test Automated Battery (CANTAB), Wechsler

Abbreviated Scale of Intelligence (WASI), Wechsler Intelligence Scale for Children, Third Revision (WISC-III) that assess not only intelligence but also working memory, attention, executive function, and processing speed.

Measures of cognitive ability selected for this study needed to meet two primary criteria. First, selected measures needed to invoke bilateral brain activations. Bilateral activations suggest that commissural fibers such as those traveling in the corpus callosum are involved in integration and active recruitment of resources from areas in the opposite hemisphere in service of a goal-oriented task.

Second, selected measures need to be of relatively high level of complexity/difficulty. Complexity/difficulty and inter-hemispheric transfer are likely to be related. Complexity/difficulty of a task influences to what extent the task taxes the processing resources of a hemisphere (Belger & Banich, 1992). Banich and Brown (2000) pointed out that inter-hemispheric transfer takes time and therefore for the inter-hemispheric integration to be beneficial the gains in redistributing information processing need to exceed losses of time associated with the inter-hemispheric relay (Banich, Hugdahl et al., 2003). Based on the data on inter-hemispheric transfer collected in the Poffenberger paradigm (Poffenberger, 1913; Zaidel & Iacoboni, 2003), for the inter-hemispheric relay to be economical, net gains due to distributed processing need to exceed 3 to 4 milliseconds. This time is believed to be required for the inter-hemispheric transfer in individuals with intact corpus callosum (Zaidel & Iacoboni, 2003).

More complex and cognitively taxing tasks are also more likely to invoke intra-hemispheric transfer. For instance, more difficult tasks often invoke both posterior and anterior attention networks (B. J. Casey, K. M. Thomas et al., 2000). Posner and Petersen (1990)'s model of attentional control the posterior (or visuo-spatial) system predominantly involving parietal lobe is credited with deploying attention to a relevant spatial location (Corbetta, Miezin, Shulman, & Petersen, 1993). Increased posterior brain activity when subjects/participants attended to the location of a stimulus have been documented in single-cell recording primate studies (Robinson, Goldberg, & Stanton, 1978), human PET studies (Corbetta & Shulman, 1998), and human fMRI studies (Corbetta, Kincade, Ollinger, McAvoy, & Shulman, 2000; Coull & Nobre, 1998). In contrast, the anterior attention system involving parts of the prefrontal cortex (anterior cingulate, dorso-lateral prefrontal cortex) is credited with the deployment of attentional control in inhibiting

rare, salient, or over learned responses (Bench et al., 1993; Carter, Mintun, & J. D. Cohen, 1995; J. V. Pardo, P. J. Pardo, Janer, & Raichle, 1990). See B. J. Casey, K. M. Thomas et al. (2000) for a more detailed discussion of this topic.

For hypotheses involving the anterior corpus callosum (region of the genu) measures selected need to invoke bilateral frontal activations. For hypotheses involving posterior corpus callosum (region of the isthmus and the splenium) measures selected need to invoke bilateral parietal activations.

Based on the preliminary review of instruments included in the repository, WASI, CANTAB, and the Coding B subtest of the WISC-III were selected as meeting the preset criteria.

Based on the evaluation of the tests that remained in the pool against the two presented criteria and evaluation of their distribution characteristics, CANTAB Spatial Working Memory along with two of the WASI subtests: the Block Design and the Matrix Reasoning were retained (see Table 2 on page 54 summarizing evaluation of CANTAB and WASI subtests against selection criteria and Table 3 on page 55 for inter- and intra-hemispheric transfer matrices for selected CANTAB and WASI tasks). In addition to the measures of cognitive ability, Coding B subtest of the WISC-III is included as an estimate of the processing speed. Processing speed closely relates to structure of white matter, and consequently to the speed of information transfer.

In the remainder of this section I will discuss measures of cognitive performance adopted as dependent measures in this study.

As part of the NIH MRI Study of Normal Brain Development participants 8 years and older but younger than 17 years received Wechsler Intelligence Scale for Children (WISC-III) Coding subtest part B. Digit Symbol was shown to be sensitive to changes in white matter associated with aging in general (Salthouse, 1996), and age related cognitive decline (Charlton et al., 2006) and age related subcortical white matter lesions (O'Brien et al., 2002) in particular (Turken et al., 2008). The digit coding test is a widely accepted measure of processing speed (Salthouse, 2005; Turken et al., 2008) and involves number of perceptual and cognitive processes including visual analysis, maintenance in memory of the visual stimulus-response associations, attentional processes, response selection, and motor planning and execution (Turken et al., 2008).

Wechsler Intelligence Scale for Children - Third Revision (WISC-III) Coding B Subtest (intended ages 8:0 – 16:11 years). The Wechsler Intelligence Scale for Children (WISC)

Table 2

Selected CANTAB and WASI tasks, their neural correlates, and the inclusion/exclusion decisions.

Task	Neural Correlate	Decision
CANTAB Spatial Working Memory	Dorsal and ventral prefrontal cortex	(+) qualifies
WASI Block Design	frontal, parietal, cingulate	(+) qualifies
WASI Matrix Reasoning	frontal, parietal, temporal, cingulate, occipital	(+) qualifies

Table 3

Inter- and intra-hemispheric transfer matrix for selected WASI and CANTAB tasks. (+) denotes presence of empirical evidence of transfer; (-) denotes lack of empirical evidence of transfer

	CANTAB Spatial Working Memory	WASI Block Design	WASI Matrix Reasoning
inter-hemispheric (CC)	+	+	+
Intra-hemispheric (medial WM)	-	+	+

is one of the most widely used intelligence tests for children populations. In this study a Coding subtest from the third revision of this test was used (WISC-III; Wechsler, 1991). The coding test is composed of two distinct parts: A and B. Because Coding A is not employed in this study it is discussed in detail elsewhere (B. D. C. Group, 2006).

In the course of the Coding B administration participant receives a key/sample sheet showing shapes marked in the upper part with a digit ranging from one to nine, and a symbol in the lower part. Each symbol is paired with a different number. The answer sheet consists of stimuli with numbers in the upper part and an empty box in the lower part. The participant's task is to fill the empty box located in the lower part of a shape with a symbol corresponding to the number written in the upper part of the shape. Thus, during this part of the test the participant transcribes the digit-symbol code as fast as possible during the 120-second time window. On the answer sheet, there are 7 practice shapes and 119 test shapes (Sattler, 1992). Each correctly coded shape receives one point. Coding B maximum score is 119 points (Sattler, 1992) and no time-bonus points can be assessed. Coding B task is appropriate for participants 8 years and older and is analogous to the Digit Symbol subtest of WAIS-R.

Psychometric properties of the WISC-III Coding. Coding is a relatively weak correlate of the g-factor yielding an average $r = .45$ across 11 age groups (range: .32, .55; Sattler, 1992). Coding loads highly on the Processing Speed factor average loading of .74 (Sattler, 1992). Digit Span shows relatively high reliability ($r = .79$) across six reported age groups (6, 7, 10, 11, 14,

15; range: .70, .90; Sattler, 1992). No reliability was reported in the test manual (Wechsler, 1991) for age groups 8, 9, 12, 13, 16 (Sattler, 1992). WISC-III Coding correlates only weakly with any of the IQ indices (FSIQ: $r = .33$; VIQ: $r = .29$; PIQ: $r = .32$; Sattler, 1992).

Cognitive Processes of the WISC-III Coding. Coding involves visuo-motor coordination, attention, visual scanning and tracking (shifting between sample and answer sheets), short-term memory/paired-associate learning, and cognitive flexibility when shifting from one pair to another (Sattler, 1992).

Neural Correlates of the WISC-III Coding. There is only a very limited data regarding neural correlates of the digit symbol substitution tests. Because of the difficulties associated with motion artifacts up to date there has been one functional study linking the digit symbol substitution test with frontal lobes (Nakahachi et al., 2008). Colom, Jung, and Haier (2006) reported significant correlation between the Digit Symbol performance and regional gray matter in a small cluster of the temporal lobe.

Cambridge Neuropsychological Test Automated Battery (CANTAB; intended ages 4:6 years and older). CANTAB is a theoretically derived test battery containing analogs of well established tests that predominantly assess the function of the frontal and temporal lobes (Luciana & C. Nelson, 2002). CANTAB assesses component subdomains of executive function: planning, working memory, visual memory, and visual attention. Each subdomain is assessed using multiple tasks, as summarized in Table 4 on page 57. CANTAB has been successfully used in both adult and children populations (Luciana & C. Nelson, 2000, 2002, 2002).

While the NIH Pediatric MRI repository provides five CANTAB tasks assessing visual attention, planning, and working memory. Those tasks include the Motor Screening Test, the Big Circle / Little Circle, the Intra-/Extra-dimensional Set-Shifting, the Spatial Memory Span, and the Spatial Working Memory (SWM) only the latter was selected for this study.

The Spatial Working Memory Task. is a computer adaptation of the radial arm maze task (Olton & Feustle, 1981; Petrides & Milner, 1982) previously employed in animal research. This task assesses spatial working memory by measuring the ability to conduct an organized search of items in order to efficiently progress toward a goal (Luciana & C. Nelson, 2002). The term working memory was coined by Baddeley (1986) and refers to temporary storage and on-line manipulation of information taking place while conducting a variety of tasks (A. Lee, A. Owen, Rogers,

Table 4

Summary of tasks in CANTAB and domains of executive function they measure. CANTAB subtests available as part of the NIH Pediatric MRI repository are marked with an asterisk.

Domain	Task	Neural Correlate
Visual Memory	Delayed Match to Sample	
	Learning of Visual Paired Associates	
	Pattern and Spatial Recognition	
Visual Attention	Reaction Time	
	Big Circle / Little Circle*	Visual association cortex
	Intra-/Extra-dimensional Set-Shifting*	Intra-dimensional: orbito-frontal Extra-dimensional: dorso-lateral prefrontal cortex
	Match-to-Sample Visual Search	
Planning and Working Memory	Motor Screening Test*	Fronto-parietal
	Spatial Memory Span*	Right dorso-lateral prefrontal
	Spatial Working Memory (Self-Ordered Search)*	Dorsal and ventral prefrontal cortex
	Tower of London (Stockings of Cambridge)	

B. Sahakian, & T. Robbins, 2000). During each trial, a number of colored squares appear on the screen. The participant is told that a token is hidden inside of one of the colored squares. In order to find the token, the participant needs to touch the colored squares one at a time until s/he discovers where the token is hidden. No square is used twice to hide a token, and once a token is discovered and moved to the storage area on the screen, another token is hidden under a different square. The participant searches through the array of squares until s/he retrieves a token from each box in the array. In order to perform the task most efficiently, the square that already contained a token during a trial should not be selected again during the same trial. At the beginning of each trial, two colored squares appear on the screen and the number increases to three, four, six, and finally eight. Each participant completes four trials. Efficient performance on this task requires remembering where tokens were found earlier in the trial.

In this study of specific interest are the between-search or "forgetting" errors taking place when a participant returns to a square where s/he already discovered a token in one of the previous trials. The forgetting error score corresponds to the participant's tendency to search a location where s/he has previously found a token in the same trial. This score is calculated based on searches of two, three, four, six, and eight-item problems. Evidence from both PET studies (A. M. Owen, Evans et al., 1996) and from the lesion patients (A. M. Owen, Downes, B. J. Sahakian, Polkey, & T. W. Robbins, 1990; A. M. Owen, R. G. Morris, B. J. Sahakian, Polkey, & T. W. Robbins, 1996) suggests that this task differentially engages the dorsal and ventral prefrontal cortices (Luciana & C. Nelson, 2000).

Cognitive Processes of the Spatial Working Memory Task. In contrast to spatial memory span and spatial recognition tasks, more demanding self-ordered search tasks such as the Spatial Working memory Task require not only independent decisions whether a spatial location was used in the past, but also arranging those decisions in a particular order that maximizes the outcomes. Consequently, this task engages processes involved in (1) the motor screening, (2) encoding of visual stimuli, maintenance of information over time, coding of the spatial location of the object and creating a cognitive map, as well as (3) series of independent decisions whether a spatial location was already used in the past and subsequent response execution.

Neural Correlates of the Spatial Working Memory Task. In contrast to spatial memory span and spatial recognition tasks that activate predominantly the right ventro-lateral prefrontal

cortex, the Spatial Working Memory task activates bilaterally the ventro-lateral and dorso-lateral prefrontal cortical areas (A. M. Owen, Evans et al., 1996). This presumably is due to increased information processing demands. Other studies also suggest hippocampal involvement in creation of the cognitive spatial map (Astur et al., 2005).

Wechsler Abbreviated Scale of Intelligence (WASI; intended ages 6 years and older). WASI is an individually administered test of intelligence (Corporation, 1999) intended to provide a brief estimate of intelligence in situations where administering more comprehensive IQ scales is not feasible. Development of WASI involved sample linking with the WISC-III and WAIS-III, thus allowing the researcher to estimate FSIQ ranges for the aforementioned tests based on WASI scores (Strauss, Sherman, & Spreen, 2006).

WASI consists of four subtests: Vocabulary, Block Design, Matrix Reasoning, and Similarities. While those subtests resemble subtests of WAIS-III and WISC-III those scales do not share any items (Strauss, Sherman et al., 2006). Selection of those subtests was based on previous empirical work, indicating that they load highly on the general intellectual ability (Spearman, 1923, g-factor) and tap into G_c and G_f components (Strauss, Sherman et al., 2006).

The Vocabulary and Similarities contribute to the Verbal IQ score (VIQ), while the Matrix Reasoning and the Block Design contribute to the Performance IQ score (PIQ). All four scales together yield a Full Scale IQ (FSIQ).

The Block Design subtest. consists of 13 cards depicting two-dimensional geometric patterns. The participant's task is to replicate a pattern presented on a card using colored blocks. This task has a limited time-response window (Sprandel, 1995).

In the course of this subtest, the participant receives sets of either four or nine three-dimensional colored blocks, and a set of cards depicting two-dimensional designs to be replicated in the course of this task. Experimenter provides participant with verbal instruction describing the task and conducts two example assemblies of blocks in order to familiarize the participant with the task. During this task, the participant needs to perform visual analysis of the (two-dimensional) pattern represented on the card, make a decision on how the blocks should to be arranged (synthesis) in order to replicate this pattern, and finally perform a visuo-spatial integration of both the analysis and synthesis stages, resulting in a three-dimensional representation of a two-dimensional pattern (Sprandel, 1995).

Cognitive Processes of the Block Design subtest. Block Design is a nonverbal measure of synthesizing and abstract abilities (Sprandel, 1995). It involves visual perception, perceptual organization, detection of part-whole relations, reproduction of visual models, and visuo-motor coordination (Sprandel, 1995).

Neural Correlates of the Block Design subtest. Performance on the Block Design test predicts brain activations in the frontal lobes of both hemispheres (right hemisphere Areas 4, 6, 8, 9, 10; left hemisphere Area 46), left and right precuneus (Area 7), left cingulate (Areas 23, 24, 31) and subcortical structures including the thalamus and basal ganglia (Fangmeier et al., 2006). Authors noted that brain activations start with the temporal-occipital region shifting to frontal regions, and then to parietal regions. Fangmeier and colleagues (Fangmeier et al., 2006) noted that activation in the parietal lobes is likely to reflect the reasoning process as this area is activated during reasoning but not during working memory tasks (Jung & Haier, 2007).

The Matrix Reasoning subtest. consists of 35 incomplete patterns each presented with a set of five possible responses. The participant's task is to select the response that completes the presented pattern. The Matrix Reasoning subtest is similar to nonverbal tests such as the Raven's Progressive Matrices and the Halstead-Reitan Category Test (Groth-Marnat, 2003). It measures visuo-spatial and abstract reasoning, visual organization, parallel processing of visual and spatial information, as well as analysis of the whole into its constituent parts (Groth-Marnat, 2003). This task is predominantly assessing the G_f.

Cognitive Processes of the Matrix Reasoning subtest. This task requires for individual to (1) infer a rule from a collection of visual elements and (2) generate next items in a series based on a rule or to verify that a presented item is a legitimate instance of a rule (G. Larson & Alderton, 1990; Strauss, Sherman et al., 2006).

Neural Correlates of the Matrix Reasoning subtest. Evidence from both the PET and fMRI studies employing variations of the matrix reasoning paradigm points to the bilateral involvement of the frontal, parietal, temporal, and to a lesser extent cingulate and occipital regions. Studies are summarized in Table 5 on page 61.

METHOD

Data used in the present study were obtained from the Pediatric MRI Data Repository Version 1 (B. D. C. Group & Evans, 2006; Waber et al., 2007; Almli, Rivkin, & McKinstry, 2007;

Table 5

Neural Correlates of Matrix Reasoning. Based on Jung and Haier (2007). Standard deviations presented in brackets. Bxx denotes bilateral activations. Lxx and Rxx denote left hemisphere and right hemisphere activations respectively. Numbers following B, L, or R refer to the approximate corresponding Brodmann's Area. RAPM denotes Raven's Advanced Progressive Matrices, WCST denotes Wisconsin Card Sorting Test. PET denotes Positron Emission Tomography. fMRI denotes functional Magnetic Resonance Imaging.

Study	N	Age of cohort	ACPC	Frontal	Parietal	Temporal	Occipital	Measure	Modality
Haier (1993) Haier, B. V. Siegel, Nuechterlein, and E. Hazlett (1988)	8	22.4 (2.3)	–	B9, B10	B39	B21, B22, B37, B38	B18, B19	RAPM	PET
Esposito, Kirkby, Van Horn, Ellmore, and Berman (1999)	41	18-42	B2, B3	B9, B46	B39, B40	B21, B37	B18, B19	WCST/ RAPM	PET
Haier (2003)	22	22.1 (2.6)	–	–	B7	B22, B37	B18, B19	RAPM	PET
Prabhakaran, J. A. L. Smith et al. (1997)	7	23-30	–	B6, B9, B44, B45, B46	L7, L39, L40	L>R21, L>R37	L>R18, L>R19	RAPM	fMRI
Kroger et al. (2002)	8	19-32	B2, B3	B6, B9, B47, L44, L46	B7	–	–	Matrix Reasoning	fMRI
J. R. Gray, Chabris et al. (2003)	48	18-37	–	L45, L46	R4, B40, L39, R31	B22	–	WM/ RAPM	fMRI

Wilke, Holland, Altaye, & Gaser, 2008), a multi-site, longitudinal study of typically developing children from ages newborn through young adulthood. The collected data provide a representative sample of the US population as described in the 2000 US Census for age ranges corresponding to employed cognitive tests [3] .

Design Statement

The employed research design is a correlational analysis of archival Magnetic Resonance Imaging and cognitive test data for age groups corresponding to recommended administration ages [3] . This analysis intends to estimate the relations between volumes of the frontal and parietal sections of the corpus callosum and the cognitive performance on cognitive tests involving inter-hemispheric transfer through those callosal sections. In addition, presented comprehensive regression model aims at testing feasibility of a mathematical formalism separating relative contributions of:

1. frontal vs. parietal structures (white matter volume, gray matter volume, volumes of sections of the corpus callosum)
2. white matter vs. gray matter (frontal and parietal white matter volumes vs. frontal and parietal gray matter volumes)
3. intra-hemispheric vs. intra-hemispheric communication (lobar white matter volumes vs. volumes of callosal subsections)

to cognitive performance on CANTAB SWM, WASI Block Design, WASI Matrix Reasoning, and WISC-III Coding B.

Data Source

Rationale for the Use of the Archival Data. Most of the studies regarding the relation between maturation of brain structures and specific cognitive abilities in normal populations (B. J. Casey, Trainor et al., 1997; E. R. Sowell, Thompson et al., 2004) were not conducted on racially, ethnically, and economically representative samples (B. D. C. Group & Evans, 2006).

[3] ages 4 years 10 months through 18 years 5 months for CANTAB SWM, 4 years 10 months through 18 years 5 months for WASI Block Design, WASI Matrix Reasoning, and 8 years 1 month through 16 years 11 months for WISC-III Coding B

Consequently, generalizibility of those reports is limited and may be a source of controversies regarding the relation between brain anatomy and intellectual performance (Finger, 1994). Due to high cost of acquiring of the magnetic resonance imaging data, need for sampling from geographically diverse locations, and a relatively large number of subjects required to built a representative sample the data collection at a single site is not feasible. Those difficulties can be overcome by data sharing initiatives such as the NIH Pediatric MRI Data Repository. While use of this sample limits age range to which results can be generalized to it also provides well screened and well constructed sample with limited selection bias and minimal risk of pathologies. In addition, longitudinal nature of this database opens possibility that with accumulation of repeated measures subsequent analyses can be conducted modeling both within and between subject effects and consequently improving efficiency of statistical modeling.

Description of the Data Source. Data used in the present study were obtained from the Pediatric MRI Data Repository (Version 1) created by the NIH MRI Study of Normal Brain Development (B. D. C. Group & Evans, 2006; Waber et al., 2007; Almli et al., 2007; Wilke et al., 2008). This is a multi-site, longitudinal study of typically developing children, from ages newborn through young adulthood, conducted by the Brain Development Cooperative Group and supported by the National Institute of Child Health and Human Development, the National Institute on Drug Abuse, the National Institute of Mental Health, and the National Institute of Neurological Disorders and Stroke (Contract numbers N01-HD02-3343, N01-MH9-0002, and N01-NS-9-2314, -2315, -2316, -2317, -2319 and -2320).[4]

Data provided in the Pediatric MRI Data Repository has been collected across seven Pediatric Study Centers (PSCs) listed in table 6 on page 65. Subjects that initially were recruited at the University of California at Irvine received subsequent follow-up scans at the University of California at Los Angeles bringing the total number of PSCs to six. All protocols and procedures were subject to approval from the Institutional Review Board at the respective PSC and a coordinating center

Participant Sample Construction.

[4] A listing of the participating sites and a complete listing of the study investigators can be found at http://www.bic.mni.mcgill.ca/nihpd/info/participating_centers.html. This manuscript reflects the views of the author and may not reflect the opinions or views of all the Study Investigators or the NIH.

Summary of the demographic data. Each of the six Pediatric Study Centers (see Table 6) was provided with a map of its vicinity with clearly identified zip codes. Based on the 2000 U.S. Census data (U.S. Census Bureau, 2000) demographics including regional median household income, and the distribution of race and ethnicity were compiled for all the zip codes in the 40 to 60 mile perimeter of the PSC (approximate 1-hour travel time). Lists of zip codes were subsequently grouped by household median income (low, medium, high) and by race and ethnicity.

Total target accruals. Total target accruals were constructed by scaling down US Census 2000 household data cross-categorized by income and ethnicity to a sample size of $N = 440$.

PSC target accruals. Stratified random samples were constructed for each PSC matching distribution of ethnicity/race, Housing and Urban Development (HUD) adjusted household income existing in the U.S. population. It was ensured that the summed accruals from all PSCs matched demographics of the U.S. population (U.S. Census Bureau, 2000).

Oversampling. In order to achieve target accrual numbers actual recruiting was oversampled by 20% in order to account for the attrition rate.

Adjustments. Some of the adjustments were needed to be dynamically implemented during data acquisition in order to maximize recruitment efficiency. Those adjustments are explained in more detail in the Sampling Strategy portion of the NIH MRI Study of Normal Brain Development protocol (B. D. C. Group, 2006). Late in the recruiting process, revised PSC-specific accruals were provided to each center. None of the adjustments affected total target accruals.

Recruitment procedure.

Mailing lists. Each PSC ordered three batches of household lists received in three-month intervals. First two batches contained information about 3000 households each, while the last one contained information about 4000 households, all cross-classified by participant's age group (4 years 6 months through 5 years; 6 years through 11 years; 12 years through 17 years) and sex (male or female). Batches were balanced by race and household income across the requested zip codes. Multiple records existed for households with multiple children but received only a single mailing. Household batches and monthly change of address updates were supplied by the national telemarketing firm InfoUSA. In order to facilitate recruiting of the lower income households (income less than 35,000 USD), contact information for additional 6,666 household were purchased from another agency, the Creative Mailers.

After each batch was received by a PSC, a random number list was requested. Random numbers were used to select 200-300 households from the list for initial contact. A follow-up phone call and additional screening provided/verified prospective participant's age, sex, ethnicity, as well as household income and parent education levels. This procedure was repeated until PSC's target stratified accruals were reached. List of PSCs and contracted accruals is presented in Table 6 on page 65.

Table 6

List of Pediatric Study Centers and corresponding contracted accruals. Modified from B. D. C. Group (2006). The MRI Study of Normal Brain Development Protocol.

Pediatric Study Center	N
Children's Hospital, Boston, MA	70
Children's Hospital Medical Center of Cincinnati, OH	100
University of Texas Health Science Center at Houston, TX	50
University of California at Irvine, CA	50
University of California at Los Angeles, CA	60
Children's Hospital of Philadelphia, PA	50
Washington University St. Louis, MO	60
Total	440

Participants

Children between the ages of 4 years, 6 months and 18 years, 3 months were recruited from the vicinity of one of the designated Pediatric Study Centers across the United States. The 2000 US Census data were scaled down to a target sample size of 440 children and young adults. Participants were recruited to participate in the Objective 1 part of the NIH MRI Study of Normal Brain Development study with equal distribution across ages and gender. From the 433 participants recruited to participate in the Objective 1, 371 received MRI scans and 361 of those scans passed the initial quality control screening. Of those scans, 327 included full three-dimensional structural MR images and not the fallback two-dimensional acquisitions. Detailed description of

the screening procedures and instrumentation of the NIH MRI Study of Normal Brain Development can be found in B. D. C. Group (2006).

Magnetic Resonance Imaging Procedures Used by the Pediatric Study Centers

For majority of subjects the magnetic resonance scanning was conducted on a subsequent day, however, participant's temperament, fatigue, preference of participant's family, and the availability of scanning equipment were all taken into consideration when scheduling MRI acquisitions. Magnetic resonance scanning sessions lasted in the upwards of 90 minutes with 30 to 40 minutes being the actual acquisition time. Participants who expressed anxiety about MR scanning and very young participants were given one or more 15 to 30 minute sessions in the mock MR scanner. All participants were asked to come back for the rest of the longitudinal study two times separated by two-year intervals. Most of the procedures described above including consent, assent, behavioral testing, full telephone interview and MR scanning were/or will be repeated during those subsequent visits.

While study collected number of MR images including three dimensional T1-weighted, two dimensional Proton Density (PD) / T2-weighted images, MR Spectroscopy (MRS), and DTI protocols in this study only T1-weighted anatomical magnetic resonance images were analyzed. Magnetic Resonance Images were acquired using Three-dimensional (3D) volumetric T1-weighted spoiled gradient recalled (SPGR) echo acquisition sequence on General Electric (GE Healthcare, Milwaukee, WI) or Siemens (Siemens AG, Erlangen, Germany) MRI scanners located at respective PSCs. In a cross-site pretesting SPGR acquisition sequence yielded higher signal-to-noise (SNR) and contrast-to-noise (CNR) ratios the than the magnetization prepared gradient echo (MPRAGE) sequence (B. D. C. Group, 2007).

Images were acquired in the sagittal orientation with Time Repetition (TR) ranging from 22 to 25 ms and Time Echo (TE) ranging from 10 to 11 ms, and flip angle of 30 degrees, and a Number of Signal Averages/Excitations (NEX) equal to 1. Field of View (FoV) inferior-superior (IS) was set to 256 mm, anterior-posterior (AP) set to 256 mm and left-right (LR) ranging from 160 to 180 mm giving sufficient coverage for the whole head. Matrix size was IS = 256 mm, AP = 256 mm and LR optimal to yield isotropic 1mm x 1mm x 1mm voxels. Some scanners where the maximum number of slices that can be acquired is 124, the slice thickness was adjusted to cover the whole head with 124 slices providing voxel size closest in size to isotropic (1 mm x 1

mm x 1.x mm; where 1.x is lower or equal to 1.5 mm; B. D. C. Group, 2007).

Image Analysis.

Cortical reconstruction and volumetric segmentation. Cortical reconstruction and volumetric segmentation was performed using the Freesurfer v 5.0. The technical details of Freesurfer have been extensively described elsewhere (A. M. Dale & Sereno, 1993; A. M. Dale, Fischl, & Sereno, 1999; Fischl, Sereno, & A. M. Dale, 1999; Fischl, Sereno, Tootell, & A. M. Dale, 1999; Fischl & A. M. Dale, 2000; Fischl, A. Liu, & A. M. Dale, 2001; Fischl, D. H. Salat, Busa et al., 2002; Fischl, A. van der Kouwe et al., 2004; Fischl, D. H. Salat, A. J. van der Kouwe et al., 2004; Han et al., 2006; Jovicich et al., 2006; Segonne, A. M. Dale et al., 2004). Image processing began with the removal of non-brain tissue using a hybrid watershed/surface deformation procedure (Segonne, A. M. Dale et al., 2004). This step was followed by the automated transformation from native subject space to Talairach space, segmentation of the subcortical white matter and deep gray matter structures such as the hippocampus, amygdala, caudate, putamen, and ventricles (Fischl, D. H. Salat, Busa et al., 2002; Fischl, D. H. Salat, A. J. van der Kouwe et al., 2004). In the next step image intensity normalization was performed (Sled, Zijdenbos, & Evans, 1998). Final steps consisted of tessellation of the gray matter white matter boundary, automated topology correction (Fischl, A. Liu et al., 2001; Segonne, Pacheco, & Fischl, 2007) and surface deformation following intensity gradients to optimally place the gray/white and gray/cerebro-spinal fluid borders at the location where the greatest shift in intensity defines the transition to the other tissue type (A. M. Dale & Sereno, 1993; A. M. Dale, Fischl et al., 1999; Fischl & A. M. Dale, 2000).

Upon completion of the cortical model, a number of deformable procedures was performed beginning with surface inflation (Fischl, Sereno, & A. M. Dale, 1999) and followed by the registration to a spherical atlas. Spherical coordinate system enables align subjects based on the individual cortical folding patterns (Fischl, Sereno, Tootell et al., 1999). Next step included parcelation of the cerebral cortex into units based on gyral and sulcal structure (Desikan et al., 2006; Fischl, A. van der Kouwe et al., 2004). Alignment based on gyral patterns is believed to be superior to traditional template based approaches. In this process instead of fusing subjects to a common template, functionally specialized areas (gyri) are aligned across subjects. Alignment based on structure-function correlation should be able to reduce impact of individual differences and is superior to Talairach-based alignment strategy.

Upon completion of the Freesurfer pipeline each subject's processing log was inspected for errors. If processing completed without errors experimenter blind to behavioral data visually inspected accuracy of skull removal, Talairach registration, volumetric tissue segmentation and created white matter and pial surfaces. In case any of the listed steps failed appropriate corrections were applied including adjustment of the watershed parameters of the skull stripping algorithm, manual removal of the skull, adjustments to the Talairach registration, addition of the control points in order to fine-tune tissue segmentation, and manual edits of the tissue partitions and subcortical segmentation with focus on the corpus callosum. Upon applying correction subject was submitted to the Freesurfer pipeline for re-processing. This process was repeated until uniformly satisfactory accuracy was achieved and in the upwards of four times. Ten images that failed any of the above steps were excluded from further analyses.

Employed screening data screening procedures represent well established practice for Freesurfer data preparation, verification, and troubleshooting (Schmansky, 2009) and follow Biomedical Informatics Research Network's recommendations for multi-site structural MRI data analysis using Freesurfer (Bockholt & Turner, 2007). During the verification process, a macroscopic atlas of the human brain (Mai, Assheuer, & Paxinos, 2004) was consulted as needed. During the screening process the experimenter remained blind to behavioral measures associated with the MR images.

Calculation of the volume. The corpus callosum was be segmented from the brain using Freesurfer v. 5.0. Five-millimeter-wide lateral sections of the corpus callosum was extracted and the corpus callosum was divided into five equal partitions. The anterior fifth of the corpus callosum consists predominantly of genu of the corpus callosum, and carries prefrontal fibers with possible contributions of pre-motor and supplementary motor fibers. The posterior two-fifths of the corpus callosum consist of the isthmus and the splenium of the corpus callosum, and carry posterior parietal, temporal, and occipital fibers. Volumes of the anterior fifth and the posterior two fifths of the corpus callosum were calculated.

Summary of Independent Measures. In this stage of data processing the following measures were derived:

F_{Wv}. Frontal white matter volume calculated separately for regions of interest defined by white matter in the frontal lobe of the left/right hemisphere. White matter volumes were cal-

culated in cubic millimeters from summed white matter volumes corresponding to the following overlying cortical gyri: Superior Frontal, Rostral and Caudal Middle Frontal, Pars Opercularis, Pars Triangularis, and Pars Orbitalis, Lateral and Medial Orbito-frontal, Precentral, Paracentral, and Frontal Pole. In order to calculate bilateral frontal white matter volume, left and right frontal white matter volumes were summed.

F_{Gv}. Frontal gray matter volume calculated separately for each hemisphere by summing white matter volumes corresponding to the following overlying cortical gyri: Superior Frontal, Rostral and Caudal Middle Frontal, Pars Opercularis, Pars Triangularis, and Pars Orbitalis, Lateral and Medial Orbito-frontal, Precentral, Paracentral, and Frontal Pole. In order to calculate bilateral frontal gray matter volume left and right gray matter volumes frontal were summed. Gray matter volumes were calculated in cubic millimeters.

P_{Wv}. Parietal white matter volume calculated separately for region of interest defined by white matter in the parietal lobe of the left/right hemisphere. White matter volume for parietal lobe is defined as sum of the white matter volumes corresponding to the following overlying cortical gyri: Superior and Inferior Parietal, Supra-marginal, Postcentral, Precuneus. In order to calculate bilateral parietal white matter volume left and right parietal white matter volumes were summed.

P_{Gv}. Parietal gray matter volume calculated separately for each hemisphere. Gray matter volume for parietal lobe is defined as sum of the volumes of the following gyri: Superior and Inferior Parietal, Supra-marginal, Postcentral, and Precuneus. In order to calculate bilateral parietal gray matter volume, left and right parietal gray matter volumes were summed.

F_{CCv}. Anterior corpus callosum volume calculated for the anterior fifth of the corpus callosum extending 5mm from the midline (2.5mm each lateral direction). Volumes were calculated in cubic millimeters.

P_{CCv}. Posterior corpus callosum volume calculated for the posterior two fifths of the corpus callosum extending 5mm from the midline (2.5mm each lateral direction). Volumes were calculated in cubic millimeters.

eTIV. Estimated Total Intracranial Volume computed according to Buckner et al. (2004) and Reuter (2009)

RESULTS

Data preparation

Extracted anatomical measures of volume were merged with demographic and behavioral data and loaded into R (Team, 2009). Quadratic age term was calculated, and handedness as well as gender were coded into binary dummy variables. Prior to conducting statistical analyses, each continuous independent variable was mean-centered in order to alleviate collinearity between age and its quadratic product (Naftali Raz, personal communication, November 9, 2009).

Sample Characteristics

Cases with missing 3D T1 MR scans were not included in the analyses. Cases with missing data on a dependent variable were excluded from the analyses involving that particular dependent variable but retained for analyses involving other dependent variables resulting in 317 subjects available for analyses with CANTAB Spatial Working Memory as a dependent measure, 209 subjects with WISC-III Coding B measure, and 294 subjects with WASI Block Design and Matrix Reasoning subtest as a dependent measure.

For the resulting sample descriptive statistics including quantiles, mean, and median are summarized in table 7 on page 71 for demographic variables and cognitive measures, and in table 9 on page 73 for anatomical measures. Means, standard deviations, as well as counts of available data points and missing data points are presented in table 8 on page 72 for demographic variables and cognitive measures, and in table 10 on page 74 for anatomical measures. Age ranges for dependent measures are presented in table 11 on page 75. Descriptive statistics separated by gender and handedness are presented in the Appendix B in Tables 27, 28, 29, 30 on pages 201–204. Inter-correlations matrix for present dataset is presented in the Appendix B in table 31 on page 206.

Outliers

Tukey fences (Tukey, 1977) were calculated for all cases and variables. Data examined employing the inner fence returned 55 suspected outliers across 9 variables with 12 suspected outliers present on anatomical variables and 43 suspected outliers present on behavioral variables. After inspecting identified cases and consulting influence plots, residual plots, and hat values most extreme observations were identified by z-score values larger or equal to 4. For each regres-

	Minimum	Q_1	Median	Mean	Q_3	Maximum
Age Days Date of Visit to DOB	1761.000	2842.000	3969.000	4054.196	5155.000	6698.000
CANTAB SWM Between Trial Return Errors	0.000	13.000	31.000	33.382	51.000	97.000
WISC-III Raw Score Coding B	18.000	41.000	53.000	53.349	63.000	97.000
WASI Total Raw Score Block	3.000	15.250	31.500	32.735	49.750	71.000
WASI Total Raw Score Matrix	3.000	21.000	25.000	23.973	28.000	34.000

Table 7

Sample distribution characteristics: descriptive statistics for continuous demographic and behavioral variables.

	Mean	SD	n	Missing	Shapiro-Wilk W	Shapiro-Wilk p
Age Days Date of Visit to DOB	4054.196	1368.066	317	0	n/a	n/a
CANTAB SWM Between Trial Return Errors	33.382	22.354	317	0	0.949	0.000
WISC-III Raw Score Coding B	53.349	15.738	209	108*	0.979	0.004
WASI Total Raw Score Block	32.735	19.269	294	23*	0.944	0.000
WASI Total Raw Score Matrix	23.973	6.486	294	23*	0.908	0.000

Table 8

*Sample characteristics: summary of continuous demographic and behavioral variables. n/a - not applicable to age, * - denotes number of participants who were outside of the age range of a cognitive measure: CANTAB SWM Between Trial Return Errors (4.8 – 18.4 years), WASI Block Design Total Raw Score (6 – 18.4 years), WASI Matrix Reasoning Total Raw Score (6 – 18.4), WISC-III Coding B (8.1 – 16.9 years).*

	Minimum	Q_1	Median	Mean	Q_3	Maximum
eTIV	1131463.928	1446646.633	1545905.418	1556915.561	1655447.189	1990277.100
CC Anterior	377.000	727.000	815.000	812.656	892.000	1253.000
CC Mid Posterior and Posterior	683.000	1121.000	1249.000	1259.991	1380.000	2267.000
ctx rlh frontallobe	153347.000	187175.000	201914.000	202594.385	216341.000	258648.000
ctx rlh parietallobe	93996.000	119926.000	129674.000	129653.514	139758.000	173692.000
wm rlh frontallobe	93232.000	125727.000	137163.000	137045.710	148037.000	183420.000
wm rlh parietallobe	58886.000	80502.000	87812.000	89535.754	98034.000	131298.000

Table 9

Sample distribution characteristics: descriptive statistics for continuous anatomical measures (in cubic millimeters).

	Mean	SD	n	Missing	Shapiro-Wilk W	Shapiro-Wilk p
eTIV	1556915.561	154846.205	317	0	0.994	0.212
CC Anterior	812.656	132.468	317	0	0.992	0.084
CC Mid Posterior and Posterior	1259.991	208.550	317	0	0.972	0.000
ctx rlh frontallobe	202594.385	20174.726	317	0	0.995	0.468
ctx rlh parietallobe	129653.514	14694.680	317	0	0.997	0.736
wm rlh frontallobe	137045.710	16844.295	317	0	0.997	0.800
wm rlh parietallobe	89535.754	12706.554	317	0	0.992	0.106

Table 10

Sample characteristics: summary of continuous anatomical measures (in cubic millimeters).

	Actual		Recommended	
Dependent measure	Minimum Age	Maximum Age	Minimum Age	Maximum Age
CANTAB SWM Between Trial Return Errors	4.8	18.4	4.5	n/a
WASI Block Design Total Raw Score	6.0	18.4	6.0	n/a
WASI Matrix Reasoning Total Raw Score	6.0	18.4	6.0	n/a
WISC-III Coding B	8.1	16.9	8.0	16.9

Table 11

Age ranges for dependent measures obtained from data and recommended administration ages for each subtest. n/a - denotes no upper age limit.

sion equation data points falling 4 or more standard deviations from the mean were examined and excluded. Number of cases used in each analysis is indicated in the results section.

Data Verification

Each variable was inspected for plausible range. For each case, values on all dependent measures must fall within the score range expected for their respective cognitive test/task.

Regression Diagnostics

Normality, linearity, homoscedasticity, and independence of residuals were screened through residuals using R (Team, 2009) and the CAR library (Fox & Weisberg, 2011).

Normality. For each variable density function was plotted over a histogram along with normal curve and visually inspected for violation of normality. In addition, quantitative metrics of normality were calculated in the form of z-skewness, z-kurtosis, and Shapiro-Wilk W statistic (Royston, 1995). Examination of Q-Q plots, distribution curves, and normality metrics revealed varying degree of departure from normality for cognitive measures but not for anatomical indices. Shapiro-Wilk statistics for demographic variables and cognitive measures are summarized in table 8 on page 72 and for anatomical measures in table 10 on page 74.

Non-constant error variance and linearity. For each variable standardized regression residuals were plotted against standardized predicted regression values and visually inspected for indication of non-normality, non-linearity, and homoscedasticity. In addition, a Non-constant Variance Test (Breusch-Pagan Test; Breusch & Pagan, 1979) was computed for each regression equation.

Multi-collinearity. For variables in each regression line a Variance Inflation Factor (VIF) was calculated along with its square root. Square root of the VIF scores often exceeded 5 for age and its quadratic term, confirming collinearity expected in the design due to inclusion of both linear and quadratic age. In order to test for possible suppression among variables, zero-level correlation coefficients were calculated for IV-DV pairs for within each hypothesis and compared to corresponding beta coefficients. For age term and to a lesser extent its quadratic term absolute differences between zero-level correlation coefficients and corresponding beta coefficients routinely approached or exceeded 1. Magnitude of this difference coupled with opposite directions of the relation between zero-order correlation coefficients and the beta weights for age or quadratic age

terms were indicative of a form of suppression between those variables. For the remaining variables, evidence of mild suppression was present but absolute differences never reached 0.5. In order to minimize suppression, each regression equation was initially run with a full set of covariates and independent variables, and final regression was re-run with only significant covariates and with all independent variables.

Sequential Volumetric Regressions

For each dependent measure separate Ordinary Least Square (OLS) regression analyses were conducted using R version 2.13.0 (Team, 2009) and the CAR library version 2.0-9 (Fox & Weisberg, 2011). Two stage hierarchical OLS regression analyses were performed between dependent measures of cognitive performance as dependent variables, with age, quadratic age-term, sex, handedness, and intracranial volume as covariates, and volume of frontal (Hypothesis 1) or parietal (Hypothesis 2) corpus callosum as independent variables. Regression analyses examined the relation between volumes of the anterior fifth (Hypothesis 1) or the posterior two fifths of the corpus callosum (Hypothesis 2) and selected measure of cognitive performance.

At the first step, WASI Block Design, WASI Matrix Reasoning, CANTAB Spatial Working Memory (number of between errors), as well as WISC-III Coding B raw scores were separately regressed onto the estimated Total Intracranial Volume (Buckner et al., 2004, eTIV), age, quadratic age term, gender, and handedness.

At the second step, measures of cognitive performance were separately regressed onto the volume of frontal or parietal portions of the corpus callosum in the series of independent regression analyses listed below:

1. Hypothesis 1: Region of the genu of the corpus callosum $Y = a + b(F_{CCv})$ where Ys are CANTAB Spatial Working Memory (number of between errors), WISC-III Coding B raw score as well as WASI Block Design, and WASI Matrix Reasoning.

2. Hypothesis 2: Region of the splenium and isthmus of the corpus callosum $Y = a + b(P_{CCv})$ where Ys are WASI Block Design, WASI Matrix Reasoning raw scores as well as WISC-III Coding B raw score.

For each hypothesis and each dependent variable initial regression runs were conducted in order to assist in selecting only significant nuisance covariates for each equation. Each regression

analysis was then repeated with only significant covariates and all independent variables for that analysis.

Correction for multiple comparisons and multiple tests. Because this study proposes a finite number of a priori specified independent inferences, planned comparisons are grouped within hypotheses. A somewhat conservative Bonferroni correction for multiple tests is applied in order to control family-wise error (FWE) at $\alpha = .05$.

Hypothesis 1: Anterior Corpus Callosum.

Hypothesis 1: CANTAB SWM Between Trial Return Errors. Summary of model stages:

$$Stage\,1: \; CANTAB\ SWM\ Between\ Trial\ Errors = Age$$

$$Stage\,2: \; CANTAB\ SWM\ Between\ Trial\ Errors = Age + Anterior\ Corpus\ Callosum$$

Because of the positive skewness present in the number of between trial return errors on the CANTAB Spatial Working Memory task a series of transforms was conducted on this variable including inverse, natural logarithm, square root, and Box-Cox $\lambda = .5$. From among those transformations square root resulted in most improvement of distribution normality. Prior to conducting analyses root square transform was applied to the number of between trial return errors on the CANTAB Spatial Working Memory task in order to allievate positive skewness present in the distribution. Square root transform resulted in a an improvement of distribution characteristics as evidenced by Shapiro-Wilk statistic changes from W = 0.925, $p > .0.00000$ for raw data with outliers to W = 0.972, $p > .00001$ after transform. Resulting distribution was examined and accepted as sufficient despite remaining departure from normality. Subsequently a two-stage hierarchical ordinary least squares regression analysis was conducted on *n* = 317 participants in order to examine the relationship between square root transformed number of between trial return errors on the CANTAB Spatial Working Memory task (CANTAB SWM Between Trial Return Errors) as the dependent variable, and centered volume of the anterior callosal partition (Cent CC Anterior) as independent variable, after controlling for nuisance covariates. Initial regression analysis conducted with a full set of covariates including centered estimated Total Intracranial Volume, centered Age, centered quadratic term of Age, gender, and handedness revealed presence of Age as a sole significant nuisance covariate. Subsequent analyses retained Age and excluded remaining non-significant nuisance covariates. In the first stage of hierarchical regression (Co-

variate Model) square root transformed number of between trial return errors on the CANTAB Spatial Working Memory task was regressed onto chronological age. In the second stage (Full Model) square root transformed number of between trial return errors on the CANTAB Spatial Working Memory task was simultaneously regressed onto age and the anterior callosal partition. Estimated regression coefficients and model statistics for covariate and full models are summarized in table 12 on page 80. Regression coefficients for the anterior callosal partition were small and non-significant predictors of square root transformed CANTAB SWM Between Trial Return Errors (Bonferroni corrected $p < 0.013$ with FWE controlled at $\alpha = .05$). At each stage of hierrahical regression amount of accounted variance was significantly different from zero with R^2 = 0.399 for the Covariate model, and R^2 = 0.399 for the Full Model. While entry of the nuisance covariates (Covariate Model) resulted in a statistically significant increment in R^2 with $F(2,315)$ = 1746.811, $p < 0.000$, entry of the the Full Model did not account for a significant amount of variance beyond that explained by the Covariate Model alone with R^2-*change* = 0.000 with $F(1,314)$ = 0.021, $p < 0.884$.

Based on the comparison of the Covariate and Full Models it can be concluded that anterior callosal partition did not account for a significant amount of variance in square root transformed number of between trial return errors on the CANTAB Spatial Working Memory task beyond that explained by nuisance variables.

Hypothesis 1: WASI Block Design Total Raw Score. Summary of model stages:

$$Stage\,1: \; WASI\ Block\ Design = Age + eTIV$$

$$Stage\,2: \; WASI\ Block\ Design = Age + eTIV + Anterior\ Corpus\ Callosum$$

Two-stage hierarchical ordinary least squares regression analysis was conducted on n = 294 participants in order to examine the relationship between total raw score on the Block Design subtest of WASI (WASI Block Design Total Raw Score) as the dependent variable, and centered volume of the region of the genu of the corpus callosum (CC Anterior) as independent variable, after controlling for a set of nuisance covariates. Preliminary regression analysis conducted with a full set of covariates including centered estimated Total Intracranial Volume (eTIV), centered age, centered quadratic term of age, gender, and handedness returned age and eTIV as two significant nuisance covariates which were retained in following hierarchical regression. In the first

Table 12

*Hypothesis 1 CANTAB SWM Between Trial Return Errors: Regression Coefficients. Significance: *** – p <0.001, ** – p <.01, * – p <.05, . – p <.1*

	Covariate Model			Full Model		
Variable	*B*	*SE B*	*Beta*	*B*	*SE B*	*Beta*
Age in Days	-0.001	0.000	-0.631***	-0.001	0.000	-0.632***
Anterior CC				0.000	0.001	0.006
R^2		0.399			0.399	
R^2 change		0.399			0.000	
F for change in R^2		1746.811***			0.021	

stage (Covariate Model) of the hierarchical regression model total raw score on the Block Design subtest of WASI was simultaneously regressed onto age and eTIV. In the second stage (Full Model) total raw score on the Block Design subtest of WASI was simultaneously regressed onto the nuisance covariates (age, eTIV) and the region of the genu of the corpus callosum. Estimated regression coefficients and model statistics for covariate and full models are summarized in table 13 on page 81.

Regression coefficients for the region of the genu of the corpus callosum were small, and non-significant predictors of WASI Block Design Total Raw Score (Bonferroni corrected $p <$ 0.006 with FWE controlled at $\alpha = .05$). At each stage of hierrahical regression amount of accounted variance was significantly different from zero with R2 = 0.621 for the Covariate model, and R^2 = 0.621 for the Full Model. While entry of the nuisance covariates (Covariate Model) resulted in a statistically significant increment in R^2 with $F(3,291) = 901.317$, $p < 0.000$, entry of the the Full Model did not account for a significant amount of variance beyond that explained by the Covariate Model alone with R^2-*change* = 0.000 with $F(1,290) = 0.005$, $p < 0.946$.

Based on the comparison of the Covariate and Full Models it can be concluded that region of the genu of the corpus callosum did not account for a significant amount of variance in total raw score on the Block Design subtest of WASI beyond that explained by nuisance variables.

Table 13

*Hypothesis 1 WASI Block Design Total Raw Score: Regression Coefficients. Significance: *** – $p < 0.001$, ** – $p < .01$, * – $p < .05$, . – $p < .1$*

	Covariate Model			Full Model		
Variable	*B*	*SE B*	*Beta*	*B*	*SE B*	*Beta*
eTIV	0.000**	0.000	0.121	0.000**	0.000	0.120
Age in Days	0.011***	0.001	0.750	0.011***	0.001	0.750
Anterior CC				0.000	0.006	0.003
R^2	0.621			0.621		
R^2 change	0.621			0.000		
F for change in R^2	901.317***			0.005		

Hypothesis 1: WASI Matrix Reasoning Total Raw Score. Summary of model stages:

$$Stage\,1: WASI\ Matrix\ Reasoning = Age + Age^2 + eTIV$$

$$Stage\,2: WASI\ Matrix\ Reasoning = Age + Age^2 + eTIV + Anterior\ Corpus\ Callosum$$

Two-stage hierarchical ordinary least squares regression analysis was conducted on n = 294 participants in order to examine the relationship between total raw score on the Matrix Reasoning subtest of WASI (WASI Matrix Reasoning Total Raw Score) as the dependent variable, and centered volume of the region of the genu of the corpus callosum (CC Anterior) as independent variable, after controlling for a set of nuisance covariates. Preliminary regression analysis conducted with a full set of covariates including centered estimated Total Intracranial Volume

(eTIV), centered age, centered quadratic term of age, gender, and handedness returned age, age quadratic, and eTIV as three significant nuisance covariates which were retained in following hierarchical regression analyses. In the first stage (Covariate Model) of the hierarchical regression model total raw score on the Matrix Reasoning subtest of WASI was simultaneously regressed onto age and eTIV. In the second stage (Full Model) total raw score on the Matrix Reasoning subtest of WASI was simultaneously regressed onto the nuisance covariates (age, age quadratic, eTIV) and the region of the genu of the corpus callosum. Estimated regression coefficients and model statistics for covariate and full models are summarized in table 14 on page 83.

Regression coefficients for the region of the genu of the corpus callosum were small, and non-significant predictors of WASI Matrix Reasoning Total Raw Score (Bonferroni corrected $p < 0.004$ with FWE controlled at $\alpha = .05$). At each stage of hierrahical regression amount of accounted variance was significantly different from zero with $R^2 = 0.595$ for the Covariate model, and $R^2 = 0.595$ for the Full Model. While entry of the nuisance covariates (Covariate Model) resulted in a statistically significant increment in R^2 with $F(4,290) = 2558.594$, $p < 0.000$, entry of the the Full Model did not account for a significant amount of variance beyond that explained by the Covariate Model alone with $R^2\text{-}change = 0.001$ with $F(1,289) = 0.378$, $p < 0.539$.

Based on the comparison of the Covariate and Full Models it can be concluded that region of the genu of the corpus callosum did not account for a significant amount of variance in total raw score on the Matrix Reasoning subtest of WASI beyond that explained by nuisance variables.

Hypothesis 1: WASI Matrix Reasoning Total Raw Score for a subset of participants 10 years or older. Summary of model stages:

$$Stage\,1: \; WASI\ Matrix\ Reasoning = Age + eTIV$$

$$Stage\,2: \; WASI\ Matrix\ Reasoning = Age + eTIV + Anterior\ Corpus\ Callosum$$

Because of a presence of quadratic relationship between age and WASI Matrix Reasoning Total Raw Score a scatterplot of the relationship was visually inspected in order to localize bend in the plotted relationship between variables. Examination of the scatterplot revealed that relationship between age and WASI Matrix Reasoning Total Raw Score stabilizes at approximately the age of 10 years. Data points of participants 10 years of age or older were selected and regression analysis was repeated on this subset of participants.

Table 14

*Hypothesis 1 WASI Matrix Reasoning Total Raw Score: Regression Coefficients. Significance: *** – $p < 0.001$, ** – $p < .01$, * – $p < .05$, . – $p < .1$*

	Covariate Model			Full Model		
Variable	*B*	*SE B*	*Beta*	*B*	*SE B*	*Beta*
eTIV	0.000***	0.000	0.132	0.000**	0.000	0.125
Age in Days	0.013***	0.001	2.621	0.013***	0.001	2.611
Age in Days quadratic	-0.000***	0.000	-1.962	-0.000***	0.000	-1.952
Anterior CC				0.001	0.002	0.024
R^2	0.595			0.595		
R^2 change	0.595			0.001		
F for change in R^2	2558.594***			0.378		

Two-stage hierarchical ordinary least squares regression analysis was conducted on a subset of n = 108 participants 10 years or older in order to examine the relationship between total raw score on the Matrix Reasoning subtest of WASI (WASI Matrix Reasoning Total Raw Score) as the dependent variable, and centered volume of the region of the genu of the corpus callosum (CC Anterior) as independent variable, after controlling for a set of nuisance covariates. Preliminary regression analysis conducted with a full set of covariates including centered estimated Total Intracranial Volume (eTIV), centered age, centered quadratic term of age, gender, and handedness returned age, age quadratic, and eTIV as three significant nuisance covariates which were retained in following hierarchical regression analyses. In the first stage (Covariate Model) of the hierarchical regression model total raw score on the Matrix Reasoning subtest of WASI was simultaneously regressed onto age and eTIV. In the second stage (Full Model) total raw score on the Matrix Reasoning subtest of WASI was simultaneously regressed onto the nuisance covariates (age, age quadratic, eTIV) and the region of the genu of the corpus callosum. Estimated regression coefficients and model statistics for covariate and full models are summarized in table 15 on page 85.

Regression coefficients for the region of the genu of the corpus callosum were very small, and non-significant predictors of WASI Matrix Reasoning Total Raw Score (Bonferroni corrected $p < 0.004$ with FWE controlled at $\alpha = .05$). At each stage of hierrahical regression amount of accounted variance was significantly different from zero with R^2 = 0.333 for the Covariate model, and R^2 = 0.336 for the Full Model. While entry of the nuisance covariates (Covariate Model) resulted in a statistically significant increment in R^2 with $F(4,104) = 331.831$, $p < 0.000$, entry of the the Full Model did not account for a significant amount of variance beyond that explained by the Covariate Model alone with R^2-change = 0.003 with $F(1,103) = 0.403$, $p < 0.527$.

Based on the comparison of the Covariate and Full Models it can be concluded that region of the genu of the corpus callosum did not account for a significant amount of variance in total raw score on the Matrix Reasoning subtest of WASI beyond that explained by nuisance variables. Presented results are consistent with results of the analysis conducted on the full sample.

Table 15

*Hypothesis 1 WASI Matrix Reasoning Total Raw Score (participants 10 years or older): Regression Coefficients.Significance: *** – $p < 0.001$, ** – $p < .01$, * – $p < .05$, . – $p < .1$*

	Covariate Model			Full Model		
Variable	*B*	*SE B*	*Beta*	*B*	*SE B*	*Beta*
eTIV	0.000**	0.000	0.240	0.000*	0.000	0.209
Age in Days	0.021	0.020	1.371	0.020	0.020	1.348
Anterior CC				-0.000	0.000	-0.899
R^2	0.333			0.336		
R^2 change	0.333			0.003		
F for change in R^2	331.831***			0.403		

Hypothesis 1: WISC–III Digit Coding B. Summary of model stages:

$$Stage\,1: WISC-III\ Coding\ B = Age + Handedness$$

$$Stage\,2: WISC-III\ Coding\ B = Age + Handedness + Anterior\ Corpus\ Callosum$$

Two-stage hierarchical ordinary least squares regression analysis was conducted on n = 209 participants in order to examine the relationship between total raw score on Coding B subtest of WISC–III (WISC–III Digit Coding B) as the dependent variable, and centered volume of the anterior callosal partition (Cent CC Anterior) as independent variable, after controlling for a set of nuissance covariates. Preliminary regression analysis conducted with a full set of covariates including centered estimated Total Intracranial Volume, centered Age, centered quadratic term of Age, gender, and handedness returned age and handedness as two significant nuisance covariates. Following analyses retained only age and handedness as nuisance covariates. In the first stage (Covariate Model) of the hierarchical regression model total raw score on Coding B subtest of WISC–III was simultaneously regressed onto age and gender. In the second stage (Full Model) total raw score on Coding B subtest of WISC–III was simultaneously regressed onto the nuisance covariates (age, gender) and the anterior callosal partition. Estimated regression coefficients and model statistics for covariate and full models are summarized in table 16 on page 87.

Regression coefficients for the anterior callosal partition were small, and non-significant predictors of WISC–III Digit Coding B (Bonferroni corrected $p < 0.008$ with FWE controlled at $\alpha = .05$). On this task right handers outperformed left handers. The average difference in performance on WISC–III Coding B for right-handers as compared to left handers holding age constant was 3.174 for the Covariate Model, and 3.145 for the Full Model. However, after correction for multiple tests handedness was no longer a significant predictor of performance on WISC–III Coding B. At each stage of hierrahical regression amount of accounted variance was significantly different from zero with R^2 = 0.667 for the Covariate model, and R^2 = 0.667 for the Full Model. While entry of the nuisance covariates (Covariate Model) resulted in a statistically significant increment in R^2 with $F(3,206) = 2517.556$, $p < 0.000$, entry of the the Full Model did not account for a significant amount of variance beyond that explained by the Covariate Model alone with R^2-*change* = 0.000 with $F(1,205) = 0.024$, $p < 0.878$.

Based on the comparison of the Covariate and Full Models it can be concluded that ante-

rior callosal partition did not account for a significant amount of variance in total raw score on Coding B subtest of WISC–III beyond that explained by nuisance variables.

Table 16

*Hypothesis 1 WISC–III Digit Coding B: Regression Coefficients. Significance: *** – $p < 0.001$, ** – $p < .01$, * – $p < .05$, . – $p < .1$ Handedness reference group: left handers.*

	Covariate Model			Full Model		
Variable	*B*	*SE B*	*Beta*	*B*	*SE B*	*Beta*
Age in days	0.014***	0.001	0.817	0.014***	0.001	0.817
Handedness	3.174*	1.271		3.145*	1.288	
Anterior CC				-0.001	0.005	-0.006
R^2	0.667			0.667		
R^2 change	0.667			0.000		
F for change in R^2	2517.556***			0.024		

Hypothesis 2: Posterior Corpus Callosum.

Hypothesis 2: WASI Block Design Total Raw Score. Summary of model stages:

$$Stage\,1: WASI\ Block\ Design = Age + eTIV$$

$$Stage\,2: WASI\ Block\ Design = Age + eTIV + Posterior\ Corpus\ Callosum$$

Two-stage hierarchical ordinary least squares regression analysis was conducted on n = 293 participants in order to examine the relationship between total raw score on the Block Design subtest of WASI (WASI Block Design Total Raw Score) as the dependent variable, and centered volume of the region of the splenium and the isthmus of the corpus callosum (CC Mid Posterior and Posterior) as independent variable, after controlling for a set of nuisance covariates. Preliminary regression analysis conducted with a full set of covariates including centered estimated Total

Intracranial Volume (eTIV), centered age, centered quadratic term of age, gender, and handedness returned age and eTIV as two significant nuisance covariates which were retained in following hierarchical regression. In the first stage (Covariate Model) of the hierarchical regression model total raw score on the Block Design subtest of WASI was simultaneously regressed onto age and eTIV. In the second stage (Full Model) total raw score on the Block Design subtest of WASI was simultaneously regressed onto the nuisance covariates (age, eTIV) and the region of the splenium and the isthmus of the corpus callosum. Estimated regression coefficients and model statistics for covariate and full models are summarized in table 17 on page 89.

Regression coefficients for the region of the splenium and the isthmus of the corpus callosum were small, and non-significant predictors of WASI Block Design Total Raw Score (Bonferroni corrected $p < 0.006$ with FWE controlled at $\alpha = .05$). At each stage of hierrahical regression amount of accounted variance was significantly different from zero with $R^2 = 0.621$ for the Covariate model, and $R^2 = 0.624$ for the Full Model. While entry of the nuisance covariates (Covariate Model) resulted in a statistically significant increment in R^2 with $F(3,291) = 901.317$, $p < 0.000$, entry of the the Full Model did not account for a significant amount of variance beyond that explained by the Covariate Model alone with R^2-*change* = 0.002 with $F(1,290) = 1.714$, $p < 0.192$.

Based on the comparison of the Covariate and Full Models it can be concluded that region of the splenium and the isthmus of the corpus callosum did not account for a significant amount of variance in total raw score on the Block Design subtest of WASI beyond that explained by nuisance variables.

Hypothesis 2: WASI Matrix Reasoning Total Raw Score. Summary of model stages:

$$Stage\,1: \; WASI\ Matrix\ Reasoning = Age + Age^2 + eTIV$$

$$Stage\,2: \; WASI\ Matrix\ Reasoning = Age + Age^2 + eTIV + Posterior\ Corpus\ Callosum$$

Two-stage hierarchical ordinary least squares regression analysis was conducted on n = 293 participants in order to examine the relationship between total raw score on the Matrix Reasoning subtest of WASI (WASI Matrix Reasoning Total Raw Score) as the dependent variable, and centered volume of the region of the splenium and the isthmus of the corpus callosum (CC Mid Posterior and Posterior) as independent variable, after controlling for a set of nuisance co-

Table 17

*Hypothesis 2 WASI Block Design Total Raw Score: Regression Coefficients. Significance: *** – $p < 0.001$, ** – $p < .01$, * – $p < .05$, . – $p < .1$*

	Covariate Model			Full Model		
Variable	*B*	*SE B*	*Beta*	*B*	*SE B*	*Beta*
eTIV	0.000**	0.000	0.121	0.000**	0.000	0.111
Age in Days	0.011***	0.001	0.750	0.011***	0.001	0.735
Posterior CC				0.005	0.004	0.051
R^2	0.621			0.624		
R^2 change	0.621			0.002		
F for change in R^2	901.317***			1.714		

variates. Preliminary regression analysis conducted with a full set of covariates including centered estimated Total Intracranial Volume (eTIV), centered age, centered quadratic term of age, gender, and handedness returned age, age quadratic, and eTIV as three significant nuisance covariates which were retained in following hierarchical regression analyses. In the first stage (Covariate Model) of the hierarchical regression model total raw score on the Matrix Reasoning subtest of WASI was simultaneously regressed onto age and eTIV. In the second stage (Full Model) total raw score on the Matrix Reasoning subtest of WASI was simultaneously regressed onto the nuisance covariates (age, eTIV) and the region of the splenium and the isthmus of the corpus callosum. Estimated regression coefficients and model statistics for covariate and full models are summarized in table 18 on page 91.

Regression coefficients for the region of the splenium and the isthmus of the corpus callosum were small, and non-significant predictors of WASI Matrix Reasoning Total Raw Score (Bonferroni corrected $p < 0.004$ with FWE controlled at $\alpha = .05$). At each stage of hierrahical regression amount of accounted variance was significantly different from zero with $R^2 = 0.595$ for the Covariate model, and $R^2 = 0.596$ for the Full Model. While entry of the nuisance covariates (Covariate Model) resulted in a statistically significant increment in R^2 with $F(4,290) = 2558.594$, $p < 0.000$, entry of the the Full Model did not account for a significant amount of variance beyond that explained by the Covariate Model alone with R^2-*change* = 0.001 with $F(1,289) = 0.973$, $p < 0.325$.

Based on the comparison of the Covariate and Full Models it can be concluded that region of the splenium and the isthmus of the corpus callosum did not account for a significant amount of variance in total raw score on the Matrix Reasoning subtest of WASI beyond that explained by nuisance variables.

Hypothesis 2: WASI Matrix Reasoning Total Raw Score for a subset of participants 10 years or older. Summary of model stages:

$$Stage\,1: \; WASI\ Matrix\ Reasoning = Age + eTIV$$

$$Stage\,2: \; WASI\ Matrix\ Reasoning = Age + eTIV + Posterior\ Corpus\ Callosum$$

Because of a presence of quadratic relationship between age and WASI Matrix Reasoning Total Raw Score a scatterplot of the relationship was visually inspected in order to localize bend

Table 18

*Hypothesis 2 WASI Matrix Reasoning Total Raw Score: Regression Coefficients. Significance: *** – $p < 0.001$, ** – $p < .01$, * – $p < .05$, . – $p < .1$*

	Covariate Model			Full Model		
Variable	*B*	*SE B*	*Beta*	*B*	*SE B*	*Beta*
eTIV	0.000***	0.000	0.132	0.000***	0.000	0.139
Age in Days	0.013***	0.001	2.621	0.013***	0.001	2.652
Age in Days quadratic	-0.000***	0.000	-1.962	-0.000***	0.000	-1.981
Posterior CC				-0.001	0.001	-0.040
R^2	0.595			0.596		
R^2 change	0.595			0.001		
F for change in R^2	2558.594***			0.973		

in the plotted relationship between variables. Examination of the scatterplot revealed that relationship between age and WASI Matrix Reasoning Total Raw Score stabilizes at approximately the age of 10 years. Data points of participants 10 years of age or older were selected and regression analysis was repeated on this subset of participants.

Two-stage hierarchical ordinary least squares regression analysis was conducted on a subset of n = 107 participants 10 years or older in order to examine the relationship between total raw score on the Matrix Reasoning subtest of WASI (WASI Matrix Reasoning Total Raw Score) as the dependent variable, and centered volume of the region of the splenium and the isthmus of the corpus callosum (CC Mid Posterior and Posterior) as independent variable, after controlling for a set of nuisance covariates. Preliminary regression analysis conducted with a full set of covariates including centered estimated Total Intracranial Volume (eTIV), centered age, centered quadratic term of age, gender, and handedness returned age, age quadratic, and eTIV as three significant nuisance covariates which were retained in following hierarchical regression analyses. In the first stage (Covariate Model) of the hierarchical regression model total raw score on the Matrix Reasoning subtest of WASI was simultaneously regressed onto age and eTIV. In the second stage (Full Model) total raw score on the Matrix Reasoning subtest of WASI was simultaneously regressed onto the nuisance covariates (age, age quadratic, eTIV) and the region of the splenium and the isthmus of the corpus callosum. Estimated regression coefficients and model statistics for covariate and full models are summarized in table 19 on page 93.

Regression coefficients for the region of the splenium and the isthmus of the corpus callosum were small, and non-significant predictors of WASI Matrix Reasoning Total Raw Score (Bonferroni corrected $p < 0.004$ with FWE controlled at $\alpha = .05$). At each stage of hierrahical regression amount of accounted variance was significantly different from zero with R^2 = 0.330 for the Covariate model, and R^2 = 0.331 for the Full Model. While entry of the nuisance covariates (Covariate Model) resulted in a statistically significant increment in R^2 with $F(4,103) = 324.696$, $p < 0.000$, entry of the the Full Model did not account for a significant amount of variance beyond that explained by the Covariate Model alone with R^2-change = 0.001 with $F(1,102) = 0.083$, $p < 0.774$.

Based on the comparison of the Covariate and Full Models it can be concluded that region of the splenium and the isthmus of the corpus callosum did not account for a significant amount

of variance in total raw score on the Matrix Reasoning subtest of WASI beyond that explained by nuisance variables. Presented results are consistent with results of the analysis conducted on the full sample.

Table 19

*Hypothesis 2 WASI Matrix Reasoning Total Raw Score (participants 10 years or older): Regression Coefficients. Significance: *** – $p < 0.001$, ** – $p < .01$, * – $p < .05$, . – $p < .1$*

	Covariate Model			Full Model		
Variable	*B*	*SE B*	*Beta*	*B*	*SE B*	*Beta*
eTIV	0.000**	0.000	0.243	0.000**	0.000	0.237
Age in Days	0.020	0.020	1.326	0.021	0.020	1.387
Posterior CC				-0.000	0.000	-0.939
R^2	0.330			0.331		
R^2 change	0.330			0.001		
F for change in R^2	324.696***			0.083		

Hypothesis 2: WISC-III Digit Coding B. Summary of model stages:

$$Stage\,1: WISC-III\ Coding\ B = Age + Gender$$

$$Stage\,2: WISC-III\ Coding\ B = Age + Gender + Posterior\ Corpus\ Callosum$$

Two-stage hierarchical ordinary least squares regression analysis was conducted on n = 208 participants in order to examine the relationship between total raw score on Coding B subtest of WISC-III (WISC-III Digit Coding B) as the dependent variable, and centered volume of the region of the splenium and the isthmus of the corpus callosum (CC Mid Posterior and Posterior) as independent variable, after controlling for a set of nuisance covariates. Preliminary regression analysis conducted with a full set of covariates including centered estimated Total Intracranial

Volume (eTIV), centered age, centered quadratic term of age, gender, and handedness returned age, age quadratic, and eTIV as three significant nuisance covariates which were retained in following hierarchical regression analyses. In the first stage (Covariate Model) of the hierarchical regression model total raw score on Coding B subtest of WISC-III was simultaneously regressed onto age and gender. In the second stage (Full Model) total raw score on Coding B subtest of WISC-III was simultaneously regressed onto the nuisance covariates (age, gender) and the region of the splenium and the isthmus of the corpus callosum. Estimated regression coefficients and model statistics for covariate and full models are summarized in table 20 on page 95.

Regression coefficients for the region of the splenium and the isthmus of the corpus callosum were small, and non-significant predictors of WISC-III Digit Coding B (Bonferroni corrected $p < 0.004$ with FWE controlled at $\alpha = .05$). Females outperformed males on WISC-III Coding B. The average difference in performance on WISC-III Coding B for females as compared to males holding age constant was approximately 4 units for both the Covariate Model and Full Models. However, after correction for multiple tests gender was no longer a significant predictor of performance on WISC-III Coding B.

At each stage of hierrahical regression amount of accounted variance was significantly different from zero with $R^2 = 0.668$ for the Covariate model, and $R^2 = 0.669$ for the Full Model. While entry of the nuisance covariates (Covariate Model) resulted in a statistically significant increment in R^2 with $F(4,205) = 1888.157$, $p < 0.000$, entry of the the Full Model did not account for a significant amount of variance beyond that explained by the Covariate Model alone with $R^2\text{-}change = 0.000$ with $F(1,204) = 0.287$, $p < 0.593$.

Based on the comparison of the Covariate and Full Models it can be concluded that region of the splenium and the isthmus of the corpus callosum did not account for a significant amount of variance in total raw score on Coding B subtest of WISC-III beyond that explained by nuisance variables.

Comprehensive Regression Model

The final three-stage hierarchical OLS regression analyses were performed between measures of cognitive performance as dependent variables, with age, its quadratic term, sex, and handedness as covariates, and volumes of frontal and parietal gray matter entered first followed by volumes of frontal and parietal white matter and anterior and posterior corpus callosum all en-

Table 20

*Hypothesis 2 WISC-III Digit Coding B: Regression Coefficients. Significance: *** – $p < 0.001$, ** – $p < .01$, * – $p < .05$, . – $p < .1$ Gender reference group: males.*

	Covariate Model			Full Model		
Variable	*B*	*SE B*	*Beta*	*B*	*SE B*	*Beta*
Age in Days	0.014***	0.001	0.812	0.014***	0.001	0.808
Gender	4.009**	1.527		4.040**	1.531	
Posterior CC				0.002	0.003	0.023
R^2	0.668			0.669		
R^2 change	0.668			0.000		
F for change in R^2	1888.157***			0.287		

tered as independent variables. Analyses were performed using R (Team, 2009) employing CAR library (Fox & Weisberg, 2011).

At the first step, WASI Block Design, WASI Matrix Reasoning, CANTAB Spatial Working Memory (number of between errors), and WISC-III Coding B raw scores were separately regressed onto the estimated Total Intracranial Volume (Buckner et al., 2004), age, quadratic transform of age, handedness score, and dummy-coded gender.

At the second step, WASI Block Design, WASI Matrix Reasoning, CANTAB Spatial Working Memory (number of between errors) as well as WISC-III Coding B raw scores were regressed in a series of equations onto left and right frontal and parietal gray mater volumes.

At the third step, WASI Block Design, WASI Matrix Reasoning, CANTAB Spatial Working Memory (number of between errors) as well as WISC-III Coding B raw scores were regressed in a series of equations onto volume of the region of the genu of the corpus callosum, volume of the region of the splenium and isthmus of the corpus callosum, the left and right frontal and parietal white mater volumes.

After accounting for nuisance covariates and elementary role of gray matter in information processing, in this model unique contributions of separate white matter structures to cognitive efficiency are being evaluated. Simultaneous entry of white matter structures allows for estimation of unique contributions of each white matter structure beyond this explained by other white matter structures, gray matter, and the nuisance covariates. This model is summarized in figure 4 on page 48.

Comprehensive Regression Model: CANTAB SWM Between Trial Return Errors. Summary of model stages:

$$\begin{aligned}
&Stage\,1: CANTAB\,SWM = Age \\
&Stage\,2: CANTAB\,SWM = Age + Frontal\ Gray\ Matter + Parietal\ Gray\ Matter \\
&Stage\,3: CANTAB\,SWM = Age + Frontal\ Gray\ Matter + Parietal\ Gray\ Matter \\
&\qquad + Frontal\ White\ Matter + Parietal\ White\ Matter + \\
&\qquad + Anterior\ Corpus\ Callosum + Posterior\ Corpus\ Callosum
\end{aligned}$$

Because of the positive skewness present in the number of between trial return errors on the CANTAB Spatial Working Memory task a series of transforms was conducted on this vari-

able including inverse, natural logarithm, square root, and Box-Cox $\lambda = .5$. From among those transformations square root resulted in most improvement of distribution normality. Prior to conducting analyses root square transform was applied to the number of between trial return errors on the CANTAB Spatial Working Memory task in order to allievate positive skewness present in the distribution. Square root transform resulted in a an improvement of distribution characteristics as evidenced by Shapiro-Wilk statistic changes from W = .925, $p > 0.00000$ for raw data with outliers to W = .972, $p > .00001$ after transform. Resulting distribution was examined and accepted as sufficient despite remaining departure from normality. Subsequently a three-stage hierarchical ordinary least squares regression analysis was conducted on n = 316 participants in order to examine the relationship between number of between trial return errors on the CANTAB Spatial Working Memory task (CANTAB SWM Between Trial Return Errors) as the dependent variable, and centered summed volume of: the left and right region of the genu of the corpus callosum (Cent CC Anterior), region of the splenium and isthmus of the corpus callosum (Cent CC Mid Posterior and Posterior), frontal white mater (Cent wm rlh frontallobe), parietal white mater (Cent wm rlh parietallobe), frontal grey mater (Cent ctx rlh frontallobe), parietal grey mater (Cent ctx rlh parietallobe) as predictor variables, after correcting for nuisance covariates. Preliminary regression analysis conducted with a full set of covariates including centered estimated Total Intracranial Volume (eTIV), centered age, centered quadratic term of age, gender, and handedness returned age as the sole significant nuisance covariate which was retained in following hierarchical regression analyses. In the first stage (Covariate Model) of the hierarchical regression model number of between trial return errors on the CANTAB Spatial Working Memory task was regressed onto age. In the second stage (Gray Matter Model) number of between trial return errors on the CANTAB Spatial Working Memory task was simultaneously regressed onto the nuisance covariate (age) and volumes of the frontal and parietal grey mater. In the third stage (Full Model) number of between trial return errors on the CANTAB Spatial Working Memory task was simultaneously regressed onto the nuisance covariate (age), volumes of the frontal and parietal grey mater, and volumes of frontal and parietal white matter, and anterior and posterior partitions of the corpus callosum. Estimated regression coefficients and model statistics for covariate and full models are summarized in table 21 on page 99. Regression coefficients for the gray and white matter variables were small, and non-significant predictors of CANTAB SWM Between Trial Re-

turn Errors (Bonferroni corrected $p < 0.002$ with FWE controlled at $\alpha = .05$). At each stage of hierrahical regression amount of accounted variance was significantly different from zero with $R^2 = 0.399$ for the Covariate model, and $R^2 = 0.400$ for the Gray Matter Model, and $R^2 = 0.405$ for the Full Model. While entry of age (Covariate Model) resulted in a statistically significant increment in R^2 with $F(2,315) = 1746.811$, $p < 0.000$, entry of the the Gray Matter Model did not account for a significant amount of variance beyond that explained by the Covariate Model alone with R^2-*change* = 0.001 with $F(2,313) = 0.383$, $p < 0.682$. Entry of the the Full Model did not account for a significant amount of variance beyond that explained by the Gray Matter Model alone with R^2-*change* = 0.005 with $F(4,309) = 0.671$, $p < 0.613$. Based on the comparison of the Covariate, Gray Matter, and Full Models it can be concluded that gray matter volume did not account for a significant amount of variance in number of between trial return errors on the CANTAB Spatial Working Memory task beyond that explained by nuisance variables, and white matter did not account for a significant amount of variance in number of between trial return errors on the CANTAB Spatial Working Memory task beyond that explained by nuisance variables and gray matter considered simultaneously.

Comprehensive Regression Model: WASI Block Design Total Raw Score. Summary of model stages:

$$\begin{aligned}
&Stage\,1: \; WASI\ Block\ Design = Age \\
&Stage\,2: \; WASI\ Block\ Design = Age + Frontal\ Gray\ Matter + Parietal\ Gray\ Matter \\
&Stage\,3: \; WASI\ Block\ Design = Age + Frontal\ Gray\ Matter + Parietal\ Gray\ Matter \\
&\qquad\qquad + Frontal\ White\ Matter + Parietal\ White\ Matter + \\
&\qquad\qquad + Anterior\ Corpus\ Callosum + Posterior\ Corpus\ Callosum
\end{aligned}$$

Three-stage hierarchical ordinary least squares regression analysis was conducted on n = 293 participants in order to examine the relationship between total raw score on the Block Design subtest of WASI (WASI Block Design Total Raw Score) as the dependent variable, and centered summed volume of: the left and right region of the genu of the corpus callosum (Cent CC Anterior), region of the splenium and isthmus of the corpus callosum (Cent CC Mid Posterior and Posterior), frontal white mater (Cent wm rlh frontallobe), parietal white mater (Cent wm rlh parietallobe), frontal grey mater (Cent ctx rlh frontallobe), parietal grey mater (Cent ctx rlh parietal-

Table 21

*Comprehensive Regression Model CANTAB SWM Between Trial Return Errors: Regression Coefficients. Significance: *** – $p < 0.001$, ** – $p < .01$, * – $p < .05$, . – $p < .1$*

	Covariate Model			Gray Matter Model			Full Model		
Variable	*B*	*SE B*	*Beta*	*B*	*SE B*	*Beta*	*B*	*SE B*	*Beta*
Age in days	-0.001***	0.000	-0.631	-0.001***	0.000	-0.644	-0.001***	0.000	-0.630
Frontal Gray				0.000	0.000	0.059	0.000	0.000	0.022
Parietal Gray				-0.000	0.000	-0.067	-0.000	0.000	-0.029
Anterior CC							0.000	0.001	0.026
Posterior CC							-0.000	0.001	-0.034
Frontal White							0.000	0.000	0.127
Parietal White							-0.000	0.000	-0.144
R^2	0.399			0.400			0.405		
R^2 change	0.399			0.001			0.005		
F for change in R^2	1746.811***			0.383			0.671		

lobe) as predictor variables, after correcting for nuisance covariates. Preliminary regression analysis conducted with a full set of covariates including centered estimated Total Intracranial Volume (eTIV), centered age, centered quadratic term of age, gender, and handedness returned age as the sole significant nuisance covariate which was retained in following hierarchical regression analyses. In the first stage (Covariate Model) of the hierarchical regression model total raw score on the Block Design subtest of WASI was regressed onto age. In the second stage (Gray Matter Model) total raw score on the Block Design subtest of WASI was simultaneously regressed onto the nuissance covariate (age) and volumes of the frontal and parietal grey mater. In the third stage (Full Model) total raw score on the Block Design subtest of WASI was simultaneously regressed onto the nuisance covariate (age), volumes of the frontal and parietal grey mater, and volumes of frontal and parietal white matter, and anterior and posterior partitions of the corpus callosum. Estimated regression coefficients and model statistics for covariate and full models are summarized in table 22 on page 101. Regression coefficients for the gray and white matter variables were small, and non-significant predictors of WASI Block Design Total Raw Score (Bonferroni corrected $p < 0.002$ with FWE controlled at $\alpha = .05$). At each stage of hierrahical regression amount of accounted variance was significantly different from zero with $R^2 = 0.608$ for the Covariate model, and $R^2 = 0.630$ for the Gray Matter Model, and $R^2 = 0.635$ for the Full Model. Entry of age (Covariate Model) and gray matter (Gray Matter Model) both resulted in a statistically significant increments in R^2 with $F(2,292) = 1304.380$, $p < 0.000$ for the Covariate Model and R^2-*change* = 0.022 with $F(2,290) = 8.575$, $p < 0.000$ for the Gray Matter Model. However, entry of the the Full Model did not account for a significant amount of variance beyond that explained by the Gray Matter Model with R^2-*change* = 0.005 with $F(4,286) = 0.962$, $p < 0.429$. Based on the comparison of the Covariate, Gray Matter, and Full Models it can be concluded that while none of the gray matter predictors reached significance, entry of gray matter significantly improved model fit over that accounted for by age alone. In contrast, white matter did not account for a significant amount of variance in total raw score on the Block Design subtest of WASI beyond that explained by nuisance variables and gray matter considered simultaneously.

Table 22

*Comprehensive Regression Model WASI Block Design Total Raw Score: Regression Coefficients. Significance: *** – $p < 0.001$, ** – $p < .01$, * – $p < .05$, . – $p < .1$*

	Covariate Model			Gray Matter Model			Full Model		
Variable	*B*	*SE B*	*Beta*	*B*	*SE B*	*Beta*	*B*	*SE B*	*Beta*
Age in days	0.012***	0.001	0.780	0.013***	0.001	0.835	0.012***	0.001	0.804
Frontal Gray				0.000.	0.000	0.106	0.000	0.000	0.109
Parietal Gray				0.000	0.000	0.060	0.000	0.000	0.045
Anterior CC							-0.007	0.007	-0.050
Posterior CC							0.007.	0.004	0.078
Frontal White							-0.000	0.000	-0.043
Parietal White							0.000	0.000	0.070
R^2	0.608			0.630			0.635		
R^2 change	0.608			0.022			0.005		
F for change in R^2	1304.380***			8.575***			0.962		

Comprehensive Regression Model: WASI Matrix Reasoning Total Raw Score. Summary of model stages:

$$\begin{aligned}
Stage\,1: WASI\ Matrix\ Reasoning &= Age + Age^2 \\
Stage\,2: WASI\ Matrix\ Reasoning &= Age + Age^2 + Frontal\ Gray\ Matter + Parietal\ Gray\ Matter \\
Stage\,3: WASI\ Matrix\ Reasoning &= Age + Age^2 + Frontal\ Gray\ Matter + Parietal\ Gray\ Matter \\
&\quad + Frontal\ White\ Matter + Parietal\ White\ Matter + \\
&\quad + Anterior\ Corpus\ Callosum + Posterior\ Corpus\ Callosum
\end{aligned}$$

Three-stage hierarchical ordinary least squares regression analysis was conducted on *n* = 293 participants in order to examine the relationship between total raw score on the Matrix Reasoning subtest of WASI (WASI Matrix Reasoning Total Raw Score) as the dependent variable, and centered summed volume of: the left and right region of the genu of the corpus callosum (Cent CC Anterior), region of the splenium and isthmus of the corpus callosum (Cent CC Mid Posterior and Posterior), frontal white mater (Cent wm rlh frontallobe), parietal white mater (Cent wm rlh parietallobe), frontal grey mater (Cent ctx rlh frontallobe), parietal grey mater (Cent ctx rlh parietallobe) as predictor variables, after correcting for nuisance covariates. Preliminary regression analysis conducted with a full set of covariates including centered estimated Total Intracranial Volume (eTIV), centered age, centered quadratic term of age, gender, and handedness returned age in its linear and quadratic forms as the significant nuisance covariate which was retained in following hierarchical regression analyses. In the first stage (Covariate Model) of the hierarchical regression model total raw score on the Matrix Reasoning subtest of WASI was simultaneously regressed onto age and its quadratic term. In the second stage (Gray Matter Model) total raw score on the Matrix Reasoning subtest of WASI was simultaneously regressed onto the nuisance covariate (age, age quadratic) and volumes of the frontal and parietal grey mater. In the third stage (Full Model) total raw score on the Matrix Reasoning subtest of WASI was simultaneously regressed onto the nuisance covariate (age, age quadratic), volumes of the frontal and parietal grey mater, and volumes of frontal and parietal white matter, and anterior and posterior partitions of the corpus callosum. Estimated regression coefficients and model statistics for covariate and full models are summarized in table 23 on page 104. Parietal gray matter volume was a significant predictor of WASI Matrix Reasoning Total Raw Score prior to correction for

multiple tests. However, after applying Bonferroni correction with $p < 0.002$ controlling FWE controlled at $\alpha = .05$ none of the gray and white matter variables were significant predictors of WASI Matrix Reasoning Total Raw Score. At each stage of hierrahical regression amount of accounted variance was significantly different from zero with $R^2 = 0.578$ for the Covariate model, and $R^2 = 0.600$ for the Gray Matter Model, and $R^2 = 0.603$ for the Full Model. Entry of age and its quadratic term (Covariate Model) and gray matter volumes (Gray Matter Model) both resulted in a statistically significant increment in R^2 with $F(3,291) = 3286.817$, $p < 0.000$ for Covariate Model, and R^2-*change* = 0.021 with $F(2,289) = 7.654$, $p < 0.001$ for the Gray Matter Model. In contrast, entry of the the Full Model including white matter structures has not accounted for a significant amount of variance beyond that explained by the Gray Matter Model alone with R^2-*change* = 0.003 with $F(4,285) = 0.604$, $p < 0.660$.

Based on the comparison of the Covariate, Gray Matter, and Full Models it can be concluded that while none of the gray matter predictors reached significance, entry of gray matter significantly improved model fit over that explained by linear and quadratic age terms alone accounting for an additional 2% of variability in total raw score on the Matrix Reasoning subtest of WASI. In contrast, white matter did not account for a significant amount of variance in total raw score on the Matrix Reasoning subtest of WASI beyond that explained by linear and quadratic age terms and gray matter considered simultaneously. While statistically significant this contribution is small and negligible.

Comprehensive Regression Model: WASI Matrix Reasoning Total Raw Score for a subset of participants 10 years or older. Summary of model stages:

$$\begin{aligned}
&Stage\,1: \; WASI\ Matrix\ Reasoning = Age \\
&Stage\,2: \; WASI\ Matrix\ Reasoning = Age + Frontal\ Gray\ Matter + Parietal\ Gray\ Matter \\
&Stage\,3: \; WASI\ Matrix\ Reasoning = Age + Frontal\ Gray\ Matter + Parietal\ Gray\ Matter \\
&\qquad\qquad + Frontal\ White\ Matter + Parietal\ White\ Matter + \\
&\qquad\qquad + Anterior\ Corpus\ Callosum + Posterior\ Corpus\ Callosum
\end{aligned}$$

Because of a presence of quadratic relationship between age and WASI Matrix Reasoning Total Raw Score a scatterplot of the relationship was visually inspected in order to localize bend in the plotted relationship between variables. Examination of the scatterplot revealed that relation-

Table 23

*Comprehensive Regression Model WASI Matrix Reasoning Total Raw Score: Regression Coefficients. Significance: *** – $p < 0.001$, ** – $p < .01$, * – $p < .05$, . – $p < .1$*

	Covariate Model			Gray Matter Model			Full Model		
Variable	*B*	*SE B*	*Beta*	*B*	*SE B*	*Beta*	*B*	*SE B*	*Beta*
Age in days	0.014***	0.001	2.703	0.014***	0.001	2.741	0.014***	0.001	2.745
Age in days quadratic	-0.000***	0.000	-2.012	-0.000***	0.000	-1.979	-0.000***	0.000	-1.982
Frontal Gray				-0.000	0.000	-0.008	-0.000	0.000	-0.002
Parietal Gray				0.000*	0.000	0.168	0.000.	0.000	0.140
Anterior CC							0.003	0.002	0.056
Posterior CC							-0.002	0.002	-0.068
Frontal White							-0.000	0.000	-0.013
Parietal White							0.000	0.000	0.035
R^2	0.578			0.600			0.603		
R^2 change	0.578			0.021			0.003		
F for change in R^2	3286.817***			7.654***			0.604		

ship between age and WASI Matrix Reasoning Total Raw Score stabilizes at approximately the age of 10 years. Data points of participants 10 years of age or older were selected and regression analysis was repeated on this subset of participants.

Three-stage hierarchical ordinary least squares regression analysis was conducted on a subset of n = 130 participants 10 years of age and older in order to examine the relationship between total raw score on the Matrix Reasoning subtest of WASI (WASI Matrix Reasoning Total Raw Score) as the dependent variable, and centered summed volume of: the left and right region of the genu of the corpus callosum (Cent CC Anterior), region of the splenium and isthmus of the corpus callosum (Cent CC Mid Posterior and Posterior), frontal white mater (Cent wm rlh frontallobe), parietal white mater (Cent wm rlh parietallobe), frontal grey mater (Cent ctx rlh frontallobe), parietal grey mater (Cent ctx rlh parietallobe) as predictor variables, after correcting for nuisance covariates. Preliminary regression analysis conducted with a full set of covariates including centered estimated Total Intracranial Volume (eTIV), centered age, centered quadratic term of age, gender, and handedness returned age in its linear and quadratic forms as the significant nuisance covariate which was retained in following hierarchical regression analyses. In the first stage (Covariate Model) of the hierarchical regression model total raw score on the Matrix Reasoning subtest of WASI was simultaneously regressed onto age. In the second stage (Gray Matter Model) total raw score on the Matrix Reasoning subtest of WASI was simultaneously regressed onto the nuisance covariate (age) and volumes of the frontal and parietal grey mater. In the third stage (Full Model) total raw score on the Matrix Reasoning subtest of WASI was simultaneously regressed onto the nuisance covariate (age), volumes of the frontal and parietal grey mater, and volumes of frontal and parietal white matter, and anterior and posterior partitions of the corpus callosum. Estimated regression coefficients and model statistics for covariate and full models are summarized in table 24 on page 107. Parietal gray matter volume was a significant predictor of WASI Matrix Reasoning Total Raw Score prior to correction for multiple tests. However, after applying Bonferroni correction with $p < 0.002$ controlling FWE controlled at $\alpha = .05$ none of the gray and white matter variables were significant predictors of WASI Matrix Reasoning Total Raw Score. At each stage of hierrahical regression amount of accounted variance was significantly different from zero with R^2 = 0.268 for the Covariate model, and R^2 = 0.330 for the Gray Matter Model, and R^2 = 0.353 for the Full Model. Entry of age and its quadratic term (Co-

variate Model) and gray matter volumes (Gray Matter Model) both resulted in a statistically significant increment in R^2 with $F(2,105) = 601.184$, $p < 0.000$ for Covariate Model, and R^2-*change* = 0.062 with $F(2,103) = 4.770$, $p < 0.010$ for the Gray Matter Model. In contrast, entry of the the Full Model including white matter structures has not accounted for a significant amount of variance beyond that explained by the Gray Matter Model alone with R^2-*change* = 0.023 with $F(4,99) = 0.891$, $p < 0.472$.

Based on the comparison of the Covariate, Gray Matter, and Full Models it can be concluded that while none of the gray matter predictors reached significance, entry of gray matter significantly improved model fit over that explained by linear and quadratic age terms alone. In contrast, white matter did not account for a significant amount of variance in total raw score on the Matrix Reasoning subtest of WASI beyond that explained by linear and quadratic age terms and gray matter considered simultaneously.

Comprehensive Regression Model: WISC-III Digit Coding B. Summary of model stages:

$$\begin{aligned}
&Stage\,1: \; WISC-III\,Coding\,B = Age + Gender \\
&Stage\,2: \; WISC-III\,Coding\,B = Age + Gender + Frontal\;Gray\;Matter + Parietal\;Gray\;Matter \\
&Stage\,3: \; WISC-III\,Coding\,B = Age + Gender + Frontal\;Gray\;Matter + Parietal\;Gray\;Matter \\
&\qquad\qquad + Frontal\;White\;Matter + Parietal\;White\;Matter + \\
&\qquad\qquad + Anterior\;Corpus\;Callosum + Posterior\;Corpus\;Callosum
\end{aligned}$$

Three-stage hierarchical ordinary least squares regression analysis was conducted on n = 208 participants in order to examine the relationship between total raw score on Coding B subtest of WISC-III (WISC-III Digit Coding B) as the dependent variable, and centered summed volume of: the left and right region of the genu of the corpus callosum (Cent CC Anterior), region of the splenium and isthmus of the corpus callosum (Cent CC Mid Posterior and Posterior), frontal white mater (Cent wm rlh frontallobe), parietal white mater (Cent wm rlh parietallobe), frontal grey mater (Cent ctx rlh frontallobe), parietal grey mater (Cent ctx rlh parietallobe) as predictor variables, after correcting for nuisance covariates. Preliminary regression analysis conducted with a full set of covariates including centered estimated Total Intracranial Volume (eTIV), centered age, centered quadratic term of age, gender, and handedness returned age and gender as the significant nuisance covariate which was retained in following hierarchical regression analyses. In

Table 24

Comprehensive Regression Model WASI Matrix Reasoning Total Raw Score (participants 10 years or older): Regression Coefficients.

*Significance: *** – $p < 0.001$, ** – $p < .01$, * – $p < .05$, . – $p < .1$*

	Covariate Model			Gray Matter Model			Full Model		
Variable	*B*	*SE B*	*Beta*	*B*	*SE B*	*Beta*	*B*	*SE B*	*Beta*
Age in days	0.008***	0.001	0.518	0.008***	0.001	0.509	0.007***	0.001	0.498
Frontal Gray				0.000	0.000	0.033	0.000	0.000	0.083
Parietal Gray				0.000.	0.000	0.224	0.000	0.000	0.165
Anterior CC							0.005	0.006	0.089
Posterior CC							0.002	0.004	0.040
Frontal White							-0.000	0.000	-0.237
Parietal White							0.000	0.000	0.230
R^2	0.268			0.330			0.353		
R^2 change	0.268			0.062			0.023		
F for change in R^2	601.184***			4.770*			0.891		

the first stage (Covariate Model) of the hierarchical regression model total raw score on Coding B subtest of WISC-III was simultaneously regressed onto age and gender. In the second stage (Gray Matter Model) total raw score on Coding B subtest of WISC-III was simultaneously regressed onto the nuisance covariate (age, gender) and volumes of the frontal and parietal grey mater. In the third stage (Full Model) total raw score on Coding B subtest of WISC-III was simultaneously regressed onto the nuissance covariate (age, gender), volumes of the frontal and parietal grey mater, and volumes of frontal and parietal white matter, and anterior and posterior partitions of the corpus callosum. Estimated regression coefficients and model statistics for covariate and full models are summarized in table 25 on page 109. Regression coefficients for the gray and white matter variables were small, and non-significant predictors of WISC-III Digit Coding B (Bonferroni corrected $p < 0.002$ with FWE controlled at $\alpha = .05$). Females outperformed males on WISC-III Coding B. The average difference in performance on WISC-III Coding B for females as compared to males holding age constant was 3.888 units for the Covariate Model and 4.328 units for the Full Model. However, after correction for multiple tests gender was no longer a significant predictor of performance on WISC-III Coding B.

At each stage of hierrahical regression amount of accounted variance was significantly different from zero with $R^2 = 0.667$ for the Covariate model, and $R^2 = 0.671$ for the Gray Matter Model, and $R^2 = 0.678$ for the Full Model. While entry of age and gender (Covariate Model) resulted in a statistically significant increment in R^2 with $F(3,206) = 2517.556$, $p < 0.000$, entry of the Gray Matter Model did not account for a significant amount of variance beyond that explained by the Covariate Model alone with R^2-*change* = 0.004 with $F(2,204) = 1.240$, $p < 0.291$.

Entry of the the Full Model including white matter structures also has not accounted for a significant amount of variance beyond that explained by the Gray Matter Model alone with R^2-*change* = 0.007 with $F(4,200) = 1.163$, $p < 0.328$.

Based on the comparison of the Covariate, Gray Matter, and Full Models it can be concluded that gray matter volume did not account for a significant amount of variance in total raw score on Coding B subtest of WISC-III beyond that explained by nuisance variables, and white matter did not account for a significant amount of variance in total raw score on Coding B subtest of WISC-III beyond that explained by nuisance variables and gray matter considered simultaneously.

Table 25

*Comprehensive Regression Model WISC-III Digit Coding B: Regression Coefficients. Significance: *** – $p < 0.001$, ** – $p < .01$, * – $p < .05$, . – $p < .1$ Gender reference group: males.*

	Covariate Model			Gray Matter Model			Full Model		
Variable	*B*	*SE B*	*Beta*	*B*	*SE B*	*Beta*	*B*	*SE B*	*Beta*
Age in days	0.014***	0.001	0.817	0.014***	0.001	0.826	0.014***	0.001	0.793
Gender	3.174*	1.271		3.888**	1.437		4.328**	1.495	
Frontal Gray				0.000	0.000	0.106	0.000	0.000	0.121
Parietal Gray				-0.000	0.000	-0.057	-0.000	0.000	-0.103
Anterior CC							-0.006	0.006	-0.046
Posterior CC							0.004	0.004	0.047
Frontal White							-0.000	0.000	-0.083
Parietal White							0.000.	0.000	0.150
R^2	0.667			0.671			0.678		
R^2 change	0.667			0.004			0.007		
F for change in R^2	2517.556***			1.240			1.163		

DISCUSSION

In the field of neuroscience in general, and neuroimaging in particular theoretical developments often lag behind basic research and advances in available tools. In the field of research on the relation between intellectual abilities and brain morphology, a body of evidence has accumulated relating morphometric measures of varying degrees of specificity to mostly general measures of cognitive ability. This study attempted to build on a more rigorous theoretical framework that focused on brain lobes along with partitions of the corpus callosum, and specific cognitive tests underlined by specific cognitive processes and well defined anatomical correlates. This study followed existing theoretical approaches stating that (1) higher cognitive abilities emerge from the integration of cognitive resources at higher levels of brain organization and (2) larger size/volume of white matter structures carries greater processing power. The selection of the anatomical target structure of interest, the corpus callosum, followed from a tradition of empirical research linking corpus callosum to higher cognition. Pairing of a specific section of the corpus callosum (e.g. anterior vs. posterior) and specific cognitive test was informed by:

1. empirical studies linking this tests to specific brain lobe or a set of brain lobes
2. theoretical knowledge of what cognitive processes are expected to underline performance on each cognitive test
3. theoretical knowledge of which lobes are differentially involved by those cognitive processes
4. topography of callosal connections with specific brain lobes
5. pairings of callosal sections carrying axons interconnecting specific brain lobes and specific cognitive tests shown to differentially engage those brain lobes

The criteria for selecting cognitive measures were that (1) the selected test is relatively difficult thus theoretically it should promote inter-hemispheric recruitments and (2) that there is relatively consistent empirical evidence of bilateral involvement during performance on those tests.

Hypothesis 1

The results of the test of hypothesis 1 suggest that upon correcting for age and other significant nuisance covariates, there is no evidence in support of a significant link between the volume of the anterior fifth of the corpus callosum and performance on CANTAB SWM Between Trial Errors, WISC-III Coding B, WASI Block Design, or WASI Matrix Reasoning. In the present study the volume of the region of the genu of the corpus callosum is neither a significant predictor of the number of between trial return errors on CANTAB Spatial Working Memory subtest, nor of performance on WISC-III Digit Coding B, or WASI Matrix Reasoning, or WASI Block Design. This null finding is unexpected provided reviewed evidence linking (1) changes in the micro- and macro-structure of the white matter and individual differences in performance on cognitive tests in normal populations, (2) changes in white matter associated with a host of pathological conditions, (3) changes in white matter associated with experience, and (4) patterns of relations between axon properties, white matter characteristics, information transfer, and efficiency of cognitive processing. However, this pattern of results is consistent with recently published analyses conducted on the same sample but employing general IQ metrics derived from WAIS (Ganjavi et al., 2011). Ganjavi et al. (2011) found a significant negative correlation between total CC midsagittal area and IQ controlled for total brain volume and age. In their analysis of callosal partitions Ganjavi et al. (2011) found no correlation between the area of segments within the anterior corpus callosum and WAIS FSIQ, PIQ, and VIQ for males, females, and the full sample. When the sample was divided into two age groups, a significant negative correlation between 3 callosal partitions and FSIQ and PIQ emerged. This finding was further qualified by an interaction with gender where significant correlations emerged for younger males but not for the females. In the present study analysis also revealed highly significant effects of age that were consistent across measures and stages. However, in contrast to Ganjavi et al. (2011), limiting age range in order to reduce non-linearity and heteroscedasticity present in WASI Matrix Reasoning for younger ages did not result in an improvement of the predictive power of entered predictors or otherwise alter pattern of results. In contrast to Ganjavi et al. (2011), handedness but not gender was a significant predictor of performance on WISC-III Coding B, a pattern that was reversed in analysis for hypothesis 2 and the comprehensive regression model.

Examination of untransformed scores on CANTAB SWM subtest (number of between

trial errors) revealed large concentration of scores at lower end of the distribution. This finding indicates that participants avoided between trial return errors and suggest that this test may not have been sufficiently difficult to invoke inter-hemispheric recruitment of processing resources.

Hypothesis 2

Results of the analysis for hypothesis 2 also suggest that upon correcting for age and other significant nuisance covariates there is no evidence in support of a significant link between the volume of the posterior two-fifths of the corpus callosum and performance on WASI Matrix Reasoning, WASI Block Design, and WISC-III Coding B. In the present study the volume of the region of the splenium and the isthmus of the corpus callosum is not a significant predictor of performance on WASI Matrix Reasoning, WASI Block Design, and WISC-III Coding B subtests. This finding, although unexpected, is largely consistent with the results presented by Ganjavi et al. (2011). In their combined sample of males and females Ganjavi et al. (2011) reported a single segment in the mid-posterior and posterior callosal region where correlation between the callosal area and FSIQ approached, but did not reach significance. This correlation was further qualified by gender becoming significant for males but not females. When further divided by age, this negative correlation in the posterior segment was significant only for younger but not older male participants. Ganjavi et al. (2011) concluded that the general negative correlation between area of midsagittal corpus callosum and IQ in their sample was driven by this posterior segment of the corpus callosum and by pre-pubescent male participants.

Comprehensive Regression Model

Results of the analysis for the comprehensive regression model suggest that upon correcting for age and other significant nuisance covariates, there is no evidence in support of a significant link between volumes of white matter in the anterior and posterior frontal and parietal lobes, as well as anterior and posterior corpus callosum, and CANTAB SWM Between Trial Errors, WASI Matrix Reasoning, WASI Block Design, and WISC-III Coding B. Across all dependent measures and steps, age remained a highly significant covariate. In addition, as in case of hypothesis 2 but not hypothesis 1, gender was a significant predictor of performance on the WASI-III Digit Coding B. As in the analysis for hypothesis 2, the quadratic term of age was a significant predictor of performance on WASI Matrix Reasoning. For Matrix Reasoning (full sample) the

addition of parietal gray matter volume resulted in a small but significant improvement of model fit. Parietal gray matter was a significant predictor of performance on Matrix Reasoning but only prior to correction for multiple comparisons, and only for the Gray Matter Model.

Overall, the proposed regression model shows a limited fit in our dataset. Because no predictors other than nuisance variables are significant in present analysis, this model is unable to allow for effective comparisons of relative unique contributions of frontal vs. parietal structures (e.g. frontal corpus callosum vs. parietal corpus callosum), and inter- vs. intra-hemispheric transfer channels (e.g. corpus callosum vs. lobar white matter volumes).

Age

Due to the fact that both the present study and Ganjavi et al. (2011) were conducted on the same sample of participants, all differences between the results of those studies need to be explained in terms of differences in study design, adopted analytic strategies, and in terms of differences in implemented methodologies. While a direct comparison of the present study and Ganjavi et al. (2011) is not possible due to the differences in implemented dependent and independent measures, results reported by both studies suggest the overpowering effect of age on tests of cognitive ability. Across all tested hypotheses, age is a single best predictor of cognitive performance irrespective of other entered covariates.

Myelination is a relatively linear process that progresses well into the second decade of life (Yakovlev & Lecours, 1967). Due to correlation of age, white matter volume and myelination, and the fact that as a covariate age was always entered in the first stage of the hierarchical regression it accounted for both shared and unique variance. As a result age effectively overpowered variables entered into hierarchical regression in the subsequent steps. Indeed, no variables entered into regression in the subsequent steps reached significance after correction for multiple tests. Examination of the correlation matrix confirms this interpretation showing the significant effects of age on cognitive measures as well as the small to moderate volume effects on cognitive measures. Correlations between age and cognitive tests ranged from $r = .81$ for WISC-III Coding B to $r = -.64$ for the CANTAB SWM subtest. In contrast, the highest correlation of volume with cognitive measures is $r = .34$ for frontal white matter and WASI Matrix Reasoning, and the lowest correlation is $r = -.04$ for anterior corpus callosum and WISC-III Coding B.

A quadratic term of age was a significant predictor of performance on WASI Matrix Rea-

soning across all hypotheses and the comprehensive regression model. Examination of the scatterplot of relation between age and WASI Matrix Reasoning reveals that quadratic effect of age is likely due to large dispersion of WASI Matrix Reasoning scores for younger participants. Variability in scores stabilizes around the age of 10-11 years. It may be the case that lower end of the age continuum encompasses transitional period where at the time of testing only subset of the younger participants developed cognitive abilities necessary for successfully performance on this task. The age period of stabilization of WASI Matrix Design scores may be marking transition from Piaget's concrete operations stage to the formal operations stage. During this transition estimated to take place around the ages of 11 to 12 years children develop ability of abstract reasoning. Ability to perform abstraction of similarities and differences between trials is crucial for effective performance on this task. Abstraction is a pre-requisite to forming hypotheses and subsequently testing them.

In Ganjavi et al. (2011) chronological, and possibly biological age, were decisive factors with regard to the relation between corpus callosum and IQ. Outside of the pre-pubescent male group, there was virtually no evidence for a link between corpus callosum and IQ. Gender effects reported by Ganjavi et al. (2011) may also be explained in terms of biological age. Gender effect can be explained by a different rate of maturation for males and females and therefore, at least to a degree, reported interaction of gender and chronological age may represent an index of biological age. In Ganjavi et al. (2011) significant correlations emerged for younger and still rapidly developing participants. This correlation was further qualified by gender because the correlation remained significant only for younger males but not for younger females. Since females mature faster, in actuality some of Ganjavi's younger female participants may have actually belonged to the older biological age group that already reached a more stable developmental stage. This interpretation is consistent with a recent large-sample, cross-sectional study of brain development (R. K. Lenroot et al., 2007) that reported brain volume peaks at 10.5 years for females, and at 14.5 years for males. While mere volume is a very simplistic metric of brain maturation, it suggests that at least in terms of some brain developmental processes, females may be years ahead of males. Since the present dataset includes both Tanner Staging data and levels of gonadal hormones from saliva samples future, analyses may consider employing those factors in order to account for individual differences in pace of development.

Quantification of Corpus Callosum Size

Possible a contributing factor in the difference in results between the present study and Ganjavi et al. (2011) is the operationalization of independent and dependent measures. While Ganjavi et al. (2011) measured the area of the midsagittal slices of the corpus callosum, present study employed volume. In addition, Ganjavi et al. (2011) implemented a much more detailed partitioning of the corpus callosum that can be only approximately mapped onto the geometric partition method implemented in this study. Ganjavi et al. (2011) focused on compound indices of cognitive ability such as scale scores on the WASI, while the present study focused on specific subtests invoking more specific subsets of cognitive processes. Ganjavi et al.'s 2011 fine-grained partitioning of the corpus callosum may have enabled the detection of very localized alterations of the callosal area that otherwise would have been averaged and diminished within larger partitions thus giving another possible explanation for null results obtained in this study.

However, in many respects results from both studies are largely consistent with each other. In both studies, after controlling for age and brain size, analyses of the combined male and female participants yielded no evidence of the link between the size of the anterior fifth of the corpus callosum and cognitive abilities. Similarly, in approximately 10 segments falling in the posterior two-fifths of the corpus callosum, Ganjavi et al. (2011) only found the trend in one segment in the full sample, which became significant for male participants only.

Another study conducted on the same dataset and investigating the link between corpus callosum morphology and IQ (Luders, Thompson et al., 2011) reported negative correlations between callosal thickness and WASI FSIQ and VIQ that were confined to the splenium of the corpus callosum. Reported correlations were small, in the -0.01 range, but survived correction for multiple tests at $FDR = .0043$ for FSIQ, and $FDR = 0.0033$ for VIQ. The remainder of correlations presented in Luders, Thompson et al. (2011) were not significant after corrections for multiple tests. While the results of Luders, Thompson et al. (2011) are somewhat at odds with the results of the present study and with the results of Ganjavi et al. (2011) two methodological differences explain differences in the results.

Both Ganjavi et al. (2011) and the present study employed related metrics of callosal size, area and volume respectively. In contrast, Luders, Thompson et al. (2011) employed thickness; a measure of distance more closely related to shape than to volume. This metric represents ad-

vancement over both, methodologies used in the present study, and the one implemented by Ganjavi et al. (2011). It appears that callosal thickness is more sensitive and consequently more capable of detecting even small and localized alterations in callosal morphology. The correlation presented in Luders, Thompson et al. (2011) was very small, in the -0.01 range, suggesting the greater sensitivity of shape as a measure of morphology. Indeed, in de Lacoste-Utamsing and Holloway (1982), significant sex difference in maximal splenial width was not accompanied by the difference in splenial area ($p = 0.08$) suggesting shape is a more sensitive metric than area. Similarly, B. S. Peterson, Feineigle, Staib, and Gore (2001) reported a negative correlation between a factor-derived indices of the size of anterior callosal body and IQ that was not present when a traditional measure of callosal size was employed.

Gender and handedness

Gender was a significant predictor of performance on WISC-III Coding B for hypothesis 2 and the comprehensive regression model. This finding is consistent with previously discussed reports (Camarata & Woodcock, 2006; Majeres, 2007; Sheppard & Vernon, 2008; Wechsler, 1997; Roivainen, 2011) indicating that females have processing speed advantage over males on digit coding tasks. This difference can be explained in terms of overall advantage in phonological processing (Majeres, 2007). This advantage is present across age groups and most pronounced during adolescence. Female processing speed advantage greatly diminishes when digits are replaced for instance by shapes indicating that gender differences exist only in phonological processing. Processing speed advantage for non-right handers present in analyses for hypothesis 1 paired with consistent finding of processing speed advantage for females suggests that performance on WISC–III Coding B might be related to lateralization and patterns of linguistic processing. Both non-right handers and females show lesser degree of language lateralization to the left hemisphere (Levy, 1972).

Brain Size

As in case of Ganjavi et al. (2011), this study also elected to control for brain size and estimated Total Intracranial Volume (eTIV) emerged as a significant predictor of performance on both WASI Block Design and Matrix Reasoning for hypotheses 1 and 2 but not on WISC-III Coding B where gender and handedness were significant covariates. It was expected that eTIV will

not be a significant predictor of cognitive performance in the comprehensive regression model because eTIV is a close correlate of a combination of volumes of gray and white matter for frontal and parietal lobes. In the present dataset, the correlation of eTIV and other volumetric measures ranged from r = .51 for the parietal gray matter to as high as r = .86 for the frontal white matter. The significance of eTIV confirms the correlation between brain size and IQ that is well documented in the literature (e.g. McDaniel, 2005; Rushton & Ankney, 2007; Toga & Thompson, 2005) and confirms the need to control for this variable in future studies. It is important to note that the effects of eTIV emerged for WASI subtests but not for CANTAB Spatial Working Memory or the WISC-III Coding B. Provided that during performance on CANTAB SWM only frontal lobes are differentially engaged, performance on this task may be dependent functions localized to frontal lobes and thus not contingent on total brain volume. This explanation, however, is not consistent with pattern of correlations between frontal white/gray matter volumes and CANTAB SWM between trail error scores. Magnitude of correlations between CANTAB SWM score and eTIV, frontal white matter, and parietal white matter was comparable. CANTAB SWM correlated with frontal white matter volume at r = -.27 and with frontal gray matter volume at r = .16. In comparison, correlation between CANTAB SWM and eTIV was r = -.24.

There was a puzzling difference separating the design implemented in the present study as well as in Ganjavi et al. (2011) from the design used by Luders, Thompson et al. (2011). Luders, Thompson et al. (2011) opted not to correct for the potentially confounding relation between brain size and cognitive performance (McDaniel, 2005; Rushton & Ankney, 2007; Toga & Thompson, 2005) while some of the previous studies by the same author implemented this correction (Luders, Narr, Thompson et al., 2009). Provided that Luders, Narr, Thompson et al. (2009) reported the presence of a correlation in only a small section of the corpus callosum, and that the magnitude of this correlation was small, it is possible that if contributions of brain size were removed, this correlation might not have been significant. In the absence of covarying effects of the brain size, the present correlation may be attributed to brain size. Jancke and Steinmetz (2003) suggested that the area of the corpus callosum and volume of the forebrain are related by geometric principles in a similar fashion to the way an area metric such as centimeter relate to a volume metrics such as cubic centimeter. Because volume is a cubic function of area, an increase in the midsagittal area of the corpus callosum is accompanied by an even steeper increase in the volume

of the brain. Consequently, larger brains tend to have a larger absolute midsagittal area of the corpus callosum, but also have smaller relative midsagittal areas in reference to brain volume. Since the midsagittal area of the corpus callosum is geometrically related to brain size, and brain size is related to intelligence, it might be the case that Luders, Narr, Thompson et al. (2009) correlations of the absolute callosal thickness and IQ are due to brain size alone. In contrast, in the Ganjavi et al. study that corrected for estimated Total Intracranial Volume, a similar argument cannot be made.

In the case of studies correcting for brain volume, what is being examined are not deviations of absolute size, but rather deviations from the expected size provided by the brain volume. Provided that the corpora callosa are geometrically related to brain size, and that brain size relates to intellectual abilities, the finding that people with larger brains happen to be "smarter" and have larger corpora callosa is not particularly enlightening. However, if in people with larger brains there were some form of departure from the expected brain to corpus callosum ratio, and if this deviation from the expected size was also related to IQ, this finding would certainly warrant further examination.

Age, Growth, Brain Size, and White Matter

Difficulty in modeling effects of brain anatomy on cognitive ability in rapidly developing systems stems from the intertwined nature of involved variables. Age, growth, myelination, and cognitive efficiency can be viewed as facets of the same process. During earlier stages of development, an increase in age is often associated with an increase in body size. Increase in body size in turn is associated with an increase in the distance that action potentials need to travel. Over the age span present in this sample, the brain increases in volume by an estimated 5%. Giedd (2008) reported that in their cohort of 475 males and 354 females, total cerebral volume was approximately at 95% of its peak size by the age of 6 years. Actual volume peaks occurred at 10.5 years in females, and 14.5 years in males (see also R. K. Lenroot et al., 2007). Because cognitive efficiency heavily depends on the timing of the arrival of neural signals, even relatively small changes in brain size require correction for delays. Both the emergence and maintenance of higher cognitive function depends on temporal synchrony. Temporal and spatial summations of neural signals are some of the mechanisms of information processing and depend on the precise timing of the arrival of action potentials. Even small delay in arrival of an action potential

at its target neuron may cause action potential to "miss" arrivals of other action potentials arriving from other neurons. This in turn may affect temporal summation and to an extent also spatial summation and may compromise target neuron's ability to initiate another action potential. Because distance action potentials need to travel increases with growth, conduction velocities need to be adjusted to account for additional distance and consequently later arrival time. In a theoretical situation of two neurons with axons of different lengths projecting to a single location, in order for a action potential from both neurons to arrive at a target point at a precise time, a conduction velocity in one of the neurons needs to be increased in order to account for longer conduction distance, and conduction velocity of the second neuron need to be decreased to account for delayed arrival of action potential in neuron one (see also Fields, 2008). One of the mechanisms that ensure maintenance of temporal synchrony during growth is increase in myelination of axons that is associated with maintenance of conduction velocity. Myelination serves additional function of secondary cellular learning mechanism as evidenced by studies of changes in white matter structure that coincide with acquisition of skill. This learning mechanism is part of cognitive tuning increasing cognitive efficiency during development (see also Fields, 2008). In many animals including horses (Szalay, 2001) and wild mice (Tessitore & Brunjes, 1988) myelination is complete at birth (Fields, 2008) while in humans complete myelination is delayed until at least second decade of life (Yakovlev & Lecours, 1967). This delay coincides with period of extensive reorganization of human cortex (Fields, 2008) reflecting effects of environment and experience aiming at adaptation to and understanding of the outside world. During this process synaptic pruning and myelination are involved in optimization of information processing (Fields, 2008). Consequently, growth, age, and myelination in essence are aspects of the same genetically pre-programmed process and share with each other a significant common component. In light of this argument, prevailing effects of age over other predictors subsequently entered into the regression equations are all but surprising. In the present dataset the notion that age and volumes of anatomical structures share a common component is supported by mild to moderate suppression evidenced by sign shifts between zero order correlation coefficients for callosal partitions and the criterion variable. For example, sign of the zero order correlation between volume of the posterior callosal partition and WASI Matrix Reasoning changes in Hypothesis 2 from r = +.24 to B = -.001 and in Hypothesis 3 from r = +.24 to B = -.002. In Hypothesis 3 sign of the zero order cor-

relation between volume of the anterior callosal partition and WASI Block Design changes from $r = +.12$ to $B = -.007$. While magnitude of those shifts is relatively small they are indicative of some form of suppression between corpus callosum and some of the other predictors. In case of hypothesis 2 this suppression clearly occurs due to age variables.

A negative pattern of correlations between gray matter volume in frontal and parietal lobes and age that was reported in the inter-correlation matrix is consistent with studies reporting pre-pubertal gray matter growth and post-pubertal gray matter loss (E. Sowell, P. Thompson, Tessner, & A. Toga, 2001; Jernigan, D. Trauner et al., 1991; Jernigan & Tallal, 1990; J. Giedd, J. Blumenthal, Jeffries, Castellanos et al., 1999; Gogtay & Thompson, 2010). J. Giedd, J. Blumenthal, Jeffries, Castellanos et al. (1999) reported in their study that frontal gray matter increased with a peak at the age of 11 years for females, and at the age of 12.1 years for males. Similarly, authors reported analogous increase in parietal gray matter with a peak at age 10.2 years for females, and at the age of 11.8 years for males. Authors noted that pre/post pubertal slopes for parietal lobes were steeper than for frontal lobes. Decrease in the volume of gray matter during post-pubertal period is consistent with synaptic pruning accelerating during adolescence and early adulthood (Bourgeois, Goldman-Rakic, & Rakic, 1994; Gogtay & Thompson, 2010). Consistent with reported differences in slopes of pre/post pubescent gray matter development for frontal and parietal lobes, present study found a weaker negative correlation between frontal gray matter volume and age ($r = -.25$) than between parietal gray matter volume and age ($r = -.40$). Given age-ranges included in this study, those correlations likely capture the slow increase, plateau, and much longer post-pubertal pruning period. Consistent with known patterns of white matter development (e.g. Yakovlev & Lecours, 1967) present study found positive correlations between lobar white matter volumes and age ($r = .41$ for frontal lobes, and $r = .35$ for parietal lobes).

Together, those results reflect opposite trajectories of pruning and myelination on brain size in our sample. Consequently, in the present study maintenance or increase in brain size must be attributed to myelination. It is not clear, however, whether this increase in white matter volume is a result of increase of axon length associated with increase of brain size, or whether it is a result of additional myelination of axons, or both processes operating in parallel. Irrespective, this finding is consistent with previous previously presented notion of relation between brain growth, increase of axon length, and additional myelination increasing speed of conduction in

axons in order to compensate for longer distance axon potentials need to travel.

A final argument in support of the notion that myelination is one of the mechanism of accounting for delays emerging from brain growth stems from the finding that delays in conduction in the central nervous system remain stable with growth. At present the only explanations for this finding involve additional myelination and related increase in axon diameter, as well as optimization of spacing between the nodes of Ranvier (Fields, 2008).

CONCLUSIONS

Inconsistencies in results of studies investigating link between corpus callosum and cognitive abilities can be attributed to several factors. First, different ways of partitioning corpus callosum (Hofer & Frahm, 2006; Witelson, 1989) could affect patterns of results as it might have been the case in differences between present study and Ganjavi et al. (2011).

Second, several factors relating to sample size and sample construction might be at roots of inconsistent results between studies present in the literature. Many of the previous studies were conducted on relatively small sample sizes and consequently may have lacked statistical power. Provided that present study was conducted on relatively large sample, it is unlikely that sample size was a key factor in obtaining null results in the present study.

Third, many previous studies employed clinical populations and/or convenience samples which may have introduced nuisance factors that complicated patterns of results. Present analyses were conducted on representative sample of US population for specified age groups. Present sample was extensively screened for physiological, neuropsychological, and neurological pathologies and other factors that could potentially confound results. Consequently, it is unlikely that obtained null results were due to sample construction or pathologies.

Fourth, developmental factors may in part account for the inconsistent pattern of results because discussed studies often examined different age groups. Previously discussed studies of Ganjavi et al. (2011) and Luders, Thompson et al. (2011) conducted on population of children and adolescents reported opposite direction of correlations between callosal size and IQ to the pattern reported in adult population (Hutchinson, Mathias, Jacobson et al., 2009). In the present study use of age as a covariate instead of dividing sample into age groups is a likely explanation for the null pattern of results. Provided that growth, myelination, and age share a common variance factor this type of design should be avoided in case of rapidly developing children and ado-

lescent populations.

Fifth, larger corpora callosa may not necessarily be also more myelinated. It is possible that simultaneous myelination and pruning complicate pattern of results slowing growth of the corpus callosum but at the same time increasing density of the myelination. Thus, larger corpus callosum might still be myelinated to a lesser extent. With anticipated addition of the diffusion tensor imaging data to present repository, future studies should address role of micro-structure of the corpus callosum along with the measures of callosal morphology.

BIBLIOGRAPHY

References

Aboitiz, F., Scheibel, A. B., Fisher, R. S., & Zaidel, E. (1992). Fiber composition of the human corpus callosum. *Brain research*, *598*(1-2), 143–53.

Allin, M., Nosarti, C., Narberhaus, A., Walshe, M., Frearson, S., Kalpakidou, A., . . . Murray, R. (2007). Growth of the corpus callosum in adolescents born preterm. *Archives of pediatrics & adolescent medicine*, *161*(12), 1183–9.

Almli, C. R., Rivkin, M. J., & McKinstry, R. C. (2007). The NIH MRI study of normal brain development (objective-2): newborns, infants, toddlers, and preschoolers. *NeuroImage*, *35*(1), 308–25.

Amacher, A. L. (1976). Midline commissurotomy for the treatment of some cases of intractable epilepsy. preliminary report. *Child's brain*, *2*(1), 54–8.

Andersen, R. A., Snyder, L. H., Bradley, D. C., & Xing, J. (1997). Multimodal representation of space in the posterior parietal cortex and its use in planning movements. *Annual review of neuroscience*, *20*, 303–30.

Anderson, B. (1999). Brain size, head size, and intelligence quotient in monozygotic twins. *Neurology*, *53*(1), 242–4.

Anderson, B., & Harvey, T. (1996). Alterations in cortical thickness and neuronal density in the frontal cortex of albert einstein. *Neuroscience letters*, *210*(3), 161–4.

Arnett, P. A., Rao, S. M., Grafman, J., Bernardin, L., Luchetta, T., Binder, J. R., & Lobeck, L. (1997). Executive functions in multiple sclerosis: an analysis of temporal ordering, semantic encoding, and planning abilities. *Neuropsychology*, *11*(4), 535–44.

Astur, R. S., St Germain, S. A., Baker, E. K., Calhoun, V., Pearlson, G. D., & Constable, R. T. (2005). Fmri hippocampal activity during a virtual radial arm maze. *Applied Psychophysiology and Biofeedback*, *30*(3), 307–17.

Atkinson, J., D. S., Abou-Khalil, B., Charles, P. D., & Welch, L. (1996). Midsagittal corpus callosum area, intelligence, and language dominance in epilepsy. *Journal of neuroimaging : official journal of the American Society of Neuroimaging*, *6*(4), 235–9.

Baddeley, A. D. (1986). *Working memory*. Oxford psychology series no. 11. Oxford: Oxford University Press.

Baker, L., & Barkovich, A. (1992). The large temporal horn: mr analysis in developmental brain anomalies versus hydrocephalus. *AJNR. American journal of neuroradiology*, *13*(1), 115–122. Retrieved from http://www.ajnr.org/cgi/content/abstract/13/1/115

Banich, M. T., & Brown, W. S. (2000). A life-span perspective on interaction between the cerebral hemispheres. *Developmental neuropsychology*, *18*(1), 1–10.

Banich, M. T., Hugdahl, K., & Davidson, R. J. (2003). Interaction between the hemispheres and its implications for the processing capacity of the brain. In *The asymmetrical brain.* (pp. 261–302). Cambridge, MA US: MIT Press.

Baumeister, A. A., & Kellas, G. (1968, March). Distribution of reaction times of retardates and normals. *American Journal of Mental Deficiency*, *72*(5), 715–718.

Baynes, K. (1990). Language and reading in the right hemisphere: highways or byways of the brain. *Journal of cognitive neuroscience*, *2*(3), 159–179.

Baynes, K., Tramo, M. J., & Gazzaniga, M. S. (1992). Reading with a limited lexicon in the right hemisphere of a callosotomy patient. *Neuropsychologia*, *30*(2), 187–200.

Beatty, W. W., & Monson, N. (1994). Picture and motor sequencing in multiple sclerosis. *Journal of clinical and experimental neuropsychology : official journal of the International Neuropsychological Society*, *16*(2), 165–72.

Behrens, S. J. (1985). The perception of stress and lateralization of prosody. *Brain and language*, *26*(2), 332–48.

Behrens, T. E., Berg, H. J., Jbabdi, S., Rushworth, M. F., & Woolrich, M. W. (2007). Probabilistic diffusion tractography with multiple fibre orientations: what can we gain? *NeuroImage*, *34*(1), 144–55.

Belger, A., & Banich, M. T. (1992). Interhemispheric interaction affected by computational complexity. *Neuropsychologia*, *30*(10), 923–9.

Ben Bashat, D., Ben Sira, L., Graif, M., Pianka, P., Hendler, T., Cohen, Y., & Assaf, Y. (2005). Normal white matter development from infancy to adulthood: comparing diffusion tensor

and high b value diffusion weighted mr images. *Journal of magnetic resonance imaging : JMRI*, *21*(5), 503–11.

Bench, C. J., Frith, C. D., Grasby, P. M., Friston, K. J., Paulesu, E., Frackowiak, R. S., & Dolan, R. J. (1993). Investigations of the functional anatomy of attention using the stroop test. *Neuropsychologia*, *31*(9), 907–22.

Benes, F. M., Turtle, M., Khan, Y., & Farol, P. (1994). Myelination of a key relay zone in the hippocampal formation occurs in the human brain during childhood, adolescence, and adulthood. *Archives of general psychiatry*, *51*(6), 477–84.

Bengtsson, S., Nagy, Z., Skare, S., Forsman, L., Forssberg, H., & Ullen, F. (2005). Extensive piano practicing has regionally specific effects on white matter development. *Nature Neuroscience*, *8*(9), 1148–1150. doi:10.1038/nn1516

Bishop, K. M., & Wahlsten, D. (1997). Sex differences in the human corpus callosum: myth or reality? *Neuroscience and biobehavioral reviews*, *21*(5), 581–601.

Bockholt, J., & Turner, J. (2007, March). Freesurfer analysis best practices as implemented in the fbirn phase ii data analysis, 2007. Biomedical Informatics Research Network.

Bogen, J. E. (1993). The callosal syndromes. In K. M. Heilman & E. Valenstein (Eds.). *Clinical neuropsychology* (3rd, Chap. 11, pp. 337–407). Oxford: Oxford University Press.

Bogen, J. E. (1998). Physiological consequences of complete or partial commissural section. In M. L. J. Apuzzo (Ed.). *Surgery of the third ventricle* (2nd, pp. 167–186). Baltimore: Williams and Wilkins.

Bogen, J. E., & Vogel, P. J. (1975). Neurologic status in the long term following complete cerebral commissurotomy. In B. Schort & F. Michel (Eds.). *Les syndromes de disconnexion calleuse chez l'homme* (pp. 227–251). Lyon: Hopital Neurologique.

Bolinger, D. L. M. (1980). *Language, the loaded weapon : the use and abuse of language today*. London ; New York: Longman.

Bourgeois, J.-P., Goldman-Rakic, P. S., & Rakic, P. (1994). Synaptogenesis in the prefrontal cortex of rhesus monkeys. *Cerebral Cortex*, *4*(1), 78–96. doi:10.1093/cercor/4.1.78. eprint: http://cercor.oxfordjournals.org/content/4/1/78.full.pdf+html

Bowers, D., Bauer, R. M., & Heilman, K. M. (1993). The nonverbal affect lexicon: theoretical perspectives from neuropsychological studies of affect perception. *Neuropsychology*, *7*(4), 433–444.

Bowers, D., Coslett, H. B., Bauer, R. M., Speedie, L. J., & Heilman, K. M. (1987). Comprehension of emotional prosody following unilateral hemispheric lesions: processing defect versus distraction defect. *Neuropsychologia*, *25*(2), 317–28.

Breusch, T. S., & Pagan, A. R. (1979). A simple test for heteroscedasticity and random coefficient variation. *Econometrica : journal of the Econometric Society*, *47*(5), pp. 1287–1294. Retrieved from http://www.jstor.org/stable/1911963

Brion, S., & Jedynak, C. P. (1972). [disorders of interhemispheric transfer (callosal disonnection). 3 cases of tumor of the corpus callosum. the strange hand sign]. *Revue neurologique*, *126*(4), 257–66.

Broca, P. (1861). Sur le volume et la forme du cerveau suivant les individus et suivant les races. *Bulletin Societe d'Anthropologie Paris*, *2*, 139–207, 301–321.

Brown, W. S., & Paul, L. K. (2000). Cognitive and psychosocial deficits in agenesis of the corpus callosum with normal intelligence. *Cognitive Neuropsychiatry*, *5*(2), 135 –157. doi:10.1080/135468000395781. eprint: http://www.tandfonline.com/doi/pdf/10.1080/135468000395781

Buchanan, T. W., Lutz, K., Mirzazade, S., Specht, K., Shah, N. J., Zilles, K., & Jancke, L. (2000). Recognition of emotional prosody and verbal components of spoken language: an fmri study. *Brain research. Cognitive brain research*, *9*(3), 227–38.

Buckner, R. L., Head, D., Parker, J., Fotenos, A. F., Marcus, D., Morris, J. C., & Snyder, A. Z. (2004). A unified approach for morphometric and functional data analysis in young, old, and demented adults using automated atlas-based head size normalization: reliability and validation against manual measurement of total intracranial volume. *NeuroImage*, *23*(2), 724–38.

Byne, W., Bleier, R., & Houston, L. (1988). Variations in human corpus callosum do not predict gender: a study using magnetic resonance imaging. *Behavioral neuroscience*, *102*(2), 222–227.

Byrd, S., Darling, C., & Wilczynski, M. (1993). White matter of the brain: maturation and myelination on magnetic resonance in infants and children. *Neuroimaging Clinics of North America*, *3*, 247–266.

Cabeza, R., & Nyberg, L. (2000). Imaging cognition ii: an empirical review of 275 pet and fmri studies. *Journal of cognitive neuroscience*, *12*(1), 1–47.

Caldu, X., Narberhaus, A., Junque, C., Gimenez, M., Vendrell, P., Bargallo, N., ... Botet, F. (2006). Corpus callosum size and neuropsychologic impairment in adolescents who were born preterm. *Journal of child neurology*, *21*(5), 406–10.

Camarata, S., & Woodcock, R. (2006). Sex differences in processing speed: developmental effects in males and females. *Intelligence*, *34*(3), 231 –252. doi:10.1016/j.intell.2005.12.001

Carroll, J. B. (1991). No demonstration that g is not unitary, but there's more to the story: comment on kranzler and jensen. *Intelligence*, *15*(4), 423 –436. doi:10.1016/0160-2896(91)90004-W

Carter, C. S., Mintun, M., & Cohen, J. D. (1995). Interference and facilitation effects during selective attention: an h215o pet study of stroop task performance. *NeuroImage*, *2*(4), 264–72.

Casey, B. J., Thomas, K. M., Welsh, T. F., Badgaiyan, R. D., Eccard, C. H., Jennings, J. R., & Crone, E. A. (2000). Dissociation of response conflict, attentional selection, and expectancy with functional magnetic resonance imaging. *Proceedings of the National Academy of Sciences of the United States of America*, *97*(15), 8728–33.

Casey, B. J., Trainor, R., Giedd, J. N., Vauss, Y., Vaituzis, C. K., Hamburger, S., ... Rapoport, J. L. (1997). The role of the anterior cingulate in automatic and controlled processes: a developmental neuroanatomical study. *Developmental psychobiology*, *30*(1), 61–9.

Cattell, R. B. (1971). *Abilities : their structure, growth, and action*. Boston: Houghton Mifflin.

Cavanna, A. E., & Trimble, M. R. (2006). The precuneus: a review of its functional anatomy and behavioural correlates. *Brain : a journal of neurology*, *129*(Pt 3), 564–83.

Charlton, R. A., Barrick, T. R., McIntyre, D. J., Shen, Y., O'Sullivan, M., Howe, F. A., ... Markus, H. S. (2006). White matter damage on diffusion tensor imaging correlates with age-related cognitive decline. *Neurology*, *66*(2), 217–22.

Chiarello, C. (1980). A house divided? cognitive functioning with callosal agenesis. *Brain and Language*, *11*(1), 128 –158. doi:10.1016/0093-934X(80)90116-9

Clarke, J. (1990). *Interhemispheric functions in humans: relationship between anatomical measures of corpus callosum, behavioral laterality effects, and cognitive profiles*. (Dissertation).

Clarke, J. M., & Zaidel, E. (1989). Simple reaction times to lateralized light flashes. varieties of interhemispheric communication routes. *Brain : a journal of neurology*, *112 (Pt 4)*, 849–70.

Clarke, S., Kraftsik, R., Van der Loos, H., & Innocenti, G. M. (1989). Forms and measures of adult and developing human corpus callosum: is there sexual dimorphism? *The Journal of comparative neurology*, *280*(2), 213–30.

Coffey, C., & Brumback, R. (2006). *Pediatric neuropsychiatry*. Lippincott Williams & Wilkins.

Cohen, J. (1988). *Statistical power analysis for the behavioral sciences (2nd edition)* (2nd). US: Hillsdale, N.J.: L. Erlbaum Associates.

Cohn, S. J., Carlson, J. S., & Jensen, A. R. (1985). Speed of information processing in academically gifted youths. *Personality and Individual Differences*, *6*(5), 621 –629. doi:10.1016/0191-8869(85)90012-1

Colom, R., Haier, R. J., Head, K., Alvarez-Linera, J., Quiroga, M. A., Shih, P. C., & Jung, R. E. (2009). Gray matter correlates of fluid, crystallized, and spatial intelligence: testing the p-fit model. *Intelligence*, *37*(2), 124–135.

Colom, R., Jung, R. E., & Haier, R. J. (2006). Distributed brain sites for the g-factor of intelligence. *NeuroImage*, *31*(3), 1359–1365.

Corbetta, M., Kincade, J. M., Ollinger, J. M., McAvoy, M. P., & Shulman, G. L. (2000). Voluntary orienting is dissociated from target detection in human posterior parietal cortex. *Nature Neuroscience*, *3*(3), 292–7.

Corbetta, M., Miezin, F. M., Shulman, G. L., & Petersen, S. E. (1993). A pet study of visuospatial attention. *Journal of Neuroscience*, *13*(3), 1202–26.

Corbetta, M., & Shulman, G. L. (1998). Human cortical mechanisms of visual attention during orienting and search. *Philosophical Transactions of the Royal Society of London. Series B, Biological Sciences*, *353*(1373), 1353–62.

Corporation, P. (1999). Manual for the wechsler abbreviated scale of intelligence. Author.

Coull, J. T., & Nobre, A. C. (1998). Where and when to pay attention: the neural systems for directing attention to spatial locations and to time intervals as revealed by both pet and fmri. *Journal of Neuroscience*, *18*(18), 7426–35.

Crystal, D. (1975). *The english tone of voice : essays in intonation, prosody and paralanguage*. London: Edward Arnold.

Dale, A. M., Fischl, B., & Sereno, M. I. (1999). Cortical surface-based analysis. i. segmentation and surface reconstruction. *NeuroImage*, *9*(2), 179–94.

Dale, A. M., & Sereno, M. I. (1993). Improved localizadon of cortical activity by combining eeg and meg with mri cortical surface reconstruction: a linear approach. *Journal of Cognitive Neuroscience*, *5*(2), 162–176.

Darwin, C. (1859). *On the origin of species by means of natural selection*. London: J. Murray.

Davison, A. N., & Dobbing, J. (1966). Myelination as a vulnerable period in brain development. *British Medical Bulletin*, *22*(1), 40–44.

de Bleser, R., & Poeck, K. (1985). Analysis of prosody in the spontaneous speech of patients with cv-recurring utterances. *Cortex; a journal devoted to the study of the nervous system and behavior*, *21*(3), 405–15.

de Lacoste, M. C., Kirkpatrick, J. B., & Ross, E. D. (1985). Topography of the human corpus callosum. *Journal of neuropathology and experimental neurology*, *44*(6), 578–91.

de Lacoste-Utamsing, C., & Holloway, R. L. (1982). Sexual dimorphism in the human corpus callosum. *Science*, *216*(4553), 1431–1432.

Demeter, S., Ringo, J. L., & Doty, R. W. (1988). Morphometric analysis of the human corpus callosum and anterior commissure. *Human neurobiology*, *6*(4), 219–26.

Denenberg, V. H., Berrebi, A. S., & Fitch, R. H. (1989). A factor analysis of the rat's corpus callosum. *Brain research*, *497*(2), 271–9.

Desikan, R. S., Segonne, F., Fischl, B., Quinn, B. T., Dickerson, B. C., Blacker, D., . . . Killiany, R. J. (2006). An automated labeling system for subdividing the human cerebral cortex on mri scans into gyral based regions of interest. *NeuroImage*, *31*(3), 968–80.

Diamond, M. C., Law, F., Rhodes, H., Lindner, B., Rosenzweig, M. R., Krech, D., & Bennett, E. L. (1966). Increases in cortical depth and glia numbers in rats subjected to enriched environment. *The Journal of Comparative Neurology*, *128*(1), 117–125.

Diamond, M. C., Scheibel, A. B., Murphy, J., G. M., & Harvey, T. (1985). On the brain of a scientist: albert einstein. *Experimental neurology*, *88*(1), 198–204.

Dimond, S. J. (1976). Depletion of attentional capacity after total commissurotomy in man. *Brain : a journal of neurology*, *99*(2), 347–56.

Dixon, R. A., & Baltes, P. B. (1986). Toward life-span research on the functions and pragmatics of intelligence. In R. J. Sternberg & R. K. Wagner (Eds.). *Practical intelligence: nature and origins of competence in the everyday world* (pp. 203–235). New York: Cambridge University Press.

Dow, C., Seidenberg, M., & Hermann, B. (2004). Relationship between information processing speed in temporal lobe epilepsy and white matter volume. *Epilepsy & behavior : E&B*, *5*(6), 919–25.

Downhill, J., J. E., Buchsbaum, M. S., Wei, T., Spiegel-Cohen, J., Hazlett, E. A., Haznedar, M. M., . . . Siever, L. J. (2000). Shape and size of the corpus callosum in schizophrenia and schizotypal personality disorder. *Schizophrenia research*, *42*(3), 193–208.

Duffy, F. H., & Burchfiel, J. L. (1971). Somatosensory system: organizational hierarchy from single units in monkey area 5. *Science*, *172*(980), 273–5.

Dugbartey, A. T., Sanchez, P. N., Gail Rosenbaum, J., Mahurin, R. K., Mark Davis, J., & Townes, B. D. (1999). Wais-iii matrix reasoning test performance in a mixed clinical sample. *The Clinical Neuropsychologist*, *13*(4), 396 –404. doi:10.1076/1385-4046(199911)13:04;1-Y;FT396

Duncan, J., Burgess, P., & Emslie, H. (1995). Fluid intelligence after frontal lobe lesions. *Neuropsychologia*, *33*(3), 261–8.

Duncan, J., Emslie, H., Williams, P., Johnson, R., & Freer, C. (1996). Intelligence and the frontal lobe: the organization of goal-directed behavior. *Cognitive psychology*, *30*(3), 257–303.

Duncan, J., & Owen, A. M. (2000). Common regions of the human frontal lobe recruited by diverse cognitive demands. *Trends in neurosciences*, *23*(10), 475–83.

Duncan, J., Seitz, R. J., Kolodny, J., Bor, D., Herzog, H., Ahmed, A., . . . Emslie, H. (2000). A neural basis for general intelligence. *Science*, *289*(5478), 457–60.

Egaas, B., Courchesne, E., & Saitoh, O. (1995). Reduced size of corpus callosum in autism. *Archives of neurology*, *52*(8), 794–801.

Eggers, R., Haug, H., & Fischer, D. (1984). Preliminary report on macroscopic age changes in the human prosencephalon. a stereologic investigation. *Journal fur Hirnforschung*, *25*(2), 129–39.

Eickhoff, S. B., Stephan, K. E., Mohlberg, H., Grefkes, C., Fink, G. R., Amunts, K., & Zilles, K. (2005). A new spm toolbox for combining probabilistic cytoarchitectonic maps and functional imaging data. *NeuroImage*, *25*(4), 1325–35.

Engel, A. K., Fries, P., & Singer, W. (2001). Dynamic predictions: oscillations and synchrony in top-down processing. *Nature reviews. Neuroscience*, *2*(10), 704–16.

Esposito, G., Kirkby, B. S., Van Horn, J. D., Ellmore, T. M., & Berman, K. F. (1999). Context-dependent, neural system-specific neurophysiological concomitants of ageing: mapping pet correlates during cognitive activation. *Brain : a journal of neurology*, *122 (Pt 5)*, 963–79.

Fangmeier, T., Knauff, M., Ruff, C. C., & Sloutsky, V. (2006). Fmri evidence for a three-stage model of deductive reasoning. *Journal of Cognitive Neuroscience*, *18*(3), 320–334.

Feingold, A. (1992). Sex differences in variability in intellectual abilities: a new look at an old controversy. *Review of Educational Research*, *62*(1), 61–84. doi:10.3102/00346543062001061. eprint: http://rer.sagepub.com/content/62/1/61.full.pdf+html

Fields, R. D. (2008). White matter in learning, cognition and psychiatric disorders. *Trends in Neurosciences*, *31*(7), 361 –370. doi:10.1016/j.tins.2008.04.001

Filley, C. M. (2001). *The behavioral neurology of white matter*. Oxford ; New York: Oxford University Press.

Finger, S. (1994). *Origins of neuroscience: a history of explorations into brain function*. New York: Oxford University Press.

Fischl, B., & Dale, A. M. (2000). Measuring the thickness of the human cerebral cortex from magnetic resonance images. *Proceedings of the National Academy of Sciences of the United States of America*, *97*(20), 11050–5.

Fischl, B., Liu, A., & Dale, A. M. (2001). Automated manifold surgery: constructing geometrically accurate and topologically correct models of the human cerebral cortex. *IEEE transactions on medical imaging*, *20*(1), 70–80.

Fischl, B., Salat, D. H., Busa, E., Albert, M., Dieterich, M., Haselgrove, C., ... Dale, A. M. (2002). Whole brain segmentation: automated labeling of neuroanatomical structures in the human brain. *Neuron*, *33*(3), 341–55.

Fischl, B., Salat, D. H., van der Kouwe, A. J., Makris, N., Segonne, F., Quinn, B. T., & Dale, A. M. (2004). Sequence-independent segmentation of magnetic resonance images. *NeuroImage*, *23 Suppl 1*, S69–84.

Fischl, B., Sereno, M. I., & Dale, A. M. (1999). Cortical surface-based analysis. ii: inflation, flattening, and a surface-based coordinate system. *NeuroImage*, *9*(2), 195–207.

Fischl, B., Sereno, M. I., Tootell, R. B., & Dale, A. M. (1999). High-resolution intersubject averaging and a coordinate system for the cortical surface. *Human brain mapping*, *8*(4), 272–84.

Fischl, B., van der Kouwe, A., Destrieux, C., Halgren, E., Segonne, F., Salat, D. H., ... Dale, A. M. (2004). Automatically parcellating the human cerebral cortex. *Cerebral cortex (New York, N.Y. : 1991)*, *14*(1), 11–22.

Fletcher, J. M., Bohan, T. P., Brandt, M. E., Brookshire, B. L., Beaver, S. R., Francis, D. J., ... Miner, M. E. (1992). Cerebral white matter and cognition in hydrocephalic children. *Archives of neurology*, *49*(8), 818–24.

Forn, C., Belenguer, A., Parcet-Ibars, M. A., & Avila, C. (2008). Information-processing speed is the primary deficit underlying the poor performance of multiple sclerosis patients in the paced auditory serial addition test (pasat). *Journal of clinical and experimental neuropsychology : official journal of the International Neuropsychological Society*, 1–8.

Foundas, A. L., Faulhaber, J. R., Kulynych, J. J., Browning, C. A., & Weinberger, D. R. (1999). Hemispheric and gender differences in sylvian fissure morphology: a quantitative approach using volumetric mri. *Neuropsychiatry Neuropsychology Behavioral Neurology*, *12*, 1–10.

Fox, J., & Weisberg, S. (2011). *An R companion to applied regression* (Second). Thousand Oaks CA: Sage. Retrieved from `http://socserv.socsci.mcmaster.ca/jfox/Books/Companion`

Friederici, A. D., von Cramon, D. Y., & Kotz, S. A. (2007). Role of the corpus callosum in speech comprehension: interfacing syntax and prosody. *Neuron*, *53*(1), 135–45.

Fry, A. F., & Hale, S. (1996). Processing speed, working memory, and fluid intelligence: evidence for a developmental cascade. *Psychological Science*, *7*(4), 237–241.

Fry, A. F., & Hale, S. (2000). Relationships among processing speed, working memory, and fluid intelligence in children. *Biological psychology*, *54*(1-3), 1–34.

Fukunaga, K. (1990). *Introduction to statistical pattern recognition* (2nd). Computer science and scientific computing. Boston: Academic Press.

Fuster, J. M. (2004). Upper processing stages of the perception-action cycle. *Trends in cognitive sciences*, *8*(4), 143–5.

Galaburda, A. M. (1999). Albert einstein's brain. *Lancet*, *354*(9192), 1821; author reply 1822.

Galin, D., Johnstone, J., Nakell, L., & Herron, J. (1979). Development of the capacity for tactile information transfer between hemispheres in normal children. *Science*, *204*(4399), 1330–2.

Ganjavi, H., Lewis, J. D., Bellec, P., MacDonald, P. A., Waber, D. P., Evans, A. C., ... Group, T. B. D. C. (2011, May). Negative associations between corpus callosum midsagittal area and iq in a representative sample of healthy children and adolescents. *PLoS ONE*, *6*(5), e19698. doi:10.1371/journal.pone.0019698

Gardner, H. (1999). *Intelligence reframed : multiple intelligences for the 21st century*. New York, NY: Basic Books.

Gazzaniga, M. S. (1970). *The bisected brain*. Neuroscience series. New York: Appleton-Century-Crofts.

Gazzaniga, M. S., & LeDoux, J. E. (1978). *The integrated mind*. New York: Plenum Press.

Geschwind, N. (1965a). Disconnexion syndromes in animals and man. i. *Brain : a journal of neurology*, *88*(2), 237–94.

Geschwind, N. (1965b). Disconnexion syndromes in animals and man. ii. *Brain : a journal of neurology*, *88*(3), 585–644.

Giedd, J. N. (2008). The teen brain: insights from neuroimaging. *Journal of Adolescent Health*, *42*(4), 335 –343. doi:10.1016/j.jadohealth.2008.01.007

Giedd, J., Blumenthal, J., Jeffries, N., Castellanos, F., Liu, H., Zijdenbos, A., ... Rapoport, J. (1999). Brain development during childhood and adolescence: a longitudinal mri study. *Nature Neuroscience*, *2*(10), 861–863. doi:10.1038/13158

Giedd, J., Blumenthal, J., Jeffries, N., Rajapakse, J., Vaituzis, A., Liu, H., . . . Castellanos, F. (1999). Development of the human corpus callosum during childhood and adolescence: a longitudinal mri study. *Progress in Neuro-Psychopharmacology and Biological Psychiatry*, *23*(4), 571–588. doi:10.1016/S0278-5846(99)00017-2

Gogtay, N., & Thompson, P. M. (2010). Mapping gray matter development: implications for typical development and vulnerability to psychopathology. *Brain and Cognition*, *72*(1), 6 – 15. Adolescent Brain Development: Current Themes and Future Directions. doi:10.1016/j.bandc.2009.08.009

Gold, B. T., Powell, D. K., Xuan, L., Jiang, Y., & Hardy, P. A. (2007). Speed of lexical decision correlates with diffusion anisotropy in left parietal and frontal white matter: evidence from diffusion tensor imaging. *Neuropsychologia*, *45*(11), 2439 –2446. doi:10.1016/j.neuropsychologia.2007.04.011

Goldman-Rakic, P. S. (1988). Topography of cognition: parallel distributed networks in primate association cortex. *Annual review of neuroscience*, *11*, 137–56.

Goldstein, J. M., Seidman, L. J., Horton, N. J., Makris, N., Kennedy, D. N., Caviness, J., V. S., . . . Tsuang, M. T. (2001). Normal sexual dimorphism of the adult human brain assessed by in vivo magnetic resonance imaging. *Cerebral cortex (New York, N.Y. : 1991)*, *11*(6), 490–7.

Gorelick, P. B., & Ross, E. D. (1987). The aprosodias: further functional-anatomical evidence for the organisation of affective language in the right hemisphere. *Journal of neurology, neurosurgery, and psychiatry*, *50*(5), 553–60.

Gould, S. J. (1996). *The mismeasure of man* (Rev. and expanded.). New York: Norton.

Gray, C. M. (1999). The temporal correlation hypothesis of visual feature integration: still alive and well. *Neuron*, *24*(1), 31–47, 111–25.

Gray, H., & Lewis, W. H. (1918). *Anatomy of the human body* (20th). Philadelphia and New York: Lea & Febiger.

Gray, J. R., Chabris, C. F., & Braver, T. S. (2003). Neural mechanisms of general fluid intelligence. *Nature neuroscience*, *6*(3), 316–22.

Gray, J. R., & Thompson, P. M. (2004). Neurobiology of intelligence: science and ethics. *Nature reviews. Neuroscience*, *5*(6), 471–82.

Groth-Marnat, G. (2003). *Handbook of psychological assessment* (4th). Hoboken, N.J.: John Wiley & Sons.

Group, B. D. C. (2006). The mri study of normal brain development mri procedure manual.

Group, B. D. C. (2007, January). The mri study of normal brain development procedure manual: objective 1. reduced format.

Group, B. D. C., & Evans, A. C. (2006). The nih mri study of normal brain development. *NeuroImage*, *30*(1), 184–202.

Gunning-Dixon, F. M., & Raz, N. (2000). The cognitive correlates of white matter abnormalities in normal aging: a quantitative review. *Neuropsychology*, *14*(2), 224–32.

Gutierrez, R., Boison, D., Heinemann, U., & Stoffel, W. (1995). Decompaction of cns myelin leads to a reduction of the conduction velocity of action potentials in optic nerve. *Neuroscience letters*, *195*(2), 93–6.

Haier, R. J. (1993). Biological approaches to the study of human intelligence. In P. A. Vernon (Ed.). *Biological approaches to the study of human intelligence* (pp. 317–322). Norwood, NJ: Ablex.

Haier, R. J. (2003). Positron emission tomography studies of intelligence: from psychometrics to neurobiology. In A. R. Jensen & H. Nyborg (Eds.). *The scientific study of general intelligence: tribute to arthur r. jensen* (1st, Chap. 3, pp. 41–52). Boston, MA: Pergamon.

Haier, R. J., Jung, R. E., Yeo, R. A., Head, K., & Alkire, M. T. (2004). Structural brain variation and general intelligence. *NeuroImage*, *23*(1), 425–33.

Haier, R. J., Jung, R. E., Yeo, R. A., Head, K., & Alkire, M. T. (2005). The neuroanatomy of general intelligence: sex matters. *NeuroImage*, *25*(1), 320 –327. doi:DOI : 10 . 101 6/j.neuroimage.2004.11.019

Haier, R. J., Siegel, B., Tang, C., Abel, L., & Buchsbaum, M. S. (1992). Intelligence and changes in regional cerebral glucose metabolic rate following learning. *Intelligence*, *16*(3-4), 415–426. doi:10.1016/0160-2896(92)90018-M

Haier, R. J., Siegel, B. V., Jr., MacLachlan, A., Soderling, E., Lottenberg, S., & Buchsbaum, M. S. (1992). Regional glucose metabolic changes after learning a complex visuospatial/motor task: a positron emission tomographic study. *Brain Research*, *570*(1-2), 134–143. doi:10 . 1016/0006-8993(92)90573-R

Haier, R. J., Siegel, B. V., Nuechterlein, K. H., & Hazlett, E. (1988). Cortical glucose metabolic rate correlates of abstract reasoning and attention studied with positron emission tomography. *Intelligence*, *12*(2), 199–217.

Hall, D. A., Anderson, C. A., Filley, C. M., Newcombe, J., & Hughes, R. L. (2003). A french accent after corpus callosum infarct. *Neurology*, *60*(9), 1551–2.

Halstead, W. (1947). *Brain and intelligence: a quantitative study of the frontal lobes*. US: Chicago, IL: University of Chicago Press.

Hamilton, C. R. (1982). Mechanisms of interocular equivalence. In D. Ingle, M. Goodale & R. Mansfield (Eds.). *Advances in the analysis of visual behavior* (pp. 693–717). Cambridge: MIT Press.

Han, X., Jovicich, J., Salat, D., van der Kouwe, A., Quinn, B., Czanner, S., . . . Fischl, B. (2006). Reliability of mri-derived measurements of human cerebral cortical thickness: the effects of field strength, scanner upgrade and manufacturer. *NeuroImage*, *32*(1), 180–94.

Harris, R. M., Sundsten, J. W., & Fischer-Wright, R. A. (1987). The human corpus callosum: an mri study varying sex, handedness and age. *Society for Neuroscience Abstracts*, *13*, 45.

Haug, H. (1984). Der einfluss der sakularen akzeleration auf das hirngewicht des menschen und dessen anderung wahrend der alterung. *Gegenbaurs morphologisches Jahrbuch*, *130*, 481–500.

Haug, H. (1987). Brain sizes, surfaces, and neuronal sizes of the cortex cerebri: a stereological investigation of man and his variability and a comparison with some mammals (primates, whales, marsupials, insectivores, and one elephant). *The American journal of anatomy*, *180*(2), 126–42.

Heaton, R. K., Nelson, L. M., Thompson, D. S., Burks, J. S., & Franklin, G. M. (1985). Neuropsychological findings in relapsing-remitting and chronic-progressive multiple sclerosis. *Journal of consulting and clinical psychology*, *53*(1), 103–10.

Heilman, K. M., Bowers, D., Speedie, L., & Coslett, H. B. (1984). Comprehension of affective and nonaffective prosody. *Neurology*, *34*(7), 917–21.

Heilman, K. M., & Gilmore, R. L. (1998). Cortical influences in emotion. *Journal of clinical neurophysiology : official publication of the American Electroencephalographic Society*, *15*(5), 409–23.

Heilman, K. M., Scholes, R., & Watson, R. T. (1975). Auditory affective agnosia. disturbed comprehension of affective speech. *Journal of Neurology, Neurosurgery & Psychiatry*, *38*(1), 69–72.

Hellige, J. B., Taylor, K. B., Lesmes, L., & Peterson, S. (1998). Relationships between brain morphology and behavioral measures of hemispheric asymmetry and interhemispheric interaction. *Brain and cognition*, *36*(2), 158–92.

Hilgetag, C. C., Burns, G. A., O'Neill, M. A., Scannell, J. W., & Young, M. P. (2000). Anatomical connectivity defines the organization of clusters of cortical areas in the macaque monkey and the cat. *Philosophical transactions of the Royal Society of London. Series B, Biological sciences*, *355*(1393), 91–110.

Hines, T. (1998). Further on einstein's brain. *Experimental Neurology*, *150*, 343–344.

Hofer, S., & Frahm, J. (2006). Topography of the human corpus callosum revisited–comprehensive fiber tractography using diffusion tensor magnetic resonance imaging. *NeuroImage*, *32*(3), 989–94.

Holloway, R. L., & de Lacoste, M. C. (1986). Sexual dimorphism in the human corpus callosum: an extension and replication study. *Human neurobiology*, *5*(2), 87–91.

Hopkins, W. D., Cantalupo, C., & Taglialatela, J. (2007). Handedness is associated with asymmetries in gyrification of the cerebral cortex of chimpanzees. *Cerebral cortex (New York, N.Y. : 1991)*, *17*(8), 1750–6.

Horn, J. L., & Cattell, R. B. (1967). Age differences in fluid and crystallized intelligence. *Acta psychologica*, *26*(2), 107–29.

Hulshoff Pol, H. E., Schnack, H. G., Posthuma, D., Mandl, R. C., Baare, W. F., van Oel, C., . . . Kahn, R. S. (2006). Genetic contributions to human brain morphology and intelligence. *The Journal of neuroscience : the official journal of the Society for Neuroscience*, *26*(40), 10235–42.

Hutchinson, A. D., Mathias, J. L., & Banich, M. T. (2008). Corpus callosum morphology in children and adolescents with attention deficit hyperactivity disorder: a meta-analytic review. *Neuropsychology*, *22*(3), 341–9.

Hutchinson, A. D., Mathias, J. L., Jacobson, B. L., Ruzic, L., Bond, A. N., & Banich, M. T. (2009). Relationship between intelligence and the size and composition of the corpus callosum.

Experimental brain research. Experimentelle Hirnforschung. Experimentation cerebrale, *192*(3), 455–64.

Hyde, K. L., Zatorre, R. J., Griffiths, T. D., Lerch, J. P., & Peretz, I. (2006). Morphometry of the amusic brain: a two-site study. *Brain : a journal of neurology*, *129*(10), 2562–2570. doi:10.1093/brain/awl204. eprint: http://brain.oxfordjournals.org/content/129/10/2562.full.pdf+html

Iacoboni, M., & Zaidel, E. (1995). Channels of the corpus callosum. evidence from simple reaction times to lateralized flashes in the normal and the split brain. *Brain : a journal of neurology*, *118 (Pt 3)*, 779–88.

Iacoboni, M., & Zaidel, E. (2003). Stable and variable aspects of callosal channels: lessons from partial disconnection. In E. Zaidel & M. Iacoboni (Eds.). *The parallel brain : the cognitive neuroscience of the corpus callosum* (Chap. 12, pp. 301–306). Cambridge, MA: MIT Press.

Innocenti, G. M. (1986). Postnatal development of corticocortical connections. *Italian journal of neurological sciences*, *Suppl 5*, 25–8.

Jambor, K. L. (1969). Cognitive functioning in multiple sclerosis. *The British journal of psychiatry : the journal of mental science*, *115*(524), 765–75.

Jancke, L., Schlaug, G., Huang, Y., & Steinmetz, H. (1994). Asymmetry of the planum parietale. *Neuroreport*, *5*(9), 1161–3.

Jancke, L., & Steinmetz, H. (2003). Brain size: a possible source of interindividual variability in corpus callosum morphology. In E. Zaidel & M. Iacoboni (Eds.). *The parallel brain: the cognitive neuroscience of the corpus callosum* (pp. 51 –63). Issues in clinical and cognitive. MIT Press.

Janowsky, J. S., Kaye, J. A., & Carper, R. A. (1996). Atrophy of the corpus callosum in alzheimer's disease versus healthy aging. *Journal of the American Geriatrics Society*, *44*(7), 798–803.

Jeeves, M., & Rajalakshmi, R. (1964). Psychological studies of a case of congenital agenesis of the corpus callosum. *Neuropsychologia*, *2*(3), 247 –252. doi:10.1016/0028-3932(64)90009-0

Jensen, A. (1992). Understanding g in terms of information processing. *Educational Psychology Review*, *4*, 271–308. 10.1007/BF01417874. Retrieved from http://dx.doi.org/10.1007/BF01417874

Jensen, A. R. (1987). Individual differences in the hick paradigm. In P. A. Vernon (Ed.). *Speed of information-processing and intelligence* (pp. 101 –175). Ablex Publishing. Retrieved from http://search.ebscohost.com/login.aspx?direct=true&db=psyh&AN=1987-98619-004&site=ehost-live

Jensen, A. R. (1990). Speed of information processing in a calculating prodigy. *Intelligence*, *14*(3), 259 –274. doi:10.1016/0160-2896(90)90019-P

Jensen, A. R., Cohn, S. J., & Cohn, C. M. G. (1989). Speed of information processing in academically gifted youths and their siblings. *Personality and Individual Differences*, *10*(1), 29 –33. doi:10.1016/0191-8869(89)90174-8

Jernigan, T., & Tallal, P. (1990). Late childhood changes in brain morphology observable with mri. *Developmental Medicine and Child Neurology*, *32*(5), 379–385.

Jernigan, T., Trauner, D., Hesselink, J., & Tallal, P. (1991). Maturation of human cerebrum observed in vivo during adolescence. *Brain : a journal of neurology*, *114*(5), 2037–2049.

Jovicich, J., Czanner, S., Greve, D., Haley, E., van der Kouwe, A., Gollub, R., . . . Dale, A. (2006). Reliability in multi-site structural mri studies: effects of gradient non-linearity correction on phantom and human data. *NeuroImage*, *30*(2), 436–43.

Jung, R. E., & Haier, R. J. (2007). The parieto-frontal integration theory (p-fit) of intelligence: converging neuroimaging evidence. *The Behavioral and brain sciences*, *30*(2), 135–54.

Juraska, J. M., & Kopcik, J. R. (1988). Sex and environmental influences on the size and ultrastructure of the rat corpus callosum. *Brain Research*, *450*(1-2), 1 –8. doi:10.1016/0006-8993(88)91538-7

Just, M. A., Cherkassky, V. L., Keller, T. A., Kana, R. K., & Minshew, N. J. (2007). Functional and anatomical cortical underconnectivity in autism: evidence from an fmri study of an executive function task and corpus callosum morphometry. *Cerebral cortex (New York, N.Y. : 1991)*, *17*(4), 951–61.

Kail, R. V. (1991). Developmental change in speed of processing during childhood and adolescence. *Psychological bulletin*, *109*(3), 490–501.

Kail, R. V. (1998). Speed of information processing in patients with multiple sclerosis. *Journal of clinical and experimental neuropsychology : official journal of the International Neuropsychological Society*, *20*(1), 98–106.

Kail, R. V. (2007). Longitudinal evidence that increases in processing speed and working memory enhance children's reasoning. *Psychological science : a journal of the American Psychological Society / APS*, *18*(4), 312–3.

Kail, R. V., & Salthouse, T. A. (1994). Processing speed as a mental capacity. *Acta psychologica*, *86*(2-3), 199–225.

Karama, S., Ad-Dab'bagh, Y., Haier, R. J., Deary, I. J., Lyttelton, O. C., Lepage, C., & Evans, A. C. (2009). Positive association between cognitive ability and cortical thickness in a representative us sample of healthy 6 to 18 year-olds. *Intelligence*, *37*(2), 145–155.

Kent, R. D., & Read, C. (2002). *The acoustic analysis of speech* (2nd). Australia ; United States: Singular/Thomson Learning.

Kertesz, A., Polk, M., Howell, J., & Black, S. E. (1987). Cerebral dominance, sex, and callosal size in mri. *Neurology*, *37*(8), 1385–8.

Kesselring, J. (1997). *Multiple sclerosis*. Cambridge; New York: Cambridge University Press.

Klingberg, T., Hedehus, M., Temple, E., Salz, T., Gabrieli, J. D., Moseley, M. E., & Poldrack, R. A. (2000). Microstructure of temporo-parietal white matter as a basis for reading ability: evidence from diffusion tensor magnetic resonance imaging. *Neuron*, *25*(2), 493 –500. doi: 10.1016/S0896-6273(00)80911-3

Klingberg, T., Vaidya, C. J., Gabrieli, J. D., Moseley, M. E., & Hedehus, M. (1999). Myelination and organization of the frontal white matter in children: a diffusion tensor mri study. *Neuroreport*, *10*(13), 2817–21.

Klouda, G. V., Robin, D. A., Graff-Radford, N. R., & Cooper, W. E. (1988). The role of callosal connections in speech prosody. *Brain and language*, *35*(1), 154–71.

Kotter, R., & Sommer, F. T. (2000). Global relationship between anatomical connectivity and activity propagation in the cerebral cortex. *Philosophical transactions of the Royal Society of London. Series B, Biological sciences*, *355*(1393), 127–34.

Kraft, R., Mitchell, O., Languis, M. L., & Wheatley, G. H. (1980). Hemispheric asymmetries during six- to eight- year-olds performance of piagetian conservation and reading tasks. *Neuropsychologia*, *18*(6), 637 –643. doi:10.1016/0028-3932(80)90103-7

Kranzler, J. H. (1997). What does the wisc-iii measure? comments on the relationship between intelligence, working memory capacity, and information processing speed and efficiency. *School Psychology Quarterly*, *12*(2), 110 –116. doi:10.1037/h0088952

Kranzler, J. H., Whang, P. A., & Jensen, A. R. (1994). Task complexity and the speed and efficiency of elemental information processing: another look at the nature of intellectual giftedness. *Contemporary Educational Psychology*, *19*(4), 447 –459. doi:10.1006/ceps.1994.1032

Kroger, J. K., Sabb, F. W., Fales, C. L., Bookheimer, S. Y., Cohen, M. S., & Holyoak, K. J. (2002). Recruitment of anterior dorsolateral prefrontal cortex in human reasoning: a parametric study of relational complexity. *Cerebral cortex (New York, N.Y. : 1991)*, *12*(5), 477–85.

Kubicki, M., Styner, M., Bouix, S., Gerig, G., Markant, D., Smith, K., . . . Shenton, M. E. (2008). Reduced interhemispheric connectivity in schizophrenia-tractography based segmentation of the corpus callosum. *Schizophrenia research*, *106*(2-3), 125–31.

Kuhn, T. S. (1996). *The structure of scientific revolutions* (3rd). Chicago, IL: University of Chicago Press.

Lacquaniti, F., Guigon, E., Bianchi, L., Ferraina, S., & Caminiti, R. (1995). Representing spatial information for limb movement: role of area 5 in the monkey. *Cerebral cortex (New York, N.Y. : 1991)*, *5*(5), 391–409.

Larson, G., & Alderton, D. (1990). Reaction time variability and intelligence: a worst performance" analysis of individual differences. *Intelligence*, *14*(3), 309–25.

Larson, G. E., Merritt, C. R., & Williams, S. E. (1988). Information processing and intelligence: some implications of task complexity. *Intelligence*, *12*(2), 131 –147. doi:10.1016/0160-2896(88)90012-8

Larson, G. E., & Saccuzzo, D. P. (1989). Cognitive correlates of general intelligence: toward a process theory of g. *Intelligence*, *13*(1), 5 –31. doi:10.1016/0160-2896(89)90003-2

Lee, A., Owen, A., Rogers, R., Sahakian, B., & Robbins, T. (2000). Utility of cantab in functional imaging. In J. M. Rumsey & M. Ernst (Eds.). *Functional neuroimaging in child psychiatry* (Chap. 22, pp. 366–378). Cambridge, UK ; New York: Cambridge University Press.

Lee, K. H., Choi, Y. Y., Gray, J. R., Cho, S. H., Chae, J. H., Lee, S., & Kim, K. (2006). Neural correlates of superior intelligence: stronger recruitment of posterior parietal cortex. *NeuroImage*, *29*(2), 578–86.

Lee, Y., Hung, J., Chang, T., & Huang, C. (2008). Agenesis of the corpus callosum in turner's syndrome: report of a case and review of the literature. *Acta Neurologica Taiwanica*, *17*(3), 194–198. Retrieved from http://www.neuro.org.tw/magz/doc/dw20093495823_17-3\%20p194.pdf

Lenroot, R. K., Gogtay, N., Greenstein, D. K., Wells, E. M., Wallace, G. L., Clasen, L. S., ... Giedd, J. N. (2007). Sexual dimorphism of brain developmental trajectories during childhood and adolescence. *NeuroImage*, *36*(4), 1065 –1073. doi:10.1016/j.neuroimage.2007.03.053

Levy, J. (1972). Lateral specialization of the human brain: behavioral manifestations and possible evolutionary basis. In J. Kiger (Ed.), *The biology of behavior* (pp. 159–180). US: Corvallis, OR: Oregon State University Press.

Liepmann, H., & Maas, O. (1907). Fall von linksseitiger agraphie und apraxie bei rechtsseitiger lahmung. *J Psychol Neurol*, *10*, 214–27.

Liston, C., Watts, R., Tottenham, N., Davidson, M. C., Niogi, S., Ulug, A. M., & Casey, B. (2006). Frontostriatal microstructure modulates efficient recruitment of cognitive control. *Cerebral Cortex*, *16*(4), 553–560. doi:10.1093/cercor/bhj003. eprint: http://cercor.oxfordjournals.org/content/16/4/553.full.pdf+html

Li, T.-Q., & Noseworthy, M. D. (2002). Mapping the development of white matter tracts with diffusion tensor imaging. *Developmental Science*, *5*(3), 293–300.

Luciana, M., & Nelson, C. (2000). Neurodevelopmental assessment of cognitive function using cantab: validation and future goals. In M. Ernst & J. M. Rumsey (Eds.). *Functional neuroimaging in child psychiatry* (pp. 379–397). New York, NY: Cambridge University Press.

Luciana, M., & Nelson, C. (2002). Assessment of neuropsychological function through use of the cambridge neuropsychological testing automated battery: performance in 4- to 12-year-old children. *Developmental neuropsychology*, *22*(3), 595–624.

Luders, E., Narr, K. L., Bilder, R. M., Thompson, P. M., Szeszko, P. R., Hamilton, L., & Toga, A. W. (2007). Positive correlations between corpus callosum thickness and intelligence. *NeuroImage*, *37*(4), 1457–64.

Luders, E., Narr, K. L., Thompson, P. M., & Toga, A. W. (2009). Neuroanatomical correlates of intelligence. *Intelligence*, *37*(2), 156–163.

Luders, E., Thompson, P. M., Narr, K. L., Zamanyan, A., Chou, Y., Gutman, B., . . . Toga, A. W. (2011). The link between callosal thickness and intelligence in healthy children and adolescents. *NeuroImage*, *54*(3), 1823 –1830. doi:10.1016/j.neuroimage.2010.09.083

Luessenhop, A. J. (1970). Interhemispheric commissurotomy: (the split brain operation) as an alternate to hemispherectomy for control of intractable seizures. *The American surgeon*, *36*(5), 265–8.

Mabbott, D. J., Noseworthy, M., Bouffet, E., Laughlin, S., & Rockel, C. (2006). White matter growth as a mechanism of cognitive development in children. *NeuroImage*, *33*(3), 936 – 946. doi:10.1016/j.neuroimage.2006.07.024

Mai, J. K., Assheuer, J., & Paxinos, G. (2004). *Atlas of the human brain* (2nd). Amsterdam ; Boston: Elsevier Academic Press.

Majeres, R. L. (2007). Sex differences in phonological coding: alphabet transformation speed. *Intelligence*, *35*(4), 335 –346. doi:10.1016/j.intell.2006.08.005

Makris, N., Kennedy, D. N., McInerney, S., Sorensen, A. G., Wang, R., Caviness, J., V. S., & Pandya, D. N. (2005). Segmentation of subcomponents within the superior longitudinal fascicle in humans: a quantitative, in vivo, dt-mri study. *Cerebral cortex (New York, N.Y. : 1991)*, *15*(6), 854–69.

Markham, J. A., & Greenough, W. T. (2004). Experience-driven brain plasticity: beyond the synapse. *Neuron glia biology*, *1*(4), 351–363. doi:10.1017/s1740925x05000219

Marzi, C. A., Bisiacchi, P., & Nicoletti, R. (1991). Is interhemispheric transfer of visuomotor information asymmetric? evidence from a meta-analysis. *Neuropsychologia*, *29*(12), 1163–77.

Mathias, J. L., Bigler, E. D., Jones, N. R., Bowden, S. C., Barrett-Woodbridge, M., Brown, G. C., & Taylor, D. J. (2004). Neuropsychological and information processing performance and

its relationship to white matter changes following moderate and severe traumatic brain injury: a preliminary study. *Applied neuropsychology*, *11*(3), 134–52.

McDaniel, M. A. (2005). Big-brained people are smarter: a meta-analysis of the relationship between in vivo brain volume and intelligence. *Intelligence*, *33*(4), 337–346.

McKeever, W. F., Sullivan, K. F., Ferguson, S. M., & Rayport, M. (1981). Typical cerebral hemisphere disconnection deficits following corpus callosum section despite sparing of the anterior commissure. *Neuropsychologia*, *19*(6), 745–755.

McKeever, W. F., Sullivan, K. F., Ferguson, S. M., & Rayport, M. (1982). Right hemisphere speech development in the anterior commissure-spared commissurotomy patient: a second case. *Clinical neuropsychology*, *4*(1), 17–22.

McLaughlin, N. C., Paul, R. H., Grieve, S. M., Williams, L. M., Laidlaw, D., DiCarlo, M., . . . Gordon, E. (2007). Diffusion tensor imaging of the corpus callosum: a cross-sectional study across the lifespan. *International journal of developmental neuroscience : the official journal of the International Society for Developmental Neuroscience*, *25*(4), 215–21.

Mesulam, M. M. (1998). From sensation to cognition. *Brain : a journal of neurology*, *121*(6), 1013–52.

Mesulam, M. M. (2000). Brain, mind, and the evolution of connectivity. *Brain and cognition*, *42*(1), 4–6.

Milner, B., Taylor, L., & Sperry, R. W. (1968). Lateralized suppression of dichotically presented digits after commissural section in man. *Science*, *161*(837), 184–6.

Monnot, M., Lovallo, W. R., Nixon, S. J., & Ross, E. (2002). Neurological basis of deficits in affective prosody comprehension among alcoholics and fetal alcohol-exposed adults. *14*(3), 321–328.

Monrad-Krohn, G. H. (1963). The third element of speech: prosody and its disorders. In L. Halpern (Ed.). *Problems in dynamic neurology* (pp. 101–118). Jerusalem: Hebrew University.

Mountcastle, V. B., Lynch, J. C., Georgopoulos, A., Sakata, H., & Acuna, C. (1975). Posterior parietal association cortex of the monkey: command functions for operations within extrapersonal space. *Journal of neurophysiology*, *38*(4), 871–908.

Nagy, Z., Westerberg, H., & Klingberg, T. (2004). Maturation of white matter is associated with the development of cognitive functions during childhood. *Journal of Cognitive Neuro-*

science, *16*(7), 1227–1233. doi:10.1162/0898929041920441. eprint: http://www.mitpressjournals.org/doi/pdf/10.1162/0898929041920441

Nakahachi, T., Ishii, R., Iwase, M., Canuet, L., Takahashi, H., Kurimoto, R., ... Takeda, M. (2008). Frontal activity during the digit symbol substitution test determined by multichannel near-infrared spectroscopy. *Neuropsychobiology*, *57*(4), 151–8.

Narberhaus, A., Segarra, D., Caldu, X., Gimenez, M., Junque, C., Pueyo, R., & Botet, F. (2007). Gestational age at preterm birth in relation to corpus callosum and general cognitive outcome in adolescents. *Journal of child neurology*, *22*(6), 761–5.

Nestor, P. G., Kubicki, M., Kuroki, N., Gurrera, R. J., Niznikiewicz, M., Shenton, M. E., & McCarley, R. W. (2007). Episodic memory and neuroimaging of hippocampus and fornix in chronic schizophrenia. *Psychiatry Research: Neuroimaging*, *155*(1), 21 –28. doi:10.1016/j.pscychresns.2006.12.020

Newman, S. D., & Just, M. A. (2005). The neural bases of intelligence: a perspective based on functional neuroimaging. In R. J. Sternberg & J. E. Pretz (Eds.). *Cognition and intelligence: identifying the mechanisms of the mind* (pp. 88–103). New York: Cambridge University Press.

Niogi, S. N., & McCandliss, B. D. (2006). Left lateralized white matter microstructure accounts for individual differences in reading ability and disability. *Neuropsychologia*, *44*(11), 2178 –2188. Advances in Developmental Cognitive Neuroscience. doi:10.1016/j.neuropsychologia.2006.01.011

Nosarti, C., Rushe, T. M., Woodruff, P. W., Stewart, A. L., Rifkin, L., & Murray, R. M. (2004). Corpus callosum size and very preterm birth: relationship to neuropsychological outcome. *Brain : a journal of neurology*, *127*(Pt 9), 2080–9.

O'Boyle, M. W. (2008). Mathematically gifted children: developmental brain characteristics and their prognosis for well-being. *Roeper Review*, *30*(3), 181–186. doi:10.1080/02783190802199594. eprint: http://www.tandfonline.com/doi/pdf/10.1080/02783190802199594

O'Boyle, M. W., Cunnington, R., Silk, T. J., Vaughan, D., Jackson, G., Syngeniotis, A., & Egan, G. F. (2005). Mathematically gifted male adolescents activate a unique brain network during mental rotation. *Brain research. Cognitive brain research*, *25*(2), 583–7.

O'Brien, J. T., Wiseman, R., Burton, E. J., Barber, B., Wesnes, K., Saxby, B., & Ford, G. A. (2002). Cognitive associations of subcortical white matter lesions in older people. *Annals of the New York Academy of Sciences*, *977*, 436–44.

O'Kusky, J., Strauss, E., Kosaka, B., Wada, J., Li, D., Druhan, M., & Petrie, J. (1988). The corpus callosum is larger with right-hemisphere cerebral speech dominance. *Annals of neurology*, *24*(3), 379–383.

Olton, D. S., & Feustle, W. A. (1981). Hippocampal function required for nonspatial working memory. *Experimental brain research. Experimentelle Hirnforschung. Experimentation cerebrale*, *41*(3-4), 380–9.

Oppenheim, J. S., Lee, B. C., Nass, R., & Gazzaniga, M. S. (1987). No sex-related differences in human corpus callosum based on magnetic resonance imagery. *Annals of neurology*, *21*(6), 604–6.

Osawa, A., Maeshima, S., Kubo, K., & Itakura, T. (2006). Neuropsychological deficits associated with a tumour in the posterior corpus callosum: a report of two cases. *Brain injury : [BI]*, *20*(6), 673–6.

Owen, A. M., Downes, J. J., Sahakian, B. J., Polkey, C. E., & Robbins, T. W. (1990). Planning and spatial working memory following frontal lobe lesions in man. *Neuropsychologia*, *28*(10), 1021–34.

Owen, A. M., Evans, A. C., & Petrides, M. (1996). Evidence for a two-stage model of spatial working memory processing within the lateral frontal cortex: a positron emission tomography study. *Cerebral cortex (New York, N.Y. : 1991)*, *6*(1), 31–8.

Owen, A. M., Morris, R. G., Sahakian, B. J., Polkey, C. E., & Robbins, T. W. (1996). Double dissociations of memory and executive functions in working memory tasks following frontal lobe excisions, temporal lobe excisions or amygdalo-hippocampectomy in man. *Brain : a journal of neurology*, *119 (Pt 5)*, 1597–615.

Pakkenberg, B., & Gundersen, H. J. G. (1997). Neocortical neuron number in humans: effect of sex and age. *The Journal of Comparative Neurology*, *384*(2), 312–320.

Pandya, D. N., Karol, E. A., & Heilbronn, D. (1971). The topographical distribution of interhemispheric projections in the corpus callosum of the rhesus monkey. *Brain research*, *32*(1), 31–43.

Pandya, D. N., & Seltzer, B. (1986). The topography of commissural fibers. In F. Lepore, M. Ptito & H. H. Jasper (Eds.). *Two hemispheres - one brain: functions of the corpus callosum* (pp. 47–73). New York: Liss.

Pardo, J. V., Pardo, P. J., Janer, K. W., & Raichle, M. E. (1990). The anterior cingulate cortex mediates processing selection in the stroop attentional conflict paradigm. *Proceedings of the National Academy of Sciences of the United States of America*, *87*(1), 256–9.

Parks, R., Loewenstein, D., Dodrill, K., Barker, W., Yoshii, F., Chang, J., . . . Duara, R. (1988). Cerebral metabolic effects of a verbal fluency test: a pet scan study. *Journal of Clinical and Experimental Neuropsychology*, *10*(5), 565–575. cited By (since 1996) 135. Retrieved from http://www.scopus.com/inward/record.url?eid=2-s2.0-0023695499\&partnerID=40\&md5=1d7de538bb00be2edaed9314a9f319fa

Parsons, O. A., Stewart, K. D., & Arenberg, D. (1957). Impairment of abstracting ability in multiple sclerosis. *The Journal of nervous and mental disease*, *125*(2), 221–5.

Paul, L., Brown, W., Adolphs, R., Tyszka, J., Richards, L., Mukherjee, P., & Sherr, E. (2007). Agenesis of the corpus callosum: genetic, developmental and functional aspects of connectivity. *Nature Reviews Neuroscience*, *8*(4), 287–299.

Pelletier, J., Suchet, L., Witjas, T., Habib, M., Guttmann, C. R., Salamon, G., . . . Cherif, A. A. (2001). A longitudinal study of callosal atrophy and interhemispheric dysfunction in relapsing-remitting multiple sclerosis. *Archives of neurology*, *58*(1), 105–11.

Pell, G. S., Briellmann, R. S., Chan, C. H. (, Pardoe, H., Abbott, D. F., & Jackson, G. D. (2008). Selection of the control group for vbm analysis: influence of covariates, matching and sample size. *NeuroImage*, *41*(4), 1324 –1335. doi:10.1016/j.neuroimage.2008.02.050

Pell, M. D. (1998). Recognition of prosody following unilateral brain lesion: influence of functional and structural attributes of prosodic contours. *Neuropsychologia*, *36*(8), 701–15.

Peterson, B. S., Feineigle, P. A., Staib, L. H., & Gore, J. C. (2001). Automated measurement of latent morphological features in the human corpus callosum. *Human brain mapping*, *12*(4), 232–45.

Peterson, B. S., Vohr, B., Staib, L. H., Cannistraci, C. J., Dolberg, A., Schneider, K. C., . . . Ment, L. R. (2000). Regional brain volume abnormalities and long-term cognitive outcome in

preterm infants. *JAMA : the journal of the American Medical Association*, *284*(15), 1939–47.

Petrides, M., & Milner, B. (1982). Deficits on subject-ordered tasks after frontal- and temporal-lobe lesions in man. *Neuropsychologia*, *20*(3), 249–62.

Peyser, J. M., Edwards, K. R., Poser, C. M., & Filskov, S. B. (1980). Cognitive function in patients with multiple sclerosis. *Archives of neurology*, *37*(9), 577–9.

Piercy, M. (1964). The effects of cerebral lesions on intellectual function: a review of current research trends. *The British journal of psychiatry : the journal of mental science*, *110*, 310–52.

Poffenberger, A. T. (1913). Reaction time to retinal stimulation, with special reference to the time lost in conduction through nerve centers. *Archives of Psychology*, *23*(1), 1–73.

Poltana, P., Poulpanich, N., Withyachumnarnkul, B., Suriyaprapadilok, L., & Inthisean, P. (2001). No significant sexual dimorphism of the corpus callosum in thai subjects: a study using stained plastinated brain slices. *ScienceAsia*, *27*, 203–209.

Posner, M. I., & Petersen, S. E. (1990). The attention system of the human brain. *Annual Review of Neuroscience*, *13*, 25–42.

Posthuma, D., De Geus, E. J., Baare, W. F., Hulshoff Pol, H. E., Kahn, R. S., & Boomsma, D. I. (2002). The association between brain volume and intelligence is of genetic origin. *Nature neuroscience*, *5*(2), 83–4.

Prabhakaran, V., Rypma, B., & Gabrieli, J. D. (2001). Neural substrates of mathematical reasoning: a functional magnetic resonance imaging study of neocortical activation during performance of the necessary arithmetic operations test. *Neuropsychology*, *15*(1), 115–27.

Prabhakaran, V., Smith, J. A. L., Desmond, J. E., Glover, G. H., & Gabrieli, J. D. E. (1997). Neural substrates of fluid reasoning: an fmri study of neocortical activation during performance of the raven's progressive matrices test. *Cognitive Psychology*, *33*(1), 43–63.

Pujol, J., Soriano-Mas, C., Ortiz, H., Sebastian-Galles, N., Losilla, J. M., & Deus, J. (2006). Myelination of language-related areas in the developing brain. *Neurology*, *66*(3), 339–343. doi:10.1212/01.wnl.0000201049.66073.8d. eprint: http://www.neurology.org/content/66/3/339.full.pdf+html

Purves, D., & Williams, S. M. (2001). *Neuroscience* (2nd). Sunderland, Mass.: Sinauer Associates.

Rao, S. M. (1996). White matter disease and dementia. *Brain and cognition*, *31*(2), 250–68.

Rao, S. M., & Hammeke, T. A. (1984). Hypothesis testing in patients with chronic progressive multiple sclerosis. *Brain and cognition*, *3*(1), 94–104.

Rao, S. M., Hammeke, T. A., & Speech, T. J. (1987). Wisconsin card sorting test performance in relapsing-remitting and chronic-progressive multiple sclerosis. *Journal of consulting and clinical psychology*, *55*(2), 263–5.

Rao, S. M., Leo, G. J., Bernardin, L., & Unverzagt, F. (1991). Cognitive dysfunction in multiple sclerosis. i. frequency, patterns, and prediction. *Neurology*, *41*(5), 685–91.

Rao, S. M., St Aubin-Faubert, P., & Leo, G. J. (1989). Information processing speed in patients with multiple sclerosis. *Journal of clinical and experimental neuropsychology : official journal of the International Neuropsychological Society*, *11*(4), 471–7.

Raven, J., Raven, J. C., & Court, J. H. (1998). *Manual for raven's advanced progressive matrices.* Oxford, England: Oxford Psychologists Press.

Reinarz, S. J., Coffman, C. E., Smoker, W. R., & Godersky, J. C. (1988). Mr imaging of the corpus callosum: normal and pathologic findings and correlation with ct. *American Journal of Roentgenology*, *151*(4), 791–798.

Reitan, R. M., & Wolfson, D. (2004). The halstead-reitan neuropsychological test battery for adults: theoretical, methodological, and validational bases. In G. Goldstein & S. Beers (Eds.), *Comprehensive handbook of psychological assessment: intellectual and neuropsychological assessment* (pp. 105 –132). US: Hoboken, NJ: Wiley.

Reitan, R. M., Reed, J. C., & Dyken, M. L. (1971). Cognitive, psychomotor, and motor correlates of multiple sclerosis. *The Journal of nervous and mental disease*, *153*(3), 218–24.

Retzius, G. (1898). Das gehirn des astronomen, hugo gylden. *Biologische Untersuchungen, neue Folge*, *8*, 1–22.

Retzius, G. (1900a). Das gehirn des physikers und padagogen per adam siljestrom. *Biologische Untersuchungen, neue Folge*, *10*, 1–14.

Retzius, G. (1900b). Gehirn des mathematikers sonja kowalewski. *Biologische Untersuchungen, neue Folge*, *9*, 1–16.

Retzius, G. (1904). Das gehirn eines staatsmannes. *Biologische Untersuchungen, neue Folge*, *11*, 89–102.

Retzius, G. (1905). Das gehirn des histologen und physiologen christian loven. *Biologische Untersuchungen, neue Folge*, *12*, 3–9.

Reuter, M. (2009). Eitv - free surfer wiki. Martinos Center for Biomedical Imaging.

Robinson, D. L., Goldberg, M. E., & Stanton, G. B. (1978). Parietal association cortex in the primate: sensory mechanisms and behavioral modulations. *Journal of Neurophysiology*, *41*(4), 910–32.

Roivainen, E. (2011). Gender differences in processing speed: a review of recent research. *Learning and Individual Differences*, *21*(2), 145 –149. doi:10.1016/j.lindif.2010.11.021

Rooy, C. V., Song, J., & Stough, C. (2005). Neurobiology of intelligence. In C. Stough (Ed.), *Neurobiology of exceptionality* (pp. 73–103). The Springer Series on Human Exceptionality. 10.1007. Springer US. Retrieved from http://dx.doi.org/10.1007/0-306-48649-04

Rose, S. E., Chen, F., Chalk, J. B., Zelaya, F. O., Strugnell, W. E., Benson, M., ... Doddrell, D. M. (2000). Loss of connectivity in alzheimer's disease: an evaluation of white matter tract integrity with colour coded mr diffusion tensor imaging. *Journal of neurology, neurosurgery, and psychiatry*, *69*(4), 528–30.

Ross, E. D. (1997). Cortical representation of the emotions. In M. R. Trimble & J. L. Cummings (Eds.). *Contemporary behavioral neurology* (pp. 107–126). Boston: Butterworth-Heineman.

Ross, E. D. (2000). Affective prosody and the aprosodias. In M. M. Mesulam (Ed.). *Principles of behavioral and cognitive neurology* (pp. 316–331). New York: Oxford University Press.

Ross, E. D., & Mesulam, M. M. (1979). Dominant language functions of the right hemisphere? prosody and emotional gesturing. *Archives of neurology*, *36*(3), 144–8.

Royston, P. (1995). Remark as r94: a remark on algorithm as 181: the w-test for normality. *Journal of the Royal Statistical Society. Series C (Applied Statistics)*, *44*(4), 547–551. Retrieved from http://www.jstor.org/stable/2986146

Ruff, C. C., Knauff, M., Fangmeier, T., & Spreer, J. (2003). Reasoning and working memory: common and distinct neuronal processes. *Neuropsychologia*, *41*(9), 1241–53.

Ruiz Villarreal, M. (2007). Complete neuron cell diagram. Wikimedia Commons.

Rushton, J. P., & Ankney, C. D. (2007). The evolution of brain size and intelligence. In S. M. Platek, J. P. Keenan & T. K. Shackelford (Eds.). *Evolutionary cognitive neuroscience* (pp. 121–161). Cambridge, MA: MIT Press.

Ryalls, J. (1988). Concerning right-hemisphere dominance for affective language. *Archives of neurology*, *45*(3), 337–8.

Sakata, H., Takaoka, Y., Kawarasaki, A., & Shibutani, H. (1973). Somatosensory properties of neurons in the superior parietal cortex (area 5) of the rhesus monkey. *Brain research*, *64*, 85–102.

Salthouse, T. A. (1996). The processing-speed theory of adult age differences in cognition. *Psychological review*, *103*(3), 403–28.

Salthouse, T. A. (2005). Relations between cognitive abilities and measures of executive functioning. *Neuropsychology*, *19*(4), 532–45.

Salvatori, R. (1999). Albert einstein's brain. *Lancet*, *354*(9192), 1821–2.

Sanchez, M. M., Hearn, E. F., Do, D., Rilling, J. K., & Herndon, J. G. (1998). Differential rearing affects corpus callosum size and cognitive function of rhesus monkeys. *Brain Research*, *812*(1-2), 38 –49. doi:10.1016/S0006-8993(98)00857-9

Sattler, J. M. (1992). *Assessment of children : wisc-iii and wppsi-r supplement*. San Diego, Calif.: J.M. Sattler.

Sauerwein, H. C., & Lassonde, M. (1994, October). Cognitive and sensori-motor functioning in the absence of the corpus callosum: neuropsychological studies in callosal agenesis and callosotomized patients. *Behavioural brain research*, *64*(1-2), 229–240.

Scepkowski, L. A., & Cronin-Golomb, A. (2003). The alien hand: cases, categorizations, and anatomical correlates. *Behavioral and cognitive neuroscience reviews*, *2*(4), 261–77.

Schatz, J., & Buzan, R. (2006). Decreased corpus callosum size in sickle cell disease: relationship with cerebral infarcts and cognitive functioning. *Journal of the International Neuropsychological Society : JINS*, *12*(1), 24–33.

Schmansky, N. (2009). Free surfer wiki. Martinos Center for Biomedical Imaging.

Schmithorst, V. J., Wilke, M., Dardzinski, B. J., & Holland, S. K. (2005). Cognitive functions correlate with white matter architecture in a normal pediatric population: a diffusion tensor mri study. *Human Brain Mapping*, *26*(2), 139–147. doi:10.1002/hbm.20149

Segonne, F., Dale, A. M., Busa, E., Glessner, M., Salat, D., Hahn, H. K., & Fischl, B. (2004). A hybrid approach to the skull stripping problem in mri. *NeuroImage*, *22*(3), 1060–75.

Segonne, F., Pacheco, J., & Fischl, B. (2007). Geometrically accurate topology-correction of cortical surfaces using nonseparating loops. *IEEE transactions on medical imaging*, *26*(4), 518–29.

Seitz, J. A. (1999). Albert einstein's brain. *Lancet*, *354*(9192), 1822–3.

Semendeferi, K., Teffer, K., Buxhoeveden, D. P., Park, M. S., Bludau, S., Amunts, K., ... Buckwalter, J. (2010). Spatial organization of neurons in the frontal pole sets humans apart from great apes. *Cerebral Cortex*. doi:10.1093/cercor/bhq191. eprint: http://cercor.oxfordjournals.org/content/early/2010/11/23/cercor.bhq191.full.pdf+html

Shadlen, M. N., & Movshon, J. A. (1999). Synchrony unbound: a critical evaluation of the temporal binding hypothesis. *Neuron*, *24*(1), 67–77, 111–25.

Shannon, C. E. (1948a). A mathematical theory of communication (part i). *Bell Systems Technical Journal*, *27*, 379–423.

Shannon, C. E. (1948b). A mathematical theory of communication (part ii). *Bell Systems Technical Journal*, *27*, 623–656.

Shannon, C. E. (2001). A mathematical theory of communication. *SIGMOBILE Mob. Comput. Commun. Rev. 5*(1), 3–55.

Shaw, P., Greenstein, D., Lerch, J., Clasen, L., Lenroot, R., Gogtay, N., ... Giedd, J. N. (2006). Intellectual ability and cortical development in children and adolescents. *Nature*, *440*(7084), 676–9.

Shaw, P., Kabani, N. J., Lerch, J. P., Eckstrand, K., Lenroot, R., Gogtay, N., ... Wise, S. P. (2008). Neurodevelopmental trajectories of the human cerebral cortex. *The Journal of neuroscience : the official journal of the Society for Neuroscience*, *28*(14), 3586–94.

Shaywitz, B. A., Shaywitz, S. E., Pugh, K. R., Constable, R. T., Skudlarski, P., Fulbright, R. K., . . . et al. (1995). Sex differences in the functional organization of the brain for language. *Nature*, *373*(6515), 607–9.

Shenton, M. E., Dickey, C. C., Frumin, M., & McCarley, R. W. (2001). A review of mri findings in schizophrenia. *Schizophrenia research*, *49*(1-2), 1–52.

Sheppard, L. D., & Vernon, P. A. (2008). Intelligence and speed of information-processing: a review of 50 years of research. *Personality and Individual Differences*, *44*(3), 535 –551. doi:10.1016/j.paid.2007.09.015

Shulman, G. L., Corbetta, M., Buckner, R. L., Raichle, M. E., Fiez, J. A., Miezin, F. M., & Petersen, S. E. (1997). Top-down modulation of early sensory cortex. *Cerebral cortex (New York, N.Y. : 1991)*, *7*(3), 193–206.

Sidtis, J. J. (1988). Dichotic listening after commissurotomy. In K. Hugdahl (Ed.). *Handbook of dichotic listening : theory, methods, and research* (pp. 161–184). New York: Wiley.

Sidtis, J. J., Volpe, B. T., Wilson, D. H., Rayport, M., & Gazzaniga, M. S. (1981). Variability in right hemisphere language function after callosal section: evidence for a continuum of generative capacity. *The Journal of neuroscience : the official journal of the Society for Neuroscience*, *1*(3), 323–31.

Singer, W. (1999). Neuronal synchrony: a versatile code for the definition of relations? *Neuron*, *24*(1), 49–65, 111–25.

Singer, W., & Gray, C. M. (1995). Visual feature integration and the temporal correlation hypothesis. *Annual review of neuroscience*, *18*, 555–86.

Sled, J. G., Zijdenbos, A. P., & Evans, A. C. (1998). A nonparametric method for automatic correction of intensity nonuniformity in mri data. *IEEE transactions on medical imaging*, *17*(1), 87–97.

Smith, E. E., & Jonides, J. (1999). Storage and executive processes in the frontal lobes. *Science*, *283*(5408), 1657–61.

Smith, R. (1997). *The norton history of the human sciences* (1st American). Norton history of science. New York: W.W. Norton.

Sowell, E. R., Peterson, B. S., Thompson, P. M., Welcome, S. E., Henkenius, A. L., & Toga, A. W. (2003). Mapping cortical change across the human life span. *Nature neuroscience*, *6*(3), 309–15.

Sowell, E., Thompson, P., Tessner, K., & Toga, A. (2001). Mapping continued brain growth and gray matter density reduction in dorsal frontal cortex: inverse relationships during postadolescent brain maturation. *Journal of Neuroscience*, *21*(22), 8819–8829.

Sowell, E. R., Thompson, P. M., & Toga, A. W. (2004). Mapping changes in the human cortex throughout the span of life. *The Neuroscientist : a review journal bringing neurobiology, neurology and psychiatry*, *10*(4), 372–92.

Spearman, C. (1923). *The nature of "intelligence" and the principles of cognition*. London: Macmillan.

Spearman, C. (1927). *The abilities of man; their nature and measurement*. New York: The Macmillan Company.

Spencer, M. D., Gibson, R. J., Moorhead, T. W., Keston, P. M., Hoare, P., Best, J. J., . . . Johnstone, E. C. (2005). Qualitative assessment of brain anomalies in adolescents with mental retardation. *AJNR. American journal of neuroradiology*, *26*(10), 2691–7.

Sperling, R. A., Guttmann, C. R., Hohol, M. J., Warfield, S. K., Jakab, M., Parente, M., . . . Weiner, H. L. (2001). Regional magnetic resonance imaging lesion burden and cognitive function in multiple sclerosis: a longitudinal study. *Archives of neurology*, *58*(1), 115–21.

Sperry, R. W., Gazzaniga, M. S., & Bogen, J. E. (1969). Interhemispheric relationships: the neocortical commissures; syndromes of hemisphere disconnection. In J. J. Vinken & G. W. Bruyn (Eds.). *Handbook of clinical neurology* (Vol. 4, pp. 273–290). Amsterdam: Elsevier.

Spitzka, E. A. (1903a). A study of the brain of the late major j. w. powell. *American Anthropologist*, *5*(4), 585–643.

Spitzka, E. A. (1903b). The brain of professor laborde. *Science*, *18*(454), 346.

Spitzka, E. A. (1904a). Professor taguchi's brain-weight. *Science*, *20*(502), 215.

Spitzka, E. A. (1904b). The brain of a swedish statesman. *Science*, *20*(514), 612–613.

Spitzka, E. A. (1905). The brain of the histologist and physiologist otto c. loven. *Science*, *21*(548), 994.

Spitzka, E. A. (1907). A study of the brains of six eminent scientists and scholars belonging to the american anthropometric society, together with a description of the skull of professor ed cope. *Transactions of the American Philosophical Society*, *21*(4), 175–308.

Sprandel, H. Z. (1995). *The psychoeducational use and interpretation of the wechsler adult intelligence scale-revised* (2nd). Springfield, Ill., U.S.A.: C.C. Thomas.

Springer, S. P., & Deutsch, G. (1997). *Left brain, right brain: perspectives from cognitive neuroscience* (5th). A Series of books in psychology. New York: Freeman.

Stepan, N. L. (1986). Race and gender: the role of analogy in science. *Isis; an international review devoted to the history of science and its cultural influences*, *77*(2), 261–277.

Sternberg, R. J. (1985). *Beyond iq : a triarchic theory of human intelligence*. Cambridge [Cambridgeshire] ; New York: Cambridge University Press.

Strauss, E., Sherman, E. M. S., & Spreen, O. (2006). *A compendium of neuropsychological tests : administration, norms, and commentary* (3rd). New York: Oxford University Press.

Strauss, E., Wada, J., & Hunter, M. (1994). Callosal morphology and performance on intelligence tests. *Journal of clinical and experimental neuropsychology : official journal of the International Neuropsychological Society*, *16*(1), 79–83.

Strub, R. L., & Black, F. W. (1977). *The mental status examination in neurology*. Philadelphia, PA: F. A. Davis Co.

Suwanwela, N. C., & Leelacheavasit, N. (2002). Isolated corpus callosal infarction secondary to pericallosal artery disease presenting as alien hand syndrome. *Journal of neurology, neurosurgery, and psychiatry*, *72*(4), 533–6.

Swirsky-Sacchetti, T., Mitchell, D. R., Seward, J., Gonzales, C., Lublin, F., Knobler, R., & Field, H. L. (1992). Neuropsychological and structural brain lesions in multiple sclerosis: a regional analysis. *Neurology*, *42*(7), 1291–5.

Szalay, F. (2001). Development of the equine brain motor system. *Neurobiology (Budapest, Hungary)*, *9*(2), 107–135.

Tabachnick, B. G., & Fidell, L. S. (2007). *Using multivariate statistics* (5th). Boston: Pearson/Allyn & Bacon.

Team, R. D. C. (2009). R: a language and environment for statistical computing. R Foundation for Statistical Computing.

Teipel, S. J., Bayer, W., Alexander, G. E., Zebuhr, Y., Teichberg, D., Kulic, L., . . . Hampel, H. (2002). Progression of corpus callosum atrophy in alzheimer disease. *Archives of neurology*, *59*(2), 243–8.

Tessitore, C., & Brunjes, P. C. (1988, September). A comparative study of myelination in precocial and altricial murid rodents. *Brain research*, *471*(1), 139–147.

Thomann, P. A., Wustenberg, T., Pantel, J., Essig, M., & Schroder, J. (2006). Structural changes of the corpus callosum in mild cognitive impairment and alzheimer's disease. *Dementia and geriatric cognitive disorders*, *21*(4), 215–20.

Thompson, P. M., Cannon, T. D., Narr, K. L., van Erp, T., Poutanen, V. P., Huttunen, M., . . . Toga, A. W. (2001). Genetic influences on brain structure. *Nature neuroscience*, *4*(12), 1253–8.

Thompson, P. M., Giedd, J. N., Woods, R. P., MacDonald, D., Evans, A. C., & Toga, A. W. (2000). Growth patterns in the developing brain detected by using continuum mechanical tensor maps. *Nature*, *404*(6774), 190–3.

Tilney, F., & Casamajor, L. (1924). Myelinogeny as applied to the study of behavior. *Archives of neurology and psychiatry*, *12*(1), 1–66. doi:10.1001/archneurpsyc.1924.02200010004001. eprint: http://archneurpsyc.ama-assn.org/cgi/reprint/12/1/1.pdf

Toga, A. W., & Thompson, P. M. (2003). Mapping brain asymmetry. *Nature reviews. Neuroscience*, *4*(1), 37–48.

Toga, A. W., & Thompson, P. M. (2005). Genetics of brain structure and intelligence. *Annual review of neuroscience*, *28*, 1–23.

Toga, A. W., Thompson, P. M., & Sowell, E. R. (2006). Mapping brain maturation. *Trends in neurosciences*, *29*(3), 148–59.

Tolhurst, D. J., & Lewis, P. R. (1992). Effect of myelination on the conduction velocity of optic nerve fibres. *Ophthalmic & physiological optics : the journal of the British College of Ophthalmic Opticians (Optometrists)*, *12*(2), 241–3.

Tomasch, J. (1954). Size, distribution, and number of fibres in the human corpus callosum. *The Anatomical record*, *119*(1), 119–35.

Tovar-Moll, F., Moll, J., de Oliveira-Souza, R., Bramati, I., Andreiuolo, P. A., & Lent, R. (2007). Neuroplasticity in human callosal dysgenesis: a diffusion tensor imaging study. *Cerebral*

Cortex, *17*(3), 531–541. doi:10.1093/cercor/bhj178. eprint: http://cercor.oxfordjournals.org/content/17/3/531.full.pdf+html

Tramo, M. J., Loftus, W. C., Stukel, T. A., Green, R. L., Weaver, J. B., & Gazzaniga, M. S. (1998). Brain size, head size, and intelligence quotient in monozygotic twins. *Neurology*, *50*(5), 1246–52.

Trauner, D. A., Ballantyne, A., Friedland, S., & Chase, C. (1996). Disorders of affective and linguistic prosody in children after early unilateral brain damage. *Annals of neurology*, *39*(3), 361–7.

Trevarthen, C. (1978). Manipulative strategies of baboons and the origins of cerebral asymmetry. In M. Kinsbourne (Ed.). *Asymmetrical function of the brain* (pp. 329–389). Cambridge: Cambridge University Press.

Tucker, D. M., Watson, R. T., & Heilman, K. M. (1977). Discrimination and evocation of affectively intoned speech in patients with right parietal disease. *Neurology*, *27*(10), 947–50.

Tukey, J. (1977). *Exploratory data analysis*. Reading: Addison-Wesley Pub. Co.

Turken, U., Whitfield-Gabrieli, S., Bammer, R., Baldo, J. V., Dronkers, N. F., & Gabrieli, J. D. E. (2008). Cognitive processing speed and the structure of white matter pathways: convergent evidence from normal variation and lesion studies. *NeuroImage*, *42*(2), 1032–1044.

Valera, E. M., Faraone, S. V., Murray, K. E., & Seidman, L. J. (2007). Meta-analysis of structural imaging findings in attention-deficit/hyperactivity disorder. *Biological psychiatry*, *61*(12), 1361–9.

van der Knaap, M. S., Valk, J., Bakker, C. J., Schooneveld, M., Faber, J. A., Willemse, J., & Gooskens, R. H. (1991). Myelination as an expression of the functional maturity of the brain. *Developmental medicine and child neurology*, *33*(10), 849–57.

Van Essen, D. (1997, January). A tension-based theory of morphogenesis and compact wiring in the central nervous system. *Nature*, *385*(6614), 313–318. doi:10.1038/385313a0

Verger, K., Junque, C., Levin, H. S., Jurado, M. A., Perez-Gomez, M., Bartres-Faz, D., . . . Mercader, J. M. (2001). Correlation of atrophy measures on mri with neuropsychological sequelae in children and adolescents with traumatic brain injury. *Brain injury : [BI]*, *15*(3), 211–21.

Vernon, P. A. (1987). *Speed of information-processing and intelligence*. Westport, CT, US: Ablex Publishing.

Vernon, P. A. (1990). An overview of chronometric measures of intelligence. *School Psychology Review*, *19*(4), 399 –410. Retrieved from http://search.ebscohost.com/login.aspx?direct=true&db=psyh&AN=1991-11744-001&site=ehost-live

Vernon, P. A. (1993). Intelligence and neural efficiency. In *Individual differences and cognition* (pp. 171 –187). Current topics in human intelligence; Vol. 3; 8755-0040. Ablex Publishing.

Vesalius, A. (1543). *De humani corporis fabrica libri septem*. Basileae: Ex officina Joannis Oporini.

Volterra, A., & Steinhauser, C. (2004). Glial modulation of synaptic transmission in the hippocampus. *Glia*, *47*(3), 249–57.

von Bechterew, W., & Weinberg, R. (1909). Das gehirn des chemikers d.j . mendelew. In W. Raux (Ed.). *Anatomische und entwicklungsgeschichtliche monographien* (Vol. 1, pp. 1–22). Leipzig: Engelmann.

von Bertalanffy, L. (1950). An outline of general system theory. *British Journal for the Philosophy of Science*, *1*(2), 134–165.

Waber, D. P., De Moor, C., Forbes, P. W., Almli, C. R., Botteron, K. N., Leonard, G., ... Rumsey, J. (2007). The nih mri study of normal brain development: performance of a population based sample of healthy children aged 6 to 18 years on a neuropsychological battery. *Journal of the International Neuropsychological Society : JINS*, *13*(5), 729–46.

Wagner, R. (1860). *Vorstudien zu einer wissenschaftlichen morphologie und physiologie des menschlichen gehirns als seelenorgan. abh. 1: uber die typischen verschiedenheiten der windungen der hemispharen und uber die lehre vom hirngewicht, mit besonderer rucksicht auf die hirnbildung intelligenter manner. mit 6 kupfertafeln*. Goettingen: Verlag der Dieterichschen Buchhandlung.

Wagner, R. (1862). *Vorstudien zu einer wissenschaftlichen morphologie und physiologie des menschlichen gehirns als seelenorgan. abh. 2: uber den hirnbau der mikrocephalen mit vergleichender rucksicht auf den bau des gehirns der normalen menschen und der quadrumanen. mit 5 tafeln*. Goettingen: Verlag der Dieterichschen Buchhandlung.

Walterfang, M., Yung, A., Wood, A. G., Reutens, D. C., Phillips, L., Wood, S. J., ... Pantelis, C. (2008). Corpus callosum shape alterations in individuals prior to the onset of psychosis. *Schizophrenia research*, *103*(1-3), 1–10.

Waltz, J. A., Knowlton, B. J., Holyoak, K. J., Boone, K. B., Mishkin, F. S., Santoa, M. d. M., . . . Miller, B. L. (1999). A system for relational reasoning in human prefrontal cortex. *Psychological Science*, *10*, 119–125.

Wang, J.-J., & Kaufman, A. S. (1993). Changes in fluid and crystallized intelligence across the 20- to 90-year age range on the k-bit. *Journal of Psychoeducational Assessment*, *11*(1), 29–37.

Wang, P. J., Saykin, A. J., Flashman, L. A., Wishart, H. A., Rabin, L. A., Santulli, R. B., . . . Mamourian, A. C. (2006). Regionally specific atrophy of the corpus callosum in ad, mci and cognitive complaints. *Neurobiology of aging*, *27*(11), 1613–7.

Waxman, S. G. (1980). Determinants of conduction velocity in myelinated nerve fibers. *Muscle & nerve*, *3*(2), 141–50.

Weber, G., & Weis, S. (1986). Morphometric analysis of the human corpus callosum fails to reveal sex-related differences. *Journal fur Hirnforschung*, *27*(2), 237–40.

Wechsler, D. (1939). *The measurement of adult intelligence*. Baltimore, MD: Williams & Wilkins.

Wechsler, D. (1991). *Wechsler intelligence scale for children-third edition.*

Wechsler, D. (1997). *Manual for the wechsler adult intelligence scale-third edition.*

Weis, S., Jellinger, K., & Wenger, E. (1991). Morphometry of the corpus callosum in normal aging and alzheimer's disease. *Journal of neural transmission. Supplementum*, *33*, 35–8.

Wilke, M., Holland, S. K., Altaye, M., & Gaser, C. (2008). Template-o-matic: a toolbox for creating customized pediatric templates. *NeuroImage*, *41*, 903–913.

Wilson, D. H., Reeves, A., & Gazzaniga, M. (1978). Division of the corpus callosum for uncontrollable epilepsy. *Neurology*, *28*(7), 649–53.

Wilson, D. H., Reeves, A., Gazzaniga, M., & Culver, C. (1977). Cerebral commissurotomy for control of intractable seizures. *Neurology*, *27*(8), 708–15.

Witelson, S. F. (1989). Hand and sex differences in the isthmus and genu of the human corpus callosum. a postmortem morphological study. *Brain : a journal of neurology*, *112*(3), 799–835.

Witelson, S. F., Kigar, D. L., & Harvey, T. (1999). The exceptional brain of albert einstein. *Lancet*, *353*(9170), 2149–53.

Yakovlev, P. I., & Lecours, A. R. (1967). The myelogenetic cycles of regional maturation of the brain. In A. Minkowski, C. for International Organizations of Medical Sciences. & F. D. generale a la recherche scientifique et technique. (Eds.). *Regional development of the brain in early life* (pp. 3–70). Edinburgh: Blackwell Scientific.

Yamauchi, H., Fukuyama, H., Ogawa, M., Ouchi, Y., & Kimura, J. (1994). Callosal atrophy in patients with lacunar infarction and extensive leukoaraiosis. an indicator of cognitive impairment. *Stroke; a journal of cerebral circulation*, *25*(9), 1788–93.

Zaidel, E. (1975). A technique for presenting lateralized visual input with prolonged exposure. *Vision Research*, *15*(2), 283 –289. doi:10.1016/0042-6989(75)90220-5

Zaidel, E. (1978). Lexical organization in the right hemisphere. In P. Buser & A. Gougeul-Buser (Eds.). *Cerebral correlates of conscious experience* (pp. 177–197). Amsterdam: Elsevier.

Zaidel, E. (1983). Disconnection syndrome as a model for laterality effects in the normal brain. In J. B. Hellige (Ed.). *Cerebral hemisphere asymmetry: method, theory, and application* (pp. 95–151). New York: Praeger.

Zaidel, E., & Iacoboni, M. (2003). Introduction: poffenberger's simple reaction time paradigm for measuring interhemispheric transfer time. In E. Zaidel & M. Iacoboni (Eds.). *The parallel brain : the cognitive neuroscience of the corpus callosum* (Chap. 1, pp. 1–7). Cambridge, MA: MIT Press.

Appendix A:
Expanded Literature Review and Historical Foundations

> Owing to this struggle for life, any variation, however slight and from whatever cause proceeding, if it be in any degree profitable to an individual of any species, in its infinitely complex relations to other organic beings and to external nature, will tend to the preservation of that individual, and will generally be inherited by its offspring (Darwin, 1859, p. p. 61).

Neurons, Information, Bandwidth, and Intelligence

Intelligence, at least viewed from the standpoint of biology, stems from the necessity to survive in the environment. It was the need to gain an edge over inter- and intra-species competitors that facilitated both the increased diversity and increased complexity of biological entities. The same force transformed dryopithecus into homo sapiens, and geared genus homo to become an increasingly complex information processor. Thus, in most general terms intelligence refers to the ability to adapt to the environment. Adaptation necessitates that biological entities are open systems (von Bertalanffy, 1950) receiving information from the environment (inputs), processing those inputs (throughputs), and executing appropriate responses (outputs). Environments are inherently ambiguous and characterized by entropy, chaos, and uncertainty. From the standpoint of information theory (Shannon, 2001, 1948a, 1948b) the goal of biological entities is to reduce entropy by acquiring information. Information is what allows making sense of what is senseless and finding patterns in what is inherently chaotic. Consequently, information is the currency of survival, and the reason why humans evolved to be complex information processors. In the context of biological systems, research on information processing and intelligence may imply studying dynamic phenomena associated with function rather than structure. Yet no function can exist in the absence of structure much like no information can be transmitted in the absence of a communications channel. This dissertation focuses on studying the infrastructure for information transfer that enables neurons to input and output information and sets the stage for distributed information processing taking place in our nervous system.

Cognition depends on underlying neural activity that in turn is influenced by the underwriting neural circuitry. While the relation between the mind and brain and between structure

and function are complex, at the most basic level, all transfer of information in the brain relies on neurons. The human brain contains approximately 100 billion neurons, creating between 1 and 10,000 connections each. In the cortex alone there are an estimated 0.15 quadrillion synapses (Pakkenberg & Gundersen, 1997). Neurons have three major components: dendrites, a cell body, and an axon (see figure 5 on page 163 for a diagram of neuron).

Dendrites are primary sites of information inputs from other neurons and constitute the first level of information processing through spatial summation of inputs from dendritic spines. The cell body is the metabolic center of a neuron and the center of information processing through spatial and temporal summation of inputs relayed by dendrites. An axon outputs information to other neurons through synaptic contacts. Axons are hair-like structures often covered by a layer of insulating fatty substance called myelin.

A collection of axons is often referred to as a tract or by the Latin term fasciculus (little bundle). In fresh tissue, myelin-rich fiber tracts have a whitish appearance and thus parts of the brain containing high density of axons are referred to as white matter. The cortical white matter contains fiber tracts that either connect cortical areas within a hemisphere (association fibers) or fiber tracts that project to the opposite hemisphere (commissures). The largest white matter commissure in the human brain is the Corpus Callosum (CC). The corpus callosum has been implicated in numerous experiments and case studies as the site of inter-hemispheric communication and is the cortical information superhighway in a mammalian brain. This connection assures that the hemispheres that evolved to specialize in processing of different kinds of information (e.g. left hemisphere specializes in verbal information) and different modes of information processing (e.g. left hemisphere is more efficient in serial information processing while the right hemisphere is more efficient in parallel information processing), can relay to each other information they are not geared to handle efficiently. Facilitation of communication between hemispheres and synchronization of this communication are among the factors that affect cognitive performance (Newman & Just, 2005).

The corpus callosum is implicated in inter-hemispheric transfer of information, the size and the number of fibers it carries may play an important role in facilitation of cognitive performance by providing the infrastructure for neuronal communication (Just, Cherkassky, Keller, Kana, & Minshew, 2007). More commissural fibers crossing the midline may provide the oppor-

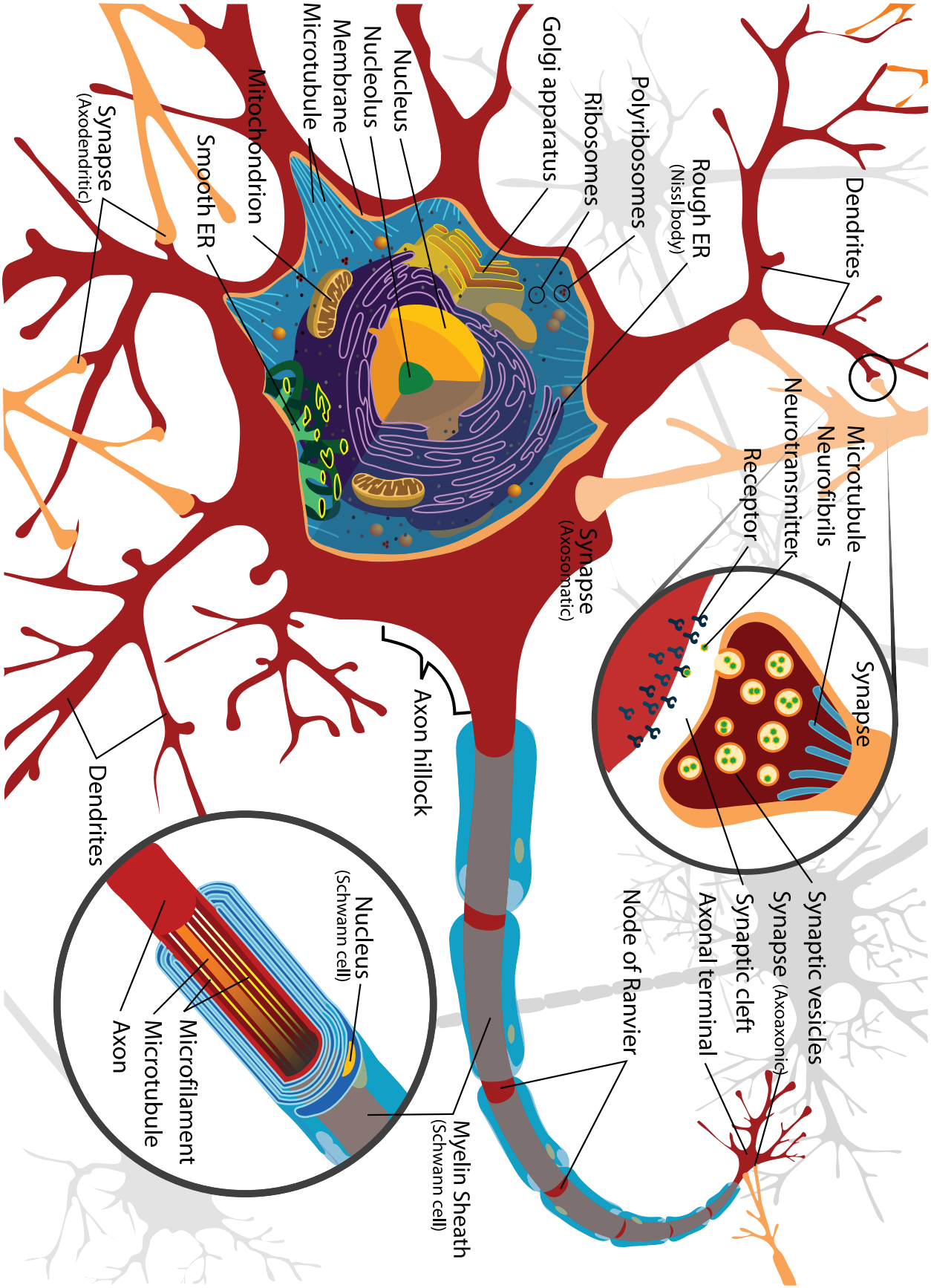

Figure 5: Diagram of a neuron (Ruiz Villarreal, 2007)

tunity for active recruiting of neurons from the contralateral hemisphere to perform challenging tasks. Inter-hemispheric connections such as the corpus callosum provide an infrastructure enabling the pooling and optimization of resources distributed across both hemispheres. In sum, commissures connect largely homologous cortical areas in each hemisphere and pool as well as optimize function-specific processing resources distributed across hemispheres. While inter-hemispheric communication pools function-specific resources distributed between hemispheres specialized in different processing modes and types of information, intra-hemispheric communication enables integration of functionally different or functionally similar areas located within a hemisphere. This pooling involves both integration of information from hierarchically organized brain areas within a single sensory system (e.g. V1 -¿ V2 -¿ V3), integration of information from various unimodal association areas (areas specialized in processing of inputs from a specific sensory system) into a multi-modal representation, as well as accessing information from a number of multi-modal association areas as in fronto-parietal integration (Jung & Haier, 2007). Two types of association fibers can be distinguished based on their projections: short and long. Short association fibers connect areas within the same lobe. For example, the fibers that connect primary auditory cortex with auditory association cortex (Wernicke's area) belong to the category of short association fibers. Long association fibers connect areas located in different lobes. For example, the superior longitudinal fasciculi (SLF) connecting the frontal lobes with the parieto-temporo-occipital junction is a long association fiber bundle. The SLF has been implicated in higher cognitive function because of its role in integrating higher-level association areas located in different brain lobes. Consequently, fiber tracts connecting brain areas within a hemisphere are also crucial for the emergence of higher cognitive function. In sum, association fibers connect functionally similar or diverse areas within a hemisphere. They pool processing resources distributed across areas within a lobe, or across lobes but within the same hemisphere. Altogether, white matter tracts connecting cortical areas both within and across hemispheres are likely to be crucial for cognitive performance, and are strong candidates for biomarkers of extraordinary ability. This thesis seeks evidence for changes in brain organization associated with increased cognitive performance. It focuses on on the Corpus Callosum that interconnects cell body-rich gray matter cortical areas, where basic information processing occurs through spatial and temporal summation of neural signals, and networks of differentially weighted dynamically changing connections.

Those networks constitute human cortex which is ontologically the newest part of the brain that separates humans from most animals, and the part of the brain we owe our consciousness and higher-level cognitive faculties.

Historical Studies of Extraordinary Ability

”Vivitur ingenio, caetera mortis erunt.” ”Man lives through his genius, all the rest is mortal.” (Vesalius, 1543, p. 164)

The search for biological landmarks of genius is marked with controversy, consistent unreliability of findings, and accusations of that quest being a new phrenology. Studies reviewed below are provided as a historical overview rather than a basis for the thesis. Case studies of brains of intellectual figures often require some caveats. In the early days of research on the relation between brain and intellect ideological beliefs led some authors to manipulate their data and samples in order to arrive at a desired conclusion (Finger, 1994). Furthermore, imprecise measurement techniques and methodological shortcomings often biased results. Early in the history of neuroscience, not all factors affecting brains has been recognized, leading to biased interpretations of the results. Perhaps the most prominent example is the lack of consideration of brain to body ratio in interpreting brain size (Spitzka, 1907). Since no definite list of factors that affect brain size exists even now modern researchers still face the dilemma of how to construct their control groups. Unfortunately, even well established factors that may influence brain size have been blatantly ignored. For instance in the studies of Einstein’s brain, the selected controls were considerably younger than Einstein (M. C. Diamond, Scheibel, Murphy, & Harvey, 1985; Witelson, Kigar, & Harvey, 1999). Case studies of the brains of intellectual figures pose one more challenge, as the experimental condition commonly consists of only one subject no firm conclusions can be drawn without further studies. Nevertheless, results of those studies should not be completely dismissed. As Kuhn (1996) pointed out many important scientific discoveries were triggered by an observed anomaly, an observation or outcome unusual enough that it could not be explained based on the current state of knowledge. Studies of brains of intellectual figures may provide a clue about where to look for answers to the question that has been puzzling generations: What makes a genius?

Anatomical Studies of Extraordinary Ability

In 1855 Wagner examined brain of a physicist, astronomer, and mathematician Carl Friedrich Gauss. This event marked the beginning of the modern study of extraordinary cognitive ability. Wagner (1862, 1860, cited in Spitzka, 1907; cf. Finger 1994) reported that Gauss' brain weighted 1492 grams and its cerebral area was 219.588 cm^2. Gauss' brain was notable for expansion of sub-parietal regions including the marginal and angular gyri as well as for complexity of the convolutions and multiplicity of fissures. Enriched fissuration was magnified in the frontal region (Spitzka, 1907). Enriched cortical folding is particularly interesting as in interspecies comparisons the degree of convolution is related to the level of phylogeny. In general, the higher an animal is on the phylogenetic ladder, the more convoluted its brain is. Cortical folding may be associated with intelligence as the animals latest in phylogeny are often considered the most intelligent, humans being a prime example. Due to limits on the size of the cranium, cortical folding could be an efficient use of space and an optimal way to spatially organize cell bodies optimizing connectivity between functionally related neurons (Van Essen, 1997). Gauss's brain became part of what came to be known as the Gottingen collection which consisted of the brains of several Gottingen's professors including pathologist and physician Konrad Heinrich Fuchs, philologist and archaeologist Carl Friedrich Hermann, mathematician Peter Gustave Lejeune Dirichlet, and mineralogist Johan Friedrich Ludwig Hausmann (Spitzka, 1907). Fuchs' brain weighted 1459 g and in its central fissures were bilaterally interrupted by bridging gyri. Frontal lobes were noted to be larger and more fissurated than average. In comparison to other brains fissuration was also more asymmetrical, in particular in the left frontal lobe. Hermann's brain weighted 1358 g and in comparison to other brains in the Gottingen collection its surface anatomy was less complex. Dirichlet's brain weighted 1520 g and in terms of complexity of fissuration it approached the brain of Gauss. Its frontal lobes were large and highly convoluted, with strikingly large and fissured superior frontal gyri. Hausmann's brain weighed 1226 g and was not only the smallest in the collection, but also the least convoluted and the most symmetrical in terms of its surface anatomy (Spitzka, 1907)

While Gauss brain's weight was only slightly higher than average his mathematical abilities were significantly higher than average. Likewise, remainder of the collection showed no consistent pattern of surface features or brain weight and Wagner concluded that weight and the ex-

tent of cortical folding are not perfect correlates of intellectual ability (Finger, 1994). The conclusion that brain size or surface anatomy is not a reliable biomarker of intellectual preciosity was inconsistent with the zeitgeist. Among the critics of Wagner's work was Broca who expressed the view that brain size relates to intelligence.[5] Broca correctly pointed out that "a professorial robe is not necessarily a certificate of genius" (Broca, 1861, p. 166 quoted in Finger, 1994, p. 306).

Following Wagner's study, donating brains became fashionable among scholars across the globe and a torrent of case studies reporting brain weights, sizes, and convolutions followed. This research has been scrupulously summarized by Spitzka (1907). In 1896, a Swedish anatomist Magnus Gustaf Retzius published first in a series of studies of brains donated by prominent figures in their professions including brains of an astronomer Hugo Gylden (Retzius, 1898 cited in Spitzka, 1907 and Finger, 1994), a female mathematician Sonya Kovalevsky (Retzius, 1900b cited in Spitzka, 1907 and Finger, 1994), a physicist Adam Siljestrom (Retzius, 1900a cited in Spitzka, 1907 and Finger, 1994), statesman (identity not revealed, Retzius, 1904 cited in Spitzka, 1904b), and a histologist and physiologist Christian Loven (Retzius, 1905 cited in Spitzka, 1905). In line with Wagner's reports, Retzius noted variations of the surface features in some of the brains. He reported presence of unusual secondary gyri, and enlarged area near the posterior end of the Sylvian fissure in the supra-marginal and angular gyri (Finger, 1994). At the beginning of the 20th Century American anatomist Edward Anthony Spitzka published a series of papers (Spitzka, 1907, 1905, 1904a, 1904b, 1903b, 1903a) providing detailed descriptions on several brains as well as an analysis of some 130 studies of brain morphology. Data gathered by Spitzka was largely archival. In his 1907 paper he provided detailed description of brains belonging to six "eminent" members of the American Anthropometric Society and compared brain-weights of 97 "eminent men" to a large group of brains belonging to "ordinary" individuals. On average brain-weights in the "eminent men" series were heavier compared with the Broca-Bischoff-Boyd series ("ordinary men") and age-related brain atrophy becomes marked in the "eminent men" series ap-

[5]Broca once wrote "all other things being equal, there is a remarkable relation between the development of intelligence and the volume of the brain" (Broca, 1861, p. 188 quoted in R. Smith, 1997, p. 398 and Finger, 1994, p. 301) and later in the same volume "In general the brain is larger in mature adults than in the elderly, in man than in woman, in eminent men than in men of mediocre talent, in superior than in inferior races" (Broca, 1861, p. 304 quoted in R. Smith, 1997, p. 398). For more accounts on Broca's view on brain size and intelligence see Finger (1994), R. Smith (1997), Stepan (1986), Gould (1996). 1994, Smith (1997), Stepan (1986), and Gould (1996).

proximately a decade later than in the ”ordinary” series (Spitzka, 1907, Fig. 2, p. 214,).

In 1909 von Bechterew and Weinberg published a study examining the brain of Dmitri Ivanovich Mendeleyev, a Russian chemist who authored periodic table of elements. von Bechterew and Weinberg (1909) reported that Mendeleyev's frontal lobes were exceptionally developed and that the left parietal region was enlarged (von Bechterew & Weinberg, 1909 cited in Finger, 1994). Later in the 20th Century it became more evident that there is significant variability in brain sizes both within and between previously reported studies (Finger, 1994). Authors reported that brain size did not seem to be a reliable predictor of intellectual ability. While no consistent pattern of gyri was found that could account for extraordinary intellectual ability, variations in the size of the frontal lobes and the parietal region were frequently reported. Among the most controversial and most widely cited case studies of brain anatomy related to intellectual performance are the studies of Einstein's brain (B. Anderson & Harvey, 1996; M. C. Diamond, Scheibel et al., 1985; Witelson, Kigar et al., 1999). While Einstein's brain was extracted, chemically fixed, and sectioned in 1955, it was not been systematically analyzed until three decades later. In 1999, Witelson, Kigar et al. compared both surface and gross anatomy of Einstein's brain (age 76 years) to a control group of 35 male brains (age M = 57 years; WAIS IQ M = 116, WAIS IQ SD = 9). Witelson, Kigar et al. (1999) reported that the weight of Einstein's brain was comparable to weights of brains in the control group (1230 g in comparison to M = 1400 g, SD = 118 g) and that weights, heights, and lengths of Einstein's hemispheres did not differ from brains of controls. However, both hemispheres in Einstein's brain were 1 cm (15%) wider than hemispheres of controls. Consequently, the width-to-height ratio for each hemisphere and for the whole brain was larger in Einstein's brain than in the brains of the controls see Witelson, Kigar et al. (1999, Figure 3; p. 2152). Based on the pictures of unsectioned brain taken in 1955, Witelson, Kigar et al. (1999) reported that in Einstein's brain the Sylvian fissure, instead of terminating with the ascending ramus, terminated at the postcentral sulcus. The ascending ramus usually divides the supra-marginal gyrus into anterior (parietal operculum) and posterior sections. Because the ascending ramus of the Sylvian fissure was not present, Einstein's parietal operculum was missing and parietal lobes were wider and more spherical. Because the ascending ramus of the Sylvian fissure is absent in about 15 to 20% of the population (Foundas, Faulhaber, Kulynych, Browning, & Weinberger, 1999), it cannot be concluded that absence of the ramus alone explains Einstein's

intellectual preciosity. For a more extensive discussion of Witelson, Kigar et al. (1999) see Galaburda (1999), Salvatori (1999), J. A. Seitz (1999).

While in most brains the parietal lobes are asymmetrical, with right parietal lobe larger than the left one, Einstein's parietal lobes were symmetrical (Witelson, Kigar et al., 1999). Witelson, Kigar et al. (1999) concluded that the decrease in asymmetry was due to Einstein's left parietal lobe being larger than usual (Witelson, Kigar et al., 1999). Parietal lobes, particularly inferior parietal lobules, are believed to be crucial for mathematical and visual reasoning, and an enlarged inferior parietal lobe is often given as an explanation of Einstein's abilities. Furthermore, an undivided supra-marginal gyrus may have allowed for better connectivity in Einstein's posterior association cortex (cf. Witelson, Kigar et al., 1999). The inferior parietal lobes host supramodal association areas integrating and translating visuo-spatial and auditory inputs. Having better connectivity in this region may have given rise to Einstein's superordinary mathematical and spatial abilities. Witelson, Kigar et al. (1999) suggested that Van Essen (1997) concept of tension systems as a driving force for brain folding may link anatomical variation in Einstein's brain (such as continuous supra-marginal gyrus) with the exceptional cognitive performance. According to Van Essen, gyri evolved in order to facilitate connections between functionally related areas. Neurons can be more efficiently connected if their cell bodies are positioned on the outer surface of a folding such as gyrus rather than arranged on a flat surface with no folds. An uninterrupted gyrus may provide better connectivity in the parietal lobes and result in better performance on tasks involving multi-modal integration such as mathematical and spatial tasks. The inferior parietal lobes are connected with the frontal lobes by the superior longitudinal fasciculus, a fiber bundle with likely involvement in higher faculties. The superior longitudinal fasciculus helps integrate resources distributed among the occipital, parietal, temporal, and frontal lobes. As much as the superior longitudinal fasciculus may allow pooling resources from different areas within a hemisphere, the corpus callosum may allow pooling resources distributed across hemispheres. As reported by Witelson, Kigar et al. (1999), Einstein's corpus callosum did not differ in size from the callosa of controls (6.8 cm^3 compared to M = 7.0 cm^3, SD = .90 cm^3 for controls). Einstein's brain differed from brains of controls in terms of its micro-architecture. B. Anderson and Harvey (1996) reported that, based on the sample obtained from the part of the right middle frontal gyrus half-way between the frontal tip and the central sulcus (corresponding to the proximity

of BA9/BA46), Einstein's cortex was thinner than average, but also more densely packed with neurons, overall yielding a number of neurons comparable to the number of neurons in brains of controls. The average thickness of Einstein's cortex was 2137 μm, considerably less than 2659 μm in matched controls (p = 0.002, U = 0.0, n's 20/4; age M = 68; age SD = 6.26). The average density of neurons in a sample of Einstein's cortex was 46,995 neurons per cubic meter. That was considerably more than the 34,962 neurons per cubic meter reported in the matched control group (p = 0.015, U = 8, n's = 19 and 4). Densely packed neurons may have given rise to better connectivity in Einstein's cortex and consequently contributed to his superior abilities. A slab obtained from the left Brodmann area (BA) 39 (the angular gyrus) of Einstein's brain yielded a smaller ratio of average estimates of neurons to glial cells than in control group of 11 males (t = 2.62, df = 9, SD = .312; p ¡ .05; age M = 64, age SD not reported, age range = ¡47, 80¿; M. C. Diamond, Scheibel et al., 1985). The authors reported that in Einstein's left BA39 they counted on average 112 glial cells for every 100 neurons. In contrast in the sample of controls there was 193.6 glial cells for every 100 neurons on average. A similar trend was present in Einstein's right BA39 and bilaterally in BA9 (part of the superior frontal gyrus), however due to large standard deviations those differences were not statistically significant (see also M. C. Diamond, Scheibel et al., 1985, , Table 1). Elsewhere Diamond's team (M. C. Diamond, Law et al., 1966) found 14% (p ¡ 0.01) increase in the number of glia among the rats raise in the enriched environment. Ratios of neurons to glial cells in Einstein's brain and controls are summarized in table 26 on page 170.

Table 26

Neuron to glial cell ratios for Einstein's brain and controls. Based on M. C. Diamond, Scheibel et al. (1985)

Region	Neuron to Glia Ratio in 11 Controls (SD)	Neuron to Glia Ratio in Einstein	p
Left Area 9	1.85 (.66)	1.04	n.s.
Right Area 9	1.75 (.76)	1.16	n.s.
Left Area 39	1.94 (.31)	1.12	0.05
Right Area 39	2.03 (.59)	0.92	n.s.

Glial cells provide physical support for the neurons including myelination, regulate extra-

cellular environment of the neural cells, and supply neurons with nutrients. During brain development glia produce neural growth factors and guide neural sprouting. Some evidence suggests that at least in some regions of the brain glia may also modulate synaptic transmission by regulating removal of the neurotransmitters from the synaptic cleft, affecting functional properties of the presynaptic terminals, and release of the neurotransmitters (Volterra & Steinhauser, 2004). Altogether glial cells are important for the optimal neural development and neural function. M. C. Diamond, Scheibel et al. (1985) have been widely criticized because controls were not age-matched (Hines, 1998). The youngest brain came from subject almost three decades younger than Einstein, and the oldest brain coming from a subject only 4 years older than Einstein. It is possible that Einstein's cortex would have a neuron to glia ratio comparable to the neuron to glia ratio in an age-matched control group. Some went as far as concluding that the M. C. Diamond, Scheibel et al. (1985) paper was so flawed that its results should not be considered at all (Hines, 1998).

Brain size and Intelligence. While previously discussed historical studies often concluded that brain size is not a reliable biomarker of genius. Closer examination of the aggregate evidence from studies involving measures of brain size and intelligence report modest but consistent positive correlations. Because of often inconsistent results this correlations often does not become apparent until collective body of evidence is examined. In their meta-analysis McDaniel (2005) based on 37 samples across 1530 people estimated the population correlation to $r = .33$. Reported correlations were higher for females than males, and for adults than children (McDaniel, 2005).

Varying magnitudes of this positive relation hold true for different metrics of brain size (Rushton & Ankney, 2007) and this relation holds true for both inter-species, and at least in case of humans, intra-species comparisons. In the context of interspecies comparisons, brain to body ratio is related to intelligence, as animals higher on the phylogenetic ladder tend to show higher degrees of cognitive ability and have larger brains. The proportion of brain-to-body weight in fish is 1 to 5000, in reptiles 1 to 1500, in birds 1 to 220, in most mammals 1 to 180, and in human 1 to 50 (Purves & S. M. Williams, 2001). In order for a fish to develop a 1 kg brain, it would need to weight on average 5000 kg, a reptile would need to weight on average 1500 kg, and a bird would need to weight on average 220 kg. Indeed, humans appear to be more intelligent that fish, reptiles, birds, and non-human mammals. This admittedly overly simple argument suggests that gains in

neural mass play some role in emergence of higher intellectual function. Gains in cortex, most notably frontal cortex, are what separate humans from other primates. However, human intellect comes not only from the bulk of neural mass, but also from the diversity of its connections. By virtue of increasing brain mass the number of neurons is increased and within bound of neural architecture number of possible combinations of neural connections increases as well. Increased number of possible combinations allows for more complex network of connections. This notion is consistent with recent report (Semendeferi et al., 2010) noting increased number and width of minicolumns in the human frontal lobe (particularly the prefrontal cortex), and increase in the space available for neuronal connections. Contemporary neuroscience accepts that consciousness and higher-order cognitive function are emergent properties of the extensive neural network present in our brain.

Possible explanation of why bigger-is-better relation is more evident in inter-species rather than intra-species comparisons likely lays in the magnitude of the weight variability. The magnitude of variability in the interspecies comparisons is relatively large, for instance there is an almost seven-fold increase in relative brain size between reptiles and birds (body-to-brain mass ratio decreased, 1:1500 in reptiles vs. 1:220 in birds). In contrast, the magnitude of variability in human brain size is estimated at only 15 to 20% (Eggers, Haug, & Fischer, 1984; Haug, 1987, 1984). Due to this is a relatively small variation in human brain size, larger samples are required in order to detect relation between brain size and intelligence and this relation becomes more apparent in meta-analytic studies.

Cortical volume and neuron density. As demonstrated by study of Einstein's cortex it is possible to have a thinner cortex more densely packed with neurons equivalent to the number of neurons of thicker cortices. In mammals the density of neurons is negatively correlated with brain volume (r = -.693, p ¡ .001, n = 27; Haug, 1987). This comparison across 27 mammalian species including human reveals that mammals with smaller brains have higher neural density, and mammals with larger brains have lower neural density. As humans fall on the large-brain end of the spectrum it may be that micro-architectural limits have not been reached in the human cortex and variability with regard to density of neurons could be present. This notion is supported by a moderate correlation between brain size and the number of neurons. Based on the sampling from different areas of the human brain in several individuals, Haug (1987) found that the num-

ber of cortical neurons correlates with brain volume at $r = .479$, $n = 81$, p ¡ .001. Alternative explanation proposed by (Semendeferi et al., 2010) states that less densely packed cortex might allow more space for neural connections.

Summary. Purves and S. M. Williams (2001) note that comparisons of brain sizes or similarly global indices ignore the brain's functional diversity. The brain is an all-encompassing entity and variations in certain regions of the brain are lost when global brain comparisons are made. Consequently, relating structure and behavior needs to focus on comparisons of specific brain regions implicated in specific functions. Because intellectual ability is an emergent property of a network spread across brain regions and hemispheres with particularly high involvement of the frontal and parietal lobes, inter- and intra-hemispheric connections between those regions are worth investigating in relation to intellectual performance. In addition to macro-structural comparisons, the micro-architecture of the tissue should be examined as size and neural density are only loosely correlated with each other.

Brain Function and Cognitive Performance

In 1892 Sir Francis Galton fathered the idea that inherited microlevel sensory and perceptual processes give rise to exceptional abilities. Functional studies although often inconsistent support Galton's notion that it is important for the exceptionality how basic nervous circuitry is used.

Electroencephalography (EEG) Studies. . Electroencephalography studies (for review see Rooy, Song, & Stough, 2005) point out to the conclusion that frequency of alpha EEG waves is positively associated with cognitive functioning. Furthermore, large power of the upper band alpha waves and small power of the theta waves are positively associated with cognitive functioning. As Rooy et al. (2005) neatly summarize the frequency of alpha waves increases from childhood to adulthood and decreases with aging and as a result of neurological disorders. Moreover, even in healthy subjects alpha frequency positively correlated with memory performance, speed of information processing. As alpha power increases from childhood to adulthood, theta power decreases, and the opposite is true during late part of the lifespan and neurological disorders, as upper alpha power decreases, theta power increases.

Positron Emission Tomography (PET) Studies. . Number of studies report a counter-intuitive finding that the performance on cognitive tasks is negatively correlated with the abso-

lute glucose metabolic rate. Haier, B. V. Siegel, Nuechterlein, and E. Hazlett (1988) in their PET study found that the absolute rate of glucose metabolic rate was negatively correlated with performance on the Raven's Advanced Progressive Matrices test, and this correlation was of moderate to strong magnitude. Parks et al. (1988) reported that overall glucose metabolic rate in the frontal, parietal, and temporal regions negatively correlated with performance on a verbal fluency test, and that this correlation was of moderate magnitude . Haier, B. Siegel, Tang, Abel, and Buchsbaum (1992), Haier, B. V. Siegel, Jr. Et al. (1992) further found within subject correlations between cortical glucose metabolic rate and performance on a visuo-spatial motor task based on the teris game. Authors found that the cortical glucose metabolic rate decreased with practice, and the magnitude of this decrease was the largest among participants who improved the most. While Raven's Advanced Progressive Matrices is a test of nonverbal reasoning, the test used by Haier, B. Siegel et al. (1992), Haier, B. V. Siegel, Jr. Et al. (1992) is a visuo-spatial motor task, and the test used by parks involved measuring verbal fluency. Thus, the negative correlation between performance on cognitive tasks has been demonstrated in a variety of reasoning tests. While it is hard to infer the nature of the mental processes underlying glucose metabolism, Parks demonstrated that as participants become more proficient in the test they also tend to metabolize less glucose. Glucose metabolism is related to neuronal activity and by extension it is likely that as participants became more proficient on the task the amount of neural activity decreased. Thus cognitive processes operating decreased but also became more efficient as evidenced by increased performance. The negative correlation between metabolic rate and performance across participants is much more ambiguous. However, it is possible that high performing participants have cognitive processes operating more efficiently in the first place and either require fewer neurons to perform the task, or require similar numbers of neurons over shorter period of time. In both cases this may be evidenced by overall less glucose being metabolized during PET scan. One of the possible micro-structural correlates of this efficiency may be myelination of axons (Rooy et al., 2005). Myelinated axons are less leaky and therefore also have higher conduction speed and in turn also higher conduction rate (e.g. rate of firing). Unfortunately PET scans are not efficient in estimating amount of white matter in the brain. This information however can be estimated from high quality MRI scans and to some extent from DTI scans.

Corpus Callosum

Gross Anatomy of the Corpus Callosum. The corpus callosum is the largest white matter structure and the largest of the commissures in the human brain. It is part of the telencephalon and consists of more than 200 million axon fibers (Aboitiz et al., 1992; Innocenti, 1986; Tomasch, 1954) interconnecting the cerebral hemispheres. The corpus callosum lacks easily identifiable landmarks that would allow easy partitioning into subunits. While a number of largely arbitrary partitioning schemes exist, the simplest divides the corpus callosum into four parts (see figure 3 on page 27): antero-ventral portion referred to as rostrum [1], antero-dorsal portion referred to as genu [2], the central portion referred to as body or trunk [3], and the posterior portion referred to as splenium [4]. In midsagittal cuts of the brain the corpus callosum appears as an approximately 10 centimeter-long rotated crescent located in the center of the brain

The anterior edge of the corpus callosum (genu) is located about 4 centimeters posterior of the anteromost corner of the frontal lobe. The posterior edge of the corpus callosum (splenium) is located about 6 cm anterior of the posteromost corner of the occipital lobe (H. Gray & W. H. Lewis, 1918). The anterior and the posterior portions of the corpus callosum, genu and splenium respectively, are among the thickest parts of the corpus callosum. The genu bends in the postero-ventral direction continuing as a much thinner rostrum (H. Gray & W. H. Lewis, 1918). The rostrum terminates connecting with lamina terminalis (H. Gray & W. H. Lewis, 1918). The genu and rostrum, as well as most of the body of the corpus callosum are supplied with nutrients by the anterior cerebral artery (ACA) and its branches. The ACA travels ventrally to the rostrum and continues dorsally along the anterior surface of the splenium and branches into the Pericallosal Artery traveling posteriorly along the dorsal surface of the body of the corpus callosum. The posterior end of the corpus callosum constitutes splenium. The splenium is located above the tela chorioidea of the third ventricle. The splenium bends ventrally and makes an acute anterior turn folding onto itself. This fold forms the thickest portion of the corpus callosum (H. Gray & W. H. Lewis, 1918). The splenium is surrounded by the supracallosal gyrus (see figure 6 point A on page 176) that ventrally continues as the fasciola cinerea and further as the fascia dentata hippocampi. The splenium is supplied with nutrients by the posterior cerebral artery (PCA).

The superior surface of the corpus callosum is about 2.5 cm wide and its medial aspect is visible at the bottom of the longitudinal fissure (see figure 6 on page 176). The superior sur-

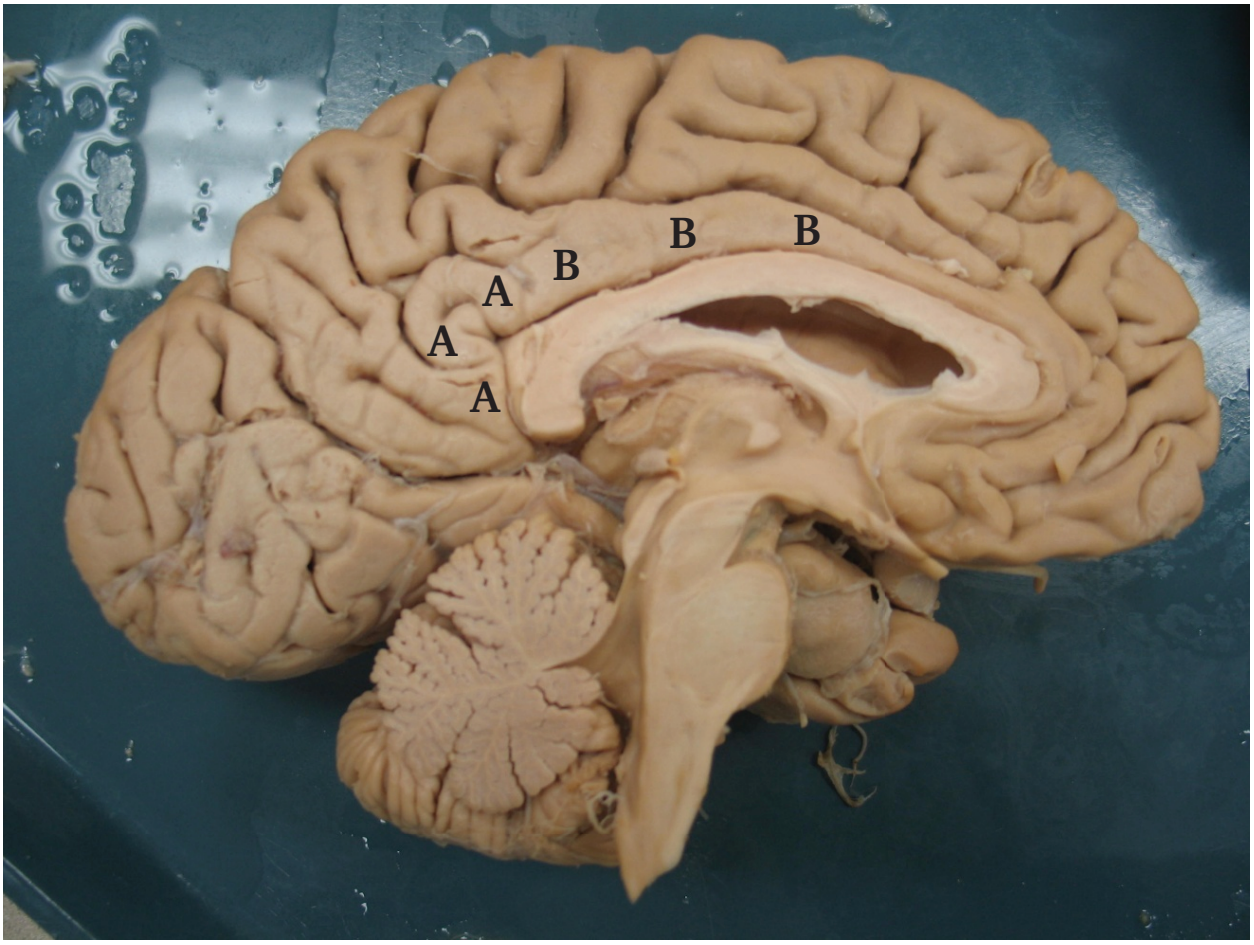

Figure 6: Midsaggital cut through the brain. Septum pellucidum removed. A – supracallocal gyrus, B – cingulate gyrus. Specimen courtesy of Dr. Steven Sawyer, Department of Rehabilitation Sciences, Texas Tech Health Sciences Center

face of the posterior corpus callosum (the splenium, parts of the posterior trunk) neighbors the falx cerebri, while the lateral aspects are covered by the supracallosal gyri. The supracallosal gyri, thin lamina of gray matter, continue laterally as the cingulate gyri (see figure 6 point B on page 176). Cingulate gyri are part of the limbic association area involved in emotions and decisions. Lateral aspects of the corpus callosum are separated from the cingulate gyri by callosal fissures. The superior surface of the corpus callosum is crossed by numerous ridges and furrows (H. Gray & W. H. Lewis, 1918). The medial part of the inferior surface of the corpus callosum attaches anteriorly to the septum pellucidum and posteriorly joins the fornix (see figure 3 point 5 on page 27). The lateral parts of the inferior surface of the corpus callosum cover the lateral ventricles. Fibers in the corpus callosum travel laterally to innervate a variety of cerebral structures. Those projections often connect homologous regions of the two hemispheres. Less common are the heterotrophic projections connecting different cortical regions in the left and right hemisphere (Innocenti, 1986; Witelson, 1989). Fibers of the corpus callosum radiate laterally traveling in the white matter of cerebral hemispheres. Based on the cortical regions they innervate, fiber tracts can be divided into three categories. Fiber tracts projecting from the genu anteriorly to the frontal lobe form forceps anterior (H. Gray & W. H. Lewis, 1918). Fiber tracts projecting from the posterior corpus callosum to the occipital lobe form the forceps posterior (H. Gray & W. H. Lewis, 1918). Fibers originating from the mid-trunk project to the temporal lobe form the tapetum. The central portion of the tapetum covers the lateral ventricles (H. Gray & W. H. Lewis, 1918).

In Vivo Morphometry of the Corpus Callosum.

Several partitioning schemes have been developed to allow a more detailed characterization of the corpus callosum. Among the most common are the geometrically based partitioning models of S. Clarke et al. (1989) and Witelson (1989) that divide the corpus callosum into quarters or fifths. Geometrical methods attempt to develop partitioning schemes that approximate the distribution of callosal fibers and their projections obtained from rhesus monkey studies. In contrast, statistical partitioning schemes do not assume any model of fiber distribution to guide partitioning but rather use patterns of variance present in the data in order to derive callosal divisions. Diffusion tensor imaging (DTI) paired with fiber tractography divide corpus callosum based on the patterns of projections modeled from diffusion tensor imaging data (Makris et al., 2005).

Geometric Schemes.

Geometric methods of partitioning the corpus callosum can be subdivided into two subcategories: methods using a straight reference line, and methods using a curved reference line.

Horizontal line geometric schemes. Horizontal line geometric schemes implement a horizontal reference line connecting the anteromost and the posteromost points of the corpus callosum to estimate the length of the corpus callosum and then divide the corpus callosum into segments corresponding to fractions of this line. For instance, the posterior fifth of the horizontal reference line is often used to define the callosal splenium. The most common horizontal line partitioning scheme was developed by Witelson (1989) (also see figure 7 on page 179). Witelson (1989) divided the corpus callosum into five segments. The first segment comprises the anterior third of the horizontal partition line and it corresponds to the genu, the rostrum, and the anterior body. The second segment comprises the area between the end of the anterior third (first segment) and the half-point of the horizontal reference line. This segment defines the anterior mid-body or anterior mid-trunk. The third segment comprises the area between the half-point and the posterior third of the horizontal reference line. This segment defines the posterior mid-body or posterior mid-trunk. The fourth segment comprises the area between the posterior third and the posterior fifth of the horizontal reference line and defines the isthmus. The fifth segment comprises the posterior fifth of the horizontal partition line and corresponds to the splenium.

Curved reference line geometric schemes. Curved reference line geometric schemes attempt to estimate the length of the corpus callosum while taking into account its curvature. First, the center of gravity of the corpus callosum is established and radial lines are drawn between the center of gravity and the corpus callosum. The lines are separated by one degree. For each of the lines crossing the corpus callosum, a midpoint between where the line enters and exits the corpus callosum is calculated. Midpoints are then connected by a curved line dividing the corpus callosum into dorsal and ventral halves. The curved reference line is then divided into 30 segments of equal length forming division points (J. Clarke, 1990). At each division point, a line is drawn to partition this structure. Each partition line is defined as the shortest line connecting dorsal and ventral halves and passing through the division point. Thirty segments establish units allowing partitioning similar to that used in the horizontal-line partitioning scheme. For instance, the posteromost six segments represent the splenium. The most common curved reference line partitioning scheme was developed by S. Clarke et al. (1989) and J. Clarke (1990).

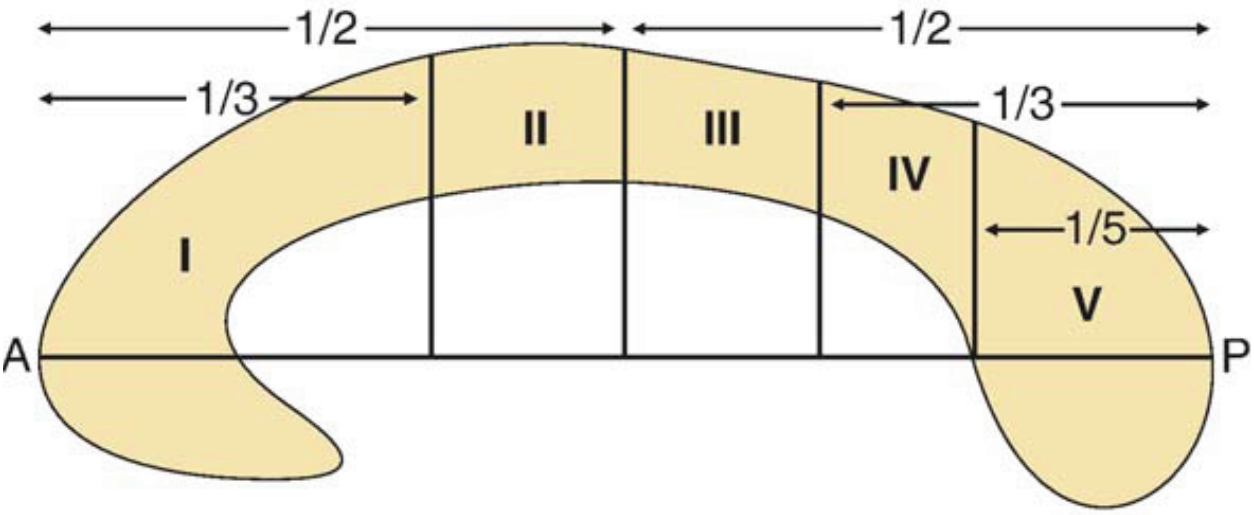

Figure 7: Witelson's Geometric Horizontal Line Partitioning Scheme. Reprinted from Neuroimage, 32, S. Hofer & J. Frahm, Topography of the human corpus callosum revisited-comprehensive fiber tractography using diffusion tensor magnetic resonance imaging, p. 992; Fig. 3 (top), Copyright 2006, with permission from Elsevier. (I) anterior third: prefrontal, premotor, and supplementary motor fibers. (II) anterior midbody: motor fibers. (III) posterior midbody: somaesthetic, posterior parietal fibers. (IV) isthmus: posterior parietal, superior temporal fibers. (V) splenium: occipital, inferior temporal fibers. A – anterior. P – posterior.

Statistical Partitioning Schemes. Instead of attempting to divide the corpus callosum using proportions that approximate distribution of fiber projections derived from primate studies, it is possible to attempt to derive callosal partitions from patterns of variability present in the data. This approach does not require a priori assumptions about callosal fiber distribution that may be violated in outliers and special populations. Most applicable statistical methods include instances of factor analysis such as principal component analysis (PCA) and common factor analysis (FA).

Principal component analysis. Principal component analysis is a popular tool of pattern recognition (Fukunaga, 1990) and data reduction (Tabachnick & Fidell, 2007). PCA conducts a linear transformation of a native coordinate system to the orthogonal coordinate system with the axes ordered according to their amount of variance. Outcome components are ordered in terms of the total amount of variance they account for with the first components accounting for the most variance. For instance, submitting data characterizing 30 segments obtained from curved reference lines to PCA will yield number of components and estimate how strongly each segment belongs to (loads on) each of those components. As a result, 30 segments may be reduced to a smaller number of callosal partitions that are grouped based on their variance. PCA derives higher order factors based on both the variance shared among the variables and the variance unique to each of the variables.

Common factor analysis. Factor analysis is a statistical technique analyzing relations among variables in order to uncover smaller number of dimensions underlying observed variability in the data. Variables in each dataset are related to each other and these relations enable common factor analysis to classify the variables along a number of dimensions termed factors. Factors that underlie variability in the data are latent and can be uncovered only by means of statistical analysis. Common factor analysis allows for the characterization of the data along a relatively small number of latent factors. This method preserves interrelations between variables since the extent to which each of the variables belongs to (loads on) a latent factor depends on the extent to which other variables load on this factor. In the course of statistical analysis, input data is deconstructed into its components and reconstructed into factors. Correlations between a component-score of a variable and each of the factors determine how closely a variable is related to each of these factors. This relation is termed a factor loading. Common factor analysis can be driven by a priori hypotheses about factor number and structure as in the confirmatory factor analysis (CFA),

or uncovered a posteriori from the data as in the exploratory factor analysis (EFA). Both CFA and EFA have applications to the partitioning of the corpus callosum. CFA can be used to statistically evaluate already formed partitioning schemes or compare existing partitioning schemes with each other in terms of their statistical fit. EFA can be used to develop partitioning schemes based on variability in datasets. The use of EFA may be particularly interesting when used on different clinical populations. Results of EFA conducted on different populations can be subsequently compared in attempt to uncover differences. Both CFA and EFA derive higher order factors based on the variance shared among the variables. Those factors may be hard to interpret and may not be theoretically informative.

Diffusion Tensor Tractography Derived Partitioning. Geometric partitioning schemes use generalized templates to approximate pattern of fiber distribution in human corpus callosum. Statistical partitioning methods use patterns in the data in order to develop partitioning tailored to a particular dataset. Diffusion tensor tractography (DTT) advanced this idea by developing idiosyncratic partitioning models for each corpus callosum. Those models could be further combined in order to develop partitioning tailored to a particular group. Unlike statistical methods, diffusion tensor tractography divides the corpus callosum based on its projections rather than pattern of variance. While statistical methods allow for developing partitioning schemes for a particular dataset, diffusion tensor tractography allows for developing partitioning schemes for both single cases and groups. DTI is an extension of the magnetic resonance imaging (MRI) where large magnetic gradient pulses are added to regular spin-echo MRI pulse sequence. This increases sensitivity of the magnetic resonance signal to Brownian motion of water molecules. In the human brain, movement of water is constricted by cell membranes and macromolecules. Cell membranes are constructed from a lipid bilayer that is largely impermeable to water, thus restricting water diffusion. In free water the diffusion is isotropic, that is equal in all directions. In the presence of a lipid bilayer the diffusion pattern of water molecules is anisotropic, that is unequal in all directions. The diffusion is constricted in the direction perpendicular to the lipid bilayer, and free in the direction parallel to the bilayer. By collecting a number of images with different diffusion weightings, also referred to as directions, it is possible to infer fiber trajectories. There are two approaches to fiber tractography. The first approach is based on streamlining fibers by connecting fiber directions computed for each voxel. The second approach creates probabilis-

tic models of fiber tracts. Based on the studies of callosal projections described in more detail in the next section it is possible to define regions of interest (ROIs) and compute fiber tracts between the corpus callosum and each of the ROIs. Since callosal projections are topographically organized, fiber bundles projecting to different areas create natural demarcation points between portions of the corpus callosum. Fiber tractography conducted on a single corpus callosum allows for developing of an individualized partitioning scheme. This partitioning method takes into account individual differences in callosal projections creating data driven divisions of the corpus callosum. This partitioning does not require any assumptions and divides the corpus callosum based on bundling of fibers projecting to a particular part of the brain (e.g. occipital lobe). As brain areas are functionally specialized, fiber bundles share both the target structure they innervate and the function they serve. For instance, fibers interconnecting occipital lobes in the left and right hemisphere predominantly carry vision-related information. Aggregation of fiber-tractography-derived idiosyncratic partitions from a number of individuals allows creating a population template analogous in function to the templates used by geometric partitioning schemes. However, this template in contrast to templates used in geometric schemes requires no assumption about distribution of fiber projections along the corpus callosum. Geometric templates use fractions of the line to divide corpus callosum into segments that would approximate partitions of the corpus callosum shown in primate studies to project to distinct anatomical areas. Diffusion fiber tractography-derived templates use bundles of fibers projecting to specified brain areas to define each partition of the corpus callosum and aggregate across those single-individual models to compute a population-mean template. Because diffusion fiber tractography allows for anatomical variations of projections across individuals, it is possible to statistically estimate accuracy of a composite template. If a composite template was computed from an infinite number of subjects, and if variability in callosal fiber distribution follows normal distribution, then such composite template would partition corpus callosum with accuracy of 1 *SD* in 68% of observations, with accuracy of 2 *SD* in 95% of observations, and with accuracy of 3 *SD* in 99.7% of observations. Shape and parameters of the callosal fiber distribution can be empirically specified for a population. If parameters of this distribution are known it is possible to construct a probabilistic partitioning template where each pixel carries specified probability of belonging to a particular partition or more specifically of projecting to a particular brain region (see also Eickhoff et al.,

2005).

Discussion of Callosal Partitioning Methods. While geometrical schemes are very common and easy to implement they are prone to error due to individual differences in the brain morphology. Statistical methods whether PCA or factor analysis can partition the corpus callosum based on a pattern of variance. These partitions may be statistical abstractions that are not anatomically meaningful or hard to interpret due to a multitude of correlations. Furthermore, the success of statistical partitioning schemes depends on researcher's ability to identify and include crucial properties of the corpus callosum and include them in the analysis (e.g. proper indices of size and shape). While selecting important geometric attributes should not pose challenge, it is not clear what micro-structural attributes should be included. Likely candidates include DTI derived descriptions of the micro-structure including eigenvectors (V1-V3), eigenvalues (λ1- λ3), mean diffusivity, and fractional anisotropy values. The exclusion of important attributes sharply decreases the utility of statistical methods. Inclusion of unnecessary attributes increases the number of required observations, and inclusion of highly correlated attributes causes multicollinearity and may affect analyses or make the interpretation of results difficult. While both FA (Denenberg, Berrebi, & Fitch, 1989) and PCA (J. Clarke, 1990) have been applied to partition the corpus callosum, the use of PCA is preferred in most cases (J. Clarke, 1990). PCA calculates components using both shared and unique variance whereas FA takes into account only shared variance. J. Clarke (1990) argued that PCA is more fit for partitioning of the corpus callosum as both shared and unshared variance are important for the separation of the parts of the corpus callosum. While J. Clarke did not provide an explanation of why total variance is a better fit for partitioning, presumably shared variance should allow grouping of "similar" parts of the corpus callosum together and unique variance should highlight differences between parts of the corpus callosum enabling better separation of dissimilar regions. FA is more appropriate for building testable models of relations among variables, when PCA is more appropriate for data reduction. While knowledge of the relations between the parts of the corpus callosum could be quite useful, the purpose of partitioning is not to uncover those relations, but rather to develop meaningful models of dividing the corpus callosum that would allow a more detailed characterization of this structure. Furthermore, gross geometric characteristics are unlikely to shed light on the interrelations between parts of the corpus callosum. These methodological concerns should not preclude the use of variants of

FA such as CFA that may help evaluate new partitioning schemes in terms of statistical fit. However, the results of statistical partitioning models should be interpreted with caution and should not be used as a primary criterion for selecting or accepting partitioning schemes. The final challenge to statistical methods is practical as relatively large datasets are required to conduct most of multivariate analyses. An increasing number of variables demands an increased number of observations to allow extraction of patterns from the data. DTI accompanied by fiber tractography combines the strengths of geometric and statistical schemes. First, it enables both idiosyncratic partitioning on a case-by-case basis, and building of generalized composite partitioning schemes. Second, it bundles (clusters) fibers based on their targets. Idiosyncratic and composite approaches represent improvements in accuracy over rigid geometric partitioning. Recent years brought many improvements in fiber tracking algorithms, scanning sequences optimization, and magnet hardware, yet uncertainty is inherent in fiber tractography. Voxels where multiple fibers cross are particularly ambiguous. Recent advances allow for the modeling of fiber crossings provided that at least 60 diffusions directions were acquired (T. E. Behrens, Berg, Jbabdi, Rushworth, & Woolrich, 2007). Increases in number of diffusion directions result in longer acquisition time and increase probability of subject movement.

Summary of Callosal Partitioning Methods. The choice of a partitioning method should take into consideration the research question, the accuracy required to address the research question, the accuracy of available partitioning methods, and available resources. Geometric methods are parsimonious, inexpensive, and easy to implement. When an area of interest within the corpus callosum is mid-size to large, geometric methods represent a viable solution. Statistical methods of partitioning are exclusively data-driven, prone to produce hard-to-interpret or artifactual results, and sensitive to a variety of methodological factors. Among the critical methodological issues is the identification of an optimal and complete set of important dimensions along which the corpus callosum needs to be characterized. It remains unclear whether characterization of the corpus callosum exclusively on the macro-structural level enables adequate partitioning. Coupling DTI and fiber tractography provides alternative to both geometric and statistical partitioning. Diffusion tensor tractography allows for the development of idiosyncratic partitioning defined by callosal projections. However, this method is relatively expensive, time and resource consuming, and not widely available, as most clinical MRI scanners do not have DTI capability. Despite the

required time and resource investments, DTI coupled with fiber tractography provides the most flexible method for characterizing the corpus callosum. When applied to single cases, DTI and fiber tractography enable development of highly accurate idiosyncratic corpus callosum partitions. When aggregated across subjects belonging to a particular population those methods provide an accurate group-level partitioning model.

Callosal Projections. Increased complexity of central nervous system and growth of cerebral cortex are associated with decreased variability in callosal projections. The more phylogenetically advanced an organism is, the more restricted is pattern of inter-hemispheric connections (Pandya & Seltzer, 1986). Callosal projections were initially mapped in the rhesus monkey by lesioning parts of the corpus callosum and observing patterns of subsequent Wallerian degeneration in different cortical regions (Pandya, Karol, & Heilbronn, 1971) or by injecting radioactive labeled amino acids into parts of the cortex and subsequently measuring radioactivity in the corpus callosum (Pandya & Seltzer, 1986). Postmortem examinations of the corpus callosum extracted from human brains that have undergone Wallerian degeneration due to localized lesions to the cerebral cortex suggest that inter-hemispheric fibers consistently cross midline in specific locations, and that the topographical organization of callosal fibers shows significant similarity between humans and rhesus monkey (de Lacoste et al., 1985). Similar patterns of topographic organization was also documented during neurosurgery in humans by electrically stimulating different parts of the corpus callosum and recording electrical responses in the cortex (cf. J. Clarke, 1990). More recent evidence in support of this pattern of connectivity comes from probabilistic models of fiber tracts computed from the diffusion tensor imaging data (Hofer & Frahm, 2006). The topographic organization of the corpus callosum mapped in primate studies (Pandya & Seltzer, 1986) grossly corresponds to the topographic distribution of the regions of overlying cortex. Medial and ventral prefrontal fibers cross the midline in the rostrum and ventral genu of the corpus callosum. Lateral prefrontal fibers cross the midline in the dorsal genu. Premotor fibers cross the midline in the rostral portion of the trunk of the corpus callosum. Sensorimotor fibers cross the midline in the mid-trunk of the corpus callosum. Fibers from the posterior parietal cortex and the middle and caudal superior temporal region cross the midline in the posterior trunk of the corpus callosum (Pandya & Seltzer, 1986). Fibers originating in the superior parietal lobules, the temporo-parieto-occipital region including the planum temporale, and the occipital lobes cross the midline

in the splenium (de Lacoste et al., 1985; Pandya & Seltzer, 1986). Fibers originating from the caudal infero-temporal cortex and caudal parahippocampal gyrus cross the midline at the intersection of the callosal trunk and splenium. Fibers originating from the cingulate gyrus cross the midline in the dorsal portion of the trunk of the corpus callosum. Fibers originating from the insula cross the midline in the ventral portion of the trunk of the corpus callosum (Pandya & Seltzer, 1986). In Witelson's (1989) partitioning scheme, fibers crossing the midline in the anterior third of the corpus callosum connect higher association areas including prefrontal, premotor, and supplementary motor areas. The anterior midbody connects motor areas while the posterior midbody connects somatosensory and posterior parietal areas. The isthmus connects posterior parietal and superior temporal areas, and the splenium connects occipital and inferior temporal areas. Witelson's partitioning scheme that was developed in large part based on Pandya and Seltzer (1986) rhesus monkey data provides a general overview of the callosal projections. It offers a very parsimonious model of the functional distribution of fibers in the corpus callosum. In Witelson's model the anterior third of the corpus callosum represents a single segment that encompasses traditional anatomical divisions such as the genu, rostrum and parts of the trunk. Others attempted to extend the division presented by Witelson (1989) by introducing additional partition for a more detailed characterization of callosal projections. Hellige, K. B. Taylor, Lesmes, and S. Peterson (1998) extended Witelson's scheme by introducing the rostral body, a small section of the corpus callosum drawn from posterior portion of the anterior third. In Hellige's (1998) scheme, the genu carries fibers connecting caudal-orbital prefrontal and inferior premotor areas while the rostral body connects premotor and supplementary motor areas. While Hellige's (1998) division may represent an improvement over Witelson's model by presenting more detailed information, it is not clear whether this model can be accurately implemented solely based on geometric information. The rostral body is the smallest partition and given the anatomical variability it may not be possible to isolate premotor and supplementary motor fibers by means of geometric divisions alone. Geometric partitioning schemes are appropriate for answering very general questions while DTI and fiber tractography should be preferred to answer questions demanding a high degree of anatomical localization and high degree of accuracy. Perhaps the best example on how diffusion tensor imaging and fiber tractography can improve accuracy over geometrical methods was presented by Hofer and Frahm (2006) (also see figure 8 on page 188). Based on fiber tractog-

raphy of DTI data Hofer and Frahm (2006) identified five partitions of the corpus callosum corresponding to five fiber bundles that emerged from clustering of DTI-derived fibers. The first segment contained fibers projecting to prefrontal areas, the second segment contained fibers projecting to premotor and supplementary motor areas, the third segment contained fibers projecting to motor areas, the fourth segment contained fibers projecting to sensory areas, and the fifth segment contained fibers projecting to parietal, temporal, and occipital areas. There are significant differences between the 5-segment partitioning scheme proposed by Witelson (1989) and results of Hoffer & Frahm's (2006) study. First, genu of approximately 1/6 of the length of the corpus callosum emerged replacing the anterior third segment proposed in Witelson's (1989) scheme. Second, motor fibers began to cross the midline in a much more anterior location. As a result, motor segments mapped onto the remainder of the anterior third and the whole anterior body. The posterior body in Witelson's scheme and the third segment in Hoffer & Frahm's scheme were found to be the same. The isthmus was found to be much smaller. The isthmus mapped onto the area between the end of the posterior body and the posterior quarter of the corpus callosum, a decrease from the posterior fifth in Witelson (1989). Decreased size of the isthmus resulted in the increased size of the splenium. The splenium increased from the posterior fifth in Witelson (1989) to the posterior quarter in Hoffer & Frahm (2006). In Hoffer and Frahm's partitioning fibers in the splenium carry projections from the area of the parieto-temporo-occipital junction.

Callosal Function. The corpus callosum is the largest white-matter structure in human brain providing inter-hemispheric communication for homologous areas located in all brain lobes. Consequently, the corpus callosum relays a wide range of information types and is involved is a wide range of brain functions. Corpus callosum is topologically organized and partitions of the corpus callosum carry functionally diverse projections. Consequently, each part of the corpus callosum is involved in various brain functions to a different extent. In this section I provide a short survey of the disorders of the corpus callosum in order to demonstrate the breadth of callosal involvement in brain function.

Disorders of the Corpus Callosum. Inferring callosal function from case studies can be challenging. Spontaneously occurring lesions such as tumors or infarcts differ in their extent and location. Consequently, those lesions affect different sections of the corpus callosum, to a different extent, and often involve neighboring structures. For instance, butterfly glioma can develop in

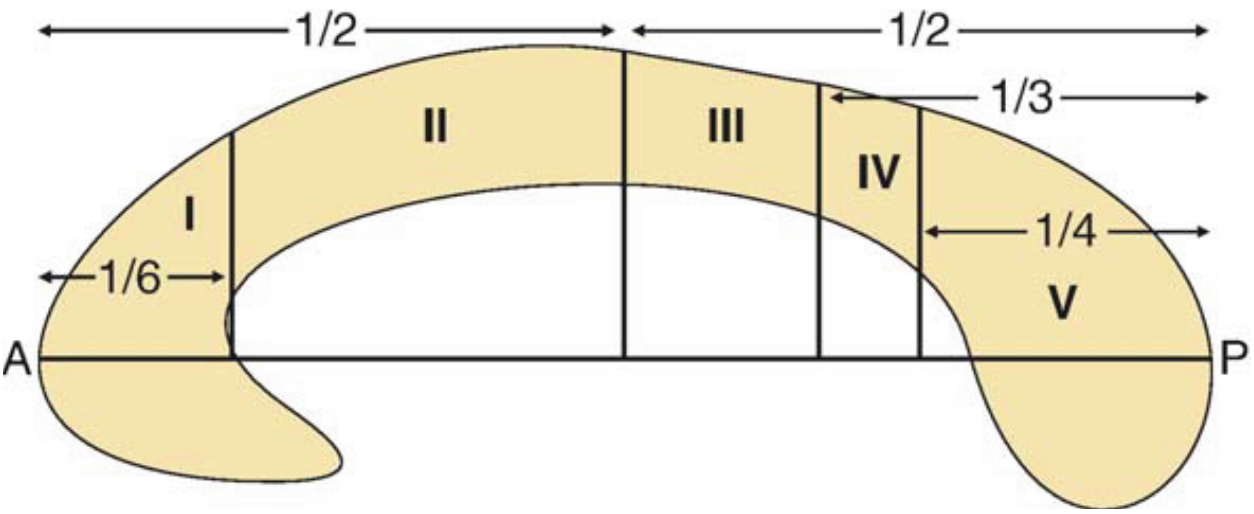

Figure 8: Hoffer & Frahm's Diffusion Tensor Tractography Derived Geometric Partitions. Reprinted from Neuroimage, 32, S. Hofer & J. Frahm, Topography of the human corpus callosum revisited-comprehensive fiber tractography using diffusion tensor magnetic resonance imaging, p. 992; Fig. 3 (bottom), Copyright 2006, with permission from Elsevier (Appendix 1). (I) prefrontal fibers. (II) premotor and supplementary motor fibers. (III) motor fibers. (IV) somatosensory fibers. (V) parietal, temporal, and occipital fibers. A – anterior. P – posterior.

the corpus callosum and spread into the frontal lobes forming ”wings” and producing a syndrome where callosal and frontal symptoms may be hard to tease apart. Due to the variability of lesions, inferences about the callosal function need to be meta-analytic where inferences are drawn from a large number of cases that allow extracting shared signs associated exclusively with callosal damage.

Alien hand syndrome. The most controversial of callosal syndromes is the Alien Hand Syndrome (Brion & Jedynak, 1972). Although etiology of the Alien Hand Syndrome varies (see Scepkowski & Cronin-Golomb, 2003, for review) the cases described by Brion and Jedynak (1972) involved patients with tumors of the corpus callosum resulting in a body-image disorder involving perception that one of patients' upper limbs did not belong to them. When patients' hands were placed behind their back and one of the hands was placed into the other, patients did not recognize the ownership of that hand (cf. Suwanwela & Leelacheavasit, 2002). Definition of this syndrome was later extended to also include cases of patients who perform complex upper limb motor activities outside of volitional control (Brion & Jedynak, 1972).

Apraxia and agraphia. In 1907, Liepmann and Mass reported a case of a right-handed patient with a lesion to the corpus callosum who suffered from left apraxia and left agraphia (cf. Bogen, 1993). Apraxia is a disorder of motor planning in the absence of damage to the muscles and pathways innervating them. Apraxia involves partial to complete inability to sequence, coordinate, and execute voluntary movements in the absence of sensory impairments or damage to the motor unit or its pathways. A special case of this disorder is verbal apraxia (speech apraxia) characterized by difficulties in articulation due to difficulties in sequencing, coordination, and execution of muscle movements. Agraphia, a form of aphasia is an inability to express language in writing or print. Liepmann and Mass' observations combined with the idea of hemispheric specialization led to development of the callosal concept (Liepmann & Maas, 1907; Bogen, 1993). The callosal concept draws attention to the fact that while verbal instructions in most right-handers are comprehended by the language centers located most frequently in the left hemisphere, movements of the muscles on the left side of the body are largely governed by the motor areas located in the right hemisphere. The corpus callosum provides connectivity between the left-hemisphere language network responsible for understanding verbal commands, and the right-hemisphere motor areas responsible for planning and execution of the movements on the left side

of the body. In patients with lesions to the corpus callosum verbal instructions are comprehended in the left hemisphere, however the motor reaction cannot be carried out as the semantic content of the instruction cannot be relayed to the right hemisphere where most of the motor planning and execution of movements of left digits occurs.

Aprosody. Prosody refers to elements of language expressed in the speech articulation. There are four prosodic systems: affective, linguistic, dialectical, and idiosyncratic (Monnot, Lovallo, Nixon, & E. Ross, 2002). Linguistic prosody refers to the semantics and punctuation. Linguistic prosody is predominantly, yet incompletely localized in the left hemisphere and in most cases does not invoke inter-hemispheric transfer through the corpus callosum (for accounts of linguistic prosody see S. J. Behrens, 1985; Monrad-Krohn, 1963; M. D. Pell, 1998; E. D. Ross, 2000; Ryalls, 1988; D. A. Trauner, Ballantyne, Friedland, & Chase, 1996)

Dialectical prosody refers to the geographic (regional) differences in speech, idiosyncratic prosody refers to individual differences in speech (cf. Monnot et al., 2002; Monrad-Krohn, 1963; E. D. Ross, 2000). Affective prosody refers to the emotional aspects of speech. Affective prosody describes the encoding of a speaker's emotional and attitudinal state during speech, as well as the decoding emotional state of others based on their speech. Nonverbal cues encoded in language carry information for social interaction. Because nonverbal aspects of speech (i.e. affective prosody) are harder to control, when the affective layer contradicts the semantic layer of a message, the affective information is more diagnostic and in turn more credible (E. D. Ross, 1997). The ability to modulate the flow of the affective information is crucial for the regulation of social interaction. Most of the evidence points to the conclusion that the modulation of affective prosody depends on the right hemisphere (Bowers, Bauer, & Heilman, 1993; Bowers, Coslett, Bauer, L. J. Speedie, & Heilman, 1987; Heilman, Bowers, L. Speedie, & Coslett, 1984; Heilman, Scholes, & Watson, 1975; Buchanan et al., 2000; Gorelick & E. D. Ross, 1987; Monnot et al., 2002), however, there are also reports of affective prosody in aphasic patients with lesions to the left hemisphere (de Bleser & Poeck, 1985; M. D. Pell, 1998). Based on patterns of deficits following lesions to the right hemisphere the location of affective prosody is inferred to be in the area of the Sylvian fissure. In the right hemisphere lesions to the anterior part of the Sylvian fissure produce deficits in spontaneous production of the affective information during speech, while lesions to the posterior part of the Sylvian fissure produce deficits in comprehension of affective informa-

tion during speech (Gorelick & E. D. Ross, 1987; Heilman & Gilmore, 1998; Heilman, Scholes et al., 1975; E. D. Ross & Mesulam, 1979; Tucker, Watson, & Heilman, 1977). The posterior aspect of the Sylvian fissure in the left hemisphere neighbors Wernicke's area (and more generally the posterior speech area) involved in the linguistic aspects of language comprehension, and in the right hemisphere it neighbors the homolog of Wernicke's area involved in the non-linguistic aspects of language comprehension. The anterior aspect of the Sylvian fissure in the left hemisphere neighbors Broca's area which is involved in the linguistic aspects of language production, and in the right hemisphere it neighbors the homolog of Broca's area which is involved in the non-linguistic aspects of language production (e.g intonation). Nonlinguistic acoustic features of speech such as intonation, pitch, stress, rate, timing, rhythm and differential pausing complement linguistic elements of language in the transport of meaning (Bolinger, 1980; Crystal, 1975; Kent & Read, 2002; Monnot et al., 2002; Monrad-Krohn, 1963). While linguistic elements of language are largely processed by the left hemisphere, the non-linguistic features are processed by the right hemisphere. The corpus callosum is part of the distributed network responsible for language production and comprehension by allowing integration of the linguistic elements of language from the left hemisphere and the non-linguistic elements of language from the right hemisphere (Klouda, Robin, Graff-Radford, & Cooper, 1988). Klouda et al. (1988) reported a case of a 39-year-old female who suffered from a burst aneurysm in the ACA and subsequent hemorrhage damaging the anterior four-fifths of the corpus callosum. At about a month following the accident, the patient showed very little prosodic differentiation when asked to read sentences while emphasizing happy, sad, angry, neutral, and questioning moods. Expression of emotive states in language is encoded in fundamental frequency (F0) by the right hemisphere, that communicates through the corpus callosum with Broca's area involved in language production. Previous research on lesion patients leads to the conclusion that both the anterior (Klouda et al., 1988) and posterior (Friederici, von Cramon, & Kotz, 2007) portions of the corpus callosum are involved in prosody. Friederici et al. (2007) points to the posterior third of the corpus callosum as relaying the suprasegmental prosodic and syntactic information.

Foreign Accent Syndrome. At least one case has been reported (Hall, C. A. Anderson, Filley, Newcombe, & Hughes, 2003) of a corpus callosum infarct resulting in a Foreign Accent Syndrome (FAS). A right-handed 53-year-old female reported a sudden onset of a speaking difficulty.

On the day of examination the patient's speech was fluent but with marked linguistic aprosody evident in altered patterns of intonation, accent, stress and pause. The patient's speech was rated by French and English speakers as characteristic to a native speaker of French or French Canadian. No apraxia or tacile anomia was present and the patient showed normal understanding and production of emotional prosody. Mild alexia (impaired reading comprehension), agraphia (impaired ability to write), and mild fluent aphasia were present. The MRI scan revealed an ischemic infarct confined to the body of the corpus callosum localized in the midline with slight extension to the left side and no direct involvement of language centers. These signs are consistent with disruption in the language network. Marked linguistic aprosody is consistent with disruption of inter-hemispheric connections between Broca's area and its homolog in the right hemisphere that is likely to be involved in expression of linguistic prosody. Mild alexia, agraphia, and mild fluent aphasia may either stem from the general disruption in the language network, or specifically from disrupted connectivity between homologous language areas in the left and right hemispheres.

Split-brain. In patients with intractable epilepsy the last treatment option is surgical transsection of cortical commissures (Amacher, 1976; Luessenhop, 1970; Wilson, Reeves, & M. Gazzaniga, 1978; Wilson, Reeves, M. Gazzaniga, & Culver, 1977). Cutting major communication pathways between hemispheres to a large extent isolates hemispheric functions creating the ultimate left-brain, right-brain. Elimination of a bulk of hemispheric connections produces a group of neurological signs collectively referred to as the split-brain syndrome or hemispheric disconnection syndrome (Sperry et al., 1969). Those neurological signs, much like the signs produced by spontaneous lesions of the corpus callosum, may help us map its functions in humans. Surgical transsection of the corpus callosum attempts to sever the cortical commissure and at the same time minimize damage to other structures. This approach is analogous to that in experimental neurology where parts of animal brain are severed and subsequent signs are recorded. Lesions produced in those procedures are highly localized and largely circumscribed to the corpus callosum. Only a limited number of those procedures have been performed and access to split-brain subjects is limited. In contrast, spontaneous lesions to the corpus callosum are more frequent but also are more diffuse as they involve more damage to neighboring structures. Pooling neurological signs following a small number of highly localized callosotomies and neurological signs following diffuse callosal lesions should allow for detailed mapping of callosal function in hu-

mans. The extent of surgical transection during callosotomy varies due to anatomical differences and the variability of surgical procedures. Severity of neurological signs depends on the extent and location of the lesion, and on brain reorganization following the surgery. As pointed out by Bogen (1998) three types of neurological signs are present following commissurotomies: hemispheric disconnection signs, neighborhood signs, and diffuse signs. Hemispheric disconnection signs are of primary interest in mapping callosal function. Neighborhood signs result from unintended damage to surrounding structures and are responsible for complicating the clinical picture following surgery. Diffuse signs results from general disruption in the neural subsystems. As intracranial pressure lowers and the edema reduces in the weeks to months following surgery, diffuse signs tend to diminish or disappear. During the Acute Hemisphere Disconnection Syndrome stage that immediately follows the surgery, all of the aforementioned signs are present. The signs that persist only for a period of the first one to two weeks can be attributed to the retraction edema due to the surgeon's attempt to pull aside one of the hemispheres in order to gain clearance to the corpus callosum. Those signs can be considered diffuse. In right-handers operated from the right side signs often include bilateral toe sign and contralateral hypotonia (Bogen, 1998). This review will focus only on the disconnection signs as they are crucial for mapping callosal function. For a comprehensive review of other neurological signs associated with commissurotomies, reader should consult Bogen (1998).

Stabilized Hemisphere Disconnection Syndrome. In the months following the disappearance of retraction edema, some degree of brain reorganization occurs paired with patients developing compensation strategies allowing them to adapt to new circumstances. In everyday interaction, the behavior of many split-brain patients is indistinguishable from before the surgery. The effects of a split-brain become salient under conditions of lateralized sensory input. Under conditions where only one hemisphere receives sensory input, (e.g. presentation of visual stimuli only to left visual field and preventing eye movements) behavior suggests that hemispheres function largely independently from each other (Bogen, 1998). Double hemianopia. It is possible to provide sensory input only to one hemisphere by presenting information to only the left or right visual field a while at simultaneously preventing eye movements (e.g. using the so called Z Lens; Zaidel, 1975). When a stimulus is presented only to the right visual field, it is projected only to the left hemisphere. Given that in most right-handers language centers are located predominantly

in the left hemisphere, most of the split-brain patients can correctly read, name, or describe stimuli in presented in the right visual field (Bogen, 1998). However, if stimuli are presented to the left visual field and therefore projected to the right hemisphere, split-brain patients deny seeing stimuli. Since the language faculty is present predominantly in the left hemisphere, objects or pictures projected to the right hemisphere cannot be named or described. Split-brain patient asked what did he or she see may answer Nothing, just a flash of light (Springer & Deutsch, 1997, , p. 36). This indicates that stimuli enter the visual system but did not reach a level of conscious perception. Double hemianopia is distinct from the hemi-inattention. When instead of naming split-brain patients are asked to reach for the object present in the left visual field, they can correctly select it from among other objects. This suggests that split-brain patients are not simply inattentive to the left visual field but rather cannot name or describe objects in the left visual field (Bogen, 1998). Contralateral auditory suppression. Central auditory pathways provide bilateral representation for auditory input from each ear with ipsilateral ear dominance. For each ear, axons in the ventral cochlear nucleus form projections with both the ipsilateral and contralateral superior olive in the medulla. The superior olive projects in the medial leminiscus to the ipsilateral inferior colliculus. In addition, axons in the dorsal cochlear nucleus form direct projections with both the ipsilateral and contralateral inferior colliculi. Each inferior colliculus projects ipsilaterally to the medial geniculate nucleus in the thalamus. The medial geniculate nucleus (MGN) projects ipsilaterally to the primary auditory cortex. Auditory pathways remain largely intact following a commissurotomy. Auditory information processing in split-brain patients appears to be unaffected when auditory stimuli are presented to one ear at a time. However, when different words are simultaneously presented to each ear, only the word presented to the right ear is reliably reported (Bogen, 1998; Milner, L. Taylor, & Sperry, 1968). The ipsilateral pathway connecting the ear with the auditory cortex does not cross the midline and therefore is not affected by a commissurotomy. However, in both split-brain and non split-brain individuals, ipsilateral inputs traveling in this pathway are suppressed if different stimuli are received by both ears. For instance, if the stimulus presented in the left ear is different from the stimulus presented to the right ear, then ipsilateral inputs from right ear to right auditory cortex and from left ear to left auditory cortex are suppressed. This mechanism helps divide attention between auditory stimuli from both ears (Sidtis, 1988) and is quite adaptive when inter-hemispheric pathways are intact. Under those

conditions information from unsuppressed contralateral pathways can always be relayed back to the side it originated from through corpus callosum functionally replacing suppressed ipsilateral inputs. However, in split-brain patients inputs carried by the auditory pathway projecting contralaterally from the left ear to the right auditory cortex cannot be relayed back to the language centers in the left hemisphere as callosal projections are severed. Apraxia. In split-brain patients apraxia is almost always present during the acute hemisphere disconnection syndrome. However, during the subsequent stabilized hemisphere disconnection syndrome stage the presence and the degree of apraxia varies widely. This variation can be explained by the existence of compensatory processes. When present, apraxia is lateralized to the left side and can be caused by either a deficit in comprehending instruction or a deficit in executing motor response (Bogen, 1998). Since language centers are predominantly located in the left hemisphere and apraxia in split-brain patients is localized to the left side of the body, it is likely that in the split-brain syndrome apraxia emerges on the side ipsilateral to the hemisphere where the language centers are located. Muscle movements on the side ipsilateral to the language centers are controlled by the contralateral motor cortex. Severing the corpus callosum disrupts communication between language centers that comprehend verbal commands and the contralateral motor cortex that executes movements on the body side ipsilateral to language centers. Replication of hand postures. In split-brain patients, hand postures presented only in one-half of the visual field are perceived by only one hemisphere. Those hand postures can be mimicked with the hand ipsilateral to the visual field where the pattern was presented, and cannot be mimicked with the hand contralateral to the visual field where the pattern was presented. When a patients' hand is formed to mimic certain shape in the absence of visual information, split-brain patients cannot replicate this shape with the other hand (Bogen, 1998). Localization of sensory stimulation. Split-brain patients show a diminished ability to localize sensory stimulation on the left side of the body. This deficit increases in magnitude towards the extremities and is most pronounced in the fingertips (Bogen, 1998). While a trained non-split-brain subjects can correctly localize pen tip pressure on one of the fingertips on at least 90trials, a trained split-brain patients correctly localize pen tip pressure on one of the fingertips at chance level or worse (=¡25%). The simplest explanation for this deficit is that split-brain patients can spatially localize sensory stimulation on the left side of the body but simply cannot verbalize it as the link between the right somatosensory cortex and the language areas in the left hemisphere is

broken. However, Bogen (1998) argued that this deficit is not mediated by the language deficits, as it is also present when the nonverbal picture identification task is used. Deficits in localization of sensory stimulation are normal developmental signs in young children (Bogen, 1998; Galin, J. Johnstone, Nakell, & Herron, 1979) presumably because of incomplete myelination of the commissures (Bogen, 1998; Yakovlev & Lecours, 1967). Retrieval of objects. When an object is placed in a split-brain patient's right palm, the patient can name and describe the object even without any visual input. In contrast, if the same object is placed in patient's left palm the patient cannot name or describe the object. However, if a patient is asked to use this object or retrieve it from amongst other objects using left hand s/he is often correct. That indicates that split-brain patients recognized the object but could not name it. This is consistent with the callosal concept because language centers are lateralized to the left, and somatosensory inputs from they left side of the body are located in the right postcentral gyrus. With the inter-hemispheric communication disrupted somatosensory and language centers are largely disconnected. In addition, split-brain patients show good retrieval of objects with the same hand they initially used to feel them, and poor retrieval of objects with hand contralateral to the one they used to initially feel them. Both motor and somatosensory areas are adjacent to each other and control the contralateral side of the body. Retrieval of objects with the same hand with which they were initially felt does not invoke inter-hemispheric transfer while retrieval of objects with the other hand requires a connection between the somatosensory areas and the contralateral motor areas. Even though the language centers are predominantly located in the left hemisphere, there is evidence that split-brain patients comprehend language even if it is presented only to the right hemisphere. Split-brain patients can retrieve objects with their left hand upon verbal command. Since left hand movements are governed by the right hemisphere, verbal command needs to be either comprehended by the right hemisphere, or comprehended by the left hemisphere and relayed to the right hemisphere through incompletely sectioned corpus callosum or other commissures that has not been severed. Split-brain patients can retrieve objects with their left hand even when name of the object is tachistoscopically presented only to the left visual field and consequently only to the right hemisphere (Bogen, 1998). However, even after selecting the correct object they provide an incorrect verbal description. Split-brain patients presented with stimuli exclusively to the right hemisphere rarely can comprehend more than single words. While lexicon comprehended by the right hemisphere

may grow with time, the understanding of language syntax remains heavily impaired. Language ability in the right hemisphere emerges from a general-purpose information processing rather than from language-specialized information processing as in case of the language centers that evolved in the left hemisphere. The right hemisphere lacks rules for transcribing graphemes to phonemes and the ability to represent information phonetically (Zaidel, 1978; Bogen, 1998)

Bogen (1998) reported two cases of split-brain patients with sparred anterior commissures that demonstrated right hemisphere language ability (Baynes, 1990; Baynes, Tramo, & Gazzaniga, 1992; Bogen, 1998; McKeever, Sullivan, Ferguson, & Rayport, 1982; Sidtis, Volpe, Wilson, Rayport, & Gazzaniga, 1981). In monkeys an intact anterior commissure allows for transfer of learning between hemispheres, while in humans the anterior commissure helps to compensate for loss of callosal connections carried in the splenium but only with regard to specific types of visual information (C. R. Hamilton, 1982). Most of the symptoms associated with the split-brain syndrome appear even if anterior commissure is sparred (Gazzaniga & LeDoux, 1978; McKeever, Sullivan, Ferguson, & Rayport, 1981, , cf. Bogen, 1998). Agraphia and dysgraphia. Agraphia refers to the inability to write while dysgraphia refers to the diminished ability to write. Both agraphia and dysgraphia can be unilateral or bilateral depending on where one or both sides of the body are affected. In a majority of individuals, both language centers and areas responsible for motor control of the dominant hand are located in the hemisphere contralateral to a dominant hand. In contrast, areas responsible for motor control of the non-dominant hand are usually located in the hemisphere contralateral to the hemisphere where the language centers are located. Most non-split-brain individuals can write slowly but legibly with their non-dominant hand as the corpus callosum enables inter-hemispheric communication between language centers and areas responsible for motor control of a non-dominant hand. In split-brain patients this ability disappears. With the corpus callosum severed, the ability of left hemisphere to relay information to motor areas in the right hemisphere is compromised, and since the right motor areas command movements of left extremities, writing using the left hand is compromised as well. Loss of the ability to write with the left hand is particularly common when apraxia is present (Bogen, 1998). Dysgraphia. Severing the corpus callosum often results in dysgraphia, specifically loss of ability to write to dictation. This deficit is not due to a general loss of coordination or paresis as motor tasks that require similar degree of control and dexterity can be performed (e.g. pattern copying,

diagram copying, design copying). Tactile anomia. While anomia refers to the inability to evoke a desired word, a tactile anomia refers to the inability to either name or describe an object based on tactile information. In majority of individuals, both language centers and areas responsible for somatosensation in the palm of the dominant hand are located in the hemisphere contralateral to the dominant hand. In contrast, areas responsible for somatosensation in the palm of a non-dominant hand are usually located in the hemisphere contralateral to the hemisphere where the language centers are located. As in case of agraphia in split-brain patients, tactile anomia is usually lateralized to the left side of the body. In Bogen's Caltech series, tactile anomia was present in the left hand of twelve right-handers, and in the right hand on one left-hander. This finding has been also replicated in patients with sparred anterior commissures (Gazzaniga & LeDoux, 1978; McKeever, Sullivan, Ferguson, & Rayport, 1981, , cf. Bogen, 1998). With the corpus callosum severed, the ability of right somatosensory cortex to relay information to the language areas in left hemisphere is compromised. Since in the majority of the population language centers are lateralized to the left, and since sensation in the left hand is localized in the right hemisphere, split-brain patients cannot verbalize (name or describe an object) their sensations. Alien hand incidents. As in spontaneously occurring lesions to the corpus callosum alien-hand-like symptoms are often present in the early postoperative period (Bogen, 1998). Gazzaniga (1970) and Springer and Deutsch (1997) described the case of a commissurotomy patient who had difficulty dressing up. When one of his hands was pulling his pants up, the other was pulling them down. In another patient when one hand was buttoning his shirt, the other hand was immediately following unbuttoning it (Bogen & Vogel, 1975).On another occasion a patient discussed by Gazzaniga (1970) and Springer and Deutsch (1997) in anger forcefully reached for his wife with his left hand, while at the same time having right hand grab left hand in an effort to stop it. Reported incidents demonstrate that left hand movements can occur outside of consciousness, even many years after the callosotomy (Bogen, 1998; Zaidel, 1983). The most interesting are the well-coordinated left-hand movements that seem at cross purposes with movements of the right hand as if cerebral hemispheres were battling over the control of one's actions. The presence of such conflicting movements suggests that more areas remain activated after split-brain surgery than before as both hemispheres attempt to simultaneously execute movements. For instance in Trevarthen (1978), split-brain baboons reached for objects with both limbs instead of using just one limb and previ-

ously mentioned split-brain patients performed simultaneous (and conflicting) movements of both upper-limbs. Altogether this suggests that the loss of callosal projections is associated with an increase in the number areas that are simultaneously activated (Trevarthen, 1978) suggests that corpus callosum carries inhibitory information (Springer & Deutsch, 1997). Regulation in biological systems often involves opponent processes resulting in a heterostasis oscillating around the desired state. Movements of human limbs result from simultaneous stretching or relaxing agonist or antagonist muscles and a constant corrective mechanism fine-tuning those operations. Bodily functions are regulated by the autonomic nervous system composed of two opposing divisions that complement each other in regulating such indispensable aspects of bodily functions as blood pressure, digestion, or breathing. All of the above regulatory mechanisms are the outcome of the interplay of opposing but complementary processes. This sheds light on the possible aftermath of the callosotomy where cerebral hemispheres lose bulk of commissural inhibitory and excitatory inputs. Inter-manual conflict resulting from this disconnection diminishes with time as new ways of integrating the functions of left and right hemispheres emerge.

Commissural Functions and the Hemispheric Specialization. The corpus callosum is the largest cortical commissure and the largest white matter structure in the brain relaying a wide variety of information across hemispheres. This may enable each hemisphere to form a complete representation of sensory inputs (Springer & Deutsch, 1997). The corpus callosum is also involved in the integration of hemispheric functions. The left hemisphere evolved to specialize in serial, and analytic information processing predisposing it to language-related functions. The right hemisphere is a more fit for parallel and holistic information processing predisposing it to spatial information processing. While the cerebral hemispheres specialize in different modes of information processing they often are both able to handle the same tasks, or process the same types of information. However, the cerebral hemispheres are not equally efficient in processing all types of information. The information processing capabilities could be divided into general information processing that can be handled efficiently by either hemisphere, and the specialized information processing that can be processed more efficiently by one of the hemispheres. For an optimal performance, each hemisphere should handle information it is more or equally efficient to process. Cerebral commissures may be the information pathways that help optimize performance and integrate hemispheric functions. This process may be modeled after a team perfor-

mance task where team members perform a complex task that requires a high degree of interdependence. Each member is assigned a part of the task where he or she is best fit to perform. At each particular point in time each team member needs to know what his/her part of the task is, the current progress of this part of the task, and the current process of each of the other members is. If any of the members falls behind, any or all of the other members can assume parts of his task in order to collectively complete the task. If no help is given, the whole team will stall. Functions distributed amongst team members are pooled and synchronized with the help of information exchanged amongst the members (current progress, specialty etc.). In a similar way commissures may allow for optimal use of brain processing resources by exchanging information with each other (e.g. progress report) and partially controlling each other's function (e.g. inhibition). The symptoms of the split-brain syndrome discussed above stem from either the disconnection of sensory relays resulting in an incomplete sensory representation in each hemisphere or from the elimination of regulatory inputs including inhibitory connections. Regulatory projections allow for the integration of functions served by hemispheres, and help in avoiding cross-talk and conflicting actions.

Appendix B:

Supplementary Result Tables

Variable	Levels	n	Min	$\widetilde{x}$	$\bar{x}_{trim}$	Max	IQR	c_v	s	#NA
Age Days Date of Visit to DOB	Male	136	2192.0	4353.5	4272.3	6698.0	2248.5	0.3	1314.3	0
	Female	157	2210.0	3987.0	4143.6	6663.0	2060.0	0.3	1264.2	0
p = 0.45823	all	293	2192.0	4183.0	4202.4	6698.0	2159.0	0.3	1286.8	0
CANTAB IED Stages Completed	Male	136	2.0	9.0	8.3	9.0	2.0	0.2	1.3	0
	Female	157	0.0	9.0	8.1	9.0	2.0	0.2	1.6	0
p = 0.068377	all	293	0.0	9.0	8.2	9.0	2.0	0.2	1.5	0
CANTAB SWM Between Trial Return Errors	Male	136	0.0	29.5	30.2	97.0	38.2	0.7	21.9	0
	Female	157	0.0	26.0	31.3	85.0	34.0	0.7	20.9	0
p = 0.52021	all	293	0.0	29.0	30.8	97.0	36.0	0.7	21.3	0
CANTAB SWM Strategy	Male	136	0.0	34.0	32.5	45.0	8.0	0.3	8.4	0
	Female	157	0.0	34.0	33.3	44.0	6.0	0.2	6.9	0
p = 0.45914	all	293	0.0	34.0	33.0	45.0	7.0	0.2	7.6	0
WAIS R Percent Digit Symbol	Male	12	46.2	63.4	68.0	100.0	10.2	0.2	13.0	124
	Female	10	63.4	76.9	78.9	92.5	17.7	0.1	10.3	147
p = 0.036397	all	22	46.2	73.1	73.0	100.0	15.1	0.2	12.8	271
WAIS R Raw Score Digit Symbol	Male	12	43.0	59.0	63.2	93.0	9.5	0.2	12.1	124
	Female	10	59.0	71.5	73.4	86.0	16.5	0.1	9.6	147
p = 0.036397	all	22	43.0	68.0	67.8	93.0	14.0	0.2	11.9	271
WAISWISC Digit Coding B Percent	Male	106	15.1	45.4	46.6	100.0	21.1	0.3	15.5	30
	Female	124	22.7	46.6	47.3	92.5	24.4	0.3	15.7	33
p = 0.69013	all	230	15.1	45.4	47.0	100.0	22.3	0.3	15.6	63
WASI Total Raw Score Block	Male	136	5.0	35.0	34.6	71.0	31.0	0.5	18.8	0
	Female	157	3.0	28.0	30.4	70.0	36.0	0.6	19.6	0
p = 0.074069	all	293	3.0	31.0	32.3	71.0	35.0	0.6	19.3	0
WASI Total Raw Score Matrix	Male	136	4.0	26.0	24.7	33.0	8.2	0.3	6.8	0
	Female	157	3.0	25.0	24.1	34.0	7.0	0.3	6.3	0
p = 0.23382	all	293	3.0	25.0	24.4	34.0	7.0	0.3	6.5	0
WISC III Percent Coding B	Male	94	15.1	43.3	44.1	74.8	14.7	0.3	13.6	42
	Female	114	22.7	44.5	45.0	81.5	20.6	0.3	13.0	43
p = 0.5243	all	208	15.1	44.5	44.6	81.5	18.7	0.3	13.2	85

Table 27

Sample characteristics: summary of continuous demographic and behavioral variables by gender.

Variable	Levels	n	Min	$\widetilde{x}$	$\bar{x}_{trim}$	Max	IQR	c_v	s	#NA
Age Days Date of Visit to DOB	Non-Right-Handed	36	2198.0	4020.5	4045.6	6456.0	1955.8	0.3	1296.7	0
	Right-handed	257	2192.0	4209.0	4226.5	6698.0	2176.0	0.3	1286.3	0
p = 0.45209	all	293	2192.0	4183.0	4202.4	6698.0	2159.0	0.3	1286.8	0
CANTAB IED Stages Completed	Non-Right-Handed	36	2.0	8.5	7.9	9.0	2.0	0.2	1.7	0
	Right-handed	257	0.0	9.0	8.2	9.0	2.0	0.2	1.4	0
p = 0.5796	all	293	0.0	9.0	8.2	9.0	2.0	0.2	1.5	0
CANTAB SWM Between Trial Return Errors	Non-Right-Handed	36	0.0	25.5	29.8	85.0	43.2	0.8	24.4	0
	Right-handed	257	0.0	30.0	31.0	97.0	36.0	0.7	20.9	0
p = 0.52992	all	293	0.0	29.0	30.8	97.0	36.0	0.7	21.3	0
CANTAB SWM Strategy	Non-Right-Handed	36	0.0	33.5	32.4	45.0	15.0	0.3	9.2	0
	Right-handed	257	0.0	34.0	33.1	44.0	7.0	0.2	7.4	0
p = 0.99161	all	293	0.0	34.0	33.0	45.0	7.0	0.2	7.6	0
WAIS R Percent Digit Symbol	Non-Right-Handed	4	63.4	63.4	65.9	73.1	2.4	0.1	4.8	32
	Right-handed	18	46.2	73.7	74.6	100.0	19.6	0.2	13.6	239
p = 0.17003	all	22	46.2	73.1	73.0	100.0	15.1	0.2	12.8	271
WAIS R Raw Score Digit Symbol	Non-Right-Handed	4	59.0	59.0	61.2	68.0	2.2	0.1	4.5	32
	Right-handed	18	43.0	68.5	69.3	93.0	18.2	0.2	12.6	239
p = 0.17003	all	22	43.0	68.0	67.8	93.0	14.0	0.2	11.9	271
WAISWISC Digit Coding B Percent	Non-Right-Handed	27	24.4	45.4	45.8	73.1	23.9	0.3	14.3	9
	Right-handed	203	15.1	46.2	47.1	100.0	21.5	0.3	15.7	54
p = 0.60924	all	230	15.1	45.4	47.0	100.0	22.3	0.3	15.6	63
WASI Total Raw Score Block	Non-Right-Handed	36	3.0	31.5	33.2	67.0	27.8	0.6	18.7	0
	Right-handed	257	4.0	31.0	32.2	71.0	36.0	0.6	19.4	0
p = 0.90135	all	293	3.0	31.0	32.3	71.0	35.0	0.6	19.3	0
WASI Total Raw Score Matrix	Non-Right-Handed	36	3.0	24.5	23.3	33.0	10.0	0.3	7.2	0
	Right-handed	257	4.0	26.0	24.5	34.0	6.0	0.3	6.4	0
p = 0.41543	all	293	3.0	25.0	24.4	34.0	7.0	0.3	6.5	0
WISC III Percent Coding B	Non-Right-Handed	23	24.4	41.2	42.1	68.9	18.1	0.3	12.5	13
	Right-handed	185	15.1	44.5	44.9	81.5	19.3	0.3	13.3	72
p = 0.32837	all	208	15.1	44.5	44.6	81.5	18.7	0.3	13.2	85

Table 28

Sample characteristics: summary of continuous demographic and behavioral variables by handedness.

Variable	Levels	n	Min	$\tilde{x}$	$\bar{x}_{trim}$	Max	IQR	c_v	s	#NA
eTIV	Male	136	1342025.6	1642567.6	1651072.3	1990277.1	168760.4	0.1	130067.8	0
	Female	157	1131463.9	1480107.1	1490620.7	1912683.8	140297.4	0.1	128222.2	0
p ¡ 0.0001	all	293	1131463.9	1552762.7	1565278.0	1990277.1	208112.7	0.1	151847.4	0
CC Anterior	Male	136	445.0	834.5	828.3	1253.0	163.2	0.2	137.4	0
	Female	157	377.0	798.0	802.8	1181.0	162.0	0.2	127.0	0
p = 0.096254	all	293	377.0	819.0	814.4	1253.0	162.0	0.2	132.5	0
CC Mid Posterior and Posterior	Male	136	683.0	1284.5	1287.0	1889.0	234.8	0.2	201.7	0
	Female	157	874.0	1236.0	1242.2	1932.0	260.0	0.2	195.5	0
p = 0.036821	all	293	683.0	1258.0	1262.8	1932.0	260.0	0.2	199.2	0
ctx rlh frontallobe	Male	136	160417.0	211856.0	210611.9	258648.0	25440.8	0.1	18509.0	0
	Female	157	153347.0	194157.0	195132.4	247083.0	21801.0	0.1	18175.8	0
p ¡ 0.0001	all	293	153347.0	201914.0	202301.8	258648.0	28304.0	0.1	19811.0	0
ctx rlh parietallobe	Male	136	93996.0	135765.0	135279.5	166028.0	17825.0	0.1	13481.9	0
	Female	157	94596.0	124014.0	124079.7	173692.0	18904.0	0.1	13640.3	0
p ¡ 0.0001	all	293	93996.0	129038.0	129255.9	173692.0	20052.0	0.1	14551.7	0
wm rlh frontallobe	Male	136	106751.0	146018.5	145940.8	183420.0	16659.5	0.1	14247.6	0
	Female	157	93414.0	130195.0	131316.1	181131.0	17941.0	0.1	14935.8	0
p ¡ 0.0001	all	293	93414.0	138171.0	138137.7	183420.0	22329.0	0.1	16217.0	0
wm rlh parietallobe	Male	136	71024.0	94948.0	95876.3	122188.0	15830.0	0.1	10723.2	0
	Female	157	59946.0	84482.0	85354.8	131298.0	15412.0	0.1	11866.0	0
p ¡ 0.0001	all	293	59946.0	89614.0	90276.2	131298.0	17858.0	0.1	12408.0	0

Table 29

Sample characteristics: summary of continuous volumetric anatomical measures by gender (unit of measurement: cubic millimeters).

Variable	Levels	n	Min	$\tilde{x}$	$\bar{x}_{trim}$	Max	IQR	c_v	s	#NA
eTIV	Non-Right-Handed	36	1131481.2	1570097.3	1581093.2	1988160.2	135242.3	0.1	158823.4	0
	Right-handed	257	1131463.9	1548628.9	1563482.8	1990277.1	209511.3	0.1	151076.5	0
p = 0.50956	all	293	1131463.9	1552762.7	1565278.0	1990277.1	208112.7	0.1	151847.4	0
CC Anterior	Non-Right-Handed	36	443.0	808.5	798.9	1253.0	215.5	0.2	178.1	0
	Right-handed	257	377.0	820.0	816.9	1234.0	158.0	0.2	125.1	0
p = 0.42845	all	293	377.0	819.0	814.4	1253.0	162.0	0.2	132.5	0
CC Mid Posterior and Posterior	Non-Right-Handed	36	683.0	1211.5	1226.9	1889.0	257.5	0.2	235.9	0
	Right-handed	257	829.0	1267.0	1268.7	1932.0	255.0	0.2	193.4	0
p = 0.1725	all	293	683.0	1258.0	1262.8	1932.0	260.0	0.2	199.2	0
ctx rlh frontallobe	Non-Right-Handed	36	153347.0	205408.5	205287.9	246455.0	23141.0	0.1	21249.0	0
	Right-handed	257	154506.0	201285.0	201858.5	258648.0	28611.0	0.1	19616.5	0
p = 0.26834	all	293	153347.0	201914.0	202301.8	258648.0	28304.0	0.1	19811.0	0
ctx rlh parietallobe	Non-Right-Handed	36	94534.0	135765.0	131749.2	162044.0	20699.5	0.1	16499.3	0
	Right-handed	257	93996.0	128706.0	128910.2	173692.0	18880.0	0.1	14265.5	0
p = 0.23369	all	293	93996.0	129038.0	129255.9	173692.0	20052.0	0.1	14551.7	0
wm rlh frontallobe	Non-Right-Handed	36	99033.0	138510.5	138522.3	175690.0	19868.0	0.1	16576.8	0
	Right-handed	257	93414.0	138171.0	138095.5	183420.0	22426.0	0.1	16198.8	0
p = 0.89639	all	293	93414.0	138171.0	138137.7	183420.0	22329.0	0.1	16217.0	0
wm rlh parietallobe	Non-Right-Handed	36	70552.0	89000.0	91176.3	115100.0	16733.5	0.1	11907.5	0
	Right-handed	257	59946.0	89638.0	90161.6	131298.0	18088.0	0.1	12495.0	0
p = 0.74714	all	293	59946.0	89614.0	90276.2	131298.0	17858.0	0.1	12408.0	0

Table 30

Sample characteristics: summary of continuous volumetric anatomical measures by handedness (unit of measurement: cubic millimeters).

Table 31

Correlation table for variables included in the dataset

	Age	Age^2	CANTAB SWM BT Errors	WISC-III Raw Score Coding B	WASI Block Design Raw Score	WASI Matrix Reasoning Raw Score	eTIV	CC Anterior 1/5	CC Posterior 2/5	Cortex R+L Frontal	Cortex R+L Parietal	WM R+L Frontal	WM R+L Parietal
Age	**1.00**	0.99	-0.64	0.81	0.78	0.71	0.31	0.14	0.38	-0.25	-0.40	0.41	0.35
Age^2	0.99	**1.00**	-0.63	0.80	0.77	0.67	0.29	0.13	0.36	-0.28	-0.41	0.39	0.33
CANTAB SWM BT Errors	-0.64	-0.63	**1.00**	-0.56	-0.62	-0.59	-0.24	-0.09	-0.26	0.16	0.23	-0.27	-0.27
WISC-III Raw Score Coding B	0.81	0.80	-0.56	**1.00**	0.63	0.52	0.09	-0.04	0.20	-0.22	-0.34	0.21	0.18
WASI Block Design Raw Score	0.78	0.77	-0.62	0.63	**1.00**	0.70	0.31	0.12	0.32	-0.08	-0.22	0.37	0.32
WASI Matrix Reasoning Raw Score	0.71	0.67	-0.59	0.52	0.70	**1.00**	0.31	0.16	0.24	-0.04	-0.17	0.34	0.30
eTIV	0.31	0.29	-0.24	0.09	0.31	0.31	**1.00**	0.33	0.30	0.64	0.51	0.86	0.77
CC Anterior 1/5	0.14	0.13	-0.09	-0.04	0.12	0.16	0.33	**1.00**	0.59	0.21	0.21	0.38	0.32
CC Posterior 2/5	0.38	0.36	-0.26	0.20	0.32	0.24	0.30	0.59	**1.00**	0.06	-0.02	0.39	0.31
Cortex R+L Frontal	-0.25	-0.28	0.16	-0.22	-0.08	-0.04	0.64	0.21	0.06	**1.00**	0.80	0.51	0.40
Cortex R+L Parietal	-0.40	-0.41	0.23	-0.34	-0.22	-0.17	0.51	0.21	-0.02	0.80	**1.00**	0.33	0.36
WM R+L Frontal	0.41	0.39	-0.27	0.21	0.37	0.34	0.86	0.38	0.39	0.51	0.33	**1.00**	0.87
WM R+L Parietal	0.35	0.33	-0.27	0.18	0.32	0.30	0.77	0.32	0.31	0.40	0.36	0.87	**1.00**

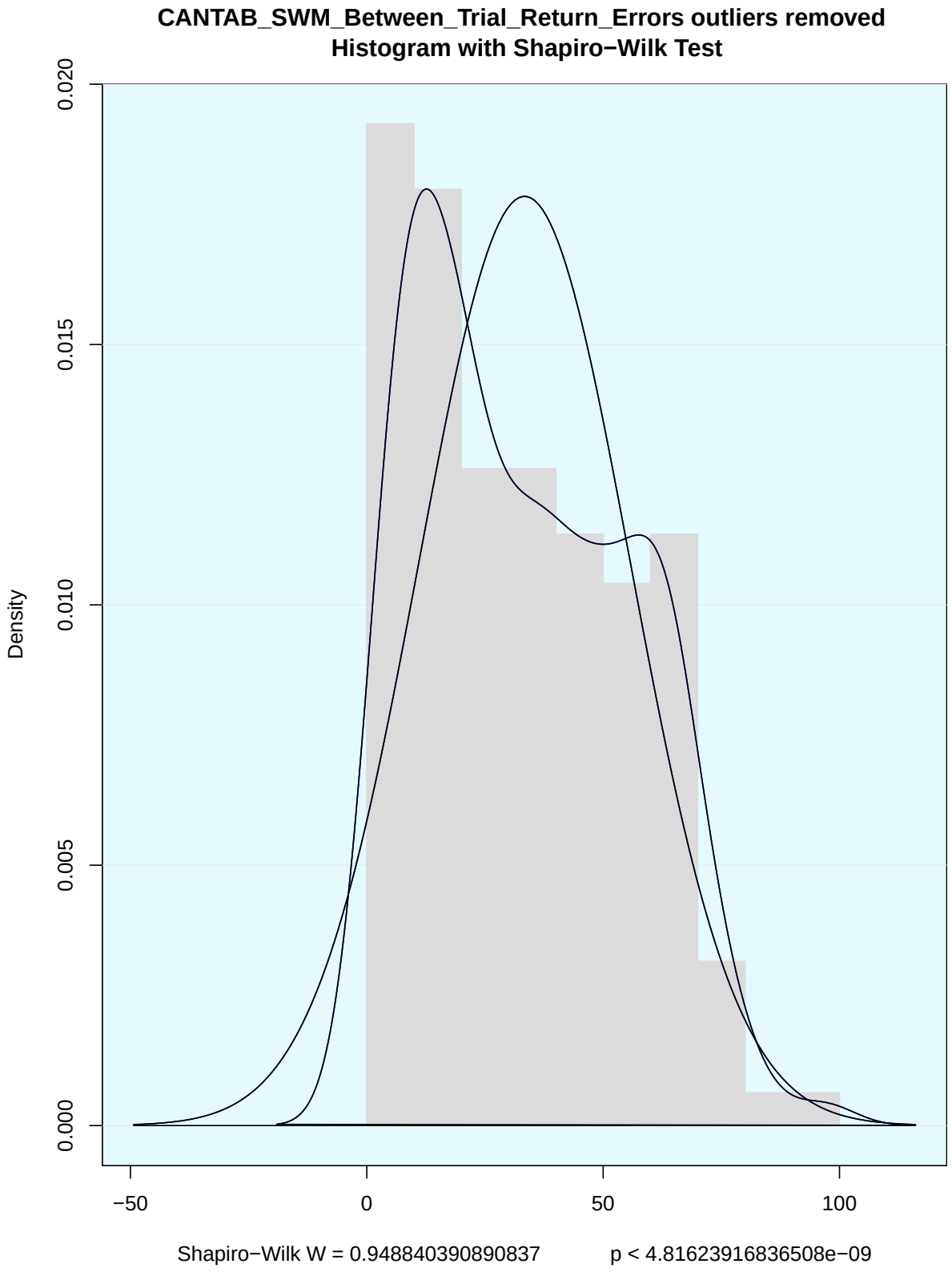

Figure 9: Distribution of CANTAB Spatial Working Memory Between Trial Return Errors

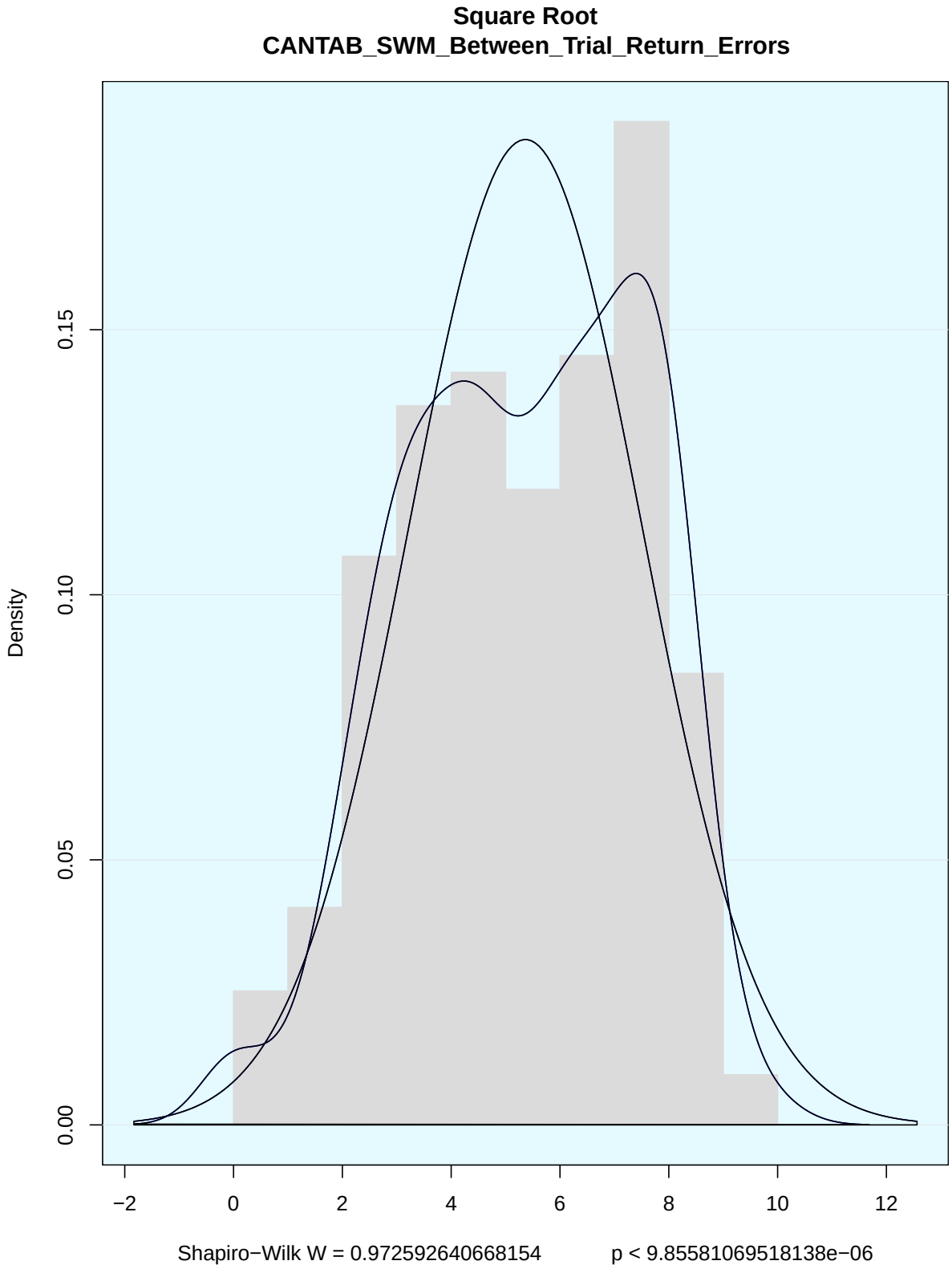

Figure 10: Distribution of square root transformed CANTAB Spatial Working Memory Between Trial Return Errors

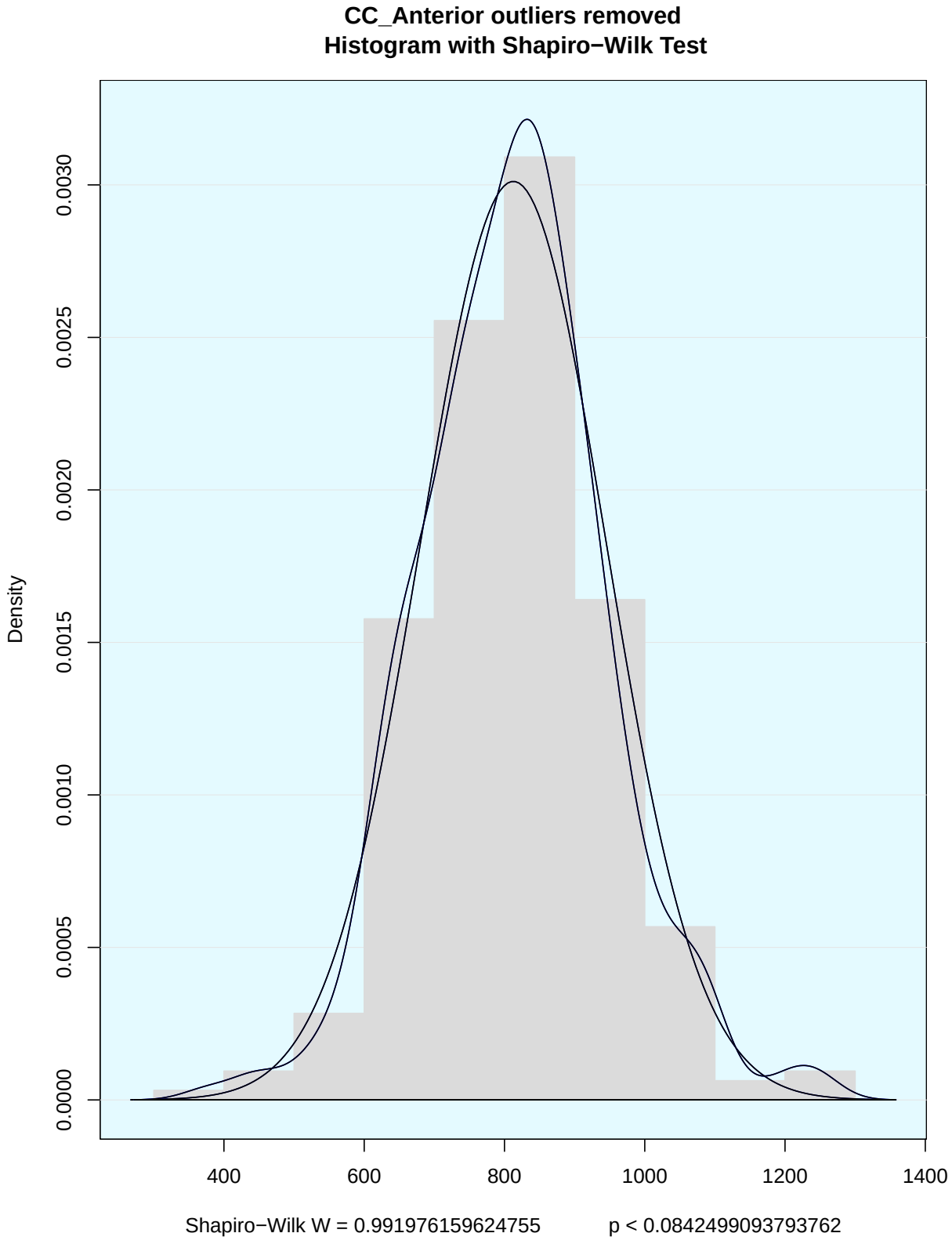

Figure 11: Distribution of the volume of the anterior one-fifth of the Corpus Callosum

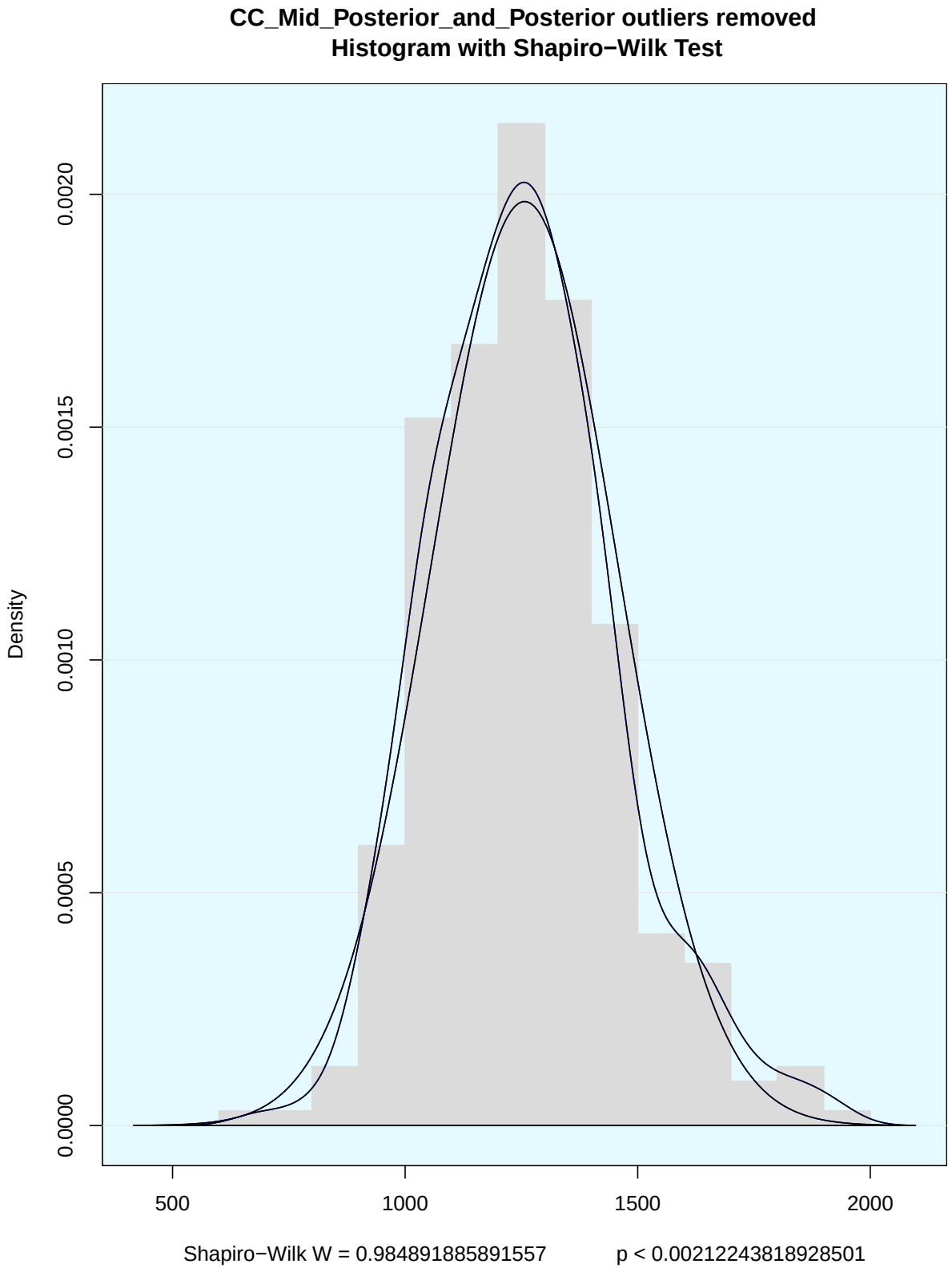

Figure 12: Distribution of the volume of the posterior two-fifths of the Corpus Callosum

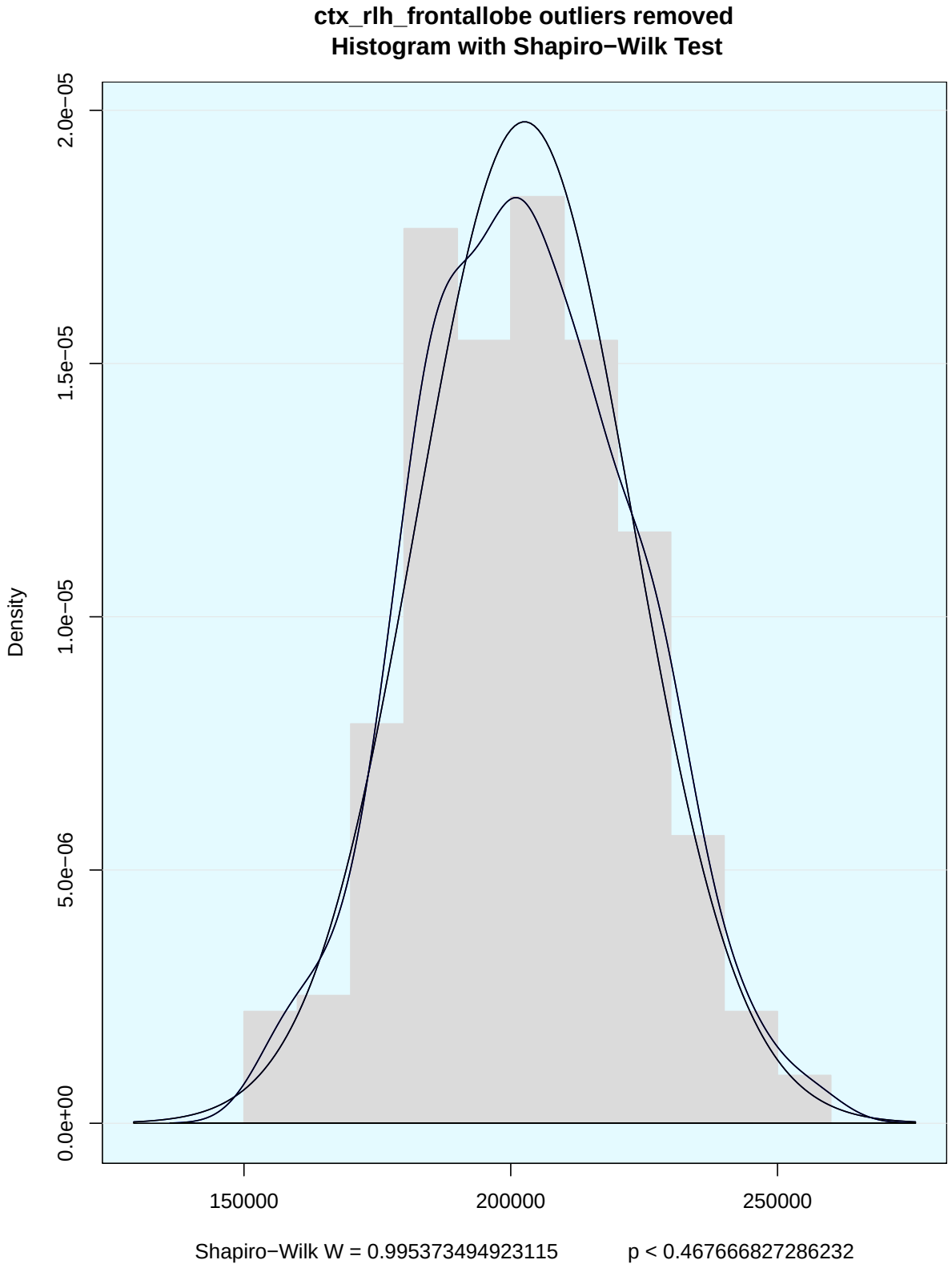

Figure 13: Distribution of volume of the frontal gray matter

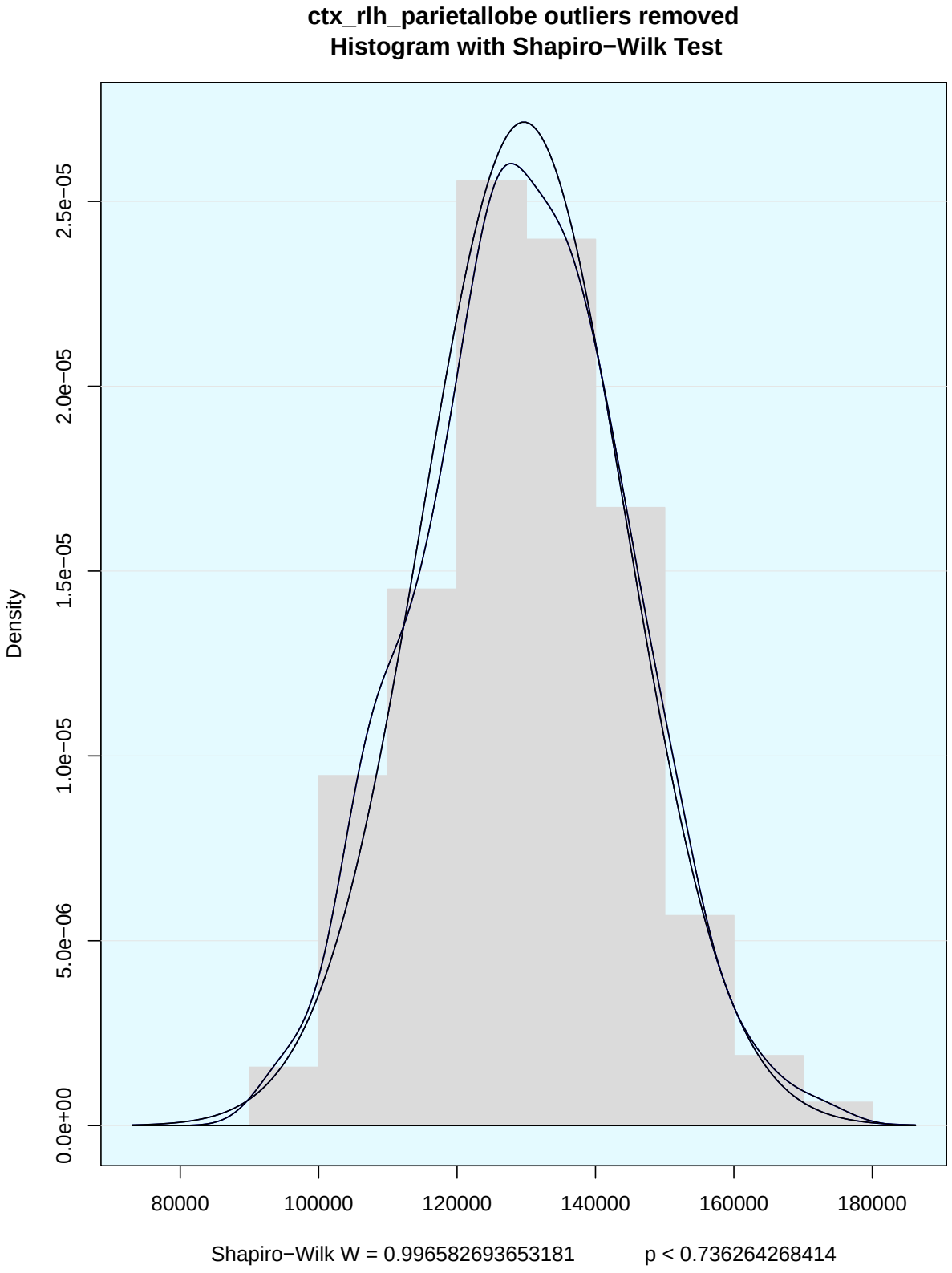

Figure 14: Distribution of volume of the parietal gray matter

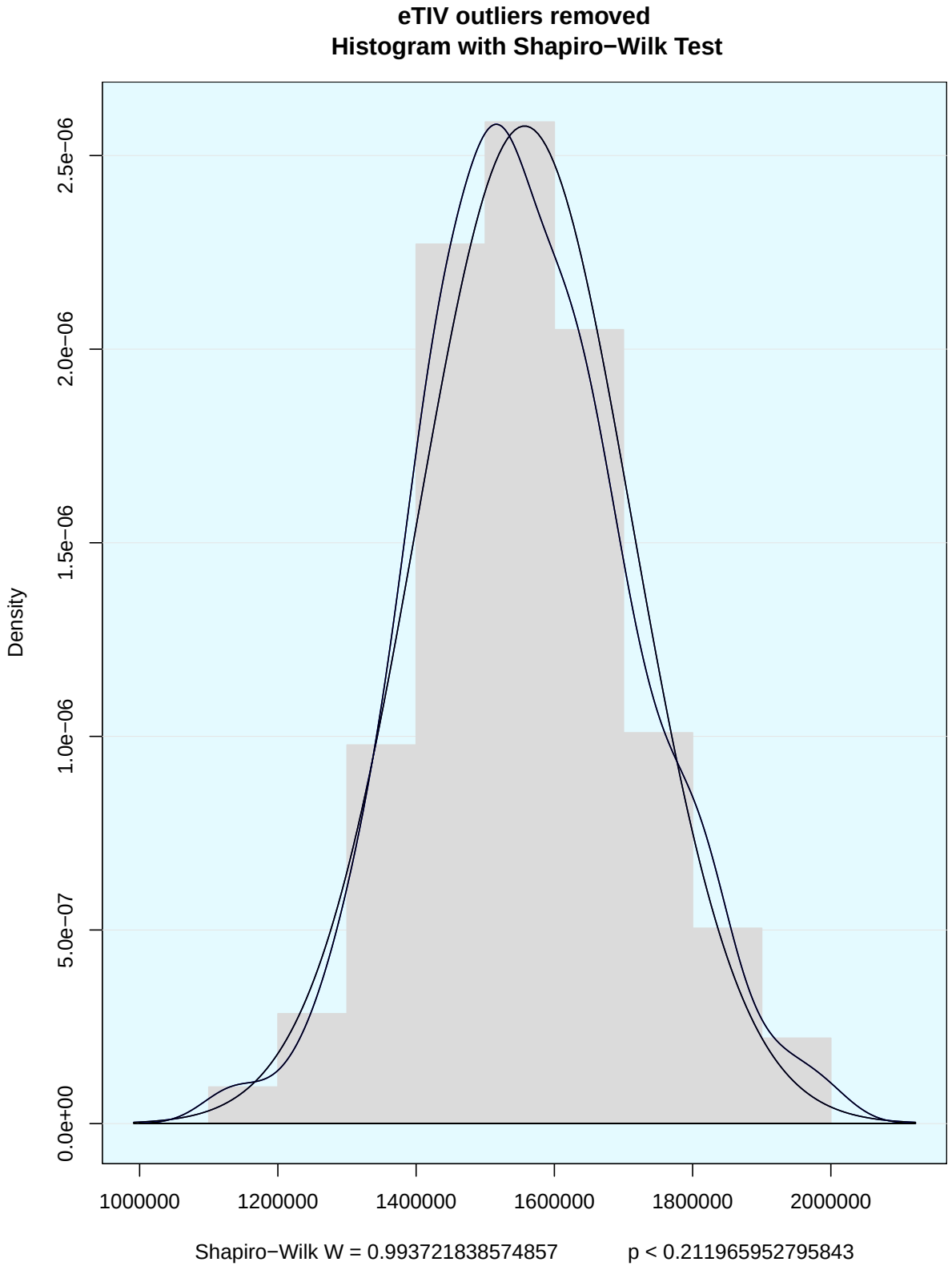

Figure 15: Distribution of volume of the estimated Total Intracranial Volume

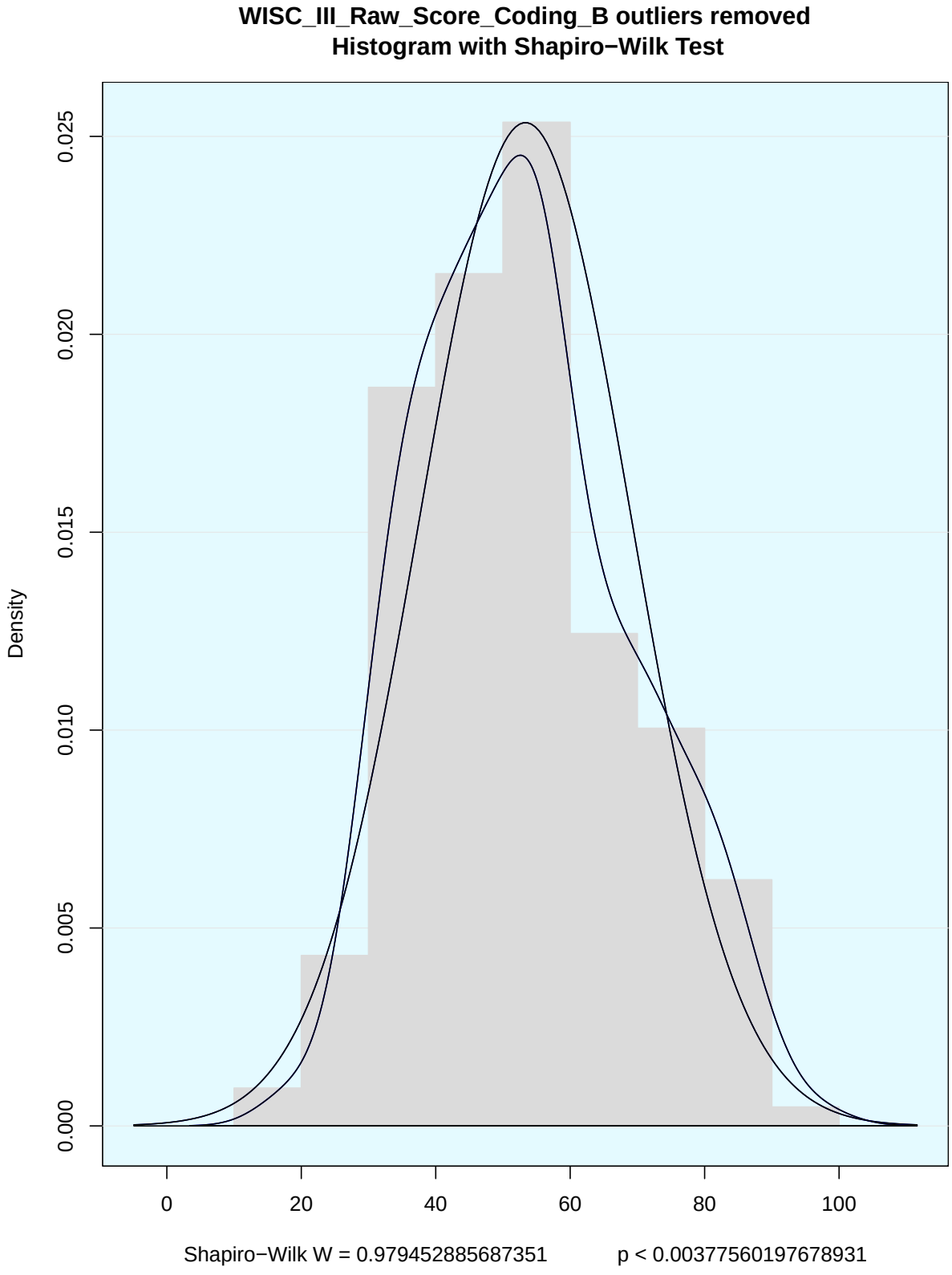

Figure 16: Distribution of the WISC-III Coding B Raw Scores

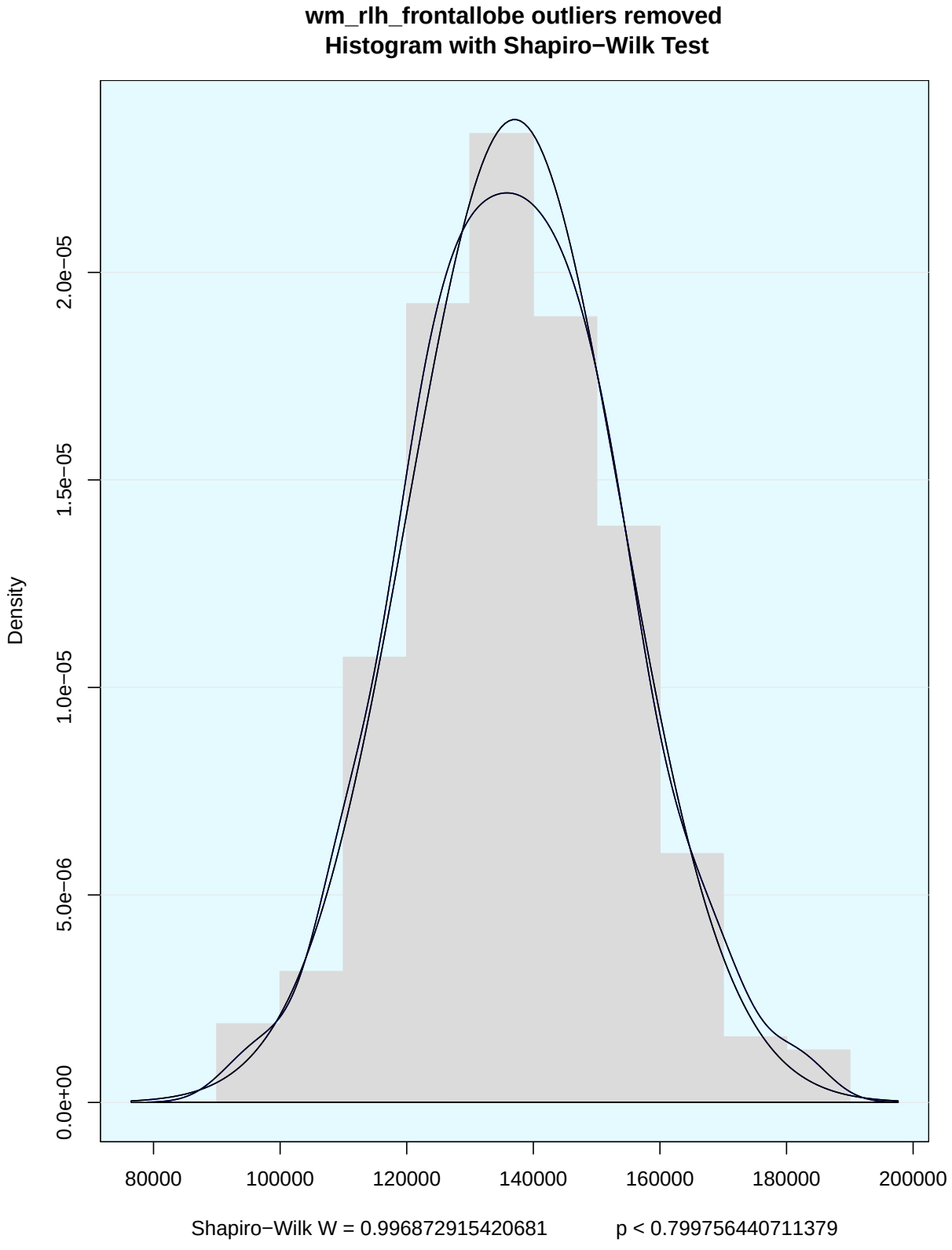

Figure 17: Distribution of volume of the frontal white matter

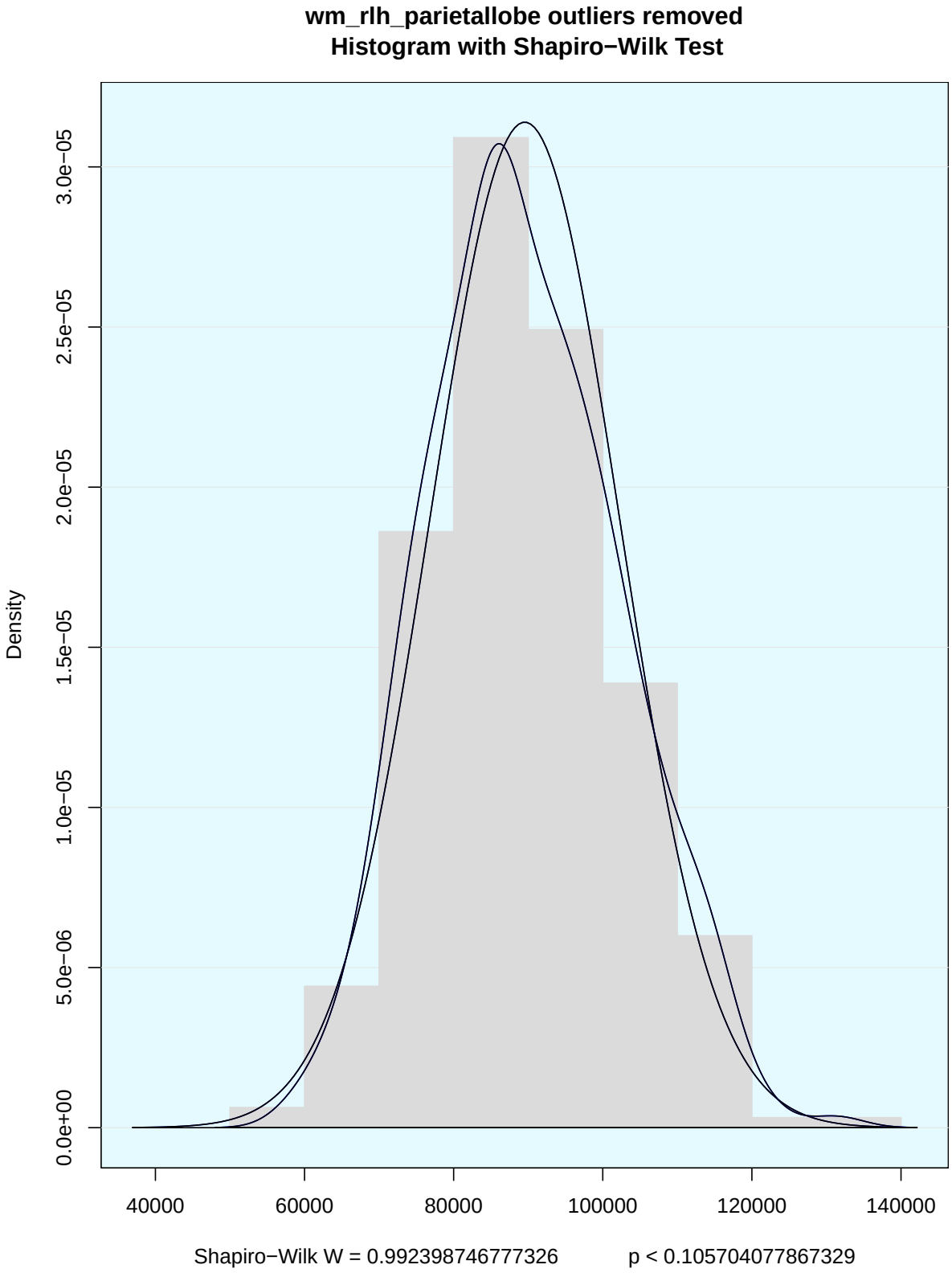

Figure 18: Distribution of volume of the parietal white matter

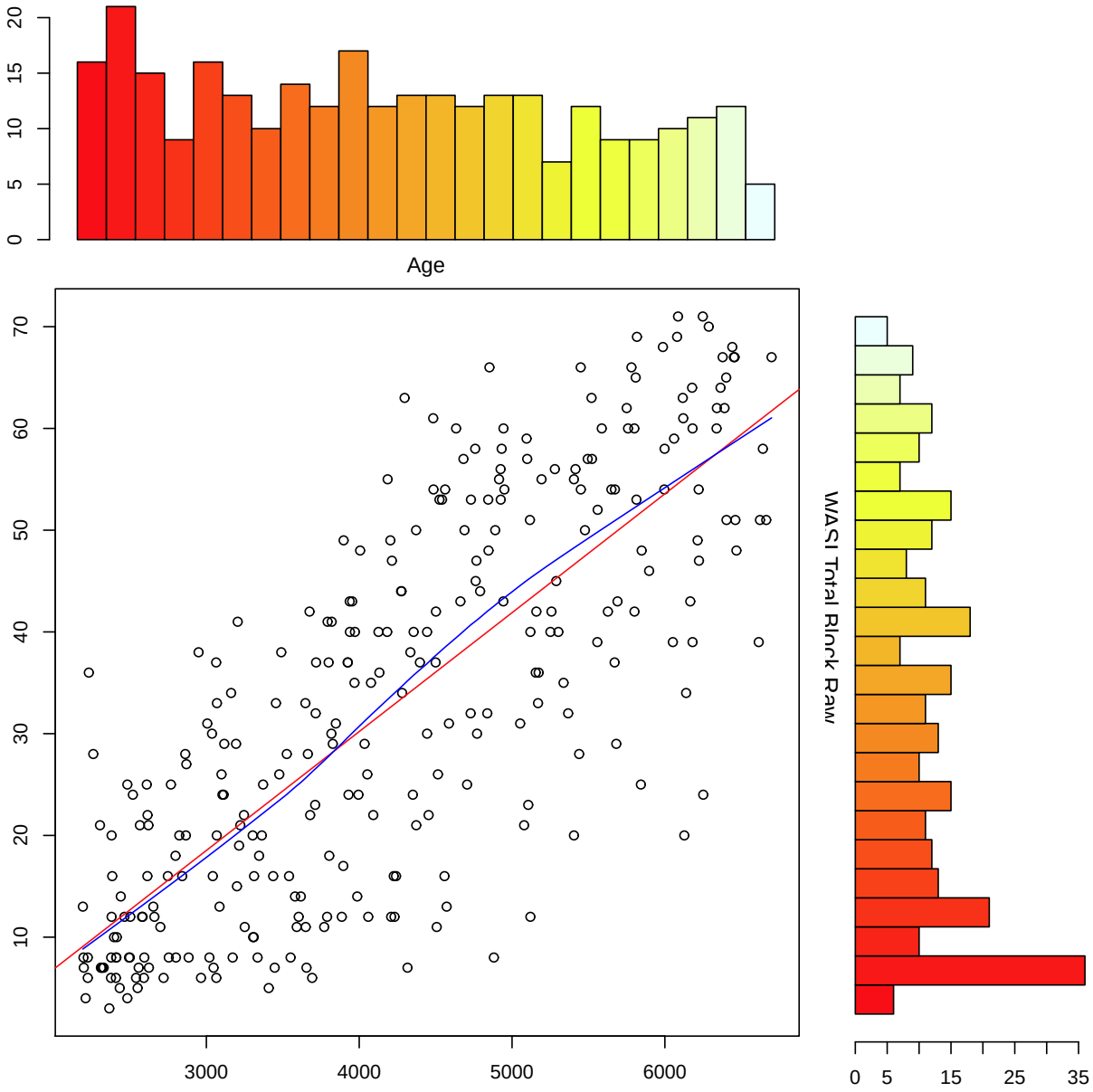

Figure 19: Scatterplot of Age (in days) vs. WASI Block Design Raw Score

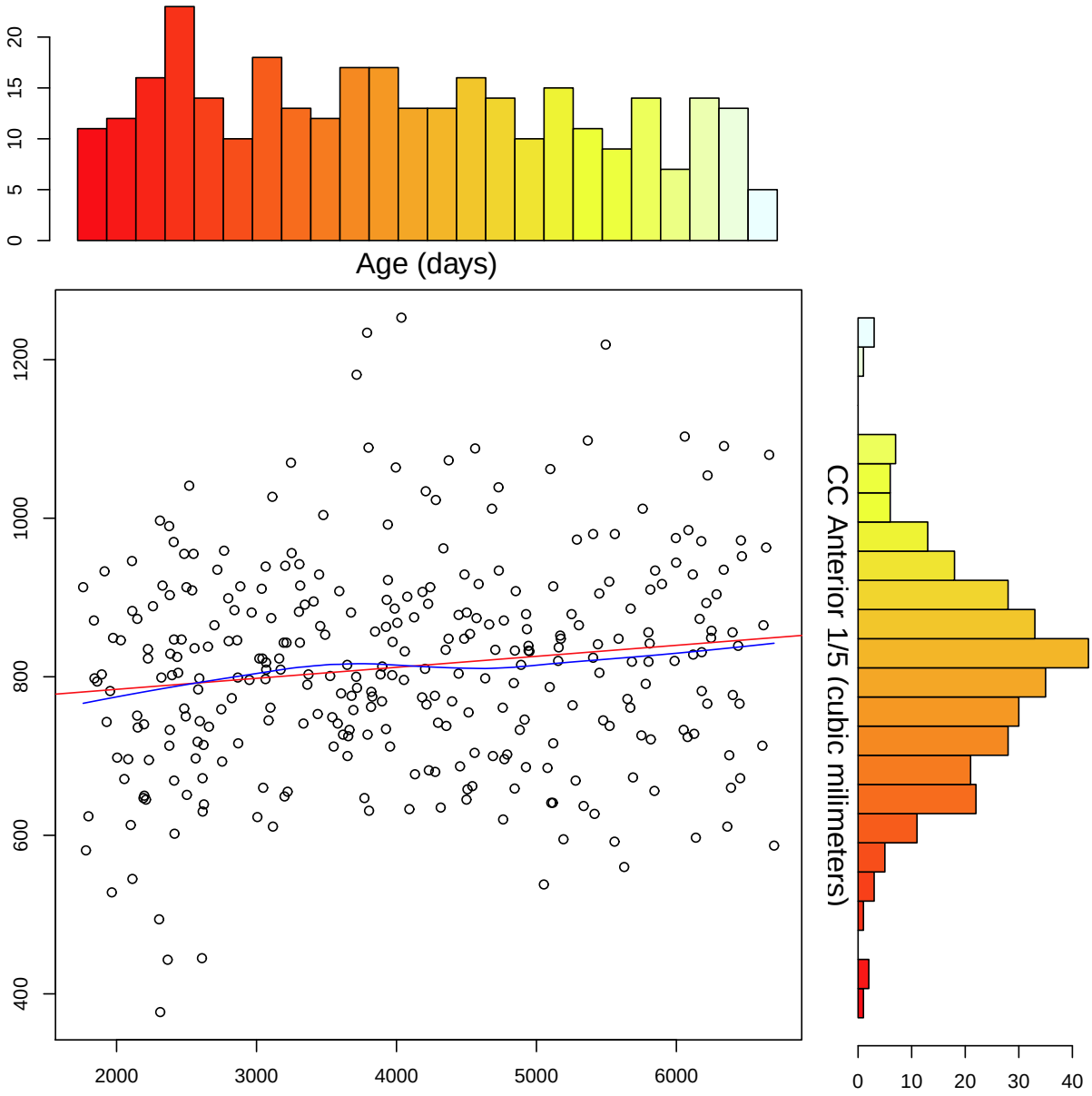

Figure 20: Scatterplot of Age (in days) vs. volume of anterior one-fifth of the corpus callosum

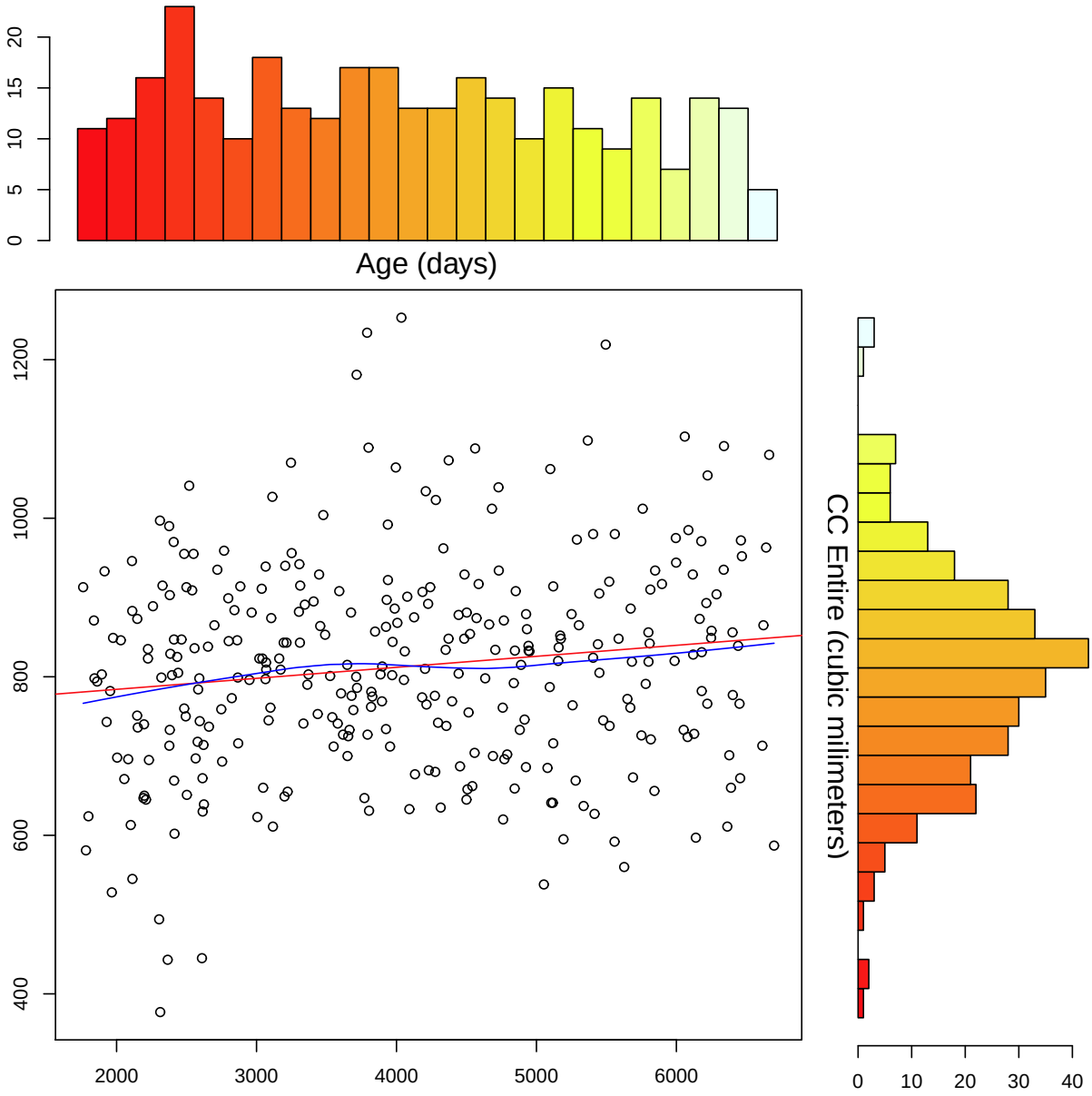

Figure 21: Scatterplot of Age (in days) vs. volume of the corpus callosum

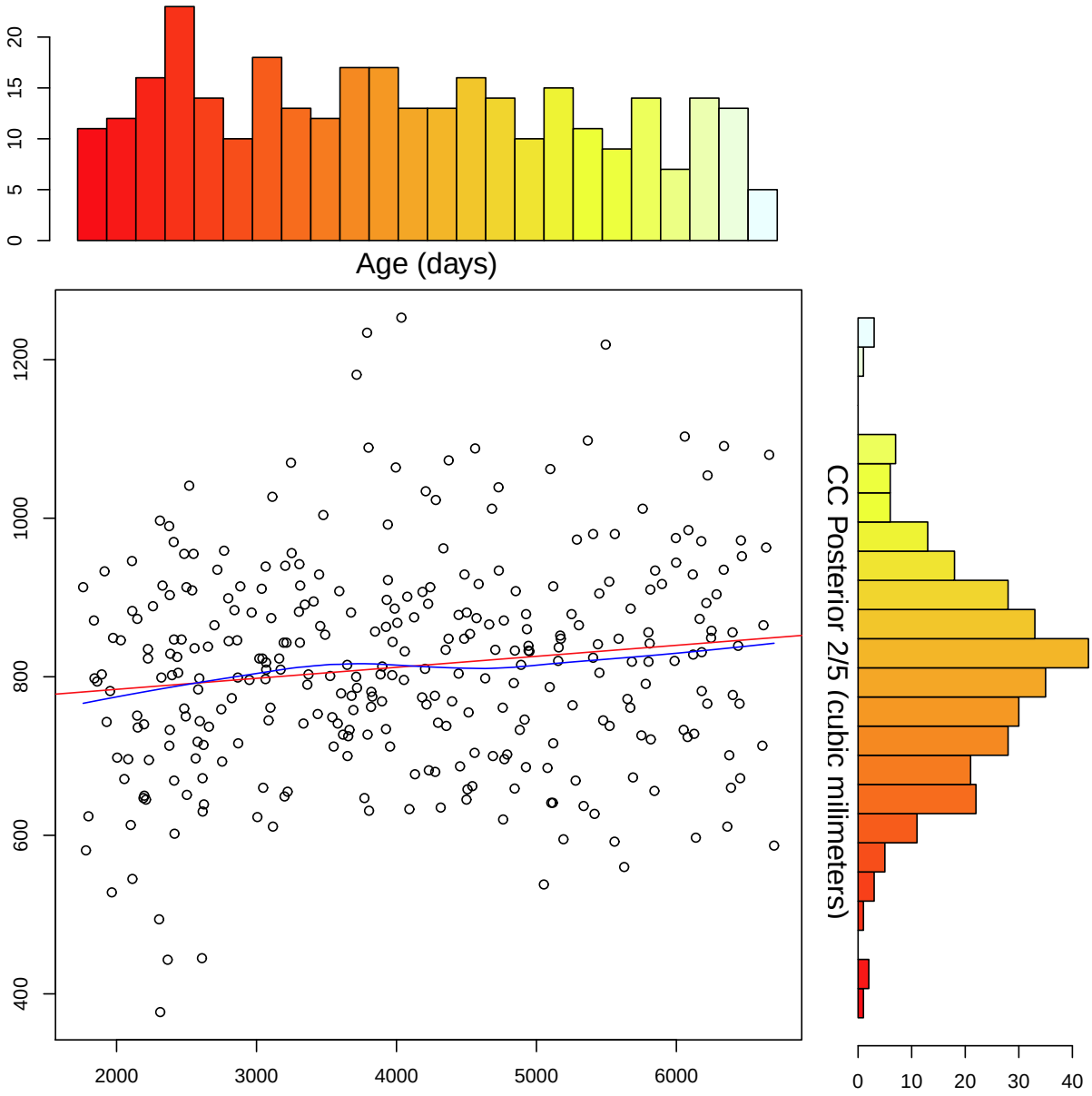

Figure 22: Scatterplot of Age (in days) vs. volume of posterior two-fifths of the corpus callosum

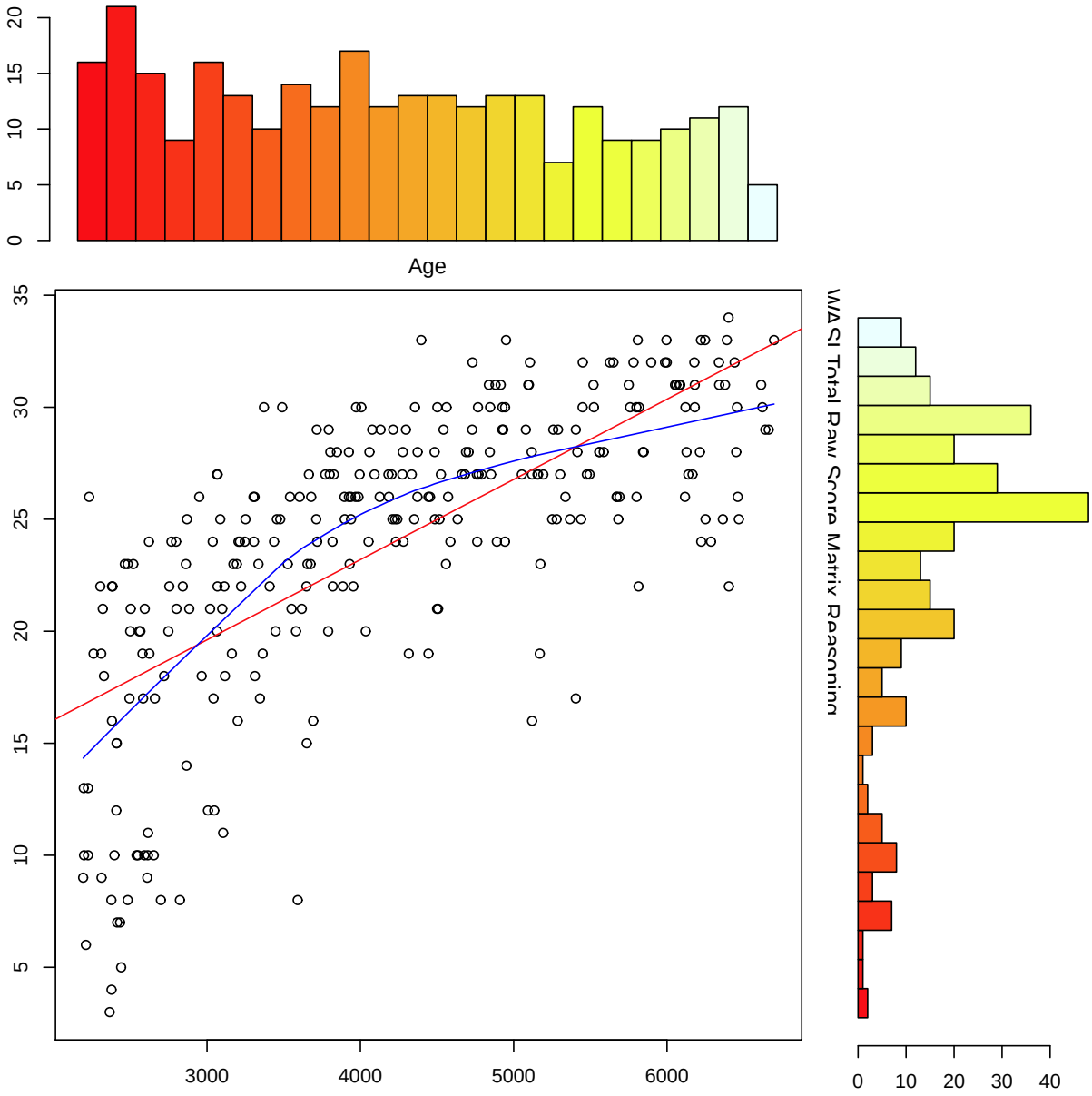

Figure 23: Scatterplot of Age (in days) vs. WASI Matrix Reasoning Raw Score

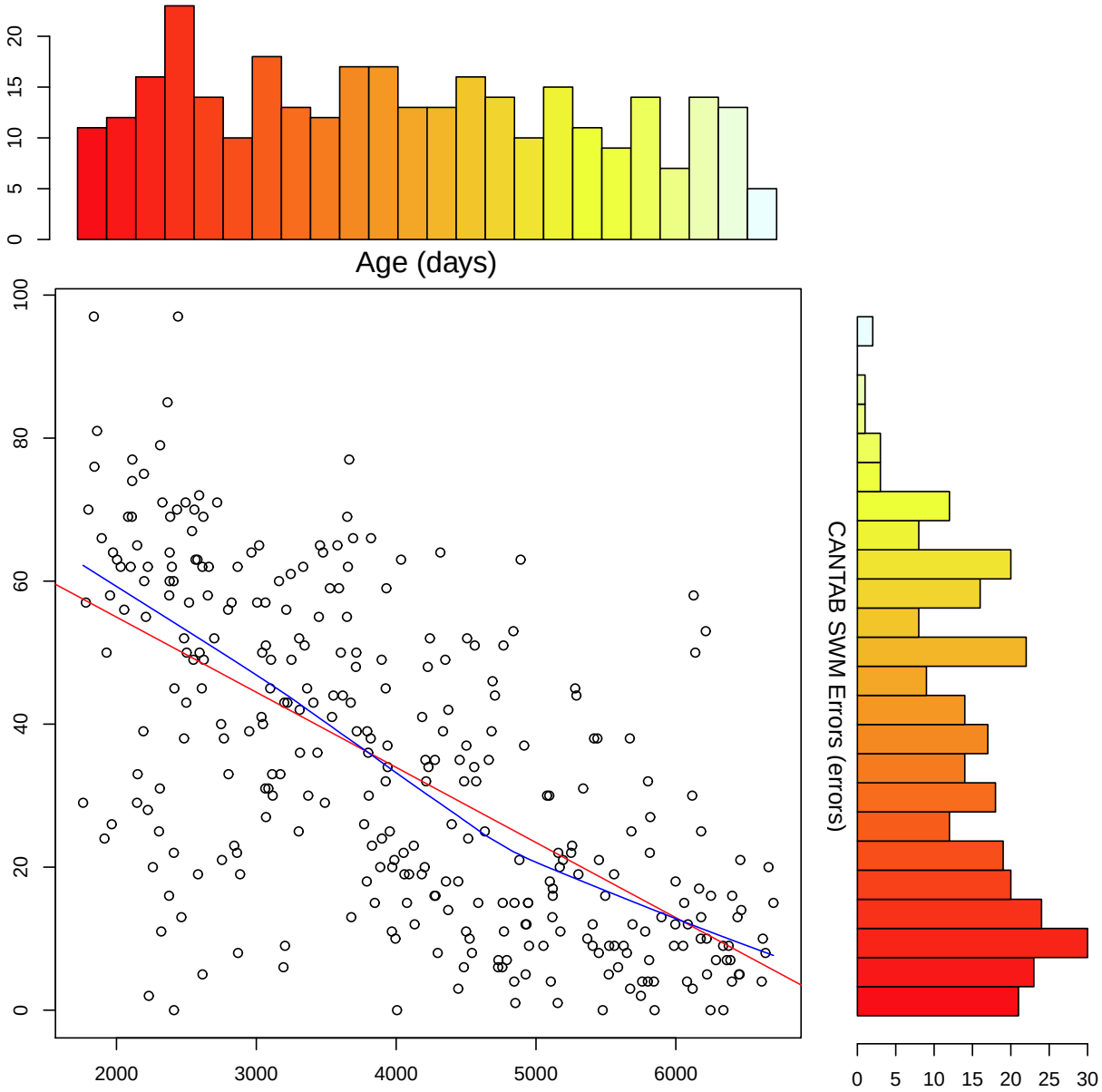

Figure 24: Scatterplot of Age (in days) vs. CANTAB Spatial Working Memory Between Trial Errors

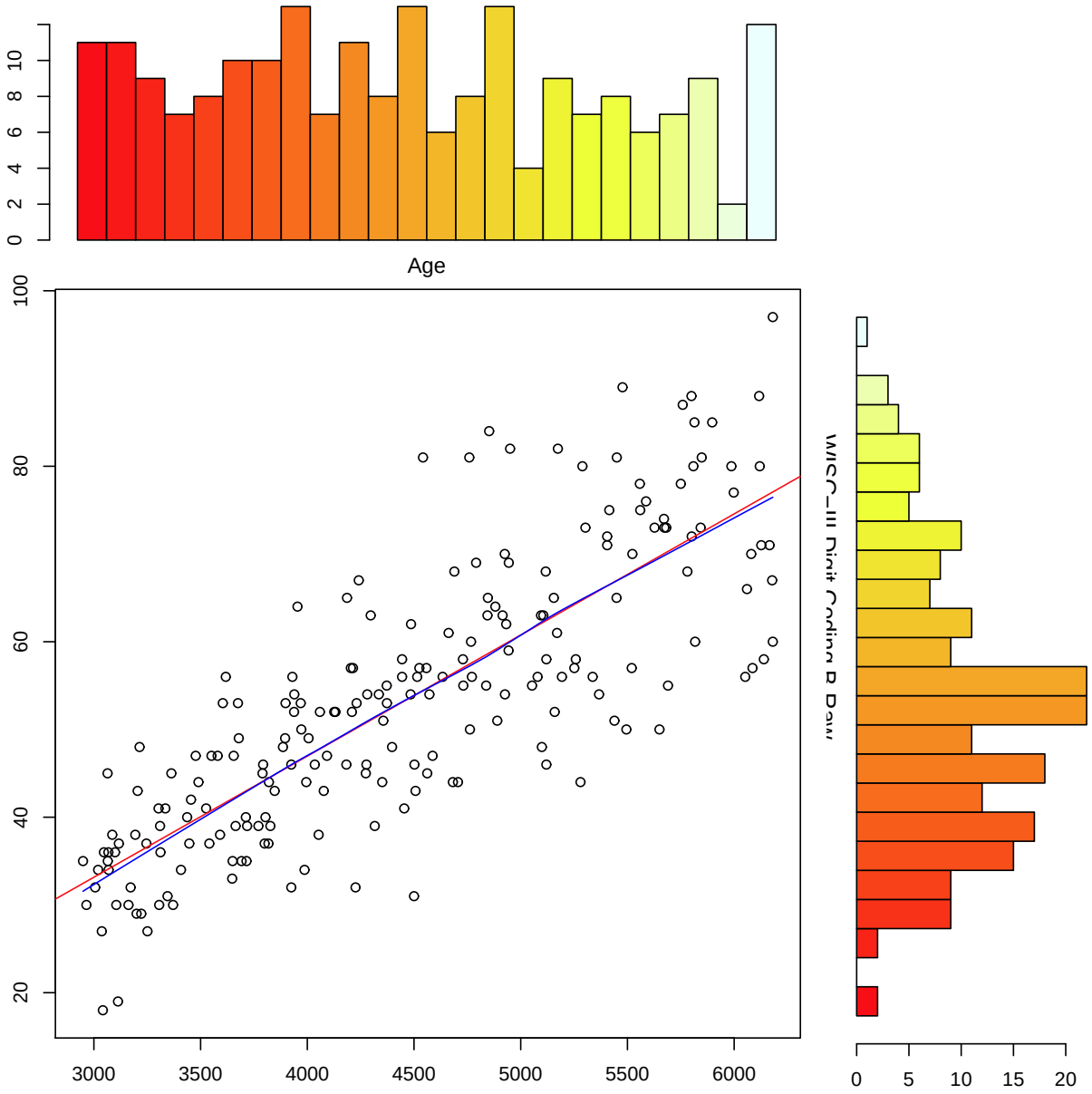

Figure 25: Scatterplot of Age (in days) vs. WISC-III Coding B Raw Score